

STORCUSU

LIBRARY  
SIM 95-011A

# SIMRAC PROJECT GAP032

## STOPE AND GULLY SUPPORT

### FINAL REPORT

DECEMBER 1995

Project Manager M.K.C. Roberts



## EXECUTIVE SUMMARY

### SIMRAC PROJECT GAP032

#### STOPE AND GULLY SUPPORT

This project had two objectives namely

- 'Develop a rationale for the design of stope support systems.'
- 'Determine support resistance criteria for the support of stope gullies for both static and dynamic loading and develop improved support systems for gullies.'

The main areas of work to meet these objectives were:

- establishing a fatal rock related accident database.
- developing and using numerical models in order to test the sensitivity of support spacing and support force on the stability of the immediate hangingwall rockmass for rockfall and rockburst conditions.
- develop a methodology so that the design of stope support systems can be evaluated against rockfall and rockburst criteria derived from the accident data base.
- determining the support behaviour and subsequent requirements of gully packs and the gully hangingwall support requirements in order to reduce rockfalls and minimise rockburst damage.

The report describes a number of outputs below.

- i) The determination of a support resistance criteria for rockfalls and an energy absorption criteria for rockbursts for the Ventersdorp Contact reef, the Carbon Leader reef and Vaal reef has been an important output from the fatal accident database.
- ii) The development of a stope design methodology allows support systems, subject to stope closure, to be evaluated against rockfall and rockburst criteria. Importantly, the stope face and the stope back area have been evaluated separately and each should meet the required criteria.
- iii) The development of a numerical model of stope support - hangingwall interaction has been a laborious process with the objective of obtaining insight into the changes that occur to hangingwall stability when the support spacing and support resistance is varied. The qualitative data obtained to date shows that the mechanisms are complex, however some insight has been obtained with respect to how inter-unit span stability varies with different support resistance's. The full potential of this model is still to be realised particularly when fracture angles are changed and contrasted and when support systems are evaluated under dynamic behaviour.

iv) The support of stope gullies was addressed in two ways, firstly the problem of gully pack stability and foundation stability was investigated by underground monitoring. This resulted in an understanding of the force - deformation behaviour of gully packs with time and stope closure and led to a recommendation with respect to a desirable force - deformation curve for gully packs. This was considered as an important output from this project.

v) The determination of gully hangingwall fallout thicknesses between the gully packs in order to evaluate support resistance criteria and energy absorption criteria for the prevention of rockfalls and reduction of rockburst damage was the second part of the work undertaken on stope gullies. The work concentrated on the Vaal reef, the Ventersdorp Contact reef and the Carbon Leader reef and gully support criteria have been derived for cumulative fallout percentages between 90 % and 100 %. Some rockbolting support requirements have been given which would meet these criteria.

vi) A support catalogue was produced in which the support - deformation curves of all common support units used in Witwatersrand gold mine stopes are arranged with respect to the relevant gold mining region and are further subdivided into face support, back area support and gully support types.

## CONTENTS

### Introduction

1. The determination of support resistance and energy absorption criteria for the Vaal reef, the Ventersdorp Contact reef and the Carbon Leader reef.
  - 1.1 Control of rockfalls - An estimation of the support resistance requirements for the Vaal reef, the Ventersdorp Contact reef and the Carbon Leader reef.
  - 1.2 Reduction of rockburst damage - An estimation of the Energy Absorption Criteria for the Vaal reef, the Ventersdorp Contact reef and the Carbon Leader reef.
2. The evaluation of stope support systems
  - 2.1 Factors affecting the force - deformation behaviour of the support units constituting the stope support system
  - 2.2 The influence of the rock mass on support systems
  - 2.3 Stope support design methodology for rockfall and rockburst conditions
3. The support of stope gullies
  - 3.1 The determination of a gully specific pack support system
  - 3.2 Numerical modelling of gully pack behaviour
  - 3.3 Gully support requirements
4. Project conclusions and outputs
5. Future work
6. References

## GAP 032 FINAL REPORT ----- DECEMBER 1995

Project Manager M.K.C. Roberts

## INTRODUCTION

The final report of the SIMRAC project, GAP 032, Stope and Gully Support, addresses the projects two main objectives, namely:

- 'Develop a rationale for the design of stope support systems.'
- 'Determine support resistance criteria for the support of stope gullies for both static and dynamic loading and develop improved support systems for gullies.'

This report covers both of these objectives in sequence. Both objectives have in common the design of support so that stope and gully support systems can be evaluated against rockfall and rockburst criteria and modified, if necessary, until they meet that criteria. The main areas of work to meet these objectives were:

- establishing a database of rock related fatal accidents,
- determining what support systems are in use in South African mines and establishing a catalogue of the force - deformation of support units making up these support systems.
- developing and using numerical models in order to test the sensitivity of support spacing and support force on the stability of the immediate hangingwall rockmass for rockfall and rockburst conditions,
- evaluate appropriate methods in order to develop a rationale for the design of stope support systems.'
- determining the support behaviour and subsequent requirements of gully packs and the gully hangingwall support requirements in order to reduce rockfalls and minimise rockburst damage.

In South African mines with tabular ore bodies, the design of stope support systems has in most cases been based on experience, past practices and cost considerations. Approximately 130 support systems have been identified in current use in the industry. These include various support unit types with variations in spacing and support dimensions. Clearly, only a number of these systems are optimised with the rest being either over or under designed.

The objective of this report is to define a methodology by which a stope support system may be designed and then evaluated in order to determine how efficiently it would behave under either rockfall or rockburst conditions.

The variables that need to be considered in evaluating a stope support system are;

- the force - deformation behaviour of the support units that constitute the stope support system
- the mining height
- the stope closure rate
- the stope closure during rockbursts and the associated velocity of closure (dynamic closure)
- the spacing of stope support units
- the support resistance generated by the stope support system
- the ability of the support system to absorb energy

In addition, an analysis of the thickness of fall of ground and rockburst ejection has been undertaken for the Vaal reef, the Ventersdorp Contact reef and the Carbon Leader reef. The data is part of the accident database which was set up for the project. The analytical procedure was to derive, from this data, a support resistance criterion for the prevention of rockfalls and an energy absorption criterion for the reduction of rockburst damage. It was intended that any support system design or existing support system would need to be evaluated against these criteria.

A similar process was undertaken to determine criteria for the support of stope gullies for these three reefs. This was done by measuring fallout thicknesses directly underground.

Data derived from laboratory testing, numerical modelling and underground instrumentation has been used when evaluating stope support systems. Clearly there will be areas where the technical knowledge is incomplete and areas where future work will be required are highlighted.

Due to the detailed technical nature of the work, this report has been structured so that the technical detail is presented as appendices or suitably referenced in order to keep the main body of the report focused on results and outputs.

## **1. The determination of support resistance and energy absorption criteria for the Vaal reef, the Ventersdorp Contact reef and the Carbon Leader reef.**

A stope support resistance of 50 kN/m<sup>2</sup> is the rockfall support resistance criterion that has been generally used by the industry as a guide for the design of stope support systems in stopes where the major hazard are rockfalls.

In stopes which are subject to seismicity and rockbursts a general energy absorption criterion has applied, namely that the support system should be capable of absorbing 60 kJ of energy per square metre of hangingwall, which requires the support system to have a yielding capability. These criteria have been re-evaluated for the three specific reefs using the data from the accident database.

### 1.1 Control of rockfalls - An estimation of the support resistance requirements for the Vaal reef, the Ventersdorp Contact reef and the Carbon Leader reef.

Although most mines mining these reefs are subject to seismicity and therefore the rockburst energy absorption criterion should apply, it is also necessary to analyse the fallout thickness in order to determine a support resistance criteria that would prevent rockfalls for those areas not subject to seismic events. The accident data base has been used to derive this data and the cumulative percentage fallout thickness are shown in Figures 1, 2 and 3 for the Vaal reef, the Ventersdorp Contact reef and the Carbon leader reef respectively.

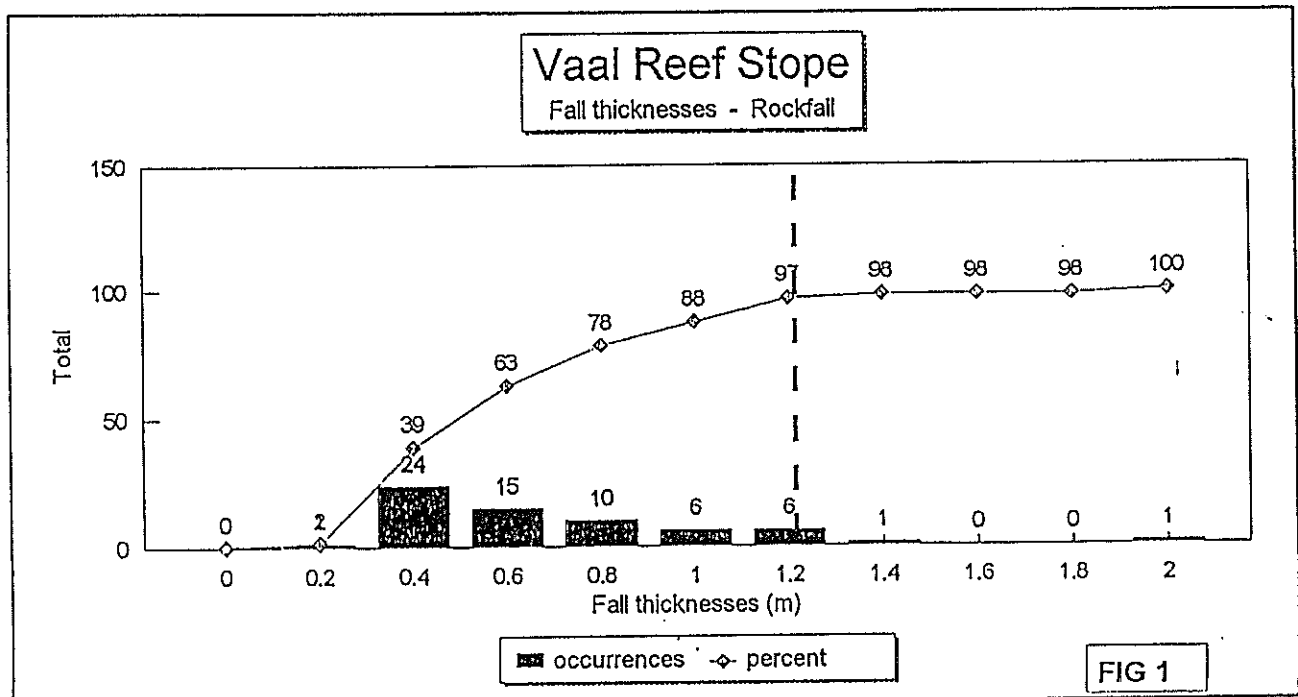


Figure 1. Cumulative fallout thicknesses for the Vaal reef

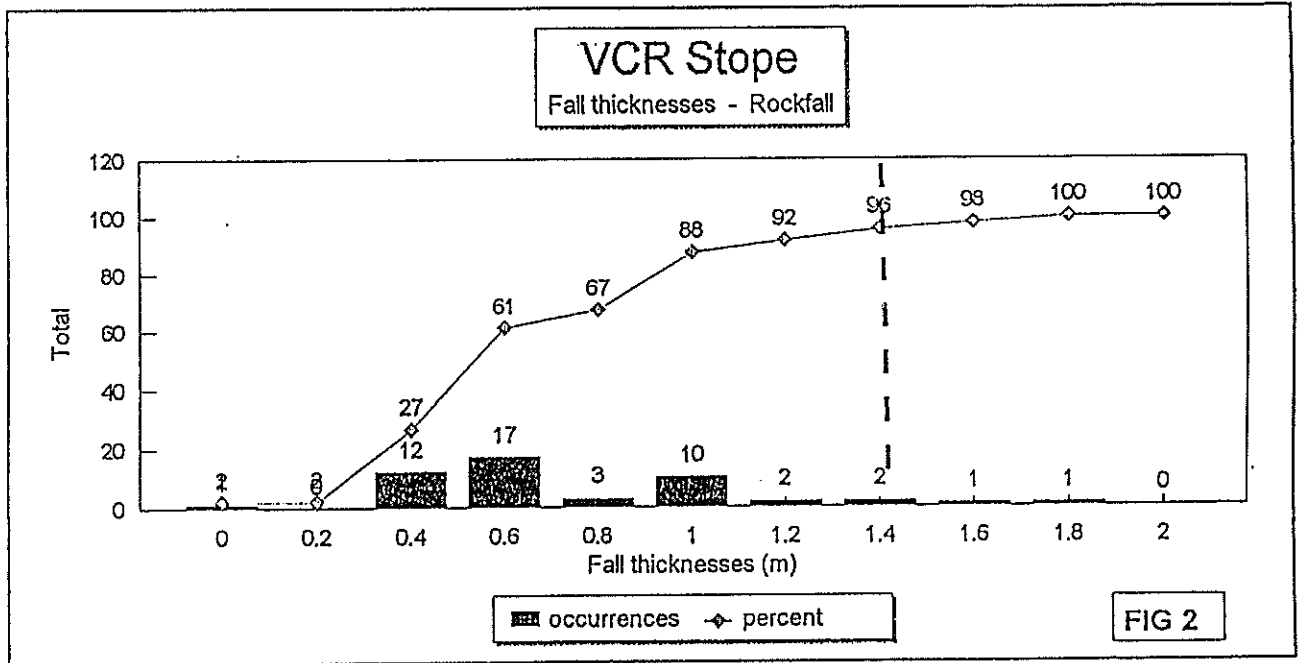


Figure 2 Cumulative fallout thicknesses for the Ventersdorp Contact reef

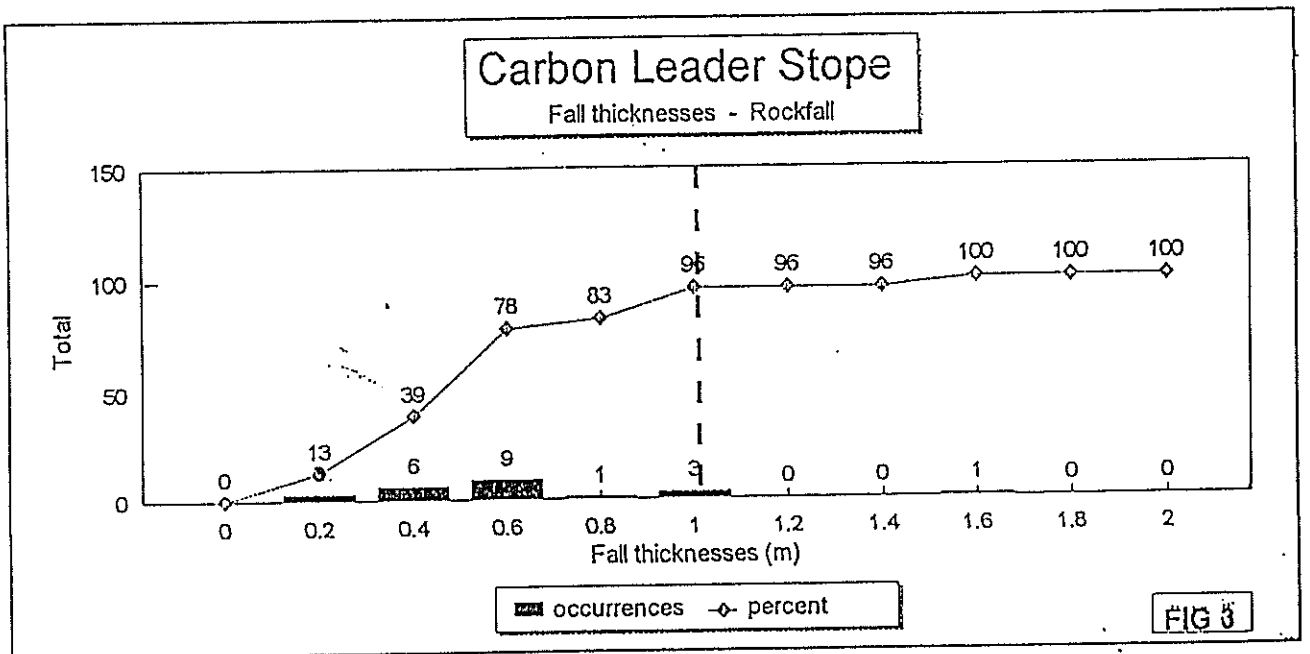


Figure 3 Cumulative fallout thicknesses for the Carbon Leader reef.



To use this data it is assumed that the support system should prevent 95% of all fallouts and the table below shows the fallout thickness for 95% frequency levels i.e. 95% of all falls were the indicated thickness or less. The table also shows the associated support resistance criteria.

Reef	95% fallout frequency	Support resistance criteria kN/m <sup>2</sup>
Vaal reef	1,2 m	33 kN/m <sup>2</sup>
Ventersdorp Contact reef	1,4 m	38 kN/m <sup>2</sup>
Carbon Leader reef	1,0 m	28 kN/m <sup>2</sup>

The support resistance of stope support systems that have been designed, or are in current use, should be evaluated against the support resistance required for the appropriate reef above to ensure that they exceed the criterion. The methodology to do this is shown in section 2.3 in this report.

### 1.2 Reduction of rockburst damage - An estimation of the Energy Absorption Criteria for the Vaal reef, the Ventersdorp Contact reef and the Carbon Leader reef.

The currently used energy absorption criteria of 60 kJ/m<sup>2</sup> has been considered necessary for stope support to reduce rockburst damage. The basis of this criterion was a support resistance of 200 kN/m<sup>2</sup> which could be displaced through 0,3 m at 3 m/s during a rockburst and in the process absorb 60 kJ/m<sup>2</sup> of energy.

The energy absorption ability of support systems used in rockburst prone stopes should therefore have met this criterion. In this report this criterion has been re-evaluated using quantified ejection thicknesses for the three reefs from the accident database. For the purpose of this analysis the ejection velocity is still considered to be 3m/s.

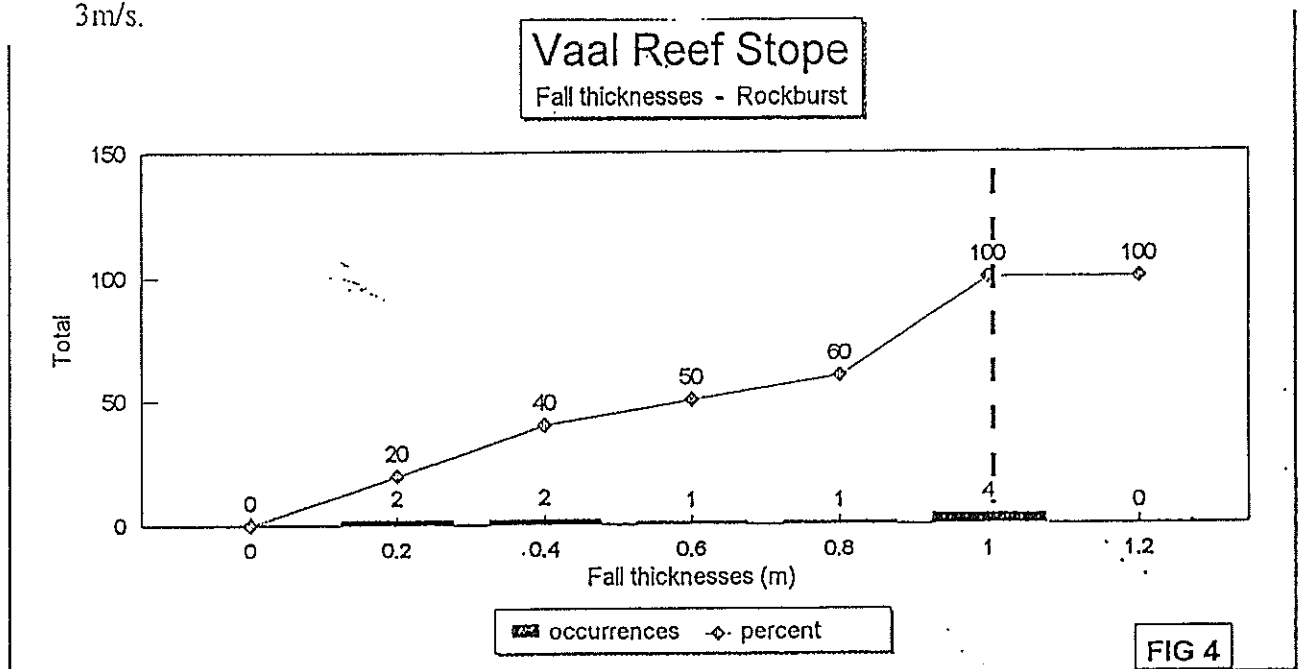


Figure 4. Cumulative percentage of ejected block thicknesses for the Vaal reef.

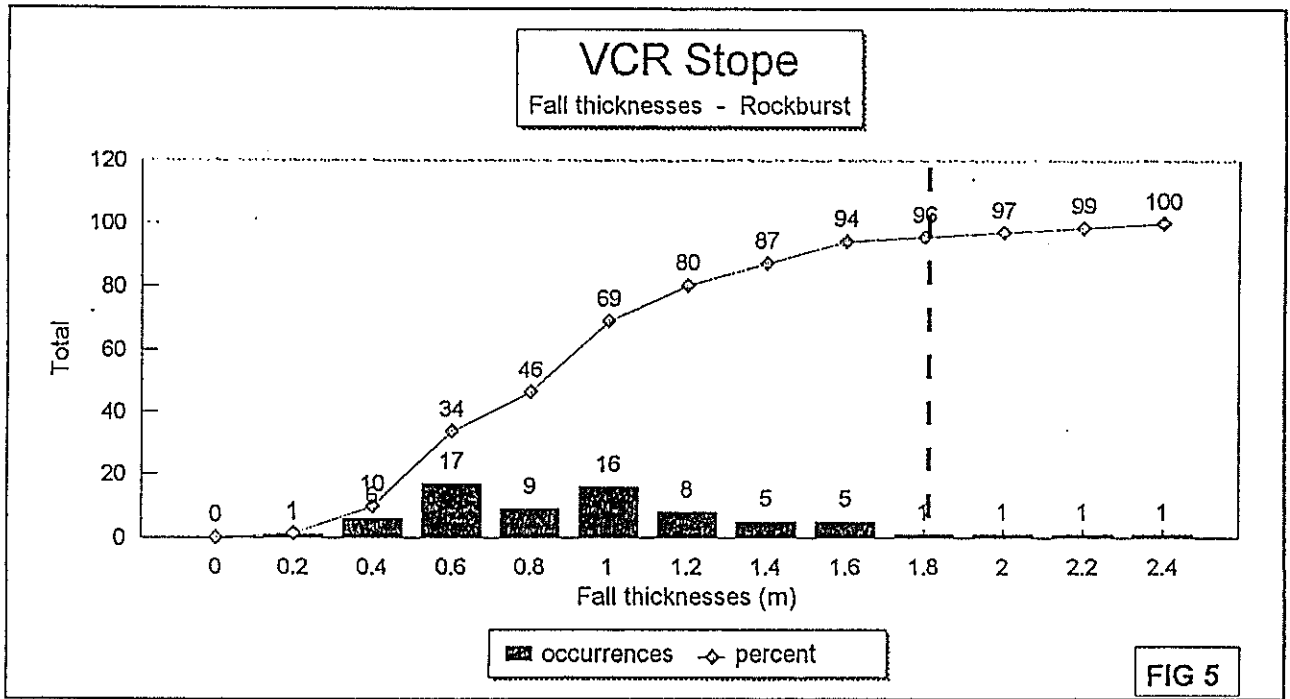


Figure 5. Cumulative percentage of ejected block thicknesses for Ventersdorp Contact reef.

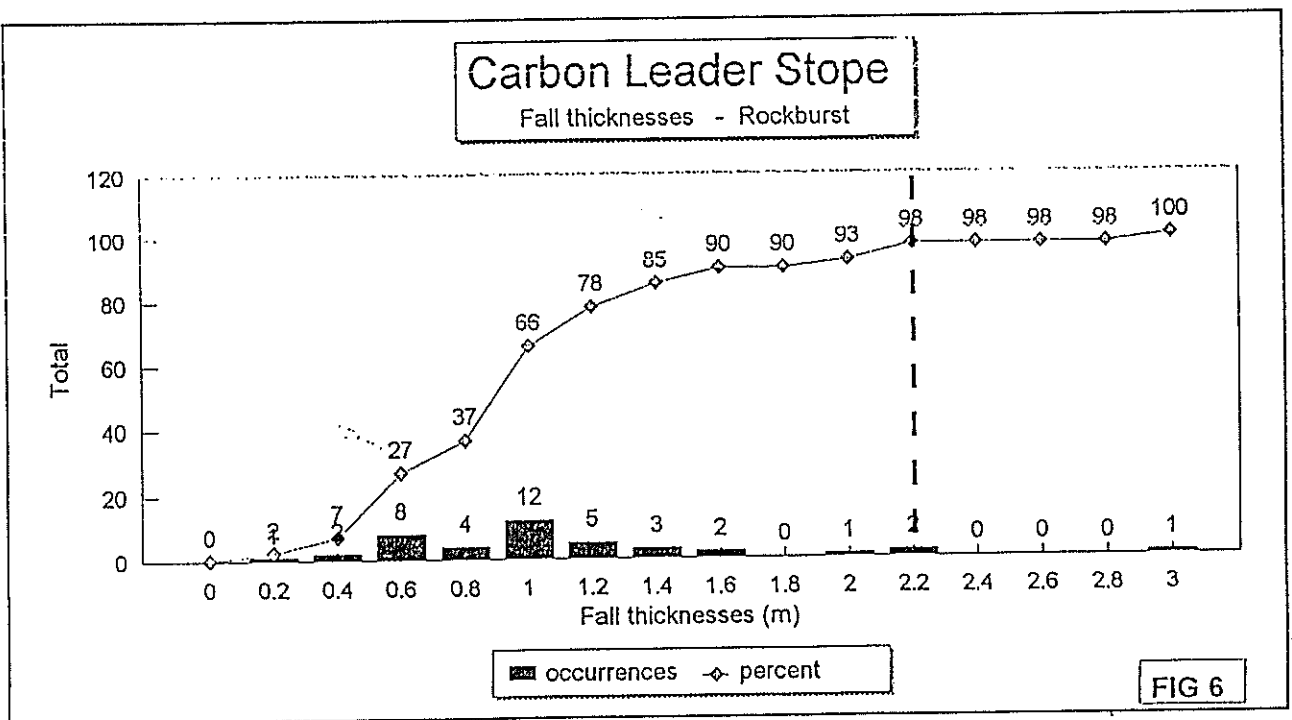


Figure 6. Cumulative percentage of ejected block thicknesses for Carbon Leader reef.

Figures 4, 5 and 6 show histograms of ejected block thickness from rockbursts as a cumulative percentage of increasing block thickness measured at the sites of fatal accidents for the Vaal reef, the Ventersdorp Contact reef and the Carbon leader reef. The ejection thickness representing 95% of the cumulative percentage will be used for the purpose of developing the energy absorption criteria. This is shown below for the various reefs.

Reef	95% rockburst ejection thickness frequency
Vaal reef	1,0 m
Ventersdorp Contact reef	1,8 m
Carbon Leader reef	2,2 m

The actual number of rockbursts used to construct the histograms are: 10 for the Vaal reef, in which 29 fatalities occurred; 71 for the Ventersdorp Contact reef in which 121 fatalities occurred, and 41 for the Carbon Leader reef in which 75 fatalities occurred. The small number of examples representing the Vaal reef are due to the fact that rockbursts are relatively uncommon across this reef with the exception of some individual shafts. For the purpose of this analysis the Vaal reef data will be evaluated although more data needs to be collected. The Carbon Leader ejection thicknesses could also vary across the ore body depending on the distance between the reef and the green bar. This type of analysis will be undertaken in future work.

Using these block ejection thicknesses it is possible to calculate a minimum energy absorption requirement per square metre of stope hangingwall that a support system should be able to provide to stabilise the stope hangingwall in 95% of the cases. The velocity of ejection is assumed to be 3m/s and it is also assumed that the support system has the ability to yield 0,2 m, typical of the yieldability of hydraulic props and yielding timber props. Packs are able to yield considerably more.

Therefore Energy absorption criterion or  $E_{ac} = 1/2 mv^2 + mgh$

Where  $m = 2700 \text{ kg} \times \text{ejection thickness}$

$v = 3,0\text{m/s}$

$h = 0,2\text{m}$

$g = 9,81$

$E_{ac}$  is the energy absorption criterion

The energy absorption criterion is detailed for the specific reefs below.

Reef	Energy absorption criteria or $E_{ac}$
Vaal reef	18 kJ/m <sup>2</sup> *
Ventersdorp Contact reef	32 kJ/m <sup>2</sup>
Carbon Leader reef	38 kJ/m <sup>2</sup>

\* small database

The energy absorption ability of stope support systems that have been designed, or are in current use, should be evaluated against the energy absorption requirement or  $E_{ac}$  for the appropriate reef above to ensure that they exceed the criterion. The methodology to do this is shown in section 2.3 in this report.

## **2. The evaluation of stope support systems**

The evaluation of a stope support system involves a technical evaluation of the support units constituting the support system, considerations of their stability at various mining heights, the behaviour of the support units with respect to the anticipated stope closure rates, the spacing of the support units in order to achieve stable spans between the units, the support resistance generated by the support system and, in rockburst conditions the ability of the support system to absorb energy. In this section these considerations will be evaluated as a step by step process of support unit evaluation.

### **2.1 Factors affecting the force - deformation behaviour of the support units constituting the stope support system**

The testing of stope support elements has been undertaken for many years in the mining industry in the belief that an understanding of the force - deformation behaviour of these units can assist in the selection of suitable stope support systems. Hundreds of support units have been designed and tested using laboratory presses and some of them have been used successfully as mine stope support. An early output of this project was the determination of which of these support units were being used by the mining industry by looking at mine codes of practice and then collation of the force - deformation behaviour of these support units into a stope support catalogue for reference.(1) The force - deformation curves were derived from laboratory tests conducted by staff from Miningtek and staff from the Anglo American rock mechanics laboratories in Welkom, who were collaborators in this portion of the project.

The force - deformation curves of the various support units shown in the catalogue with other pertinent information such as the press loading rate, the height of the unit, the dimensions of the unit and, in the case of packs, the rise of the timber.

A number of factors will affect the force - deformation behaviour of these support units and these need to be assessed before evaluating the behaviour of any support units constituting a support system.

#### **2.1.1 The loading rate effect on timber support units**

It is well known that the force - deformation behaviour, and consequently the ability of timber support units to absorb energy, changes significantly depending on the loading rate. In the case of yielding timber elongates such as pipe sticks and profile props, the work by Roberts, Jager and Riemann (2) established a procedure to adjust the force - deformation behaviour of these elongates either upwards or downwards, depending on the loading rate. However with respect to timber packs it was known that under rapid loading, the ability of timber packs to absorb energy was enhanced as the force increases with a rise in the deformation rate, however, the magnitude of the enhancement was not known.

The difference between normal stope closure, typically 5 mm/day to 20 mm/day and the closure rates that are believed to occur during some rockbursts of 1 m/s to 3 m/s is approximately 6 orders of magnitude in displacement rate. It was therefore necessary to determine an algorithm so that the force - deformation characteristic of timber packs could be adjusted upwards or downwards depending on the loading rate, thus allowing the energy absorption ability of the pack to be determined.

Roberts and Pienaar attempted to establish a relationship to determine the change in force with deformation rate (3) but the validity of the theoretical formula could not be checked as no rapid pack testing facility exists in South Africa.

An output of this project was therefore to determine such a relationship and testing of timber packs dynamically up to velocities of 3 m/s was undertaken by Miningtek and Anglo American staff in Germany where a rapid pack testing facility was located. The results of this work are of particular importance and leads directly into another part of the project, the numerical modelling of the stope support / hangingwall interaction. These models need the input of dynamic force - deformation curves for packs in order to realistically determine the hangingwall interaction with the support.

The results of the tests are described by Taggart (4 and 5) who found a linear relationship between a change in deformation rate and the resulting change in pack force of approximately 16 per cent per order of magnitude change in deformation rate and that this variance is irrespective of the size and composition of the packs. This relation is shown below:

$$F_f = F_s \left[ 1 + \frac{\%inc}{100} \right]^{\log \frac{v_f}{v_s}}$$

where :  $F_f$  is pack force at increased velocity  $v_f$

$F_s$  is pack force at lower velocity  $v_s$

and  $\%inc$  is the empirically derived per cent increase in force per increase in order of magnitude in compression velocity

Using this relationship the force - deformation behaviour and consequently the energy absorption ability of timber packs may now be determined for high deformation rates typical of some rockbursts.

### 2.1.2 The height of support units

It is known that support units installed in high stoping widths are less stable than support units at low stoping widths, however little work to quantify this has been undertaken. For example it is commonly assumed that packs whose height to width ratio exceeds 2 are considered unstable, particularly during dynamic closure. This appears to be a qualitative assessment from underground experience and is probably correct. It will only be possible to evaluate this once the dynamic pack tester is available. Such a pack tester is planned for the Miningtek test laboratory and funded by SIMRAC.

Similarly the stability of yielding timber elongates decreases with increasing height and with increasing amounts of stope closure. This has been determined by means of underground measurements in which the percentage of buckled yielding timber elongates was determined for various lengths and for various amounts of stope closure.

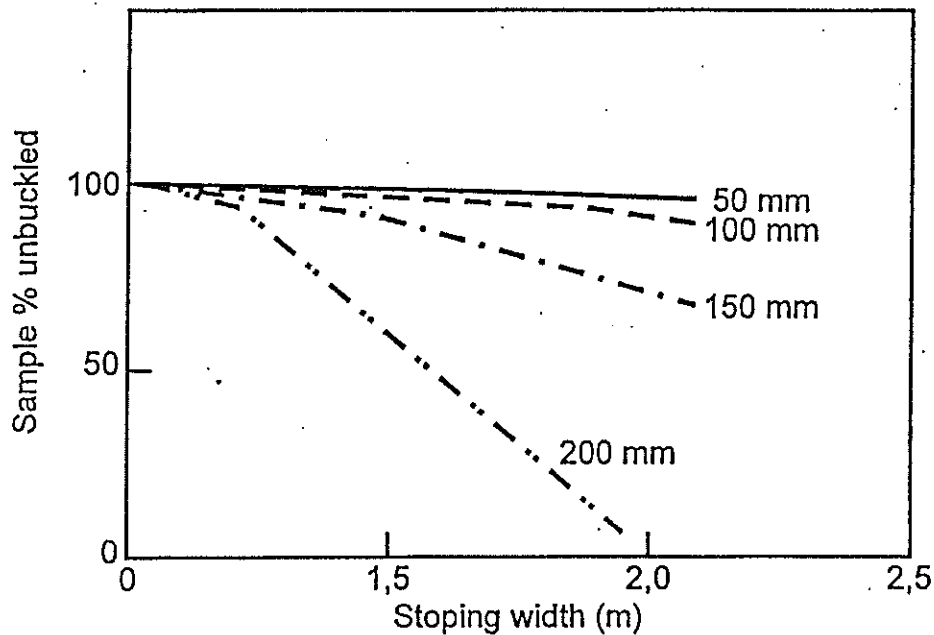


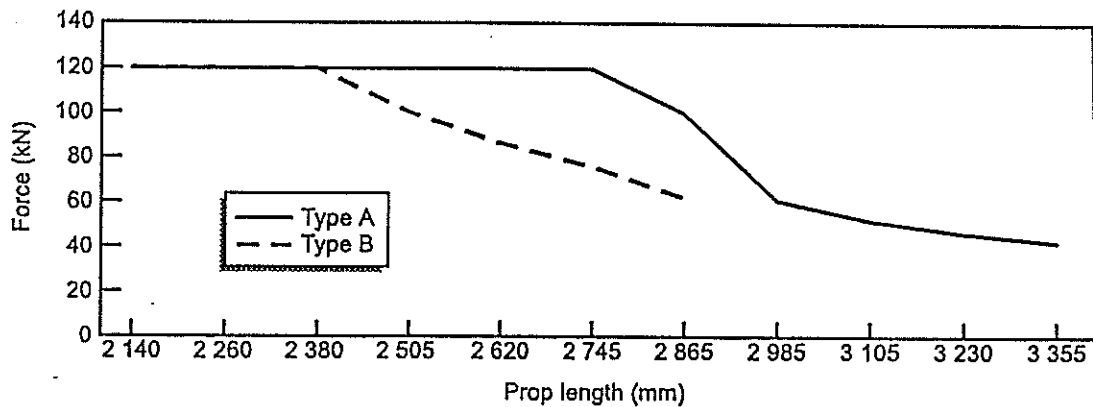
Figure 7 The buckling potential of yielding timber elongates as a function of increasing length and stope closure.

Figure 7 shows this in graphical form where each curve represents different amounts of buckling for different amounts of stope closure. It appears therefore that the height to width ratio of elongate support units should not exceed 10.

The stability of hydraulic props and extensions have been greatly improved in recent years by the adoption of conical extension pieces. The upper stability limits have not been tested although it is known that hydraulic props installed a metre from the stope face have a significantly increased blast out rate as the prop length exceeds 1,8m.

Moreover underground observations have shown that hydraulic props and extensions that exceed 2,5 m in length are unstable during dynamic loading.

Testing has been undertaken on a variety of mechanical props firstly to determine the buckling potential with increasing length and secondly to determine their ability to absorb energy.



**Figure 8 The force - length relationship for two types of medium duty mechanical props.**

Figure 8 shows two varieties of medium duty mechanical props which were tested with increasing prop lengths. Between the lengths of 2,3 m and 2,7 m the props failed by buckling at loads below 120 kN and they buckled at progressively lower loads with increasing lengths. The range of lengths between 2,3 m and 2,7 m should be regarded as the upper limit in terms of length for the use of these props.

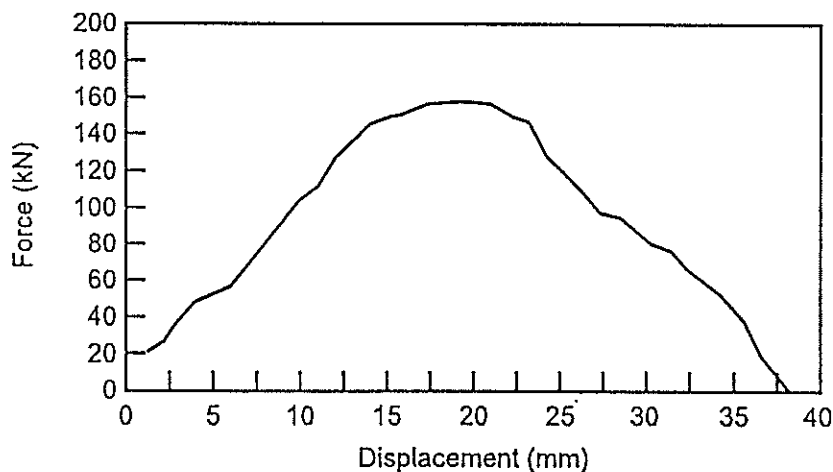


**Figure 9 The force - deformation curve of a 1.5 m long medium duty mechanical prop.**

Figure 9 shows a force - deformation curve of a typical medium duty mechanical prop. If the area under the curve is considered then its ability to absorb energy, namely 3,2 kJ is extremely limited. These props therefore have no energy absorption function as support in rockburst prone stopes.

## 2.2 The influence of the rock mass on support systems

The rock mass behaviour surrounding stopes can vary widely depending on depth, bedding thickness, jointing and the hangingwall rock types. Depth determines whether the blocks constituting the rockmass are defined by geological structures only, as

found in shallow conditions or by stress induced fractures, typical of deep mining conditions as well as geological structures. The depth of stope can also influence the stope closure rate although other factors such as mining cycle stope span and the rock types in the hangingwall and footwall also have an influence. The distribution of geological structures, bedding thickness and stress induced fractures in the rock mass will influence the spacing of support units in a support system and the closure rate will influence the choice of support system particularly if it is required to absorb energy should a rockburst occur.

### **2.2.1 The stope closure rate**

Stope closure may be negligible in shallow or multi - reef stopes but can be up to 50 mm/day in deep stopes, particularly on the Carbon Leader or Vaal reefs. Where these high closure rates occur, a large contribution is due to inelastic deformation, often due to the sliding of non - planar bedding planes in the hangingwall and footwall of the stope as a result of the dilation in the stope face and the consequent generation of horizontal stresses in the various strata. Stope closure, and hence the rock mass behaviour, in deep mines is only reduced when the support resistance exceeds 1000 kN/ m<sup>2</sup> or 1 mPa. This high support resistance can only be achieved by backfill and in practice, conventional stope support such as packs and props rarely exceed 300 kN/ m<sup>2</sup> or 0,3 mPa.

It is important to know the expected stope closure rate and mining cycle when designing or evaluating a support system in order to determine the absolute amount of stope closure that has acted on the support system in order to determine if the remaining yieldability will allow sufficient energy to be absorbed should a rockburst occur.

### **2.2.2 Dynamic closure velocity during rockbursts**

Dynamic closure which occurs during some rockbursts is particularly difficult to measure. However some measurements have been made, in particular at Blyvooruitzigt where a velocity of 2.1m/s over 50mm was recorded. At East Driefontein a minimum velocity of 1.4 m/s was back calculated from a block ejected from a tunnel hangingwall in which a single shepherd crook had failed in tension. Historically, the old 40 ton hydraulic props were occasionally known to burst in significant numbers during rockbursts. The designed yield velocity was 1 m/s and this must have been exceeded in these cases. For the purpose of assessing support system behaviour the closure velocity is therefore assumed to be 3 m/s until further data comes available.

### **2.2.3 The spacing of stope support units**

An important step in the application of the stope support design methodology presented in this report is the determination of the support systems resistance and energy absorbing capacity. Support system resistance curves can be derived by simply determining the area associated with each support and dividing the support unit resistance by this area to obtain the average support resistance per square metre. A system's energy absorption capacity is derived in a similar way. Critical to the validity of this approach is that the supports deliver their resistance to hangingwall movements in a stable manner.



At the outset of the project the importance of support parameters such as spacing, support unit force and the use of load spreaders, or head-boards, was recognised. It was also established that there is little documented information available concerning the influences of these support parameters on hangingwall stability. A study of trends in hangingwall stability with variations in these parameters was therefore undertaken. A numerical modelling approach was used; a detailed account of the background to and technical aspects of this work is presented in an appended document entitled *Numerical modelling of stope support-rockmass interaction* (see Appendix 1). The advantages of the modelling approach over a programme of underground monitoring are also discussed in this document. It was acknowledged from the outset of this study that a modelling approach would not provide quantitative results. The objective of the study was therefore simply stated as:

- to establish the relative stability of the hangingwall with changes in
- a) **support spacing,**
  - b) **support unit force, and**
  - c) **the use of load spreaders.**

The intention was to consider hangingwall stability under both static and dynamic conditions. Some results have been obtained under quasi-static conditions, that is, under the loading encountered during typical face advances. Modelling of support performance under dynamic loading, typical of mine induced seismicity has also been done but insufficient data has been generated to establish any trends. Results of the static analysis are presented below, although in all modelling work the values used for support parameters were realistic, detailed calibration of the model has not been possible and hence the values of support forces and spacings in the results should not be considered as definitive.

Attention has been focused on support units in the face area while two different back area support systems have been considered. The models used take into account the blocky nature of the skin of deep level mining excavations but the pattern of fracturing in the rock surrounding the stope has to be pre-determined and is fixed while support parameters are varied. Most of the results presented have been obtained with a model that includes reef parallel bedding planes at a spacing of half a metre; some other results have also been obtained with a one metre spacing, but no further testing of the sensitivity of the results to details of the fracture pattern has been attempted.

### 2.2.3.1 Trends with varying spacing and support force

A support systems average resistance per square metre is the parameter used in current design practice. Variation of support spacing, while holding a support system's average resistance constant requires variation in support unit resistance (*support force*). Conversely, variation of spacing while holding support unit resistances constant, results in changes to the support system's average resistance. Trends in support performance can be interpreted in different ways by taking into account this coupling. Figures 10(a) and (b) show the trends in hangingwall stability obtained by varying spacing and support unit resistances. A constant dip spacing of 1m is assumed

as all modelling was carried out in two dimensions. The method used to rate hangingwall stability is described in Appendix 1.

Figure 10(a) shows three lines; these lines indicate trends in hangingwall stability with increasing average support system resistance. The support spacing is constant for each trend line, the three lines correspond to spacings of 1m, 2m and 3m.

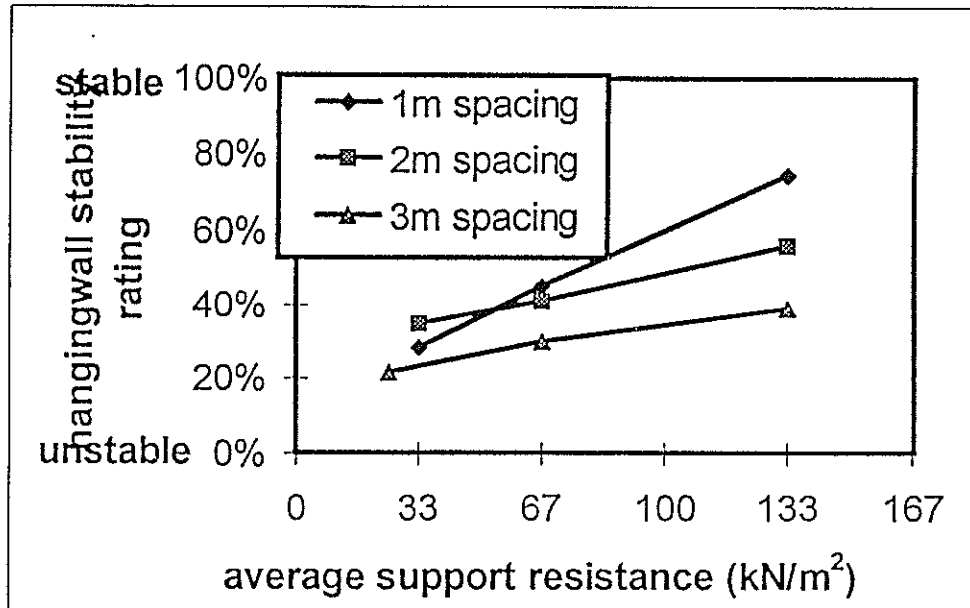


Figure 10(a) Hangingwall stability vs average support resistance at different support spacings (0.5m bedding, back area packs)

In this Figure, the support unit resistances change along each curve; for example, for the case of 1m spacing, the unit resistances, at average resistances of 33 kN/m², 66 kN/m² and 133 kN/m² are 5t, 10t and 20t respectively. Note however that the support unit resistances also differ for points on the three curves representing a specific resistance; for example, at a support system average resistance of 33 kN/m², 5t units are used with a spacing of 1m, while 10t and 20t units are used with spacings of 2m and 3m respectively, and at a support system average resistance of 133 kN/m², 20t, 40t and 80t units are used with spacings of 1, 2 and 3m respectively.

Figure 10(b) is an alternative representation of the data used to obtain Figure 10(a), it also shows three curves. These curves indicate trends in hangingwall stability with varying spacing, holding the system average resistance constant on each curve by varying unit resistances.

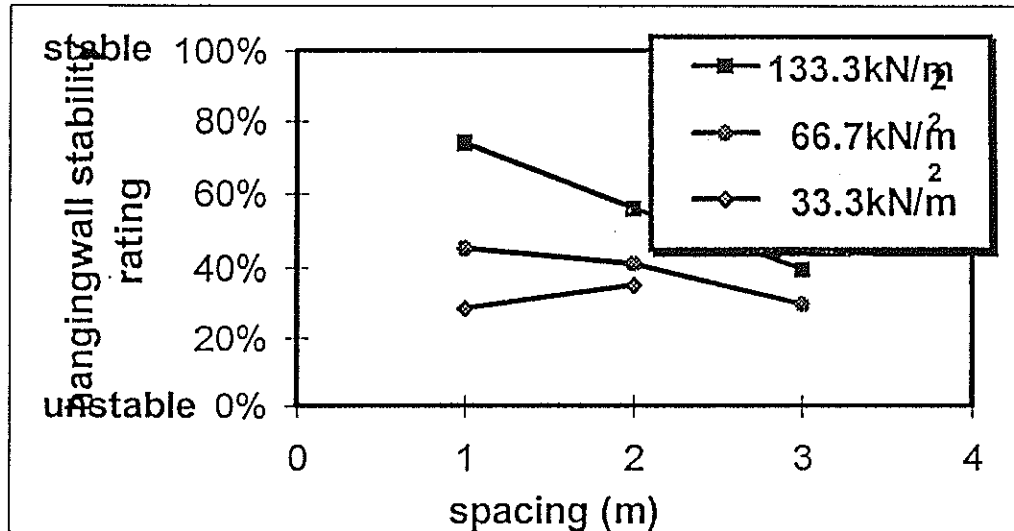


Figure 10(b) Hangingwall stability vs support spacing at different average support resistances (0.5m bedding, back area packs)

The improvement in hangingwall conditions with increasing average support resistance that is observed for the case of supports at a 1m spacing in Figure 10(a) was expected. Of interest is the indication that the rate of improvement rapidly decreases with increasing support spacing. This result is clearly illustrated in Figure 10(b) by comparing the slopes of the three lines in the figure. In the case of a 3m spacing there is no improvement with increasing average resistance, in this case the benefit of additional average resistance is countered by the negative influence of high unit force that tends to destabilise the hanging wall by causing a type of punching mechanism to take place. The influence of this mechanism is also illustrated by the worsening of hangingwall conditions with increasing spacing in Figure 10(b).

#### 2.2.3.2 The use of the trends associated with varying spacing and support force in design.

The following conclusion shows how, at least conceptually, trends such as those indicated above can be used to make adjustments to a support system design. This process only takes into account support system performance under static conditions, and other constraints may become important under dynamic conditions. It is reiterated that, the results of the study are purely qualitative and values used and derived in the examples given below should not be applied in practice without first collecting sufficient data from an underground support monitoring programme and using it to calibrate the results.

The trends show that, if an increase in spacings is desired without changing the hangingwall stability, an increase in average support resistance will be needed, except where punching mechanisms become active. The impact of this is particularly true where the average support resistance required is already high. In other words, if support spacing is increased the capacity of the units required increases by more than the amount simply derived by maintaining average resistance. Conversely, it may be

possible to reduce the support unit force by more than the amount simply derived by maintaining average resistance if support spacing is reduced. The benefit derived from reducing spacing is, however likely to be the better option in improving hangingwall conditions, that is, to reduce the rockfall hazard.

The following example illustrate the concepts, to simplify calculations the trend lines indicated in Figures 10(a) and (b) have been replaced by straight lines in the area of interest.

### Example

#### (a) increasing support spacing

A system with an average support resistance of  $66 \text{ kN/m}^2$  and a support spacing of  $1\text{m}$  is first considered;  $10\text{t}$  units are required to achieve this (the face area considered is  $6\text{m}^2$  and 4 units are used so that a minimum  $2\text{m}$  face to first support distance is maintained, see Appendix A). This system is represented by the point (A,P) in Figure 11(a), where P is the level of hangingwall stability achieved. An increase in support spacing to  $2\text{m}$  is considered. If no increase in support unit resistance is made the average support resistance is reduced to  $33 \text{ kN/m}^2$  (as 2 units are then used), B, and the hangingwall condition is degraded to Q. To maintain the average support resistance at  $66 \text{ kN/m}^2$  requires increasing the support unit resistance to  $20\text{t}$ , this system is represented by the point (A,R), but a deterioration in hangingwall condition still results. To maintaining the hangingwall condition at P the average support resistance must be increased to C, equal to  $99 \text{ kN/m}^2$  using simplified curves (the true value would be obtained from calibrated curves). To achieve this  $15\text{t}$  units would be required.

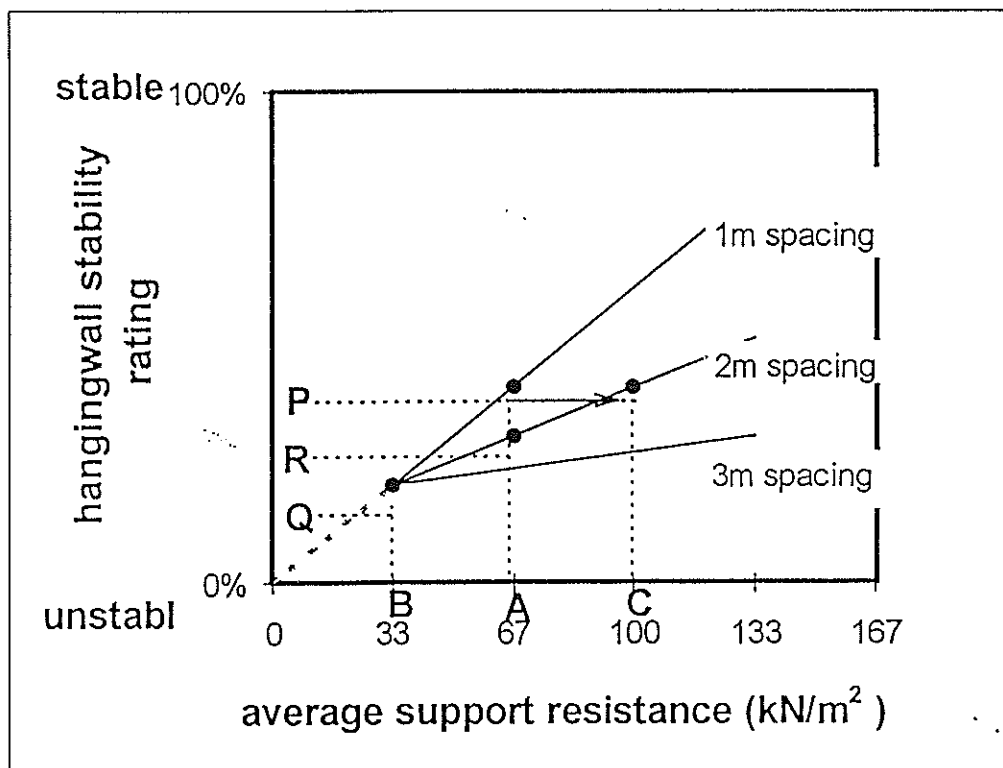


Fig 11(a) Example (a) increasing support spacing

**(b) decreasing support spacing**

A system with an average support resistance of 66 kN/m<sup>2</sup> but with a support spacing of 2m, for which 20t units are required is now considered. This system is represented by the point (A,R) in Figure 11(b). A decrease in support spacing to 1m while maintaining the hangingwall stability rating allows the average support resistance to be reduced to 50 kN/m<sup>2</sup>, the required support unit resistance to achieve this is only 7.5t, this is represented by the point (D,R). Maintaining the support unit force at 20t results in an improvement in hangingwall conditions as is represented by point (A,P).

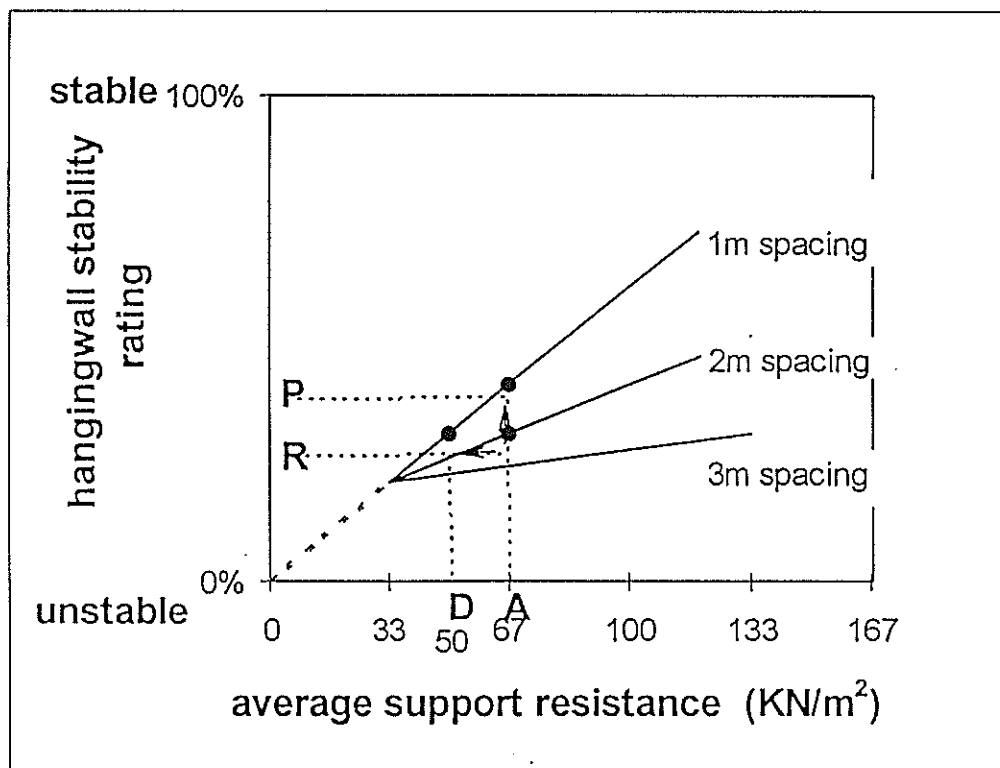


Figure 11(b) Example (b) decreasing support spacing

**2.2.3.3 Taking changes in dip spacing into account**

All modelling was done in two dimensions using a plane strain assumption. This assumption implies that dip spacing of supports is 1m. Trend lines for dip spacings other than 1m could be generated by multiplying support unit resistances by the dip spacing or, alternatively, dividing the system's average resistance by the dip spacing. This procedure relies on an assumption that the mechanisms effecting hangingwall stability are not different for ratios of dip to strike spacing and strike to dip spacing that are equal; this assumption is probably valid only for limited dip spacings greater than 1m and will be determined by the frequency of discontinuities running on or close to strike. Figure 12 shows the trend lines generated for dip spacings of 1.5m and 2m for a strike spacing of 1m.

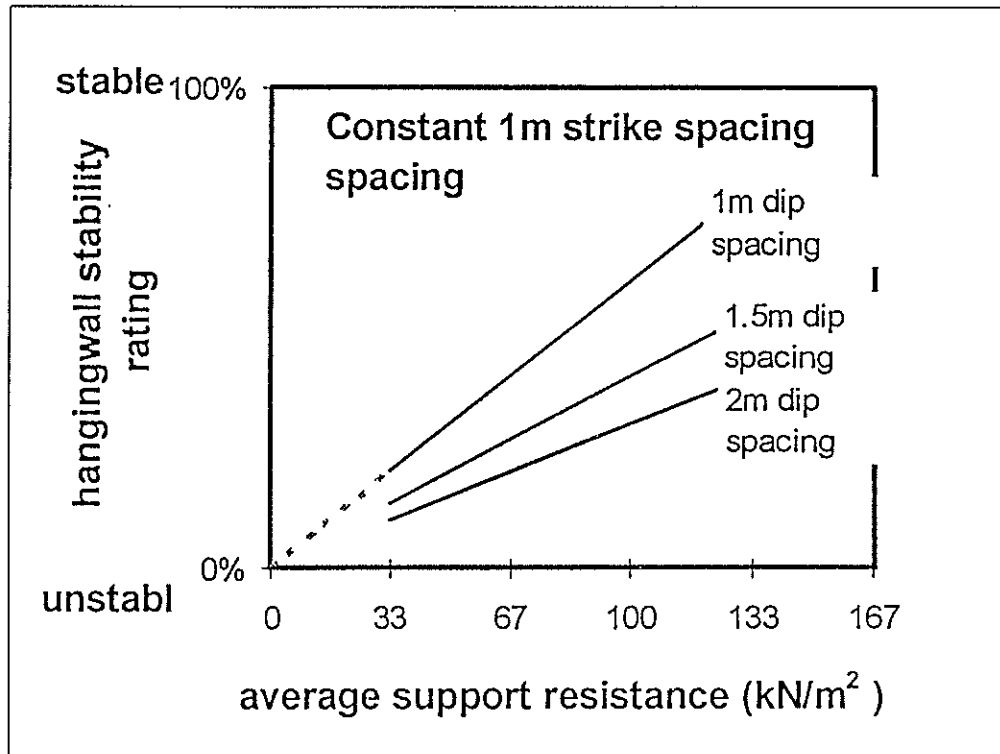


Figure 12 Extending 2D results to consider dip spacing of supports

#### 2.2.3.4 The influence of load spreaders

Figure 13 shows how the use of load spreaders improves hangingwall stability. This result was obtained with the average support resistance held constant at 66 kN/m<sup>2</sup> and spacing held constant at 2m. In this case the detrimental effects of the punching mechanism are present, though not as pronounced as they are for a 3m spacing. A result obtained with a load spreader for a 3m spacing indicate that the relative improvement may be greater in this case but that it is unlikely that hangingwall conditions will improve beyond those achieved with the lesser support spacing.

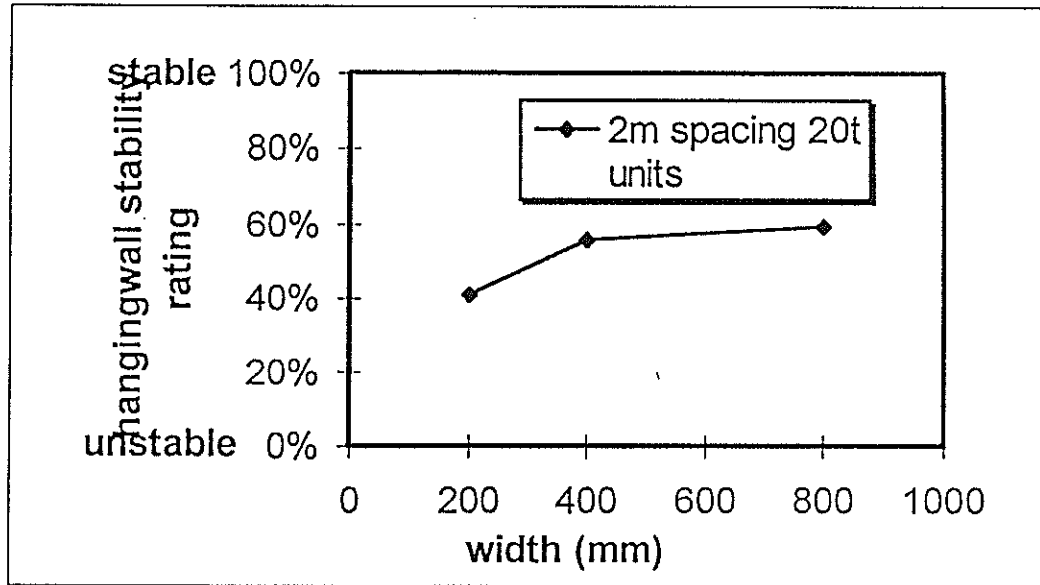


Figure 13 Hangingwall stability vs length of load spreaders  
(0.5m bedding, back area packs)

#### 2.2.3.5 Sensitivity to bedding plane spacing

A similar set of results to those obtained for the case of a half metre bedding thickness was produced for the case of a one metre bedding. Comparison of results was possible by applying a suitable normalising procedure. On the whole the hangingwall stability improves significantly with this doubling of the bedding plane spacing. The influence of changes in support parameters also seem to be less marked. This is illustrated in Figure 14. This would seem to indicate that lower support resistances may be used, however, this trend is not supported by fallout data which appears to show some correlation between the thickness of bedding and fallouts. Further work is required to obtain a full picture of the trends in hangingwall stability

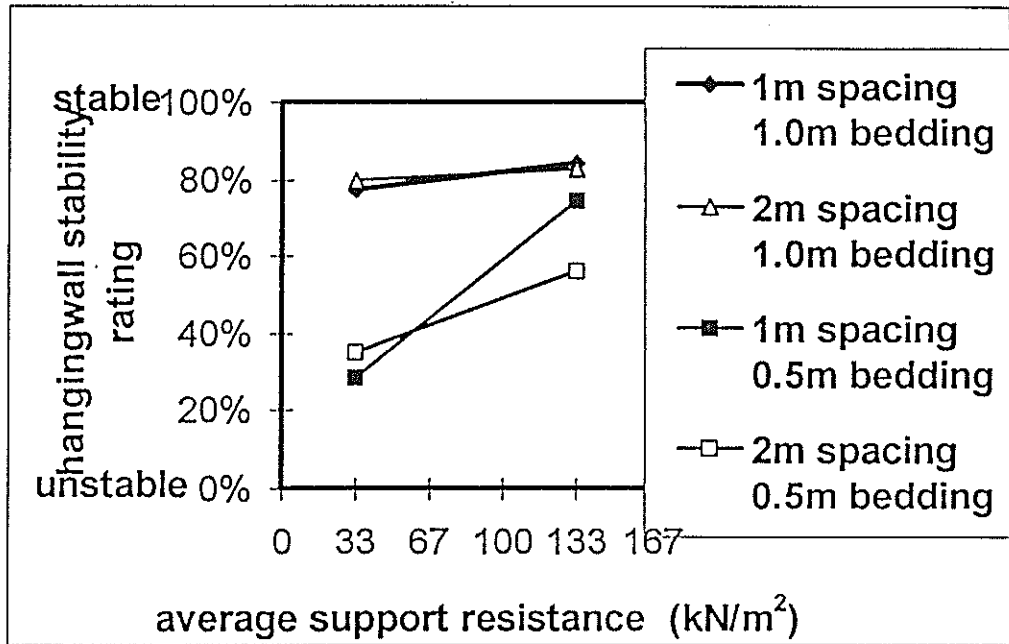


Figure 14 Hangingwall stability vs average support resistance for support spacings of 1m and 2m with different bedding thicknesses

#### 2.2.3.6 The influence of back area support

In the above examples 1.1m square Mat packs at 3m centres were used as back area support (the pack resistance used in the model has been adjusted to take into account a 3m dip spacing). A second set of results was generated using the model with a half metre bedding spacing, in this analysis the back area support system used represented a 46% porosity backfill. A significant improvement in hangingwall conditions was obtained, however, the modelling method used to represent the backfill will tend to exaggerate the influence of the backfill on the face area as the lack of confinement along the face of the backfill is not taken into account. This result is illustrated in Figure 15.



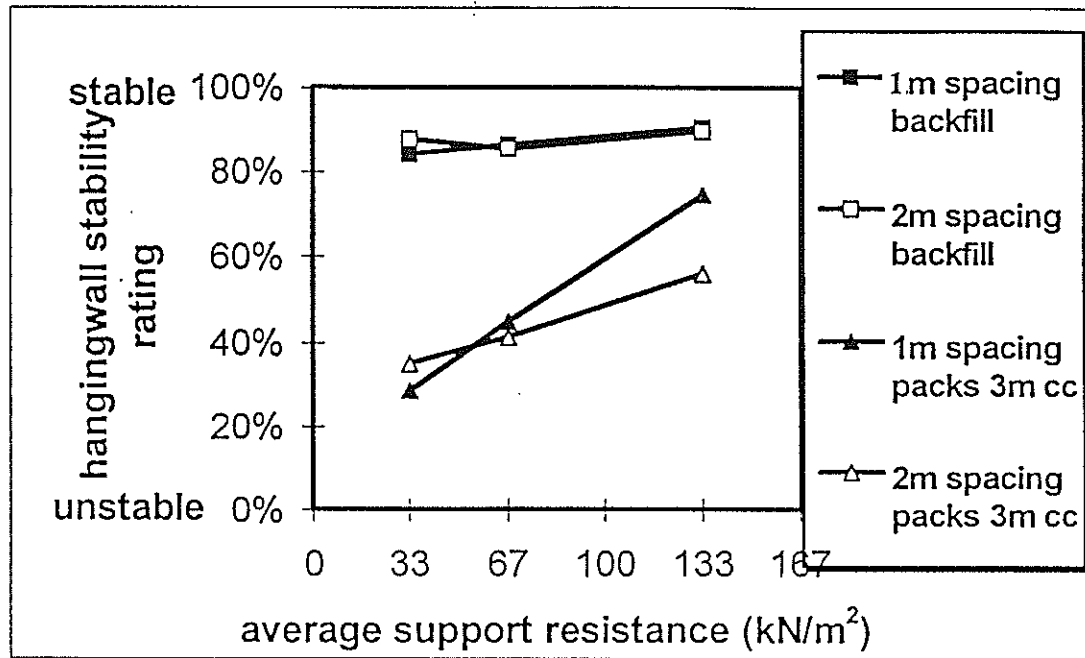


Figure 15 Hangingwall stability vs average support resistance for spacings of 1m and 2m and different types of back area support (0.5m bedding)

#### 2.2.3.7 Rationale for determining support spacing

The trends established provide some rationale for selecting a support system, but are not as yet sufficient to establish a complete design procedure for determining support spacing. In particular, validated quantitative results are required before the results can be used in such a procedure. The work provides a starting point from which to design and initiate a programme of underground monitoring that will provide the data needed to calibrate models and hence provide the necessary quantitative dimension to the results. An acceptable method of assessing hangingwall stability needs to be developed to include in such a programme.

### 2.3 Stope support design methodology for rockfall and rockburst conditions

The support system reacts to the influence of the rock mass behaviour in the stope both under static and dynamic loading. With respect to the control of rockfalls, the support resistance requirement needs to be at least equalled by the support resistance designed into the support system. With respect to dynamic loading of support systems that occurs in some rockbursts, the energy absorption requirement needs to be compared to the ability of the support system to absorb the required energy.

### 2.3.1 The evaluation of the support resistance and energy absorption ability of various support systems

The support resistance of a support system is defined as the force applied by the support system per square metre of hangingwall and is typically represented as  $\text{kN/m}^2$  or as  $\text{kPa}$ . The support resistance will depend upon the force - deformation behaviour of individual support units, their spacing and the amount of stope closure that has acted on the support system. Support resistance - deformation curves for any support system can readily be determined and a number of support systems can be plotted in this way for purposes of comparison.

The determination of the ability of a stope support system to absorb energy with the objective of reducing rockburst damage is not simple since it depends on a number of variables, the most important of which is the ability of the support system to yield during rapid deformation and so absorb energy. It is also necessary to have a good estimate of the normal slope closure rate that would occur prior to any dynamic closure. Other variables which effect the ability of stope support systems to absorb energy are the spacing of the support units and the velocity of the dynamic stope closure.

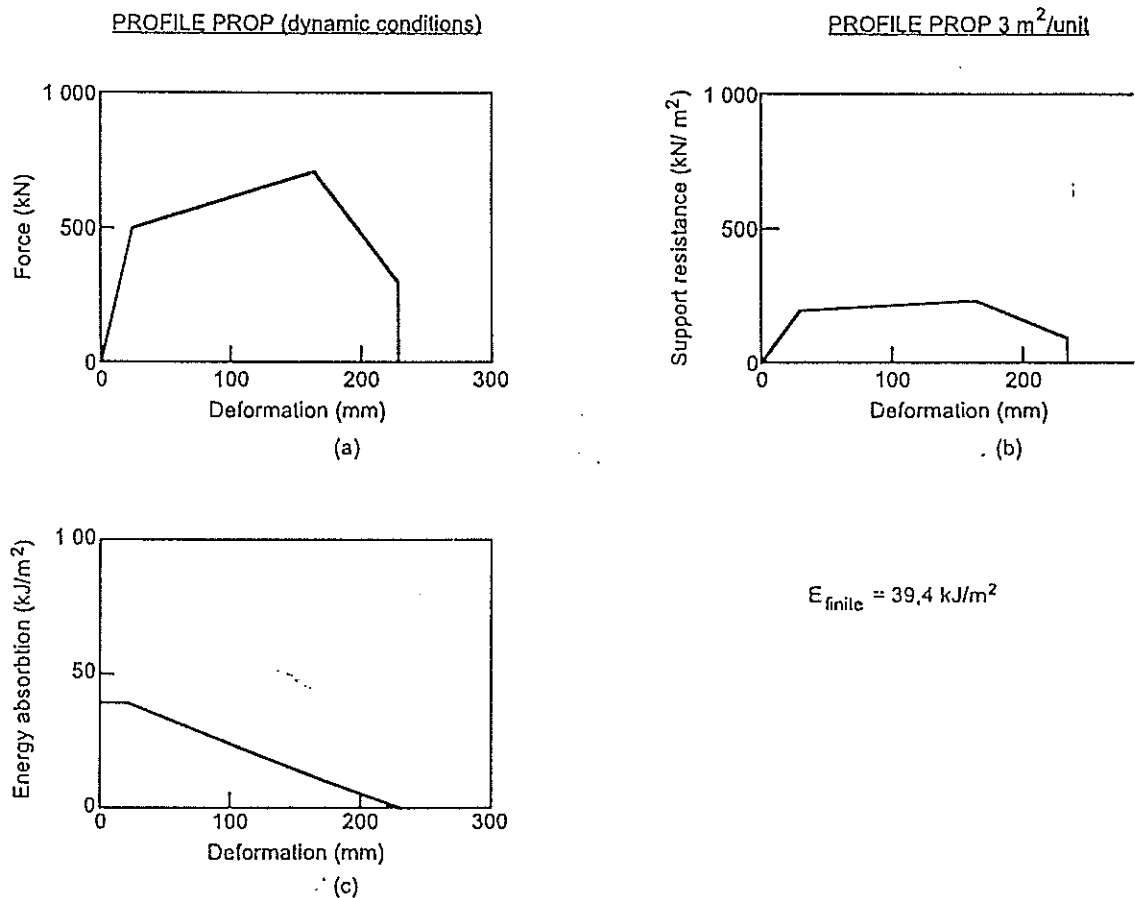


Figure 16 The force - deformation, support resistance - deformation and energy absorption - deformation behaviour of profile props.

Consider Figure 16 in which Figure 16(a) shows the force - deformation curve of a profile prop for a closure rate of 3 m/s. A support system made up of profile props can best be represented as a support resistance - deformation curve, as shown in Figure 16(b), the support force has been divided by the number of square metres per unit (in this case 3 m<sup>2</sup> per unit) in order to determine the values for the support resistance axis. Figure 16(b) shows how the support resistance of this profile prop support system changes with deformation. The area under the curve represents the energy absorption ability of the support system in terms of kJ/ m<sup>2</sup> which in this case is 40 kJ/ m<sup>2</sup>. This represents the finite amount of energy ( $E_{finite}$ ) that can be absorbed during deformation by the support system per square metre of hangingwall. If Figure 16(c) is considered where the energy absorbing ability of the support system is plotted against deformation then it can be seen that this finite amount of energy ( $E_{finite} = 40 \text{ kJ/ m}^2$ ) plots on the y - axis. However, as deformation occurs the amount of energy ( $E_{available}$ ) that the support system can absorb decreases with increasing deformation. The absolute amount of normal stope closure that occurs prior to any dynamic closure increases from the stope face towards the back areas and by implication the ability of the stope support system to absorb energy during dynamic closure reduces from the face towards the back areas. The following general equation illustrates the process that was used to assess a profile prop support system as in Figure 16(c).

$$E_{available} = E_{finite} - E_{stope\ closure}$$

Where;  $E_{finite}$  is the amount of energy available to be absorbed by the support system prior to any stope closure.

$E_{available}$  is the available energy that can be absorbed by the support system, during a rockburst for example taking into account previous stope closure.

and  $E_{stope\ closure}$  is the energy absorbed by normal stope closure prior to a rockburst.

This may be shown graphically as in Figure 17 below.

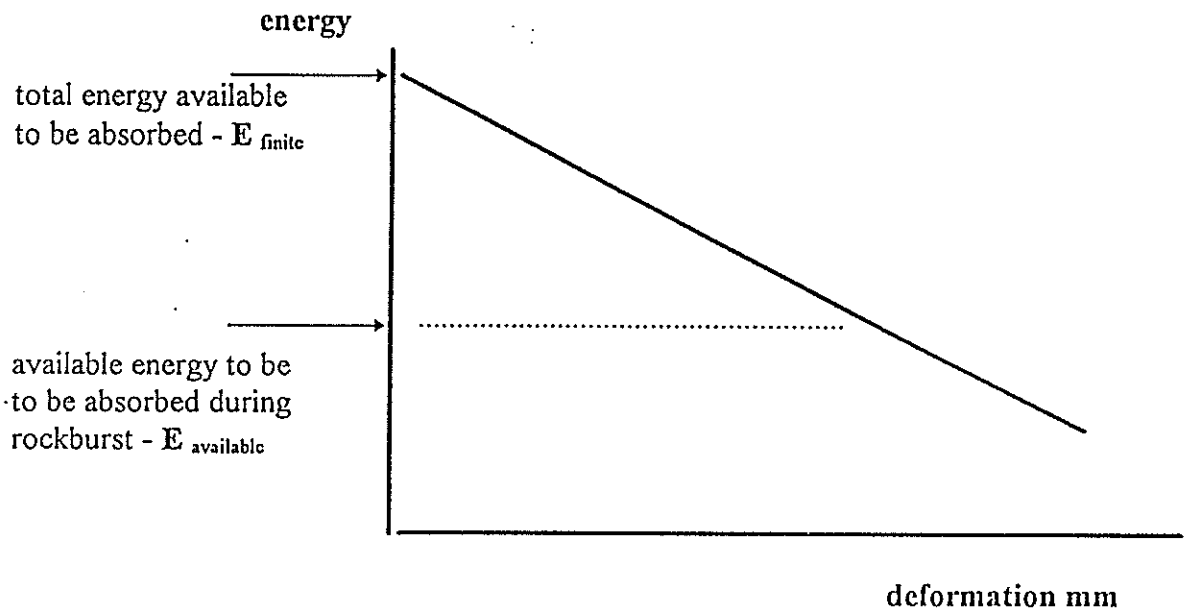


**Figure 17 Energy - deformation curve showing the decrease in energy absorption ability with increasing deformation.**

Most support units and support systems have a finite amount of energy that can be absorbed during deformation, the main exception being backfill. Pack support systems are often portrayed as having a continuing increasing support resistance and consequent energy absorption ability, with increasing deformation. However for the purpose of this analysis it is assumed that the energy absorption ability of pack support systems is limited to 50% deformation. Some pack types, notably composite packs, RSS grout packs and grout based timber packs clearly do lose structural integrity after large deformations and in some timber packs structural integrity can also become questionable at this amount of deformation.

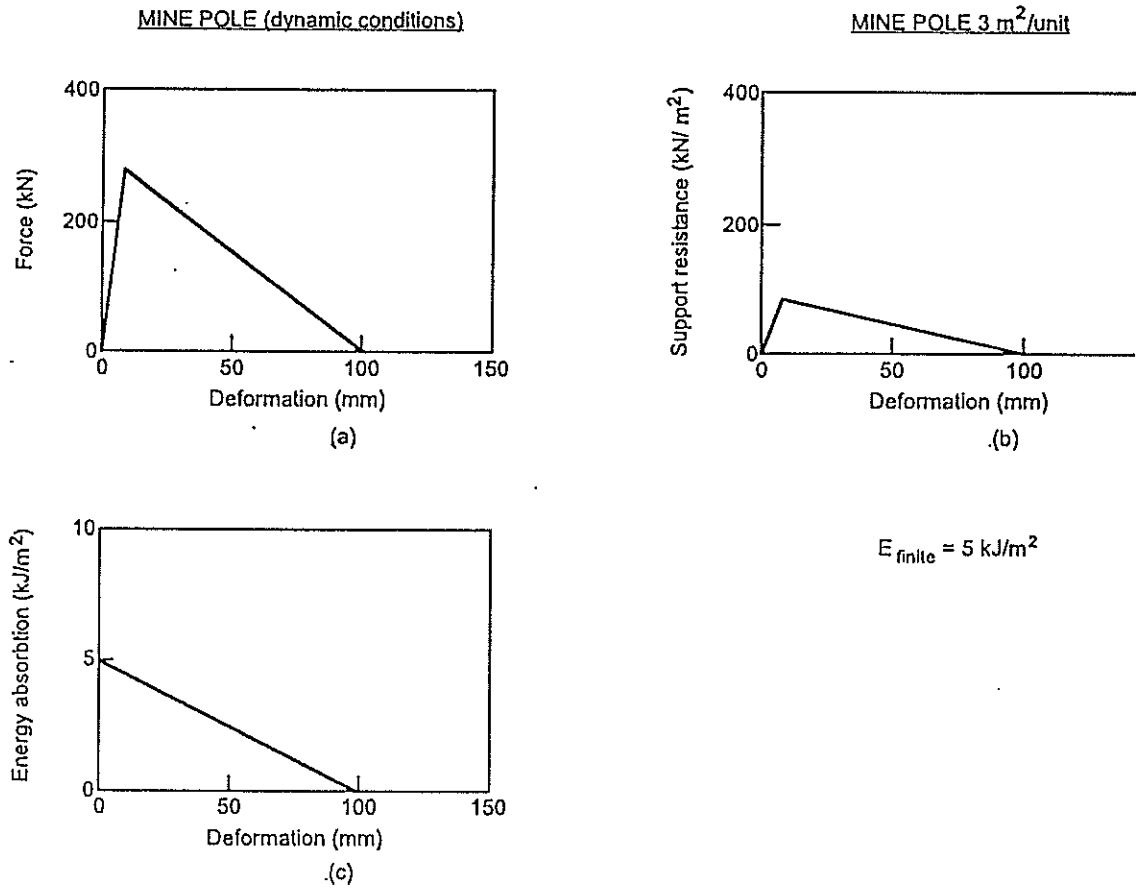


Figure 18 The force - deformation, support resistance - deformation and energy absorption - deformation behaviour of mine poles.

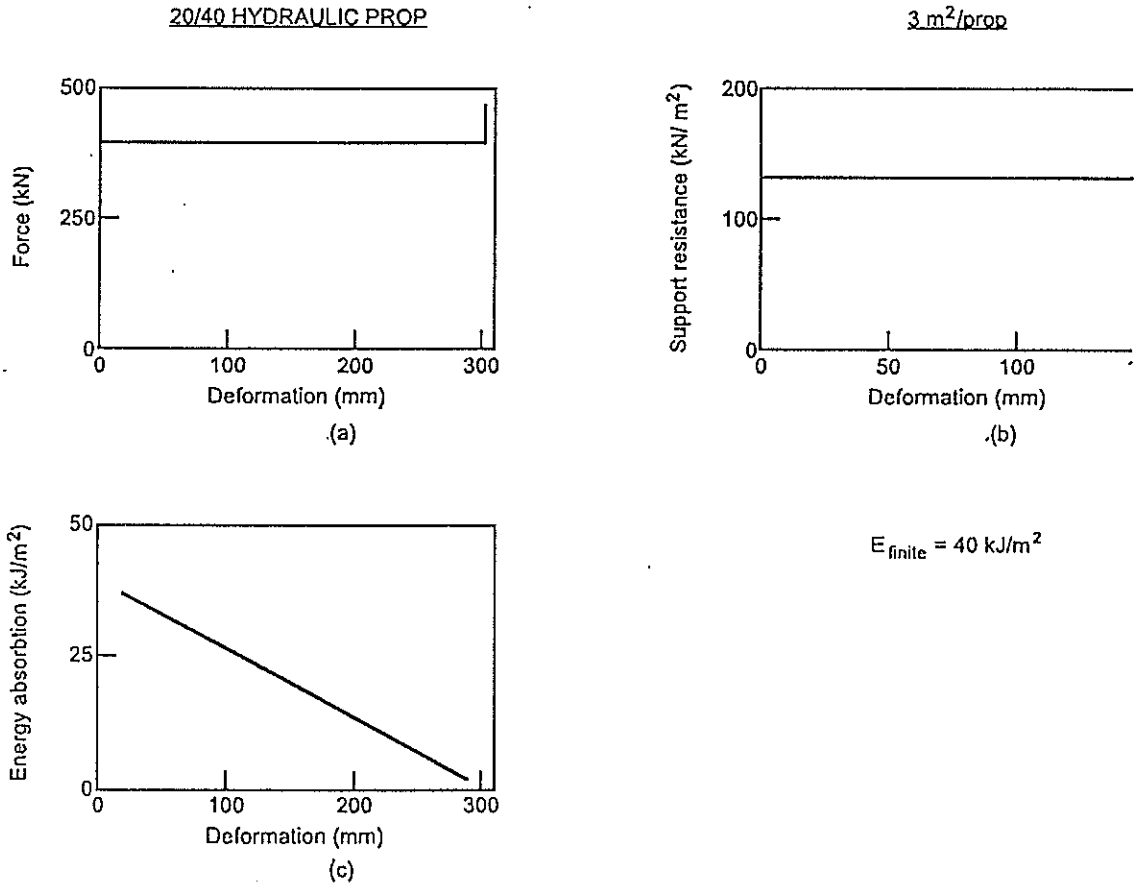


Figure 19 The force - deformation, support resistance - deformation and energy absorption - deformation behaviour of hydraulic props.

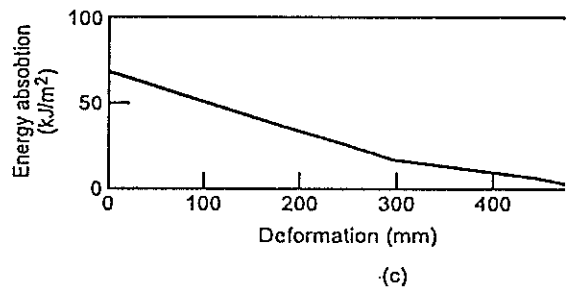
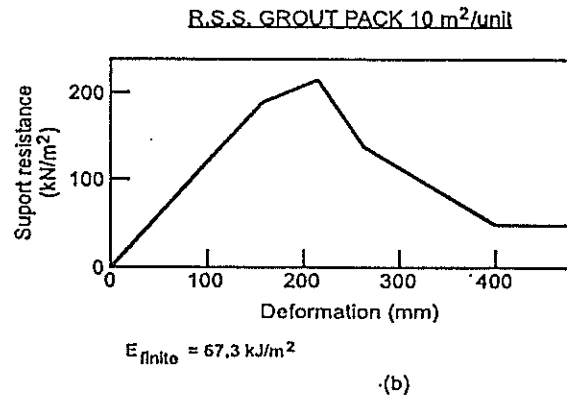
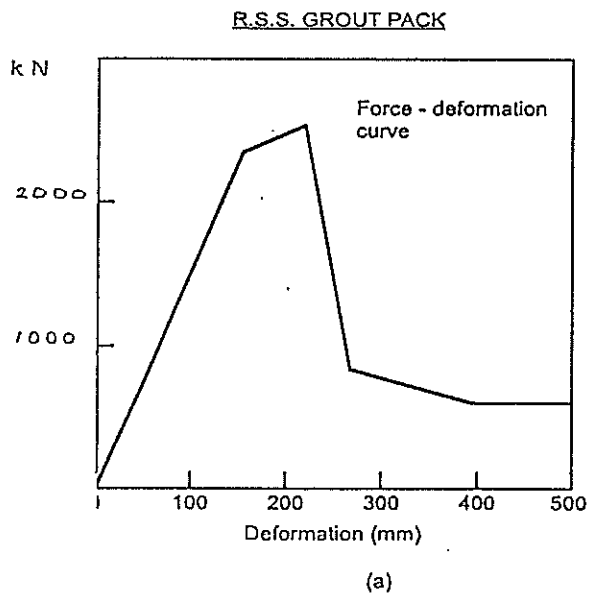


Figure 20 The force - deformation, support resistance - deformation and energy absorption - deformation behaviour of RSS grout packs.

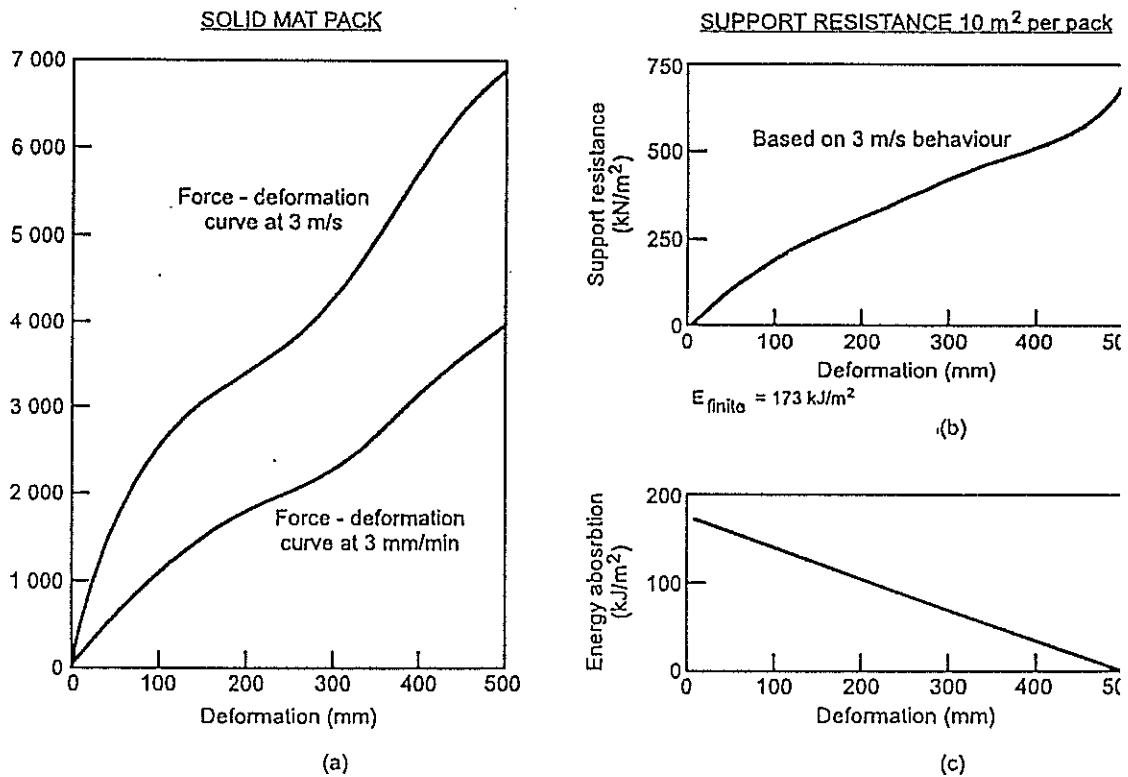


Figure 21 The force - deformation, support resistance - deformation and energy absorption - deformation behaviour of timber packs.

Similarly to Figure 16(a) Figures 18(a), 19(a), 20(a) and 21(a) show the force - deformation curves of a mine pole, a hydraulic prop, an RSS grout pack and a timber pack respectively. Similarly Figures 18(b and c), 19(b and c), 20(b and c) and 21(b and c) show support resistance - deformation curves and energy absorption - deformation curves for a mine pole support system, a hydraulic prop support system, an RSS grout pack support system and a timber pack support system respectively. The ability of these support systems to absorb energy will be influenced by the amount that the available energy absorption ability of the support system is degraded by the normal stope closure that occurs between installation of the units and the time the rockburst closure occurs. The determination of the energy absorption capability of a support system is of great importance because should a rockburst occur it's the  $E_{available}$  that is required to reduce rockburst damage.

### 2.3.1.1 Methodology for testing support resistance - deformation curves of support systems against support resistance criteria for different reefs

Any support units installed in a stope are immediately acted upon by stope closure which can be up to 50 mm/day. Depending on the force - deformation characteristics of the support unit this closure could either degrade its ability to generate load or increase its ability to generate load. In order to take this into account it is necessary to



represent a support system as a number of support resistance - deformation curves which are functions of stope closure and of the distance behind the stope face.

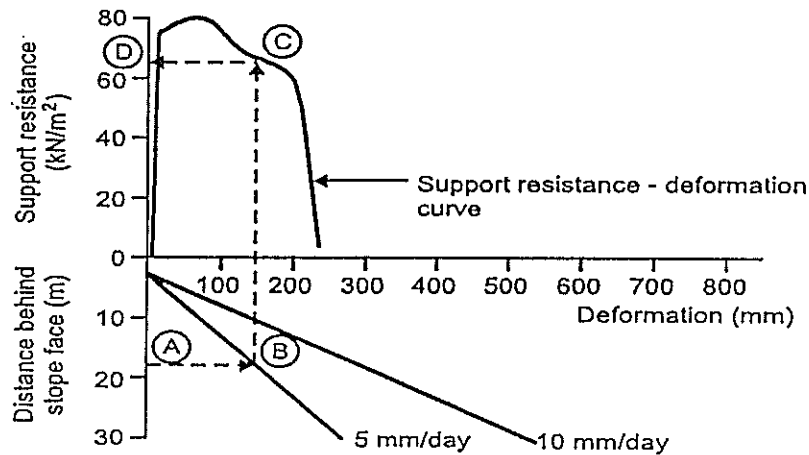
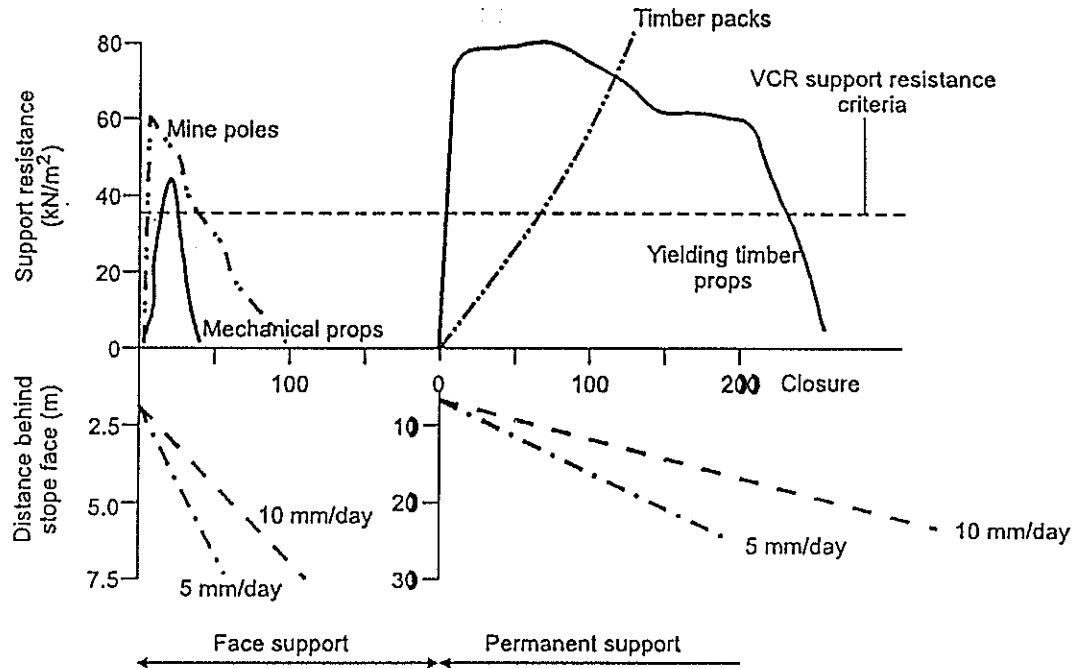


Figure 22 A support resistance - deformation curve which is a function of stope closure and of the distance behind the stope face.

Figure 22 illustrates how these graphical representations may be used to determine the support resistance for any distance behind the stope face and for any closure rate. Consider point A some distance behind the stope face, a horizontal line is traced until it intersects with the line representing the stopes closure rate, Point B. From B a vertical line is traced to point C on the support resistance - deformation curve of the support system. From C a horizontal line is traced back to the x - axis to D where the support resistance of that particular support system for the specific closure rate can be determined for those graphs. The support is assumed to have been initially installed 3,0 m from the stope face and the stoping is on a two day cycle.



**Figure 23** The support resistance - deformation curves of various support systems as a function of stope closure and of the distance behind the stope face for both the face and permanent support areas.

This graphical representation may be further extended by separating the face and permanent support areas and plotting the support resistance - deformation curves of the support systems used in both the face and permanent support areas. This is shown in Figure 23 where a mine pole support system and a mechanical prop support system are shown in the face area for comparison. In the permanent support area a timber pack support system is compared with a yielding timber prop support system. This allows the support resistance of a specific support system to be tested against the support resistance requirement of a particular reef as determined in section 1.1 is reproduced here for convenience.

Reef	95% fallout frequency	Support resistance criteria $\text{kN/m}^2$
Vaal reef	1,2 m	33 $\text{kN/m}^2$
Ventersdorp Contact reef	1,4 m	38 $\text{kN/m}^2$
Carbon Leader reef	1,0 m	28 $\text{kN/m}^2$

From above, in order to prevent 95% of rockfalls on the Ventersdorp Contact reef the support resistance requirement would have to be 38  $\text{kN/m}^2$  or greater.

This criteria is shown on Figure 23 and it is significant that some of the support systems shown fail to meet this criteria under certain conditions. For example, for a closure rate of 10 mm/day the mine pole support system will fail to meet this support resistance criteria once it is 4,0 m or more behind the stope face. For a closure rate of 5 mm/day the equivalent distance is 6,5 m. The mechanical prop support system will

fail to meet this criteria 3,5 m ad 4,5 m behind the stope for a closure rate of 10 mm/day and 5 mm/day respectively.

These support systems can be evaluated for different reefs with different support resistance criteria.

### 2.3.2.1 Methodology for testing the energy absorbing ability of support systems against the energy absorption criteria for different reefs

The development of a methodology for evaluating the energy absorbing ability of support systems with respect to the energy absorption criteria for different reefs will allow existing support systems to be evaluated or will allows support systems to be designed so that it will meet the required energy absorption criteria. These energy absorption criteria for the Vaal reef, Ventersdorp Contact reef and Carbon Leader reef were derived in section 1.2 and are reproduced below for convenience.

Reef	Energy absorption requirement or $E_{ac}$
Vaal reef	18 kJ/m <sup>2</sup>
Ventersdorp Contact reef	32 kJ/m <sup>2</sup>
Carbon Leader reef	38 kJ/m <sup>2</sup>

The ability of support systems to meet these criteria is therefore the test when evaluating or designing a support system to be used on any of the above reefs. Most support units and support systems have a finite amount of energy that can be absorbed during deformation, A profile prop support system, spaced at 3m<sup>2</sup> per prop for example can absorb 40 kJ/m<sup>2</sup> of energy before failure, similarly a hydraulic prop support system at a similar spacing is able to absorb 47 kJ/m<sup>2</sup> of energy before failure. The determination of the amount of energy that a support system can absorb can be evaluated using a similar process as described in section 2.3.1.1

Any support units installed in a stope are acted upon by stope closure which can be up to 50 mm/day. Depending on the yieldability of the support units making up the support system this closure degrades the support systems' ability to absorb energy. In order to evaluate this it is necessary to represent a support system as shown in **Figure 17** in section 2.3.1 but it is also necessary to consider the decrease in the ability of the support system to absorb energy as a function of stope closure and of the distance behind the stope face.

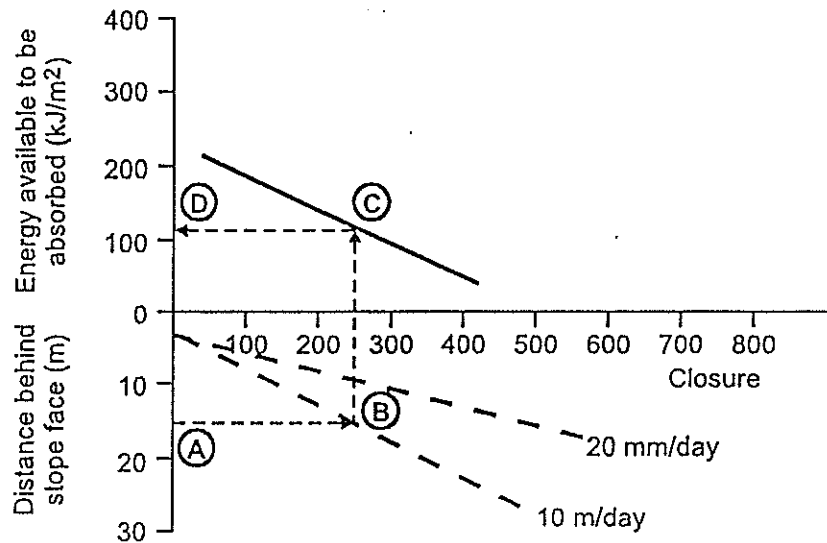


**Figure 24** An energy absorption - deformation curve which is a function of slope closure and of the distance behind the slope face.

Figure 24 illustrates how this graphical representation may be used to determine the energy that can be absorbed ( $E_{\text{available}}$ ) for any distance behind the slope face and for any closure rate in the following way.

Consider point A in Figure 24 some distance behind the slope face, a horizontal line is traced until it intersects with the line representing the slopes closure rate, Point B. From B a vertical line is traced to point C on the energy - deformation curve of the support system. From C a horizontal line is traced back to the x - axis to D where the energy that can be absorbed ( $E_{\text{available}}$ ) can be determined for that particular support system and for that specific closure rate. The support is assumed to have been initially installed 3,0 m from the slope face and the stoping is on a two day cycle.

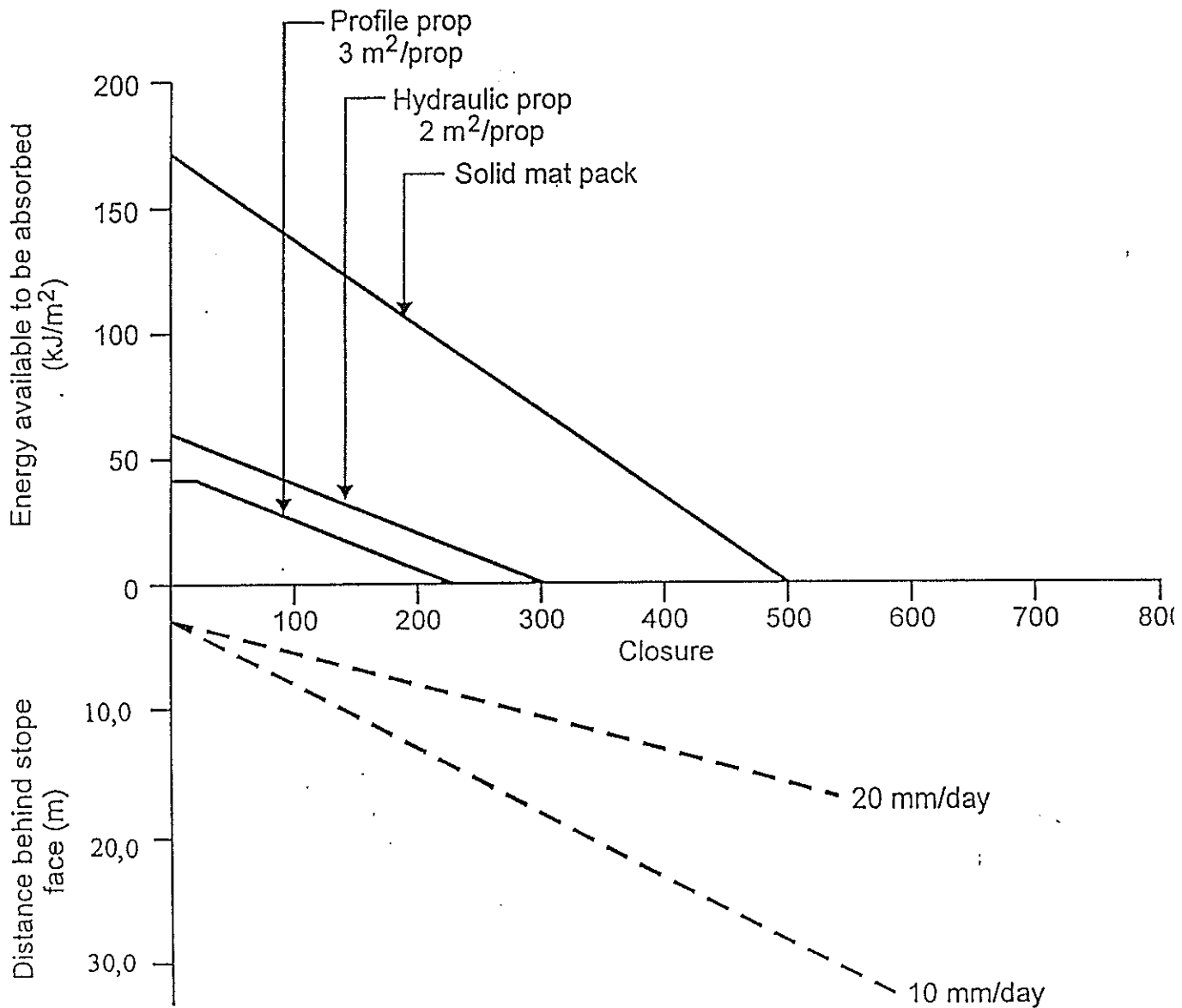


**Figure 25** An energy absorption - deformation curve which is a function of stope closure and of the distance behind the stope face for various support systems.

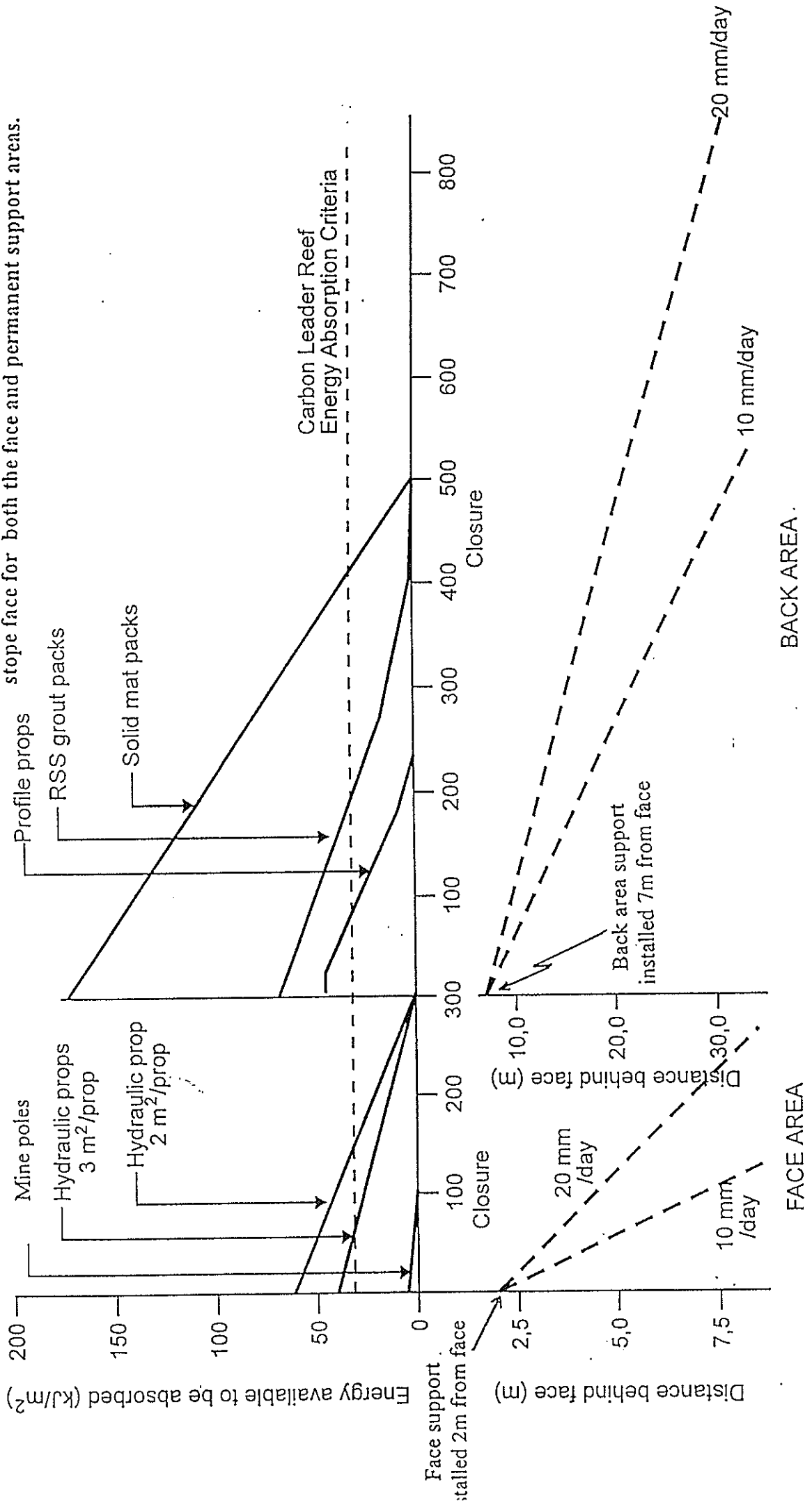
Figure 25 shows some typical support systems made up of timber packs, hydraulic props and profile props plotted in the way described above.

This graphical representation may be further extended by separating the face and permanent support areas and plotting the energy - deformation curves of the support systems used in both the face and permanent support areas.

This is shown in Figure 26 where a mine pole support system and a hydraulic support system are shown in the face area for comparison. In the permanent support area a timber pack support system is compared with a profile support system and with a RSS grout pack support system.

If the energy absorption requirement for the Vaal reef, the Ventersdorp Contact reef and the Carbon Leader reef is plotted on Figure 26 then support systems can be evaluated or designed to ensure that the required energy absorption criteria is met, both in the stope face and in the permanent support area. This would be evaluated by using the A to B to C to D technique described above.

Figure 26 The energy absorption-deformation curves of various support systems as a function of stope closure and of the distance behind the stope face for both the face and permanent support areas.



Below are some of the support characteristics of support units constituting common support systems.  $E_{finite} / m^2$  has been determined on the basis of typical support spacing used in the industry, for support under dynamic loading.

Units	Force	Yielding range	Spacing	$E_{finite} / m^2$
Mine Poles	300kN	0,1m	2m <sup>2</sup> unit	= 7,5 kJ/m <sup>2</sup>
Mechanical Props	120kN	0,05m	2m <sup>2</sup> unit	= 3 kJ/m <sup>2</sup>
Hydraulic Props	400kN	0,30m	2m <sup>2</sup> unit	= 60 kJ/m <sup>2</sup>
Profile props	500kN	0,250m	2m <sup>2</sup> unit	= 62,5 kJ/m <sup>2</sup>
Packs	4000kN	0,500m	10m <sup>2</sup> unit	= 175 kJ/m <sup>2</sup>
RSS grout packs	2000kN	0,40m	10m <sup>2</sup> unit	= 50 kJ/m <sup>2</sup>

### 3. The support of stope gullies

The support of stope gullies was addressed in two ways, firstly the problem of gully pack stability and foundation stability was investigated by underground monitoring. This resulted in an understanding of the force - deformation behaviour of gully packs with time and stope closure and led to a recommendation with respect to a suitable force - deformation curve for gully packs.

The second area of investigation was the determination of gully hangingwall fallout thicknesses between the gully packs in order to evaluate the support resistance requirements to prevent rockfalls and the energy absorption requirements in order to reduce rockburst damage. The investigation concentrated on the Vaal reef, the Ventersdorp Contact reef and the Carbon leader reef. Appendix 2 gives a comprehensive record of this research. The section below shows pertinent results from this research and gives gully support guidelines for the Vaal reef, the Ventersdorp Contact reef and the Carbon Leader reef.

The need for this area of research is demonstrated by the incidence of accidents which occur in stope gullies and the observation that a large number of gully packs are undermined by the collapse of the underlying gully sidewall. Accident data from 1991 and 1992 show that stope gullies account for the second highest incidence of in-stope fatalities after the stope face (Figure 27).

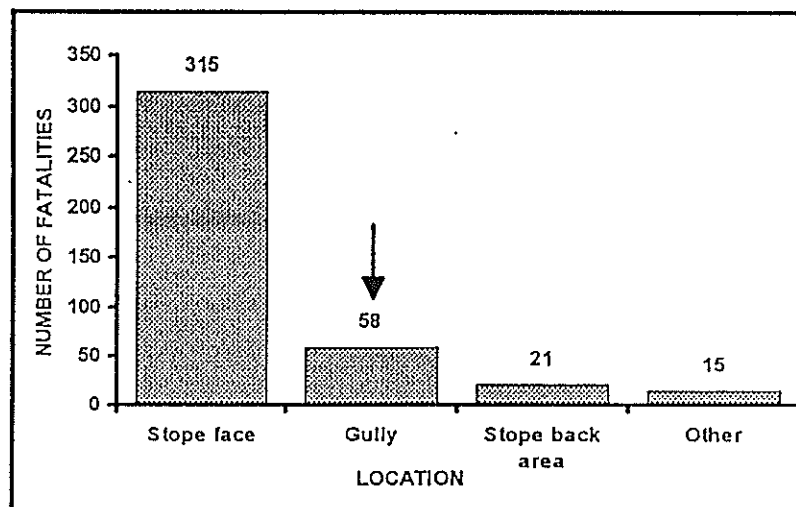


Figure 27 Distribution of in-stope rock related fatalities for all mining districts during 1991 and 1992

### 3.1 The determination of a gully specific pack support system

#### 3.1.1 In situ gully pack monitoring

Monitoring of gully packs has been undertaken at sites on Hartebeestfontein Gold Mine, Western Deep Levels South Mine and Western Holdings Gold Mine. At each underground monitoring site a series of three gully packs which were in standard use on the mine were installed and instrumented as part of the normal mining sequence of a gully and panel. The instrumentation consisted of four flat pressure load-cells sandwiched between two 10 mm thick steel plates which were built into each pack during its construction. After pack construction was complete pegs were installed into the hangingwall and footwall at each corner of the pack to enable stope closure to be measured and therefore the pack deformation. Figure 28 shows some of the results from Western Deep Levels which are typical of many of the results obtained and shown in Appendix 2.

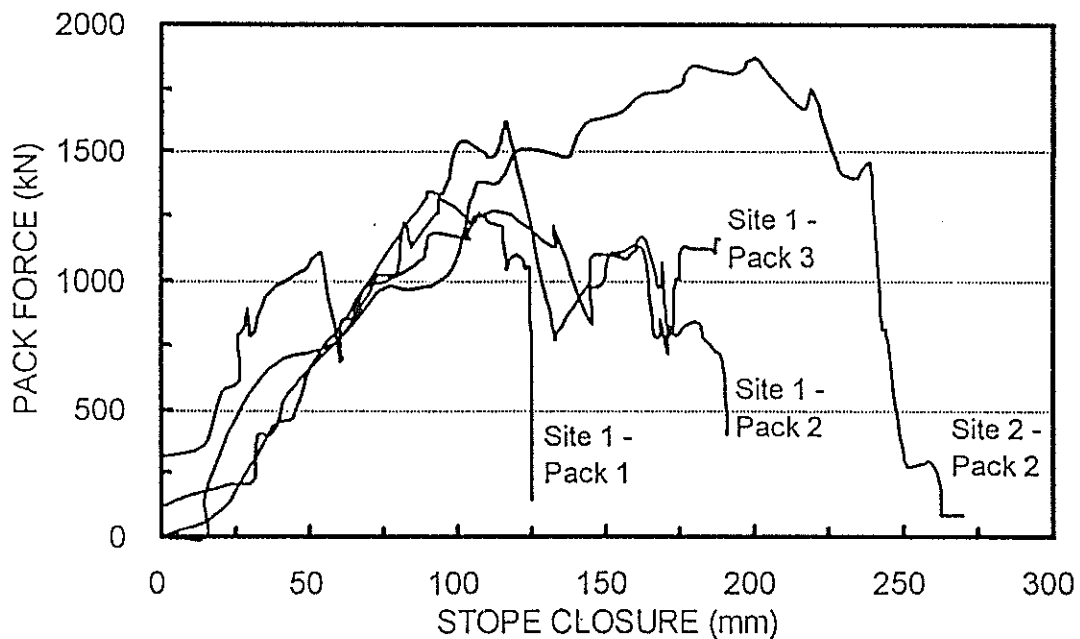


Figure 28 Pack force-deformation behaviour at Western Deep Levels South, Sites 1 and 2

From these graphs it can be seen that pack forces of between 1250 kN and 1600 kN are reached after stope closure of about 110 mm. After these forces are reached, there is a levelling off and even a drop in force with increasing time and closure. This levelling or dropping off of load is accompanied by gully sidewall convergence. The large drops in pack force are associated with the mining of the gully past the packs.

#### 3.1.2 Proposed yielding gully pack

The results presented in Figure 28 indicate that damage to the gully sidewall under gully packs occurs at pack loads near or below 2000 kN. Even though the packs are capable of sustaining higher loads their potential is not realised and could be detrimental to the situation. It is therefore proposed that gully packs be designed to yield below 2000 kN preferably at 1000 kN which forms the lower limit of "failure



load” in the majority of cases. **Figure 29** shows the force - deformation curve of such a proposed gully pack with a yield load of 1000 kN.

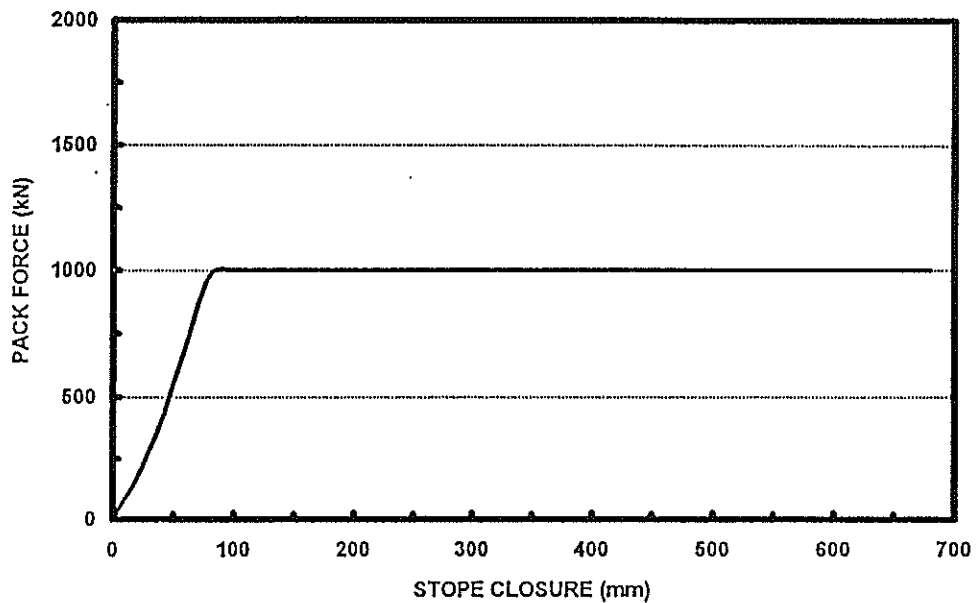


**Figure 29** Graph showing proposed gully pack 1000 kN yielding behaviour

In order to test the validity of the above proposal, Grinaker was asked to develop a variation of their 90 x 120 cm “hollow” construction Duraset (reinforced foamed concrete) packs (**Figure 30**) that would yield at 1000 kN. The laboratory determined load-deformation behaviour of one these customised packs is reproduced in **Figure 31**.

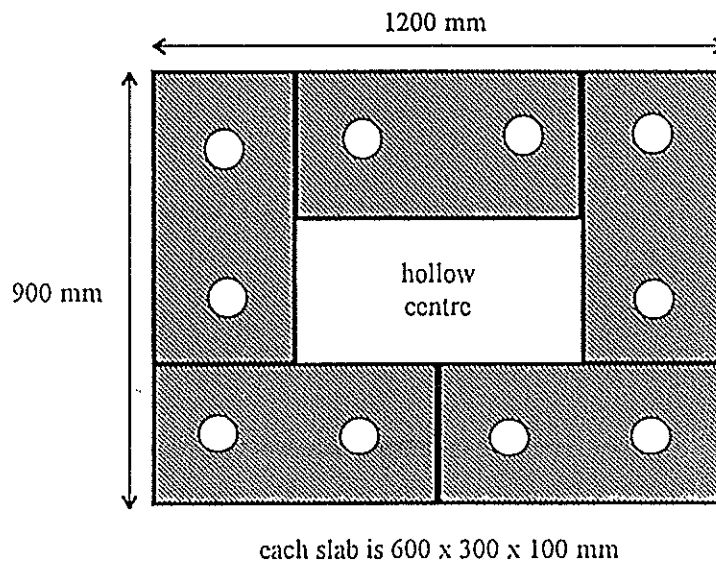


**Figure 30** Schematic of trial 1000 kN yielding Duraset pack construction

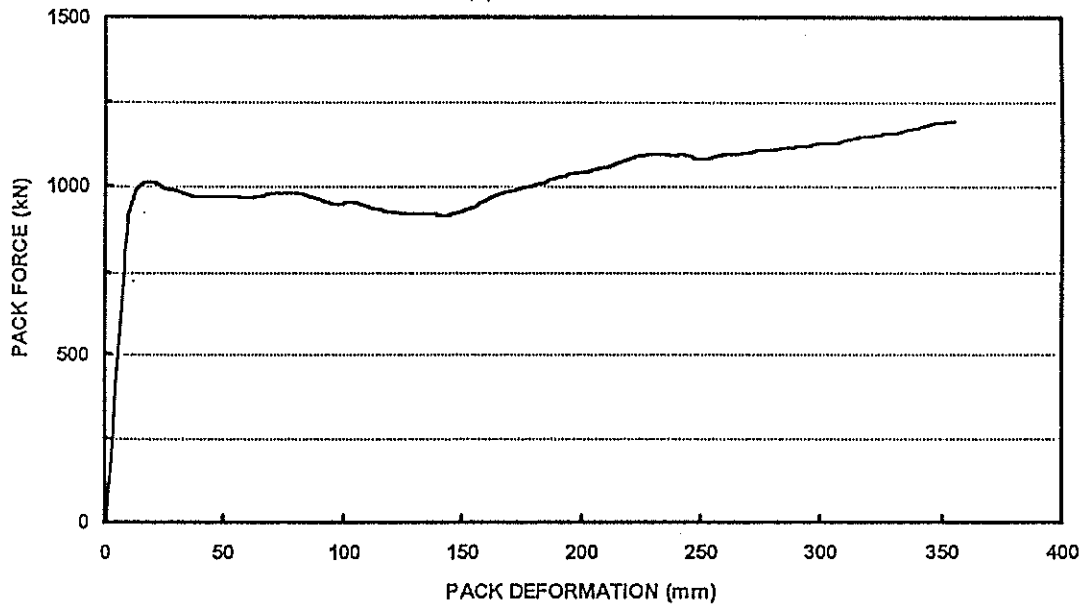


Figure 31 Laboratory curve obtained for a 1,3 m high, 1000 kN yielding Duraset pack

Three trial packs with a design yield of 1000 kN were installed at Western Deep Levels South Mine in the 87-49 VCR stope, W1 panel at a depth below surface of 2691 m. These packs and the associated stope and gully closures were monitored for about 100 days in conjunction with the gully displacement of some adjacent 'mine standard' timber packs as a means of assessing the success of the trial packs in reducing gully sidewall damage. The results are shown in Appendix 2.

### 3.2 Numerical modelling of gully pack behaviour.

Numerical modelling was carried out to investigate possible reasons for the observed and measured *in situ* behaviour of gully packs and gully sidewall (6) and to predict the behaviour of the proposed gully pack support. Both FLAC and UDEC were used and the results are shown in Appendix 2.

### 3.3 Gully support requirements

In addition to providing support along the sides of the gullies by means of gully packs, support needs to be considered for the exposed section of gully hangingwall which is not directly supported by the two rows of gully packs. It is therefore necessary to be able to design support systems to function in this region of stope gullies.

To do this it is first necessary to determine the support requirements that must be met and this in turn depends on knowing the thicknesses (heights) of fallouts which have to be prevented. One source of data for fallout dimensions is the GME's fatal accident investigation files. However, due to the relatively small dataset for accidents occurring between the rows of gully packs, the analysis of the GME's fatal accident records has only been able to provide limited information with respect to the thicknesses of

fallouts. This problem becomes especially evident when the data is broken down on the basis of reef type or mining district.

In order to address this deficiency, a programme of underground measurements was undertaken to determine fallout thicknesses in a series of representative gullies located on the three major reef horizons, namely Ventersdorp Contact reef, Carbon Leader reef and Vaal reef. In each case a cumulative frequency distribution is plotted and fallout thicknesses determined for various percentage limits. This data was then used to calculate the support resistance requirement for static conditions and an energy absorption requirement for rockburst conditions.

### 3.3.1 Fallout thickness distributions

The graphs of cumulative percentage fallouts measured in gullies on the VCR, Carbon Leader Reef and Vaal Reef are given in Figures 32, 33 and 34, respectively. These graphs are based on 416 measurements on the VCR, 538 measurements on the Carbon Leader and 433 measurements on the Vaal Reef. A total of 27 gullies were surveyed, on a number of mines and at a variety of depths.

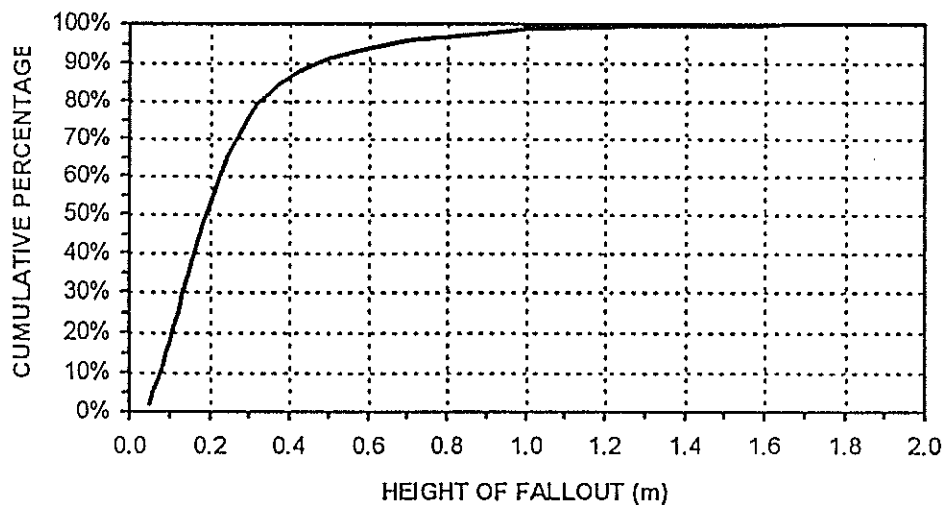


Figure 32 Distribution of fallouts in sampled Ventersdorp Contact Reef (VCR) gullies

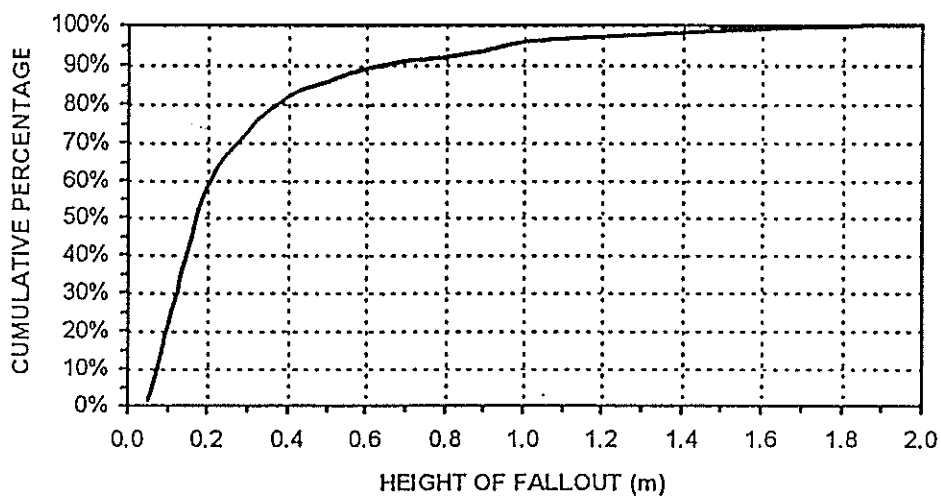


Figure 33 Distribution of fallouts in sampled Carbon Leader Reef gullies

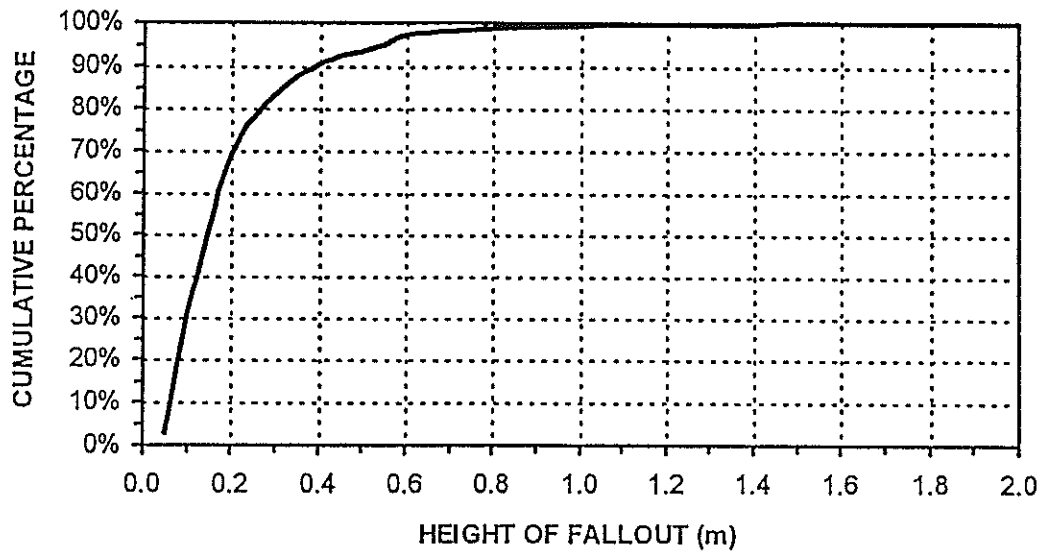


Figure 34 Distribution of fallouts in sampled Vaal Reef gullies

### 3.3.2 Support requirements

Using the fallout distribution graphs together with the fallout values for the 90, 95 and 100 per cent frequency levels of static (support resistance) and dynamic (energy absorption) support requirements are compiled in the table below. In all calculations a density of  $2700 \text{ kg/m}^3$ , a gravity value of  $9.81 \text{ m/s}^2$ , a velocity of  $3 \text{ m/s}$ , and an arresting distance of  $0,1 \text{ m}$  is used for a  $1 \text{ m}^2$  area of hangingwall.

#### Support Requirements for VCR, Carbon Leader Reef and Vaal Reef

Reef Type	Cumulative frequency percentage limit	Fallout thickness m	Support resistance $\text{kN/m}^2$	Energy absorption $\text{kJ/m}^2$
VCR				
	90%	0.50	13	7
	95%	0.70	19	10
	100%	1.70	45	25
Carbon Leader				
	90%	0.70	19	10
	95%	1.00	26	15
	100%	2.00	53	30
Vaal Reef				
	90%	0.40	11	6
	95%	0.55	15	8
	100%	2.00	53	30

These support requirements in turn relate to the following support densities as shown in the table below when using yielding tendons to address dynamic conditions. It is

assuming that a yielding tendon functions with a yield load of 100 kN under dynamic conditions.

#### Yielding tendon support densities

Cumulative frequency percentage limit	VCR Yielding tendon per m <sup>2</sup>	Carbon Leader Reef Yielding tendon per m <sup>2</sup>	Vaal Reef Yielding tendon per m <sup>2</sup>
90%	0.7	1.0	0.6
95%	1.0	1.5	0.8
100%	2.5	3.0	3.0

In order for the cone bolts to work effectively and maintain the integrity of the hangingwall during rockburst shakedown it will be necessary to use straps to connect the cone bolts together and create areal coverage. Careful consideration must also be given to the length of bolt used so that the bolt can fulfil its function both during the dynamic phase and the static situation afterwards.

#### 4. Project conclusions and outputs.

- The determination of a support resistance criteria for rockfalls and an energy absorption criteria for rockbursts for the Ventersdorp Contact reef, the Carbon Leader reef and Vaal reef has been an important output from the fatal accident database. The decision to base the ejected block thickness on 95 % cumulative percentage for the three reefs can be debated and a higher or lower percentage used to determine these criteria by individual mines. The determination of further criteria for other reefs, notably the Leader and Basal reefs in the Free State still needs to be undertaken. This can be done relatively rapidly as much of the data required is part of the database
- The development of the stope design methodology has been the second important output of this project and allows support systems, subject to stope closure, to be designed and evaluated against rockfall and rockburst criteria. Importantly, the stope face and the stope back area are evaluated separately and each should meet the required criteria. The methodology does assume that the hangingwall spans between support units are stable. The determination of stable spans is complex and was a major objective of the numerical modelling output.
- The development of a numerical model of stope support - hangingwall interaction has been a laborious process with the objective of obtaining insight into the changes that occur to hangingwall stability when the support spacing and support resistance is varied. The qualitative data obtained to date shows that the mechanisms are complex, however some insight has been obtained with respect to how inter-unit span stability varies with different support resistances. The full potential of this model is still to be realised particularly when fracture angles are changed and contrasted and when dynamic behaviour is evaluated.
- The support of stope gullies was addressed in two ways, firstly the problem of gully pack stability and foundation stability was investigated by underground monitoring.

This resulted in an understanding of the force - deformation behaviour of gully packs with time and stope closure and led to a recommendation with respect to a desirable force - deformation curve for gully packs, this was considered as an important output from this project.

- The determination of gully hangingwall fallout thicknesses between the gully packs in order to evaluate support resistance and energy absorption criteria for the prevention of rockfalls and reduction of rockburst damage was the second part of the work undertaken on stope gullies.. The work concentrated on the Vaal reef, the Ventersdorp Contact reef and the Carbon leader reef and gully support criteria have been derived for cumulative fallout percentages between 90 % and 100 %. Some rockbolting support requirements have been given which would meet these criteria.

It should be noted that with respect to the various methodologies described in this report it has been assumed that the support systems have been perfectly installed and that there are no missing or malfunctioning units. This is not always the case underground and the rock engineer should take this into account when evaluating a proposed support system against the relevant criterion. It would be prudent to estimate how well the support system would be installed in practice and then adjust the required support resistance or energy absorption requirement upwards.

## 5. Future directions.

The database has been particularly useful for the determination of the rockburst and rockfall criteria for the Vaal reef, the Ventersdorp Contact reef and the Carbon Leader reef. Determination of these criteria for other reefs is still required to be done and expansion of the database will be required. This will be undertaken in the SIMRAC project GAP 330, Stope Face Support Systems.

The determination of the rockburst energy absorption criteria for the various reefs assumes a closure velocity of 3 m/s. In section 2.2.2 some justification for using this velocity is given, however further investigation is required. The rockburst closure velocity is different for different reefs and is likely to be different within geotechnical areas of individual reefs. This will be addressed by SIMRAC project GAP 201, Site Response to Rockbursts and also by GAP 330.

The numerical modelling of stope support offers great potential to assist in the design of stope support systems. Work required in the future would be the assessment of stable spans between support units for the different fracture patterns which are characteristic of various geotechnical areas and how dynamic loading, that occurs during some rockbursts, effects the stability of spans between support units for different fracture patterns. This will be addressed by GAP 330.

The stope support design methodology proposed above will require further development. The criteria and design methodology should be determined and applied to other reefs not considered in the report above. This will determine a deeper understanding of the rockmass behaviour around these reefs and the determination of geotechnical areas within these reefs. This will be addressed by GAP 330.

## 6. References.

Two papers not directly referenced in this report but that were outputs of this SIMRAC project are referenced below as (7, 8 and 9).

1. CSIR Mining Technology. Rock Engineering. Stope Support Catalogue 1993.
2. Roberts, M.K.C. Jager, A.J. and Reimann, K.P. The performance characteristics of props. Chamber of Mines, Research. Report no. 35/87. 1987.
3. M.K.C Roberts F.R.P Pienaar and F.C. Kruger. "Properties of Pack Supports - Comparison of the Laboratory and Underground Performance". Symposium, From Stump to Stope. C.S.I.R. 1987.
4. Taggart P.N. Dynamic laboratory testing of pack based support elements. Part I. The laboratory evaluation of timber and composite packs, single rise pack elements and grout based prestressing. Interim project report, GAP 032. 1994.
5. Taggart P.N. Dynamic laboratory testing of pack based support elements. Part II. The laboratory evaluation of two types of grout based pack prestressing systems. Interim project report, GAP 032. 1994.
6. Eve R.A. and Squelch A.R. Modeling of stope and gully support systems The proceedings of The ISRM symposium on the application of numerical modeling in geotechnical engineering. September 1994.
7. Squelch, A.P., Roberts, M.K.C. and Taggart, P.N. 'The development of a rationale for the design of stope and gully support in tabular South African mines'. Proceedings of the 1st North American Rock Mechanics Symposium, University of Texas at Austin, June 1994. Ed. Nelson & Laubach. Balkema, Rotterdam. pp 919-926.
8. Eve R.A. Modelling of stope support-rockmass interaction. SIMRAC Symposium, September 1995.
9. Daehnke A. ' A method for evaluating the influence of grout pre-stressing systems on the performance of packs: Static and dynamic considerations. Interim project report, GAP 032. 1994.

# APPENDIX 1

## NUMERICAL MODELLING OF STOPE SUPPORT - ROCK MASS INTERACTION

### TABLE OF CONTENTS

	page
1. INTRODUCTION	
1.1 Modelling objectives	1
2. MODELLING REQUIREMENTS	
2.1 Initial Assessment	2
2.2 Modelling tools	2
2.3 Two-dimensional models of tabular excavations	3
3. DEVELOPMENT OF A DISCONTINUUM MODEL	
3.1 Overview	4
3.2 Determination of fracture patterns	4
3.3 Model development	5
3.3.1 Phase I : Initial full stope model	5
3.3.2 Phase II : Local models	6
3.3.3 Phase III : Very blocky models	7
3.3.4 Phase IV : Increased span blocky model	11
3.3.5 Phase V : The final model	12
4. FINAL MODEL	
4.1 Geometry	12
4.2 Material and joint properties	16
4.3 Boundary and initial conditions	17
4.5 Mining history	18
4.5.1 Excavation	18
4.5.2 Supports	18
4.4.3 Mining of back areas	21
4.4.4 Mining of the area of interest	21
4.4.5 Dynamic loadings	23
5. RESULTS	
5.1 Quasi-static analysis	24
5.2 Dynamic loading	37
6. PARAMETER STUDIES	
6.1 Evaluation of hangingwall stability	40
6.2 Trends with varying spacing and support	40
6.2.1 Taking changes in dip spacing into account force	42
6.3 The influence of load spreaders	43
6.4 Sensitivity to bedding plane spacing	43
6.5 The influence of back area support	44
7. CONCLUSION AND RECOMMENDATIONS	45



# NUMERICAL MODELLING OF STOPE SUPPORT-ROCK MASS INTERACTION

## 1. INTRODUCTION

The results of the numerical modelling work described in this appendix are summarised and their application discussed in the main body of this project report.

The work reported here was carried out as part of the SIMRAC project GAP032 the primary objective of which was to *develop a rationale for the design of support systems*. The research programme has been carried out over a period of three years (1993 to 1995). From the outset it was realised that direct physical underground measurement of controlled support system installations was impractical, particularly in view of the extremely high costs that may be incurred for such a monitoring programme. A two pronged approach was employed to obtain a basis on which to develop a support design rationale. The establishment and analysis of a complete database of accident records was the first approach used. The second approach adopted was use of numerical modelling.

It was accepted that a full simulation of support system performance would not be possible with current modelling tools. The objective of the modelling approach was, therefore, limited to determining trends in support performance with a few simple support parameters. An account of technical aspects of this research is given in this appendix. The precise objectives of the numerical modelling are first stated. This is followed by an account of an initial assessment of the requirements necessary to meet these objectives. A brief review of the available modelling tools is then given. Considerable time and effort was expended in developing an acceptable model to use in performing the required parameter studies. The main purpose of this report is to document the final model used and the results of the parameter studies. In spite of success achieved using the current model there undoubtedly remains considerable scope for further improvements. Some understanding of the history of the development of this model is of importance as its structure is, in many respects, a consequence of this process. The main phases in this development process are described before detailed information about the final model is given. The parameter studies performed under quasi-static conditions are discussed and results presented. Some discussion of the few dynamic results obtained follows. In conclusion, the success of the work is reviewed, the limitations of the modelling are reiterated and the main conclusions of the work are summarised. Finally, the need for further work and the potential for other applications of the models developed are remarked upon, recommendations for further refinements are also made.

### 1.1 Modelling Objectives

The following are the objectives of the numerical modelling component of the project as stated in the original project proposal:

*Using numerical modelling conduct a sensitivity analysis on the following:*

- 1 The effect of spacing of support units on the stability of hangingwall blocks between units.*
- 2 The effect of varying support unit force on the stability of hanging wall blocks between support units.*
- 3 The effect of point loads or area support on the stability of hangingwall blocks between support units.*
- 4 Determine the effect of increasing or decreasing the support resistance of various support systems on the skin of the excavation.*

*under both static and dynamic conditions.*

## 2. MODELLING REQUIREMENTS

### 2.1 Initial Assessment

The rockmass surrounding deep level excavations is transected by many discontinuities in the form of geological faults, joints, bedding or parting planes and mining induced fractures. The behaviour of the rockmass is to a large extent dependant on the intensity and nature of such discontinuities. This is most evident near free surfaces where confinement is low and so relative displacement and movement, in particular rotation, of blocks is possible. The intensity of discontinuities is also particularly high in the immediate skin of the excavation where fracturing is dominant. Capturing the influence of discontinuities is therefore essential for the assessment of hangingwall stability.

The behaviour of blocky systems is highly non-linear and greatly dependant on history of past loading and deformation. The rock surrounding the stope is subjected to a reasonably complex loading history as a consequence of the incremental nature of mining. The rock is initially stressed but as the excavation advances the rock ahead of a stope face is subjected to an extreme concentration in the vertical stress, this is accompanied by reduced confinement in the horizontal direction. Behind the face stresses in the stope footwall and hangingwall are greatly reduced and considerable deformation of the rockmass takes place, particularly in the hangingwall. Reasonably accurate modelling of the excavation process is therefore considered essential.

An important aspect of support design is response to dynamic loadings caused by mining induced seismicity. Detailed investigation of these phenomena by direct underground observation is almost impossible as considerable instrumentation is necessary to establish magnitude and characteristics of seismic events as well as the response of supports and the skin of the excavation. Seismic events are unpredictable hence a high density of instrumented sites would be needed to capture even a few events. Modelling provides perhaps the only viable method of investigation of this important aspect of support design. In the past there has been little detailed investigation into how seismic energy is dissipated in highly discontinuous rock and in particular how energy is focused into the ejection of loose surface blocks. The initial contact conditions between blocks of rock determine the way in which dynamic waves are reflected, refracted, attenuated and dispersed in a blocky rockmass, hence, a critical aspect of assessing dynamic loading is the establishment of a realistic initial state. The initial state is that reached by considering the excavation and support installation sequence that takes place during mining. Establishment of modelling techniques that adequately represent support-rockmass interaction under quasi-static conditions was therefore considered of prime importance as it was assumed that the necessary detailed initial conditions for dynamic modelling could not be established in any other way. A requirement that models constructed for quasistatic analysis should include provision for the application and analysis of dynamic loading places was proposed and adhered to.

### 2.2 Modelling tools

The underlying philosophy to the modelling work undertaken in this project was to make use of currently available software and to work within the limitations of this software. This approach was adopted to ensure that the capabilities of current tools are exploited fully in attempts to come to an understanding of the complex nature of fractured rock before new models are developed.

In rock engineering practice continuum models are widely used. Many of the currently available continuum modelling tools allow inelastic material behaviour to be modelled. The inelastic constitutive laws that are widely used to represent rock, such as the Mohr-Coulomb plasticity model, are limited in their ability to capture detailed aspects of the behaviour of discontinuous rock masses. Some attempts have been made to improve this situation, with for example introduction of strain softening and ubiquitous joint models. The stability of blocky hangingwalls, the assessment of which is central to the aims of this work, relies on the interaction of blocks of rock through the conditions on the multiple discontinuities that define them. A discontinuum model was considered to be desirable, if not the only possible way of capturing a realistic representation of the complex mechanisms of support-rockmass interaction that determine hangingwall stability.

Some preliminary investigations were carried out using a continuum model with discrete discontinuities representing bedding planes; FLAC a two-dimensional explicit finite difference code developed in Minneapolis Minnesota by Itasca Consulting Group Incorporated, was used. This work served to confirm the need for a better representation of the behaviour of blocky rock than is available in such a code.

Tools for the construction and analysis of discontinuum models have been available for some time, in particular UDEC, the Universal Distinct Element Code also developed by Itasca (first released in 1985, the distinct element method having been first proposed in 1971). UDEC is a two-dimensional modelling tool based on the distinct element method. Calculations are based on an explicit formulation of fully dynamic behaviour, deformation of blocks is taken into account by modelling their behaviour with a finite difference scheme. Application of such tools to the analysis of the highly blocky skin of the rockmass surrounding deep level tabular excavations has, to date, been limited. The considerable computational effort required to analyse problems of the size required to provide both the necessary intensity of discontinuities and the step by step mining sequence necessary to ensure the correct history of loading and deformation, has been an obstacle to progress. The increasing rate of improvement in affordable computational power has only recently made it possible to consider development of reasonably realistic models.

In this project the construction and analysis of discontinuum models of the interaction between stope support and the blocky rockmass at the skin of stope excavations have been carried out using UDEC. Some of the limitations to development of the required model associated with this tool and method are mentioned as development of models is discussed. The rapid changes in computer hardware capabilities that have occurred in the short three year life of this project have had an impact on model development; some approaches initially found to be too computationally demanding, and hence discarded, have subsequently become feasible.

Most currently available modelling tools capable of analysing the behaviour of blocky rock masses undergoing significant deformations, including UDEC, require all discontinuities to be spatially defined before any calculation steps are taken. It is, therefore, not possible to model the development of fractures in such models. The best representation of fracturing that can be achieved is obtained by construction of a mesh of potential discontinuities in a predefined pattern and using the algorithms controlling movements on discontinuities to mimic fracture, or activation, of these lines. Fracturing around stopes is considered to take place in the area of high stress concentration ahead of the face. Underground observations indicate that the intensity and direction of this fracturing is essentially independent of the support system used. The use of predefined fracture patterns is therefore a valid approximation for the purposes of current work. The choice of fracture pattern has however been found to be fairly critical to the success of such models; it was studied during the development of the models described below.

### 2.3 Two-dimensional models of tabular excavations

There exist tools that could be used to construct and analyse three-dimensional discontinuum models, but none is efficient enough to be able to consider very blocky systems. For this reason and the lack of experience in discontinuum modelling of stopes, all the work done on this project has been limited to two-dimensional modelling. It is, therefore, important to understand and keep in mind the basic assumptions of two-dimensional modelling and the limitations which these assumptions place of mechanisms that become active and the way in which results can be interpreted.

In two-dimensional modelling of three dimensional problems it is assumed that there exists a planar section that is representative of the problem geometry. It is also assumed that all model parameters vary only in the plane of this section, and therefore that all the important modes of behaviour involve only movements in this plane. The geometry of longwall mining where the angle of dip is low (less than about 30 degrees) and where breast mining on panels of reasonable length, with small leads is practised, can be represented in two-dimensions by a strike section through the centre of a panel. This representation is valid partly because of the inelastic nature of the rockmass which ensures that the effects of gullies and the lead/lag of panels are localised to the ends of panels; at least more so than they would be in an elastic medium. In such a model, dip of the stope is completely ignored. The only fractures that are actually truly represented are face parallel, these are

assumed to be infinitely long in the direction normal to the modelled section, this is compatible with the observation that the dominant sets of fractures in a typical stope are face parallel. In general, it is not easy to model the influence of jointing. Joint sets are not usually conveniently oriented in a direction consistent with the two-dimensional modelling assumptions. It is noted that the effects of non face parallel joints faults and fractures if present could have a significant influence on hangingwall stability but that such discontinuities are completely ignored in two-dimensional models.

The formulation of mechanics in two-dimensions that is appropriate for modelling of the rockmass surrounding stopes is a plane strain formulation. This formulation assumes that there is no straining, or movement, in the direction normal to the plane of the model. A unit thickness is also assumed, this has implications for the modelling of support. The dip spacing of supports can not be directly taken into account, supports modelled in the two-dimensional model are effectively like infinitely long walls parallel to the face. The support force delivered per unit length in the dip direction is the value of support resistance that should be used; for example if 10t units were placed at a dip spacing of 1m a support resistance of 10t could be used in the model, however, if a dip spacing of 2m was used the equivalent support resistance that must be used in the model would be 5t (that is 5t/m). The simple relationship between dip spacing and support force is used to interpret the final results obtained for the effect of changing dip spacing of supports. It is very important to note that the validity of the model relies partly on the use of small dip spacings.

An assumption of symmetry about the central raise is typically made when modelling longwall mining as a slot in a two-dimensional plane. This assumption implies longwall mining in both directions simultaneously and is used in most of the models analysed.

### 3. DEVELOPMENT OF A DISCONTINUUM MODEL

#### 3.1 Overview

Development of the model finally used to obtain some indication of the trends in hangingwall stability with variation in support parameters took some time. Five major sets of changes in the way in which construction of the model was tackled define a series of phases in the development process; these phases are described below. Details of results obtained with early attempts at constructing a suitable model are not given, these can be found in the annual project progress reports.

The basic approach taken in all phases of model development was to try and construct a single basic model suitable for all the proposed parametric studies. The aim was to build a model capable of capturing a wide spectrum of possible failure mechanisms; this would make it possible to detect changes in mode of failure as support parameters were varied. Great importance was placed on ensuring that the model would require no adjustment, other than to support configuration, for the determination of the required trends. In this type of study changes to parameters other than those of the study make it impossible to ensure that a meaningful comparison of results and identification of trends can be made. A stable and reasonably robust basic model was developed before starting to invest time in obtaining final results. This approach was based to some extent on the assumption that a single simple class of fracture and joint patterns, dependent on only a few simple parameters, could be identified.

#### 3.2 Determination of fracture patterns

The choice of fracture patterns used in the various models proposed during the course of this study was an issue that triggered much discussion. Several researchers have documented observations and measurements made of fracture patterns and displacements around stopes. Figures 1 shows diagrams of some of these observations. This literature was initially consulted, however, uncertainty expressed by many as to the applicability of some aspects of these observations prompted further study, by direct underground observation, of the fracture patterns present in typical stopes.

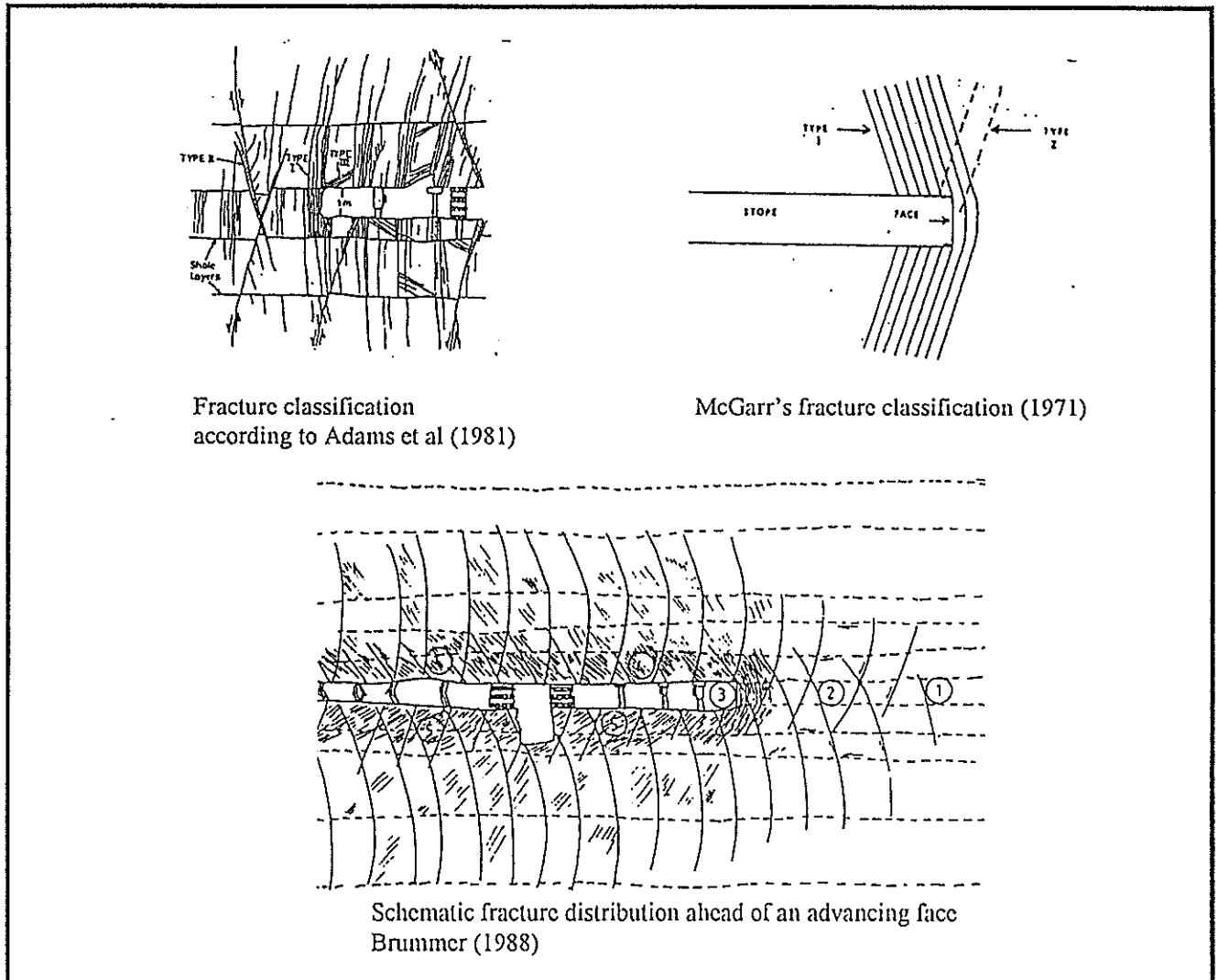


Figure 1 Examples of fracture patterns recorded in the literature.

During the second year of the project a large number of underground trips (to a variety of mines) were undertaken to gather information with respect to stope fracture patterns in different mining environments. The classical fracture pattern consisting of bedding planes, extension fractures and possibly some shear fractures, associated with typical of stopes which have quartzite hangingwall and quartzite footwalls, was quite apparent in some of the stopes visited, but occurrence of fractures that could be positively identified as shear fractures was very limited. Some fracture mapping was done at Hartebeestfontein and at Harmony gold mines. The classical extension (Type I) fractures were observed at both these sites, but no shear (Type 2) fractures were observed. The angle of extension fractures at both sites was steeper ( $70$  to  $85^\circ$ ) than had been used in early models ( $45$  to  $60^\circ$ ). These observations were used in later modelling work.

### 3.3 Model Development

#### 3.3.1 Phase I: Initial full stope model

Model development started with construction of a two-dimensional blocky model of a full stope. A strike section of the excavation was modelled assuming symmetry about the central raise, as discussed above. Provision was made for a stope of width  $1.4\text{m}$  to be excavated to a half span of  $42\text{m}$ . Initially single support type was used throughout. The mining sequence ignored differences between permanent and face area support; in subsequent developments different back area support systems were used but focus on face area support was maintained. The extent of the excavation was chosen so as to allow for the influence of closure on the supports and surrounding rockmass to become well established. A simple and somewhat course

fracture pattern was used. This pattern was based on that indicated in some literature as being characteristic of what may be found in typical stope excavations on South African mines and included both shear and extensional fractures, as well as bedding planes. Figure 2. shows a detailed view of part of the model after excavation of about 14m; note no face crushing is allowed for and complete closure occurs only 7m behind the face.

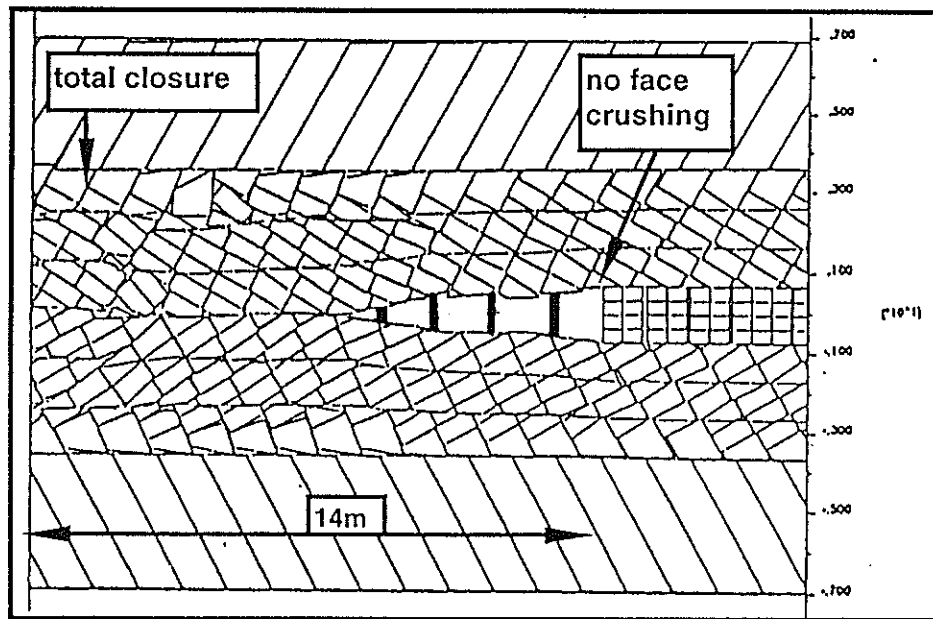


Figure 2 Initial fully stope model: a detailed view of the stope after 14m of excavation.

After several months of work on this model some aspects of the results obtained were promising although excessive closures were obtained with the parameters being used. It was noted that dilation on fractures and joints had a marked effect on the closures predicted by the model. Some difficulties were encountered in tuning the model to give good stress results while at the same time achieving a numerically stable solution. Slow progress was due mainly to the time required to run the analysis of the model, this being of the order of several days for only the first half of the proposed excavation. It was noted, that considerable further refinement of the model was necessary, that the rate at which development of the model could proceed was very low due to long run times, and that, a large number of model parameters, other than those of prime concern in the study, needed to be taken into account and optimised. At this time a 486 50Mhz PC computer was being used. The approach was considered to be very risky as too much time and effort would have been required before a good idea of the potential success of the model in achieving the set objectives could have been obtained. It was decided that this approach was not viable and an alternative approach should be used; development of the full stope discontinuum model was therefore halted.

### 3.3.2 Phase II: Local models

In this phase of model development the suggestion that smaller, *local*, models might provide enough information about support rockmass interaction, without requiring excessive computer resources, was investigated. This investigation continued until the end of the first year of the project. From the outset it was recognised that great care would be needed in interpreting the results of the analysis of these local models since the effects of boundary conditions, simplified mining history and other assumptions might dominate the models behaviour.

The first set of local models considered consisted of a short section of hangingwall supported by a set of supports (initially in some cases the footwall was also included). The model was constructed with symmetry boundary conditions on both the left and right hand sides of the model. The idealised fracture pattern used was very simple, being regular and symmetric, with extension and shear fractures at equal angles. This symmetry was imposed to keep boundary conditions as simple as possible. Various angles of fractures were used and some investigation into the consequences of varying the spacing of support units was done. Dynamic

loading in the form of a shock wave (velocity step function) applied vertically to the top boundary was used in this investigation. Examples of these models are shown in Figures 3(a) and (b).

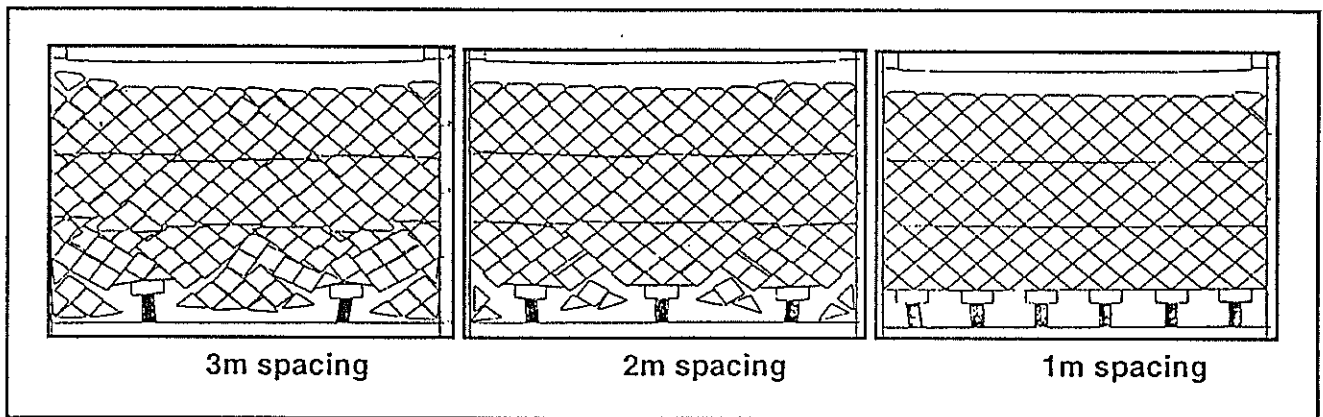


Figure 3(a) Example of a local model with blocky hangingwall and various support spacings

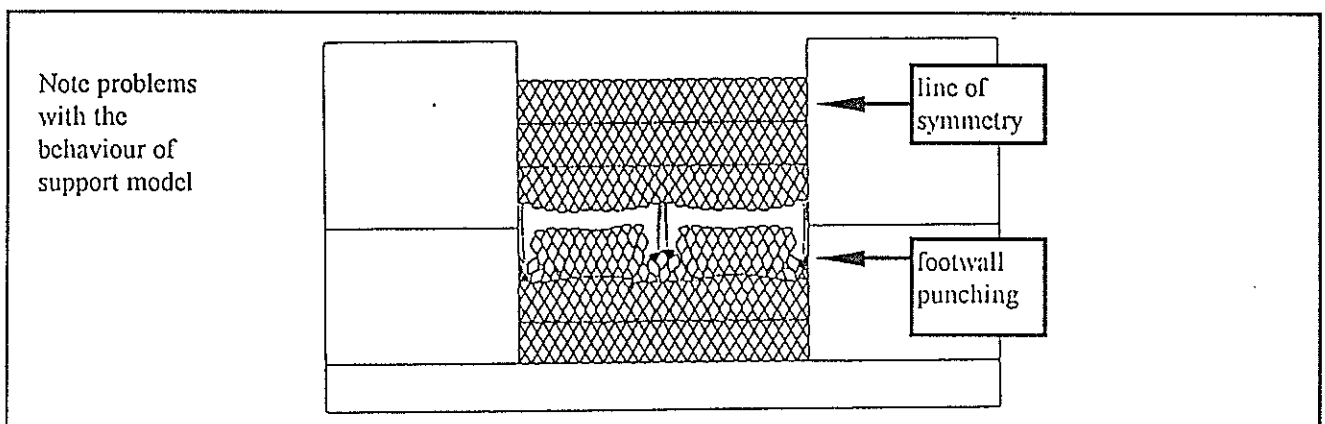


Figure 3(b) Example of a local model with blocky footwall and hangingwall.

While superficially the results from these local models looked promising a closer inspection revealed some severe limitations over and above those imposed by the simplifying assumption of symmetry. The results show the intuitively expected fall out of a triangle of material between the edges of the head boards of adjacent supports. In practice this material may have been held in place by, key block mechanisms, in a direction perpendicular to the plane, and by the development of compressive, clamping, forces in the hanging wall as a consequence of the mining process. Key block mechanisms acting in a direction at any angle to the plane of the two-dimensional model cannot be taken into account. The development of compressive stresses can be included by applying forces to the side boundaries using a system of rigid blocks. The values and the way in which these forces develop relative to vertical movements in the hangingwall are unknown. The joint properties given to fractures become critical when horizontal stresses are applied. This is partially due to the symmetric fracture pattern which allows artificial locking up of the blocky system, this in turn results in potential instability in the solution. Under these conditions minor perturbations in the joint properties, or stress distribution, such as those obtained from out of balance force calculations, may determine the solution obtained.

After some further review of the attempts at developing local models a local model with asymmetric fracturing was constructed. This unsuccessful model is shown in Figure 4. The intention was to select a set of fractures which was representative of a specific pattern identified underground; this pattern being typical of a number of sites. The fracture pattern chosen was one which showed potential for significant in-plane key blocking. In this case it was assumed that out of plane key block effects play a secondary role in determining the hangingwall stability and hence could be ignored. Since the simplifying imposition of symmetry is abandoned

the revised model included the stope face. The model again relied on assumed and idealised boundary conditions in the form of applied stresses; a notable short coming of the model is that there is no reliable method for choosing suitable values for these stresses. There was also some uncertainty as to how best to apply a dynamic boundary condition so as to simulate, at least to some degree, an impinging seismic wave. Lack of provision for face crushing is another feature of this model that is responsible for its poor performance.

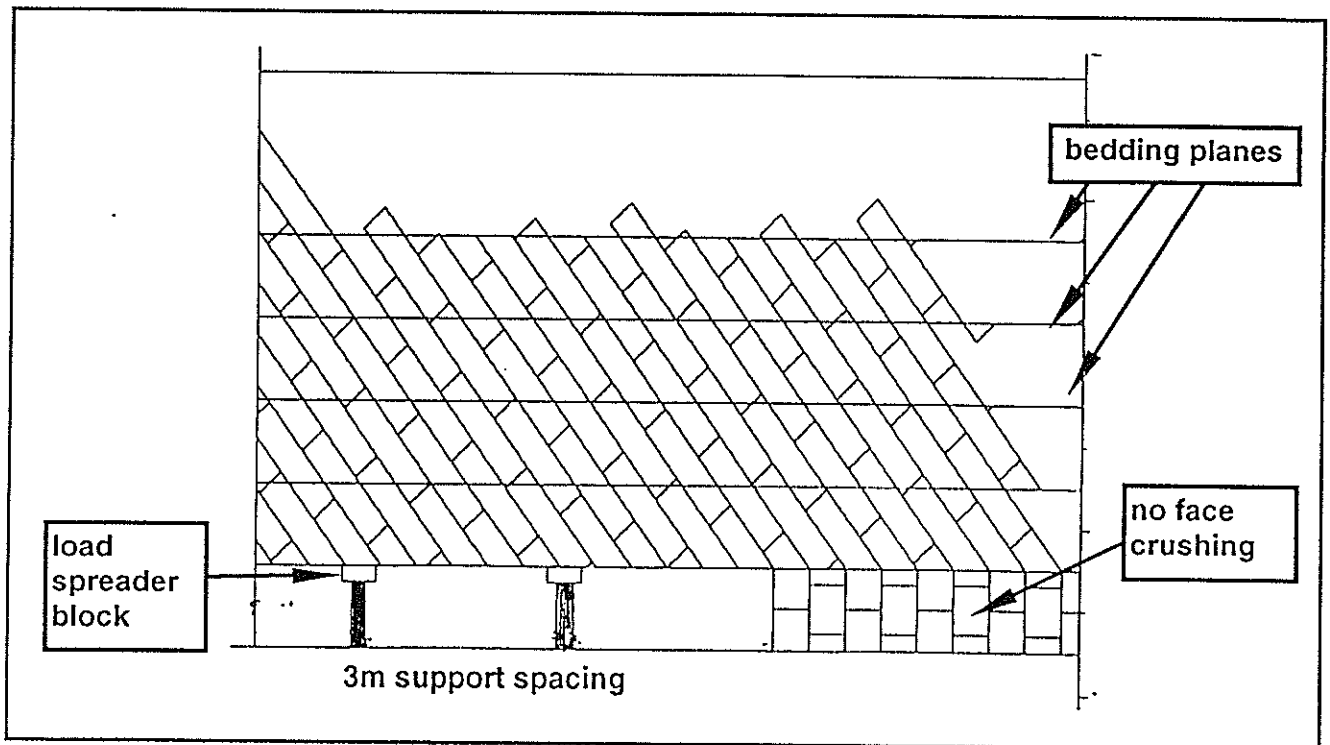


Figure 4 Unsuccessful non symmetric local model

In summary of this phase of model development, no collapse mechanism, which could be easily related to physical observations, could be identified using local models.

As part of the development of local models it was necessary to do a thorough investigation into various methods of modelling support load spreaders, *head boards*. Some problems associated with the simple method of extending the width of support unit model available in UDEC were identified. A rigid block proved the most effective way of representing load spreaders provided some analysis control parameters are adjusted so as to avoid adversely affecting the time step size. Subsequently when again considering larger models, the use of rigid blocks proved excessively cumbersome; a simple widening of supports was used. It was found that the problems found in detailed local models were not significantly manifest in larger models, at least not for quasistatic loading.

### 3.3.3 Phase III : Very blocky models

At the beginning of the second year of the project a workshop was held with the Group Rock Mechanics Engineers to discuss numerical modelling work and to assess the direction in which the work was to proceed. The main recommendation was that specific underground sites should be modelled. However, it was felt that direct calibration of the model would defeat the purpose of the study. It was concluded that it would be useful to gather more information about stopes in different geotechnical areas and to use this information to verify results obtained by modelling. The general consensus of the meeting was that there is a need to continue to try and understand the mechanisms involved and to develop suitable modelling techniques to do this. Other issues which were raised included:



- the influence of local geological variations on stability of the rockmass,
- the inherent stability of typical stopes,
- the question of stability under dynamic conditions
- the relevance of different intensities of seismic activity associated with rock bursts, and
- the importance of face crushing in determining the distribution of stresses near a stope.

After discussion of the shortcomings of local models a new approach was suggested that led to the development of another new set of models. The concept used was aimed at including face crushing and allowing shear and extension fractures to develop in a way that was dependent on the stresses in the rock at the stope face. This was achieved by constructing an extremely blocky region, the intensity of discontinuities being far greater than that of observed fracturing and choosing the joint material properties in such a way that no slip or plastic failure takes place under these initial stress conditions, that is, all joints are locked up and the blocky rock mass acts as an elastic continuum (at least as close as the program allows it to). When the stope is excavated changes in the stress regime cause slip to occur on some of the pre-defined joints, this mimics the fracturing that takes place in reality.

The large number of blocks required to implement this approach limits the extent to which the stope half span that could be modelled while maintaining a reasonable problem size with reasonable run times.

A model consisting of a very blocky region surrounded by large deformable blocks was constructed. The large blocks were added in an attempt to extend the model far enough from the excavation to avoid the influence of boundary conditions simulating the surrounding infinite rockmass. Horizontal bedding planes extending over the full width of the model were included. Initial stresses representative of a mining depth of approximately 2000m were applied. A stope of 12m half-span was excavated and support units included in a sequence representative of an actual mining process thereby allowing stresses and "fracturing" (slipping predefined joints) to develop in a manner which takes into account the mining history.

Initially sets of joints, or potential fractures were defined in a regular pattern to produce the blocky region; joints at 60°, 90° and 120° were used. In the blocky region an elastic model was used, each block being modelled with a single zone. This has the effect of making the blocks practically rigid. A Mohr-Coulomb constitutive law was used for the large deformable boundary blocks, this was done to account for slip not accounted for on explicitly defined joints. This model is shown in Figure 5.

A large number of calculation cycles were needed at each mining step to ensure that equilibrium was reached. Initially the model took seven or more days to run, this again made development of the model an extremely slow process. Pursuit of the use of this model was made possible by the acquisition of an HP workstation, this occurred approximately one and a half years into the project. Testing and experience in running UDEC on the HP showed a speed-up factor of 10 over the 486 PC used previously.

Initially results were quite promising. It was noted, however, that results for closure of the stope were largely dependent on the joint properties; exaggerated closures were initially obtained. Simply increasing cohesion and friction on joints, using the basic UDEC joint contact model, appeared to be an unsatisfactory method of controlling closure. This either fails to restrict initial slip, that is the failure or "fracturing", or inhibits post failure slipping of joints in the face and hangingwall, and hence the model loses its capability to model the fractured rock adequately. The continuously yielding joint model implemented in UDEC provides an alternative mechanism whereby initiation of slip and post failure behaviour are governed by different frictional and, more importantly, cohesive properties. The use of this model was investigated. By adjusting the continuously yielding joint model it was possible to improve closure results while preserving the formation of "fracturing" by slip on some, but not all, of the predefined joints. Optimisation of the continuously yielding joint model properties for application in this model was, however, difficult and the relationship between joint model parameters and known material properties is not clear.

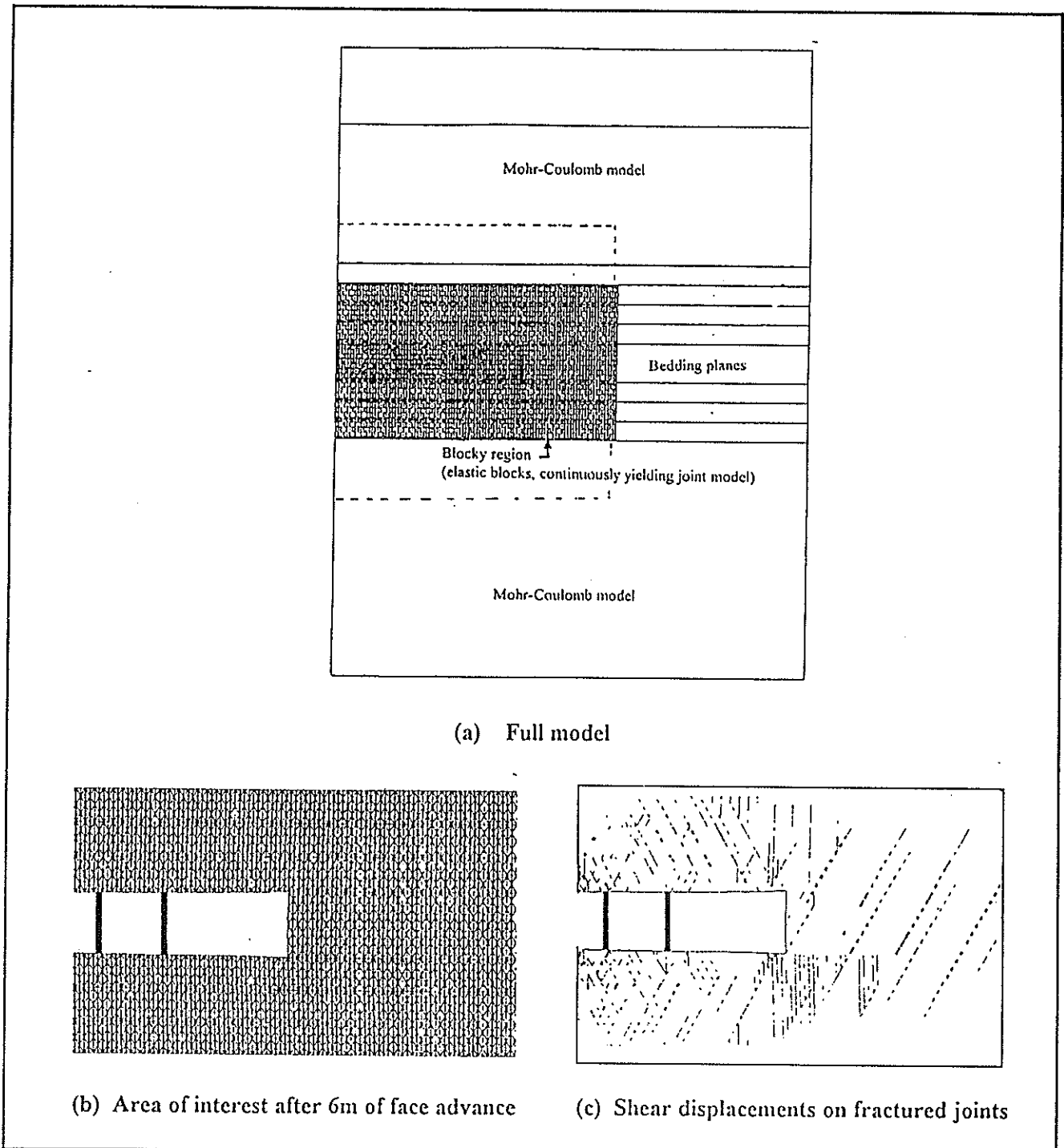


Figure 5 Very blocky model

Fractured, but stable, hangingwall conditions were achieved, however, several shortcomings in the model were noted, these included:

- the limited span resulting in among other things difficulties in verifying the models behaviour by comparing the closures obtained with those observed underground,
- closures that appeared excessive,
- a fracture pattern was considered to be artificial especially with respect to shear fractures, boundary conditions at midspan, where the discontinuum lies on the line of symmetry, that do not appear to be effective, and
- the transition from discontinuum to elasto-plastic continuum produced artificial local effects.

A first attempt at applying a simple dynamic excitation to the model was made, but was not successful. It was decided not to pursue the dynamic modelling until further success in quasi-static modelling had been achieved.

### 3.3.4 Phase IV: Increased span blocky model

The need to model wider spans necessitated some redesign of the blocky model. The following points were considered in developing another new model. Firstly, it was considered desirable to include the development of fracturing in the model, however, it was suggested that perhaps too much emphasis had been placed on modelling fracturing in the previous development phase. Secondly, it was noted that early full stope models (spans >40m) were reasonably successful but lacked a mechanism for modelling crushing of the face, the block size used was also too large to allow for local mechanisms of skin instability to develop through interaction with supports. The excessive time required to run earlier models, which initially prompted a move away from full stope models, were considered to have become acceptable in the light of experience gained in running UDEC and by use of the HP work station.

The model initially proposed in this phase of the work is shown in Figure 6. The idea of defining an area of interest, at a given stope half span, in which many blocks are defined and the assessment of supports can be made was introduced. In this approach fracturing in the back areas is only coarsely modelled, the idea was to achieve a reasonably representation of the stresses and deformations effecting the area of interest. Provision for shear fracturing was reduced to a spacing similar to that observed for active shear fractures in earlier models. The very finely fractured region is restricted to the thickness of two bedding planes. The reef horizon (material to form stope face) was only jointed enough to allow a crushing mechanism to develop but was not modelled in detail; crushing of the face away from the area of interest was ignored. All blocks were modelled with a Mohr-Coulomb material so as to avoid problems in the transition between different continuum models.

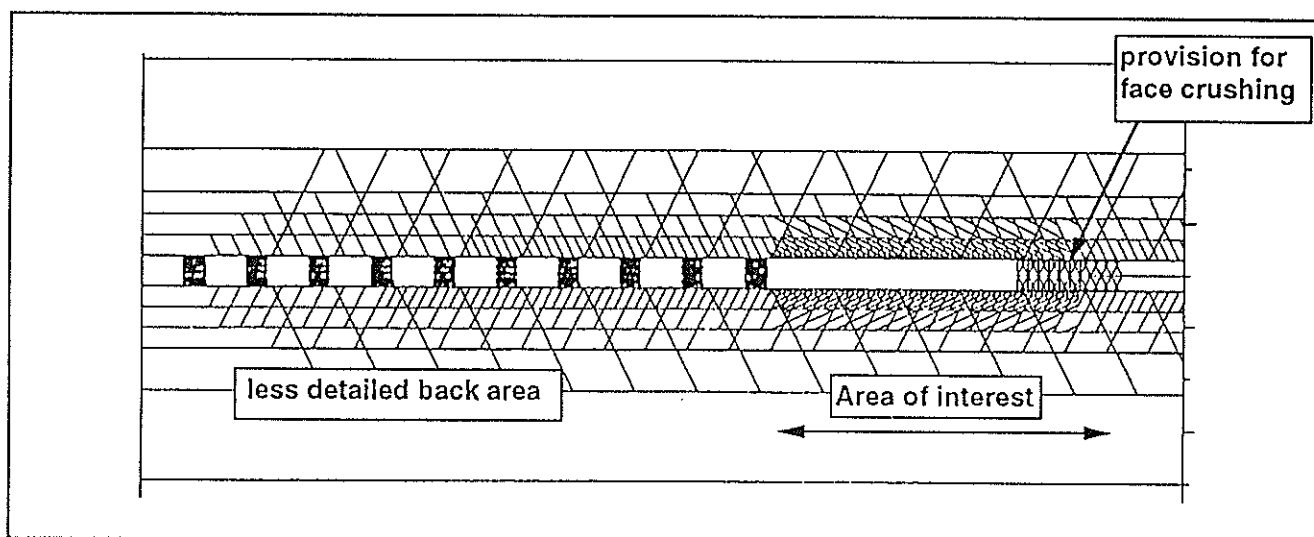


Figure 6 A view of the stope in the revised very blocky model

Initial results indicated some problems but most of these were not difficult to overcome. Closure rates appeared to be reasonable, however, a considerable number of calculation cycles, and hence run time, were necessary to achieve the required closure and for something close to equilibrium to develop at each step in the excavation sequence. Initially a simple fracturing joint model was used. The mobilisation of previously defined potential fractures still seemed to provide a reasonable assessment of the damage to the skin of the excavation resulting from advancing the face. Plasticity indicators enhanced the picture. As was observed with earlier models the hangingwall was found to be reasonably stable under static conditions, however, the shear fractures still appeared to assume an artificially dominant role.

This model was not studied in detail, firstly because of the long run times required and secondly, and more importantly, because it was felt that the fracture pattern being used was, in the light of the observation made at the time, considered not to be sufficiently representative of that which occurs in most stopes. However, the

concepts used in the construction of this model proved to be the key to success when applied and refined in the final phase of model development in this project.

### 3.3.5 Phase V : The final model

The model developed in this phase is described in detail in the next section of this document as it is the final model to be developed and has been used to obtain an indication of trends in slope support performance . The main difference between this model and that developed in phase IV was the elimination of shear fractures. The angle of extension fractures was also made steeper. These changes were based on the underground observations described in section 3.2.

In all previous phases of model development both extension and shear fractures were included. With both these sets of fractures and bedding planes it is necessary to define a regular fracture pattern, so as to avoid forming very small blocks where bedding planes, potential extension fractures and potential shear fractures intersect. Very small blocks cause a number of numerical problems, one of which is to radically reduce the critical time step size used by UDEC this makes the number of calculation cycles required prohibitive. With the elimination of shear fractures went the need to use artificially regular fracture patterns. The inclusion of some randomness in the pattern of discontinuities, and hence the shape of blocks, was another key factor in the success of the model constructed in this final phase of development. In addition some variation in the angles and spacing of extension fractures random sets of short, near horizontal, "cross fractures were introduced. The addition of this new class of fractures was also based on underground observations.

Previously in the back areas fracturing had been coarsely modelled with the objective of achieving a good representation of the stresses and deformations effecting the area of interest. It was again noted that the back area is being modelled simply to improve the "boundary condition" on the area of interest. In the final model the need to define additional blocks in the back areas was eliminated by using a ubiquitous joint model. This approach provides a reasonable representation of the rockmass behaviour in the back areas in the absence of shear fracturing.

The blocky area of interest is restricted to the thickness of a few bedding planes. A simplified jointing of the reef horizon, the material that forms the slope face, was retained to allow a crushing mechanism to develop, crushing of the face outside the area of interest was again ignored.

## 4. FINAL MODEL

A brief description of the final model used in the study has been given in section 3.3.5, above, here the model is described in more detail making direct reference to examples of the UDEC input data used. The model requires a fair amount of data, this data was divided into different parts so as to allow the variations required and parameter studies to be efficiently applied. The main components of the data are: definition of the model, excavation of the back areas with installation of supports (either packs or backfill), excavation of the face area with installation of supports of different resistances and at different spacings and application of dynamic loading. The model definition was further subdivided into: construction of the blocky geometry, definition of zoning for deformable blocks and the associated material and joint models and properties and definition of boundary and initial conditions with a consolidation phase to ensure good initialisation of the model. Further data files were used to control the calling of data to complete the final parameter studies.

### 4.1 Geometry

The model domain includes a region that extends 80m above and 80m below the slope, the total width of the model is 110m. The geometry of the model is shown in Figure 7. The origin of the co-ordinate system used is placed on the centre of the model in the vertical direction, allowing some symmetry between hanging and footwall geometry to be easily constructed, and at a distance of 30m in from the symmetry line on the left hand boundary of the model. The 30m corresponds to the distance that the slope that is excavated for the purposes of achieving the correct conditions in the area of interest. Choosing the origin in this way allows the slope

span to be easily adjusted. The model allows for a total slope half span of 42m to be excavated, the last 12m of which is considered to be of interest. Bedding planes at a spacing of 0.5m have been defined for 5m above and below the slope over most of the width of the model; a variation of the model has bedding spacing set at 1m. The slope is excavated to a width of 1.5m. The outer regions of the problem domain are divided into blocks so that the sizes of zones, defined to allow the rock mass to be modelled as a deformable region, can be controlled. In the rock surrounding the area of interest provision is also made for the application of dynamic loading. This provision takes the form of a series of thin blocks which are deleted and a pressure loading is subsequently applied in the resulting slot; this gives a crude approximation of a seismic event.

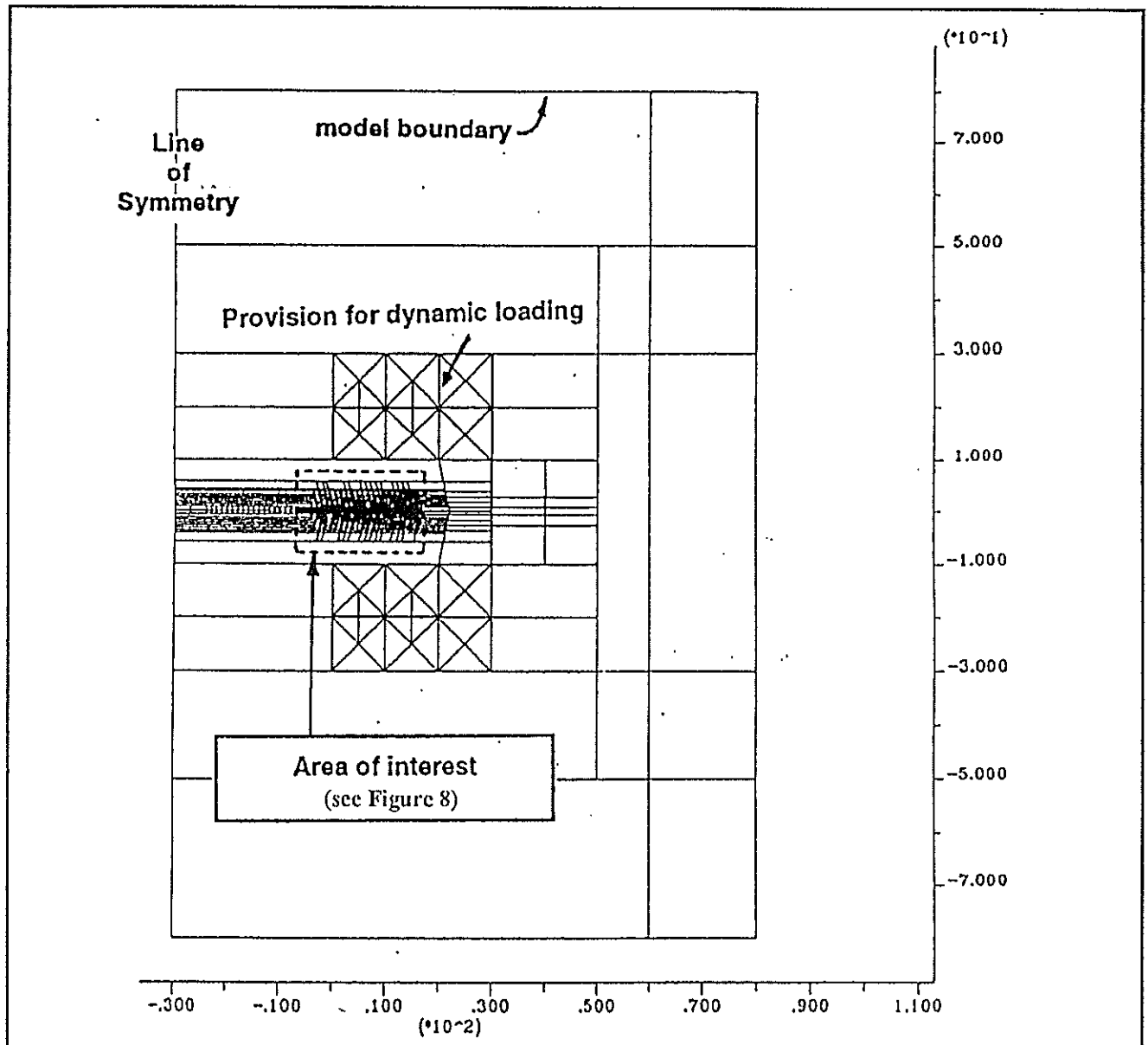


Figure 7 Final model geometry

The joints that represent the potential extension fracture pattern and the sets of randomised cross fractures, described in section 3.3.5, are only inserted in the area of interest and transition regions in the last few metres of the 30m back area excavation and in the rockmass for a distance of 5m ahead of the final face position. Two sets of extension fractures, one at an angle  $75^{\circ}$  and the other at  $80^{\circ}$ , were used, these are inserted with a random spacing of between 250 and 500mm. The cross fracturing is restricted to within each layer of bedding and are randomly distributed. The fracture pattern in the area of interest is shown in Figure 8. This figure also shows the artificial blocky model used to include the influence of face crushing. The blocks in this system are defined in such a way that vertical movements result in bulking of the face rather than in a lockup of stresses caused by pairs of blocks that jam against each other over the width of the stope.

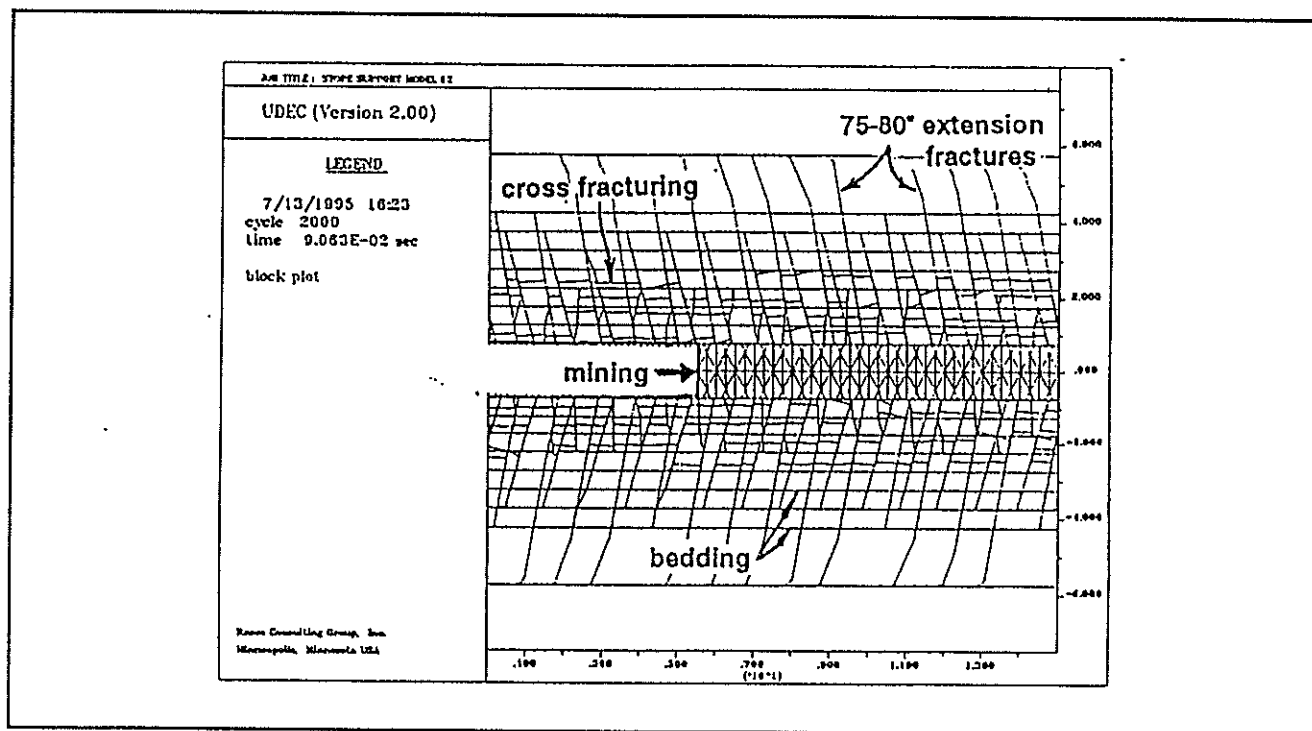


Figure 8 Final model : area of interest

The UDEC data that defines this geometry is given below

```

* STOPE MODEL GEOMETRY DEFINITION
* 0.5m bedding
new
title
STOPE SUPPORT MODEL
ro 0.06
*
* Main Problem domain
bl -30,-80 -30,80 80,80 80,-80
*
* split for gridding
cr -30, 10.00 50, 10.00
cr -30, 20.00 50, 20.00
cr -30, 30.00 80, 30.00
cr -30, 50.00 80, 50.00
cr -30,-10.00 50,-10.00
cr -30,-20.00 50,-20.00
cr -30,-30.00 80,-30.00
cr -30,-50.00 80,-50.00
cr 30, 30.00 30,-30.00
cr 40, 10.00 40,-10.00
cr 50, 50.00 50,-50.00
cr 60, 80.00 60,-80.00
cr 20, 10.00 22, 0.00
cr 20,-10.00 22, 0.00
*
* faults for dynamic runs hw
cr 0.0, 10.0 0.0, 30.0
cr 10.0, 10.0 10.0 30.0
cr 20.0, 10.0 20.0, 30.0
cr 0.0, 19.8 20.0, 19.8
cr 20.0,19.8 29.8,10.0
cr 20.0,20.0 30.0,10.0
cr 5.0,14.0 5.0,25.0
cr 15.0,14.0 15.0,25.0
cr 0.0,10.0 10.0,19.8
cr 0.0,30.0 10.0,20.0
cr 10.0,10.0 20.0,19.8
cr 10.0,30.0 20.0,20.0
cr 10.0,10.0 0.0,19.8
cr 10.0,30.0 0.0,20.0
cr 10.0,20.0 20.0,30.0
cr 20.0,10.0 10.0,19.8
cr 20.0,20.0 10.0,30.0
cr 20.0,20.0 30.0,30.0

```

```

cr 20.0,10.0 30.0,20.0
cr 20.0,30.0 30.0,20.0
*
* faults for dynamic runs fw
cr 0.0,-10.0 0.0,-30.0
cr 10.0,-10.0 10.0 -30.0
cr 20.0,-10.0 20.0,-30.0
cr 0.0,-19.8 20.0,-19.80
cr 29.8,-10.0 29.8,-10.00
cr 20.0,-19.8 29.8,-10.0
cr 20.0,-20.0 30.0,-10.0
cr 5.0,-14.0 5.0,-25.0
cr 15.0,-14.0 15.0,-25.0
cr 0.0,-10.0 10.0,-19.8
cr 0.0,-30.0 10.0,-20.0
cr 10.0,-10.0 20.0,-19.8
cr 10.0,-30.0 20.0,-20.0
cr 10.0,-10.0 0.0,-19.8
cr 10.0,-30.0 0.0,-20.0
cr 10.0,-20.0 20.0,-30.0
cr 20.0,-10.0 10.0,-19.8
cr 20.0,-20.0 10.0,-30.0
cr 20.0,-20.0 30.0,-30.0
cr 20.0,-10.0 30.0,-20.0
cr 20.0,-30.0 30.0,-20.0
*
* faults ahead of face
cr 29.8, 10.0 29.8,-10.00
*
* Slope
cr -30,-0.75 50,-0.75 ; slope footwall
cr -30, 0.00 30, 0.00 ; slope centre
cr -30, 0.75 50, 0.75 ; slope hangingwall

* Bedding
cr -30,-5.75 30,-5.75 ; lower bedding plane 9
cr -30,-4.25 22,-4.25 ; lower bedding plane 8
cr -30,-3.75 30,-3.75 ; lower bedding plane 7
cr -30,-3.25 22,-3.25 ; lower bedding plane 6
cr -30,-2.75 50,-2.75 ; lower bedding plane 5
cr -30,-2.25 22,-2.25 ; lower bedding plane 4
cr -30,-1.75 30,-1.75 ; lower bedding plane 3
cr -30,-1.25 22,-1.25 ; lower bedding plane 2
*
cr -30, 1.25 22, 1.25 ; upper bedding plane 2
cr -30, 1.75 30, 1.75 ; upper bedding plane 3
cr -30, 2.25 22, 2.25 ; upper bedding plane 4
cr -30, 2.75 50, 2.75 ; upper bedding plane 5
cr -30, 3.25 22, 3.25 ; upper bedding plane 6
cr -30, 3.75 30, 3.75 ; upper bedding plane 7
cr -40, 4.25 22, 4.25 ; upper bedding plane 8
cr -30, 5.75 30, 5.75 ; upper bedding plane 9
*
* slope crushing
jreg -7,-0.7 -7,0.7 17,0.7 17,-0.7
jset 63.435,0 100,0 0,0 0.4472,0 0,0
jset 116.565,0 100,0 0,0 0.4472,0 0,0
jreg -7.1,-0.75 -7.1,.75 16.75,.75 16.75,-.75
jset 90,0 1.5,0 0,0 0.5,0 0,-0.75
jset 90,0 1.5,0 5,0 0.5,0 0.25,-0.75
jreg -12,-0.7 -12,0.7 -7,0.7 -7,-0.7
jset 63.435,0 100,0 0,0 0.8944,0 0,0
jset 116.565,0 100,0 0,0 0.8944,0 0,0
jreg -24.1,-0.75 -24.1,.75 -7.2,0.75 -7.2,-.75
jset 90,0 1.5,0 0,0 1.0,0 0,0
cr -27,-0.75 -27,0.75
*
* hangingwall fractures
jreg -5,0.75 -3,5.60 16,5.60 17,0.75
jset 100,.2 100,0 0,0 1,0.0 10.0,0.75 ;80deg
jreg -5,0.75 -3,3.75 16,3.75 17,0.75
jset 105,.1 100,0 0,0 1,0.01 10.6,0.75 ;75deg
jreg -1,0.75 1,2.20 14,2.20 15,0.75
jset 88,.2 100,0 0,0 .8,0.01 10.3,0.75 ;92deg
jreg -4,4.50 -4,5.75 18,5.75 17,4.50
jset 110,.1 100,0 0,0 .3,0.01 10.3,0.75 ;70deg
*
* footwall fractures
jreg -3,-5.60 -5,-0.75 17,-0.75 16,-5.60
jset 80,0.2 100,0 0,0 1.0,0.0 10.0,-0.75
jreg -3,-3.75 -5,-0.75 17,-0.75 16,-3.75
jset 75,0.1 100,0 0,0 1.0,0.01 10.6,-0.75
jreg 1,-2.20 -1,-0.75 15,-0.75 14,-2.20
jset 92,0.2 100,0 0,0 0.8,0.01 10.3,-.75
jreg -4,-5.75 -4,-4.50 17,-4.50 18,-5.75
jset 70,0.1 100,0 0,0 0.3,0.01 10.3,-0.75
*
* additional fracturing
* hangingwall
jreg -3,0.85 -3,1.15 16,1.15 16,0.85
jset 179,1 0.8,0 0.10,0.1 0.3,.05 5.0,1.00 3
jreg -3,1.35 -3,1.65 16,1.65 16,1.35

```

```

jset 179,1 0.8,0 0.10,0.1 0.3,.05 5.0,1.50 3
jreg -3,1.85 -3,2.15 15,2.15 15,1.85
jset 179,1 0.8,0 0.10,0.1 0.3,.05 5.0,2.00 3
jreg -3,2.35 -3,2.65 15,2.65 15,2.35
jset 179,1 0.8,0 0.10,0.1 0.3,.05 5.0,2.50 3
* footwall
jreg -3,-1.15 -3,-0.85 16,-0.85 16,-1.15
jset 1,1 0.8,0 0.10,0.1 0.3,.05 5.0,-1.00 -3
jreg -3,-1.65 -3,-1.35 16,-1.35 16,-1.65
jset 1,1 0.8,0 0.10,0.1 0.3,.05 5.0,-1.50 -3
jreg -3,-2.15 -3,-1.85 15,-1.85 15,-2.15
jset 1,1 0.8,0 0.10,0.1 0.3,.05 5.0,-2.00 -3
jreg -3,-2.65 -3,-2.35 15,-2.35 15,-2.65
jset 1,1 0.8,0 0.10,0.1 0.3,.05 5.0,-2.50 -3
*
jdel
ret

```

### 4.3 Material and joint properties

So as to be able to treat the rockmass as deformable a mesh of finite difference zones needs to be defined in all blocks. The zoning should be as fine as possible near the slope but at the boundaries it can be coarse. For dynamic modelling it is best to have a constant zone size throughout the model but this is impractical for large models where some areas require small zones. The transition between coarse and fine zoning should be as smooth as possible particularly if dynamic loading is to be applied. In this model a total of close to 10000 zones are defined. The data used to construct this finite difference mesh is given below.

```

* zoning
* Deformable block regions
gen -20,20 -2.75, 2.75 edge 0.71
gen -30,20 -3.75, 3.75 edge 1.0
gen -30,30 -5.75, 5.75 edge 2.0
gen -20,50 5, 10 edge 2.5
gen -30,50 -10, -5 edge 2.5
gen -30,30 10, 20 edge 3.0
gen -30,30 20, 30 edge 3.5
gen -30,30 -20,-10 edge 3.0
gen -30,30 -30,-20 edge 3.5
gen 30,40 -20, 20 quad 3.5
gen 30,50 -30, 30 edge 4.5
gen -30,50 30, 50 quad 6.5
gen -30,50 -50,-30 quad 6.5
gen 50,60 -50, 50 quad 6.5
gen 60,80 -80, 80 quad 10.0
gen -30,60 -80,-50 quad 10.0
gen -30,60 50, 80 quad 10.0

```

The rock material behaviour was modelled using Mohr Coulomb plasticity over the entire domain, except in the back areas where a ubiquitous joint model was assigned. The ubiquitous joint model is based on the Mohr-Coulomb plasticity model. The ubiquitous jointing is simply a preferential direction for slip to occur, this direction being given by the joint angle. In this application of the ubiquitous joint model the “joints” represent fractures, the properties on the joints should therefore be equal to those of the rockmass. To assist in ensuring that failure first takes place on the “joints” the properties assigned to the ubiquitous joints are slightly lower than those assigned to the rock. The material properties used are those obtained for quartzite from laboratory testing. It is common practice to down grade material properties for use in modelling work, this is done to take into account the discontinuous nature of the in-situ rock, in this model the discontinuities are modelled explicitly and therefore no reduction in strength properties is applied. The following are the material data used.

```

* Mohr Coulomb continuum rock (Quartzite) -----
prop mat=3 d=3000 g=29e9 k=39e9 ; E=70GPa nu=0.2
prop mat=3 fric=25 coh=72e6 ten=10e6 dil=5
prop mat=3 jkn=400e9 jks=300e9
prop mat=3 jfric=20 jcoh=65e6 jten=10e6 jdil=5
change -30,80 -80,80 mat=3 cons=3 jcons=5
*
* Ubiquitous joints in back areas-----
* hangingwall
zone r -30,0 -30,5.75 -3,5.75 -5,0 model=ub &
bu=39e9 sh=29e9 fric=25 coh=72e6 ten=12e6 dil=5 &
jangle=105 jfric=20 jcoh=65e6 jten=10e6
* footwall
zone r -30,-5.75 -30,0 -5,0 -3,-5.75 model=ub &
bu=39e9 sh=29e9 fric=25 coh=72e6 ten=12e6 dil=5 &
jangle=75 jfric=20 jcoh=65e6 jten=10e6

```



There are three types of discontinuities used in the model, those that represent potential fractures, those that represent bedding planes and those that are necessary to construct the model. Those representing fractures are given strength properties similar to those of the rock, some dilation is assigned to take into account the fact that these discontinuities are smooth straight lines whereas in practice fracture surfaces may be rough and are not usually perfectly straight. The joint behaviour is modelled with a constitutive model that records yield. The cohesion on the joint is reduced to zero after yield, this mimics fracturing. The bedding planes are assumed to be weak and more inclined to dilate than fractures. Those crack lines introduced purely for the purposes of constructing the model, and which have no real physical meaning, are effectively glued and the fracturing constitutive model is not applied. When large deformations and movement of blocks occur new block contact points are defined, default properties are used at these points. The joint property data used is listed here.

```
* Joint (potential fracture) properties -----
prop jmat=4 jkn=400e9 jks=300e9
prop jmat=4 jfric=20 jcoh=65e6 jten=10e6 jdil=5
change -30,80 -7,7 jmat=4 jcons=5
*
* Bedding planes
prop jmat=5 jkn=400e9 jks=300e9
prop jmat=5 jfric=10.0 jcoh=10e6 jten=4e6 jdil=10
change -30,80 -6.9,6.9 angle -1 1 jmat=5 jcons=5
*
* Glued planes
prop jmat=5 jkn=400e9 jks=300e9
prop jmat=6 jfric=75.0 jcoh=2000e6 jten=2000e6 jdil=0
change -30,80 6.99,80.0 jmat=6 jcons=2
change -30,80 -80.00,-6.99 jmat=6 jcons=2
change 30,80 -7.00, 9.5 angle 89,91 jmat=6 jcons=2
*
* default joint properties
prop jmat=7 jkn=400e9 jks=300e9
prop jmat=7 jfric=20.0 jcoh=0e6 jten=0e6 jdil=5
*
set jmatdf=7 jcondf=5
```

### 4.3 Boundary and initial conditions

The stope that is considered is at a depth of approximately 2000m where in-situ stresses of 50 MPa in the vertical, y, direction and 25 MPa in the horizontal, x, direction (k ratio = 0.5) are typical of those that would be acting in virgin rock on a South African gold mine. The effects of gravity are included in the model, the stresses, therefore, vary over the model. Initial stresses that take into account these variations and maintain the k ratio are applied over the full domain.

Modelling has been restricted to considering a single stope in an infinite rockmass, the influence of any other mining is ignored. The boundary and initial conditions are used to include the influence of depth and the confining influence of the rock on the model. The use of symmetry has already been mentioned in section 2.3, the symmetry condition is applied on the left hand side of the model by simply stopping the boundary from moving in the horizontal, x, direction. The effects of confining stresses could have been applied to the remaining boundaries either by fixing these boundaries or by applying stresses. If only stresses are applied they have to be kept in equilibrium with the total weight of the rock modelled because the model would not have been fixed in the y direction and since material is removed the boundary stresses applied to the bottom boundary would need to vary. It is therefore more convenient to fix the bottom boundary in the y direction. The choice of method for the remaining top and right hand side boundaries is somewhat arbitrary. The choice of stresses results, in a slight over estimation of displacements. Fixing them in the y and x direction respectively results in an underestimation of displacements. These errors are made small by ensuring that the boundary of the model is sufficiently far from the excavation.

The data used to apply the initial and boundary conditions is listed below. It includes some calculation cycles, these ensure that all the applied values are initialised and equilibrated correctly; this is important in any very blocky model as small strains occur due to the slight interpenetration of blocks that is needed to produce the appropriate stresses on discontinuities. During this consolidation phase stress boundary conditions are applied to the top and right hand side of the model. After consolidation these two conditions are replaced with y fixity

and x fixity respectively. The left-hand side condition is also re-applied to ensure that at the corner points the correct boundary conditions are specified.

```
* Initial conditions
set grav 0,-10
ins st -25e6 0 -50e6   yg 15e3 0 30e3   szz=-32.5e6   zg= 0 22.5e3
*
* boundary conditions
bo c 37 50 st -25e6 0 -50e6   yg 15e3 0 30e3   top
bo c 50 63 st -25e6 0 -50e6   yg 15e3 0 30e3   rhs
bo c 24 37 xvel=0
bo c 63 24 yvel=0
*
* Consolidation
cy 500
* rest boundary conditions
bo c 37 50 yvel=0
bo c 24 37 xvel=0
bo c 50 63 xvel=0
cy 1500
```

## 4.4 Mining history

The history of the mining influences the deformation and generation of stresses in the rockmass surrounding the stope, modelling of this process is therefore fundamental to obtaining correct deterioration of the rockmass and loading of support units. For the purposes of modelling mining is made up of a sequence of excavations that advance the face and the installation and removal of supports. The mining is assumed to be a quasi-static process, that is, a process where the behaviour being modelled is to a large extent independent of inertial effects. The calculations which UDEC performs are based on the full equations of motion, a quasistatic solution is obtained by applying damping and allowing enough cycles to run for all velocities to become zero. Such a state of equilibrium must be found at the end of each excavation step before supports are installed.

### 4.4.1 Excavation

Blast loading and any associated fracturing is not taken into account, excavation is modelled simply by instantaneously removing the rock in the reef plane. In UDEC removal of material is done by deleting blocks; this can be done in one of two ways: by specifying a region to be deleted or by specifying each block by number. The first of the two methods is easy to use but leads to problems when applied to this model. It is therefore necessary to delete blocks by number. These numbers change whenever adjustments to the geometry are made. A method of automating the normally tedious process of determining this data, was developed. The list of delete commands required for each face advance are stored in a separate file, this makes the generation of mining sequence data simpler.

### 4.5.2 Supports

Three types of support have been used, packs, backfill and hydraulic props. The force displacement data for each support type used is stored in a separate file. The width of supports is specified when they are installed in the mining sequence discussed below.

#### *Packs*

The packs modelled are typical 1.1m x 1.1m solid Mat packs. The properties used for these packs are those recorded in the support catalogue compiled as part of this project. These laboratory values have been down graded by 30% to take into account differences in behaviour between laboratory and underground conditions. The packs forces are further adjusted for the dip spacing of 3m (2m skin to skin), this adjustment has been discussed in section 2.3. The data for these packs is given below and plotted in Figure 9.

```
* File = pack3.mat
* Pack support units 3m dip spacing
prop mat=9 kn=-9
; Solid Matpack (1.1x1.1) Ref KG PS AUG9003.rsp
; Degraded for UG installation (30%)
; Degraded for 3m dip spacing (1/3)
table 9 0,0 0.06,47e4 0.2,93e4 0.6,163e4 1.0,163e4
ret
```

The installation of packs was done with commands similar to the following.

```
support (-3.5,0) width=1.1 seg=21 mat=9 ; pack
```

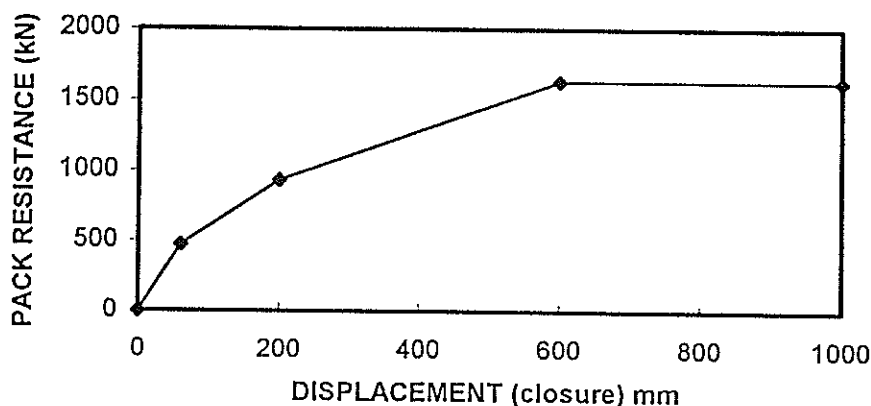


Figure 9 Pack data (down graded for 3m dip spacing)

### Backfill

Some results were obtained for models where backfill was used as back area support. Fill stiffness characteristics of classified tailings with 46% porosity were applied. This type of fill is typical of that used in much of the industry and in-situ performance data was available from a paper written by Gurtunca and Adams (1991). The response of backfill is strain related hence the data required an adjustment to make it applicable for use in the 1.5m stope width modelled. The data used is presented below and plotted in Figure 10.

```
* File back46.dat
* Classified tailings 46% porosity
prop mat=9 kn=-9
* Ref : Gurtunca RG and Adams DJ
; A rock-engineering monitoring programme at West Driefontein Gold Mine
; SA Inst Min Metall vol 91 no 12 (1991) p423-433 [Figure 12]
;
* Adjusted for 1.5m stope width from strain)
tab 9 0,0 0.015,0 0.12,3e6 0.16 6e6 0.19,9e6 0.218,12e6 0.2,15e6 0.26,18e6 0.345,30e6
*
ret
```

The installation of backfill was done with commands similar to the following.

```
support (-4.5,0) width=0.948 seg=19 mat=9 ; backfill
support (-4.5,0) width=0.948 seg=19 mat=9 ; backfill
```

The width of .0948 ensures that adjacent backfill installations result in an even distribution of the support sub elements that represent the fill.

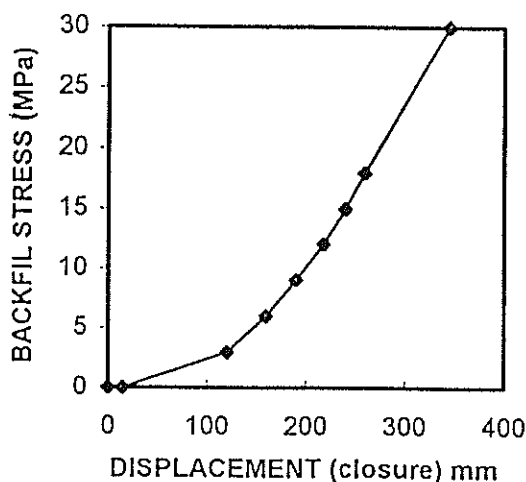


Figure 10 Backfill data

### Hydraulic props

The characteristics of hydraulic props were used for all the support units inserted as temporary face area support. The shape of the force displacement curve, illustrated in Figure 11 was held constant but the maximum force delivered was varied as required for the parameter studies. This characteristic was chosen as the simple behaviour makes these changes meaningful. The force displacement curves for other timber supports used in the industry include the effects of many different aspects of prop failure, these do not necessarily scale in a simple way. Data for typical 20t hydraulic support units are given below.

```
* file = hprop20.dat
* Hydraulic support units 20t
  prop mat=8 kn=-1 ; (kn in table 1 below)
  ; static only max travel 300mm
  ; Unfactored assumed 1m dip spacing
. table 1 0,0 .0001,150e3 .025,200e3 0.3,200e3 0.4,0 2,0
*
ret
```

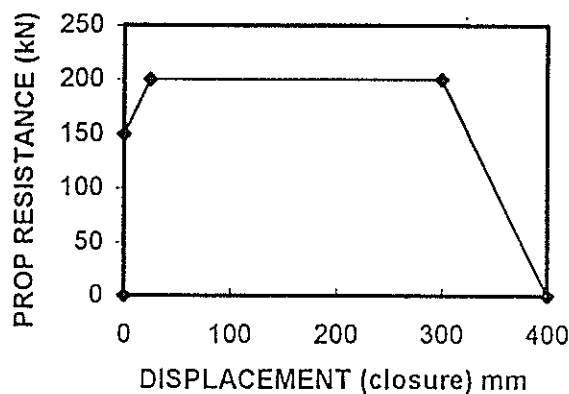


Figure 11 Typical prop data : 20t units

The installation of props was done with commands similar to the following.

```
support (3,0) width=0.2 seg=19 mat=8 ; prop
```

for a standard unit, and

```
support (3,0) width=0.8 seg=19 mat=8 ; prop
```

for a unit with a 800mm long head board.

### Head boards

The use of head boards was modelled by simply increasing the width specified for a given support unit, as is indicated above. In UDEC support units are represented by a set of sub-units each generating a part of the total resistance. Each sub-unit acts completely independently its resistance being derived from the force displacement data by looking up the force in the table corresponding to the sub-unit deformation and dividing it by the number of sub-units. Local yielding can therefore take place at some point along the width of the support without effecting the way in which the remainder of the support behaves. A poor representation of long head boards is obtained because the bending stiffness of head boards cannot be taken into account. Alternative methods of modelling supports with head boards were investigated using local models but these alternatives either proved ineffective or too cumbersome to implement in large models designed to be applied to many different support configurations.

### Supports under dynamic loading

At the start of the project it was noted that the dynamic response of support units could not be modelled with UDEC. Itasca was therefore contracted to develop a method of including a loading rate dependant support unit model. This work was completed and incorporated in a proprietary version of UDEC 1.83 during the first

year of the project. A detailed description of this model is given in a report on this development work (Itasca 1993). Unfortunately this model was not included in UDEC version 2 which was subsequently released and which is currently being used; it has therefore not been used. A copy of the source code for the rate dependent model is also available.

#### 4.4.3 Mining of the back areas

Detailed modelling of the excavation of the entire back area does not need to be done. The influence of temporary support is not included in the mining of the first 30m of the stope, detailed modelling of the skin of the excavation which these supports influence is in any event absent in this part of the model. In the case of both packs and backfill a maximum face to permanent support distance of 6m was maintained. Initially the face was advanced by 6m, this was reduced to 2m and then to 1m after a total of 12m of the back area excavation. With the exception of the first mining step a minimum face to permanent support distance of 3m was used with packs and of 4m with backfill. The packs were installed at 3m centres and the backfill placed over 2m at a time. A face advance of 1m per mining step was maintained for the remainder of the excavation of the stope including the excavation in the area of interest where the blockiness of the rockmass is modelled.

#### 4.4.4 Mining of the area of interest

As realistic as possible a mining sequence was modelled during the mining of the stope between a half span of 30 and 42m. The detail of each sequence depends on the spacing of supports being used. Strike spacings of 1m, 2m and 3m between support units were used. The minimum support to face distance was held constant at 2m for all three cases which resulted in maximum support to face distances of 3m, 4m and 5m for each of these support configurations respectively. The area of interest spans 12m, this allows any influence, that a given support configuration may have on stress and deformation history, to be accumulated before assessment of the system is made. Included in the modelling of mining history is the removal of some props and installation of either packs or backfill required to maintain the permanent support to face distances indicated above.

An example of the UDEC input data used to define mining in the area of interest is presented below, this data is for face area support spacing of 2m and permanent support consisting of backfill.

```
* EXCAVATE AND INSERT SUPPORTS AT 2m centres
* Back area support = backfill
* Face area support element properties = 20t props no load spreaders
  call hprop20.dat
-----
  support (-5.5,0) width=0.948 seg=19 mat=9 ; backfill
  support (-4.5,0) width=0.948 seg=19 mat=9 ; face of fill at 26m

* step 01 =====
  call ef.d01 ; excavate face to 31m
  call efstep.dat
  call efstep.dat
  save efbf2h20s.s01
* step 02 =====
  call ef.d02 ; excavate face to 32m
  call efstep.dat
  call efstep.dat
  save efbf2h20s.s02
  support (-3.5,0) width=0.948 seg=19 mat=9 ; backfill
  support (-2.5,0) width=0.948 seg=19 mat=9 ; face of fill at 28m
* step 03 =====
  call ef.d03 ; excavate face to 33m
  call efstep.dat
  call efstep.dat
  save efbf2h20s.s03
* step 04 =====
  call ef.d04 ; excavate face to 34m
  call efstep.dat
  save efbf2h20s.s04
  support ( 2.0,0) width=.2 seg=20 mat=8 ; prop
  call efstep.dat
  support (-1.5,0) width=0.948 seg=19 mat=9 ; backfill
  support (-0.5,0) width=0.948 seg=19 mat=9 ; face of fill at 30m
* step 05 =====
  call ef.d05 ; excavate face to 35m
  call efstep.dat
  call efstep.dat
  save efbf2h20s.s05
```

```

* step 06 =====
call ef.d06                               ; excavate face to 36m
call efstep.dat
save efbf2h20s.s06
support ( 4.0,0) width=.2 seg=20 mat=8    ; prop
call efstep.dat
support ( 2.0,0) rem
support (0.5,0) width=0.948 seg=19 mat=9  ; backfill
support (1.5,0) width=0.948 seg=19 mat=9  ; face of fill at 32m
* step 07 =====
call ef.d07                               ; excavate face to 37m
call efstep.dat
call efstep.dat
save efbf2h20s.s07
* step 08 =====
call ef.d08                               ; excavate face to 38m
call efstep.dat
save efbf2h20s.s08
support ( 6.0,0) width=.2 seg=20 mat=8    ; prop
call efstep.dat
support ( 4.0,0) rem
support ( 2.5,0) width=0.948 seg=19 mat=9 ; backfill
support ( 3.5,0) width=0.948 seg=19 mat=9 ; face of fill at 34m
* step 09 =====
call ef.d09                               ; excavate face to 39m
call efstep.dat
call efstep.dat
save efbf2h20s.s09
* step 10 =====
call ef.d10                               ; excavate face to 40m
call efstep.dat
save efbf2h20s.s10
support ( 8.0,0) width=.2 seg=20 mat=8    ; prop
call efstep.dat
support ( 6.0,0) rem
support ( 4.5,0) width=0.948 seg=19 mat=9 ; backfill
support ( 5.5,0) width=0.948 seg=19 mat=9 ; face of fill at 36
* step 11 =====
call ef.d11                               ; excavate face to 41m
call efstep.dat
call efstep.dat
save efbf2h20s.s11
* step 12 =====
call ef.d12                               ; excavate face to 42m
call efstep.dat
call efstep.dat
support (10.0,0) width=.2 seg=20 mat=8    ; prop
save efbf2h20s.s12
call efstep.dat
call efstep.dat
save efbf2h20s.sfs
return

```

In this data the files ef.d01, ef.d02 etc. contain the commands required for excavation of the each 1m face advance. The file efstep.dat contains the step command that defines the number of cycles used for each quasi-static step in the analysis.

#### 4.5 Dynamic Loadings

The state of equilibrium attained at the end of the quasistatic analysis is used as the basis for consideration of dynamic loading. The analysis of seismic waves impinging on the face area of the excavation requires changes to the boundary conditions and the removal of damping. The crude method of generating a seismic loading is to apply a pressure pulse to the interior of a slot created in the rockmass. The pressure pulse is of limited duration and its intensity is varied in a sinusoidal manner, the curve that defines the pressure load multiplier is shown in Figure 12. This pulse has a duration of 1.5 milli-seconds (msec), the a data point is defined at every 0.05 msec. This data is stored in a file (bm.d01) that is read when the loading is applied.

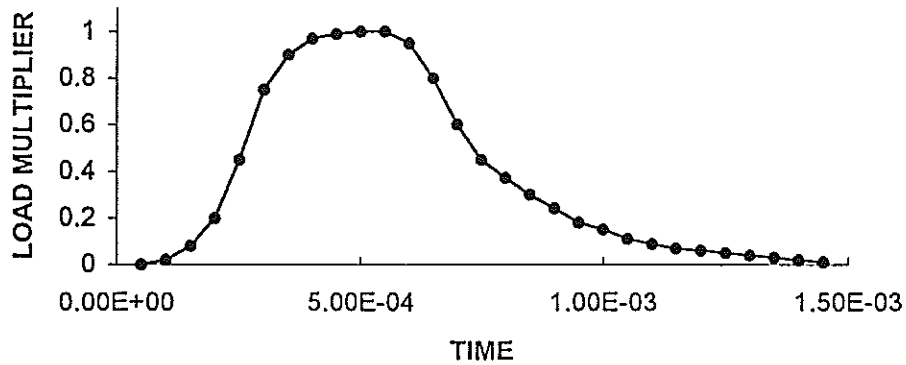


Figure 12 Load multipliers for application of dynamic loading

An abbreviated listing of the data used to generate a simulation of a seismic event is given below.

```

* file PBUMPl.a.dat
* Dynamic Analysis / Seismic Event Simulation
* Open slot
del blo 8116 7541 8547
* Apply pressure loading
bou hread 50 bm.d01
bou in -2,22 18,22 stress -50e6 0 -800e6 his 50
* Change boundary conditions to quiet
bou c 37 50 xvi yvi m=2
bou c 50 63 xvi yvi m=2
* apply Raleigh damping
damp 0.01 50 ; 1% 50 Hz
* Start dynamic time
reset time
* Define geophones
reset his
his yv 10.5 5
his yv 10.5 3
.
.      cfc
.
.-----
set vga
call bump.dmv
sav Bla.s01
* reset slot loading
bou in -2,22 18,22 str -10e6 0 -30e6
sav Bla.s02
.
.      run, add movie frames and save at intervals
.
call bump.dmv
sav Bla.s10
ret

```

The monitoring of velocities at various points in the path of the wave generated by this artificial loading provide some insight into the characteristics of the event generated. Results obtained are described below.

## 5. RESULTS

### 5.1 Quasi-static analysis

The model described above was used to analyse the influence of a number of different support configurations on hangingwall stability. Trends in support performance were obtained by comparison of combinations of results obtained with all model parameters held constant except those of interest. These parameter studies are discussed in the next section of this document (section 6). Three main sets of runs were made for the final parameter studies, the basic model parameters varied were back area support type (packs and backfill) and bedding plane spacing (0.5m and 1m). In this section the results obtained for only a few selected examples are presented and described.

The analysis of each different support configuration requires considerable computer run time. The simulation of each metre of face advance requires approximately one and a half hours on the fast machine described earlier (section 3). The excavation of the first 30m is however identical for each support configuration making use of a given type of back area support system, hence the results of this part of the run are saved and used as a starting point for application of different face area support configurations. This first part of the mining simulation takes over 40 hours to run. The subsequent excavation and installation of supports in the area of interest, that is from a half span of 30m to 42m takes a further 16 hours, this phase must be repeated for each different system considered. Due to the high demand on computer resources the number of support configurations that could be considered was limited.

Each set of results consisted of at least nine different combinations of the face area support parameters spacing and support unit force. Further runs were made to investigate the influence of different load spreader lengths. In the case of the 1m spacing a total of four units are installed in the 6m face area (measured on strike). Support unit forces of 5t, 10t and 20t were of prime interest, these giving total support forces of 20t, 40t and 80t. Since the two-dimensional model represents a 1m wide section, on dip, the total hangingwall area supported is 6m<sup>2</sup>, hence the above support configurations have average resistances of 33kN/m<sup>2</sup>, 66kN/m<sup>2</sup> and 133kN/m<sup>2</sup>, respectively. In the case of 2m spacing, two units are installed in the same face area. Support unit forces of 10t, 20t and 40t give the same set of total support forces, and hence average resistances, 33kN/m<sup>2</sup>, 66kN/m<sup>2</sup> and 133kN/m<sup>2</sup>, as those generated with the 1m spacing configurations. With the 3m spacing a single support is used in the face area, support unit forces were again chosen to produce average resistances of 33kN/m<sup>2</sup>, 66kN/m<sup>2</sup> and 133kN/m<sup>2</sup>, these being 20t, 40t and 80t units.

Little information is available for verification of results. Closure is perhaps the most commonly monitored parameter characterising rockmass behaviour around stopes. Measured closure rates include components of both time dependent rockmass behaviour and closure associated purely with face advance. The model does not take into account time dependant behaviour, hence the closures predicted with the model can be expected to be less than those measured underground. Closures of between 20mm and 90mm/m of face advance were estimated at a distance of up to approximately 10m from the face in the areas where the fracture mapping described in section 3.2 was carried out. The closure predicted by the model in the area of interest fall in the lower part of this range; closures predicted in the back area are however low. Some attempts to measure hangingwall stresses have also been made. Horizontal stresses of the order of 5 to 10MPa appear to be typical of those that have been measured in the immediate hangingwall of stopes mined in bedded strata. Modelling results show considerable variation in hangingwall stress within in the hangingwall. The horizontal stresses predicted are in general rather high with values of between 20MPa and 30MPa being generated 1m into hangingwall in most cases. Some further tuning of material properties, in particular a reduction in the angle of dilation, is still needed to improve this aspect of the models performance.

Three groups of results, typical of those obtained in each of the main studies indicated above, are described below. For each example a contour plot of the vertical displacement, y-displacement, and a tensor plot of principal stresses are presented; note that negative stresses are compressive. These plots show a view that is limited to the detail in the face area, unfortunately the black and white reproduction of the original colour plots



are not very clear but the main aspects of variations in displacement and stress can still be seen. These and other similar plots have been used to make an assessment of hangingwall stability described in section 6.1.

The first study considered was one for which a bedding plane spacing of 0.5m was modelled and back area support of packs at 3m centres on both dip and strike was used. Figure 13 shows the results obtained with out any temporary support having been used in the face area; this result is used as a reference for normalisation of all other results. In this case no blocks actually fall out but many have loosened considerably; this is indicated by changes in contour values of displacements. Some opening on the first bedding has also taken place. Very low but compressive stresses are obtained in blocks in the first half metre section of the hangingwall. This result reflects the observation that in general the hangingwalls of typical stopes with steep dipping fractures do not often collapse under normal static conditions even in the absence of face support, however, it also indicates that while the hangingwall remains intact it may be fairly unstable and that, in practice, signs of instability may not necessarily be seen from examination of the surface of the hanging wall. Figures 14, 15 and 16 show results obtained with 20t support units at spacings of 1m, 2m and 3m respectively. Note how displacements in the skin of the excavation are significantly reduced by use of these moderately high unit resistances at low spacings, in particular see Figure 14. Note, however, that there is a slight tendency for face stresses to increase with improved hanging wall conditions, this aspect of the modelling requires further investigation and some changes to the representation of face crushing are recommended, see section 7. The final result presented in this study, Figure 17, is that with the same support configuration as that in Figure 15 but with the support resistance of 20t being spread over 800mm rather than the 200mm used in all other cases. Differences in Figures 15 and 17 reflect the influence of load spreaders, note how the clamping stresses in the skin of the hangingwall are improved and opening on the first bedding plane is reduced. The support and rockmass condition shown in Figure 15 are those used as the initial conditions for the dynamic analysis described in section 5.2.

The second group of results was also obtained with the model that includes bedding planes at a spacing of 0.5m, but with the back area supported with backfill. The first result presented, Figure 18, is again the case where no face area support was installed. Comparison with Figure 13 indicates the positive influence that stiffer back area support has on stability of the face area. The other results presented for this case again show variation with support spacing but this time only those for spacings of 1m and 3m are shown, Figures 19 and 20 respectively. For these runs the support units used each have a resistance of only 5t. Note in particular how the clamping stresses in the skin of the hangingwall are enhanced and face stresses are reduced by the good distribution and greater total resistance of the temporary support as shown in Figure 19. The model does not show the development of any significant beam buckling instability which might have been expected as a result of the high horizontal stresses generated by the stiff back area support.

The final set of results shown are those for which a bedding plane spacing of 1m was modelled. The back area support used was the same as that used in the first set of results presented, that is, packs at 3m centres on both dip and strike. Figure 21, when compared to Figure 13 shows how the rockmass with wider bedding spacing is inherently more stable. The results shown in Figures 22 and 23, are again one example of variation of support spacing with the support unit resistance held constant, in this case at 20t. Comparison with the first group of results shows that in spite of the greater inherent stability of the rockmass the influence of support variations on the larger blocks in the skin of the excavation is a little less marked.

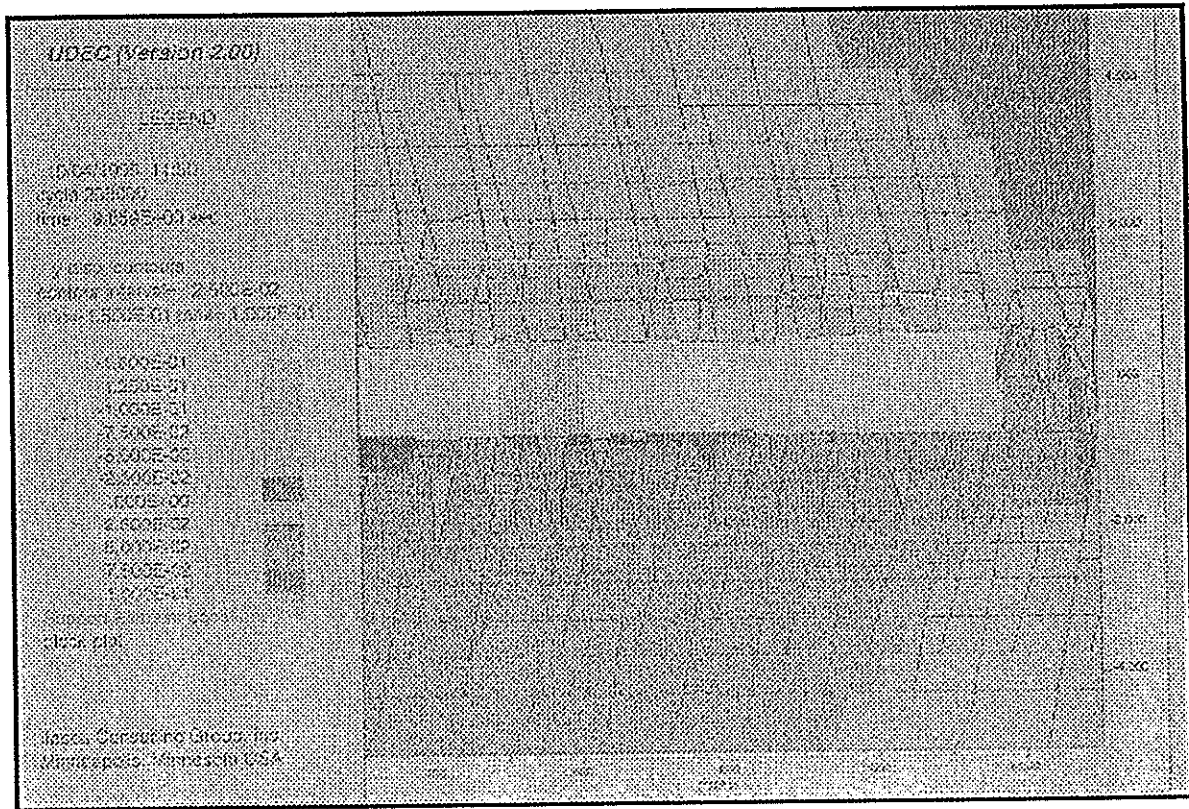


Figure 13(a) 0.5m bedding, packs, no face area support contours of y-displacement

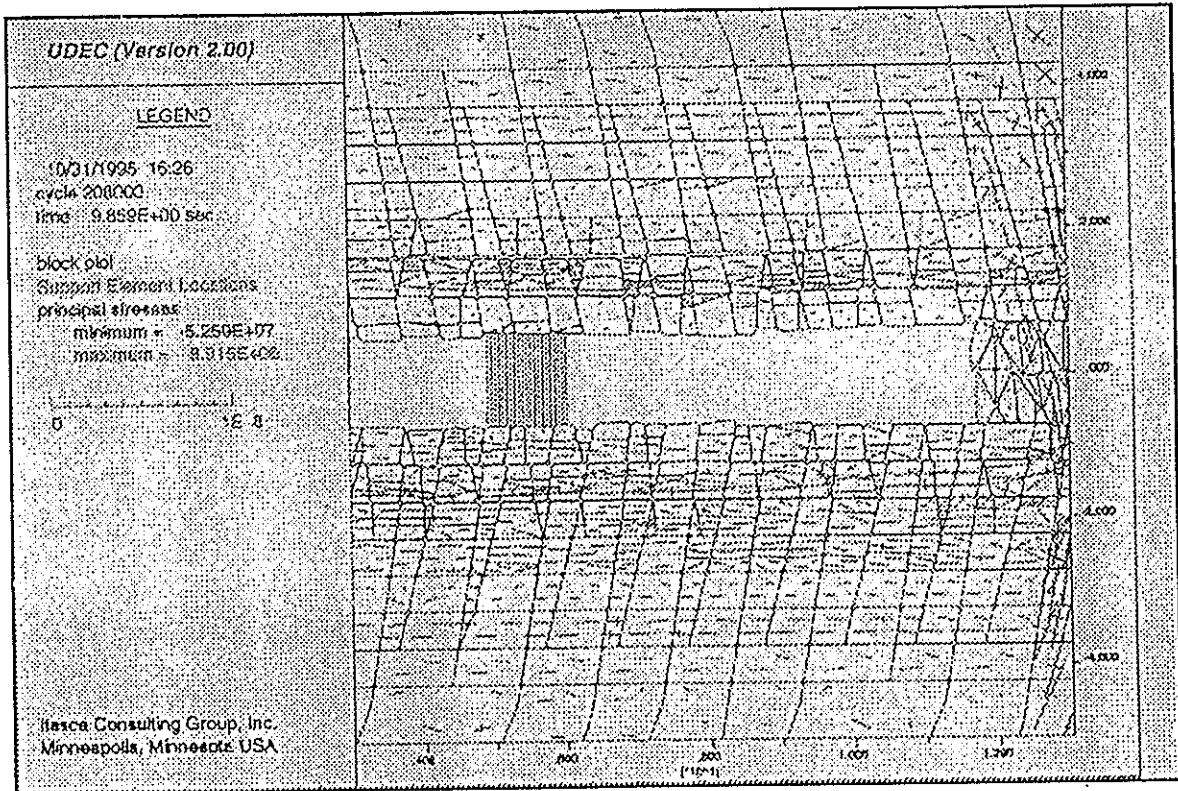


Figure 13(b) 0.5m bedding, packs, no face area support principal stress tensors

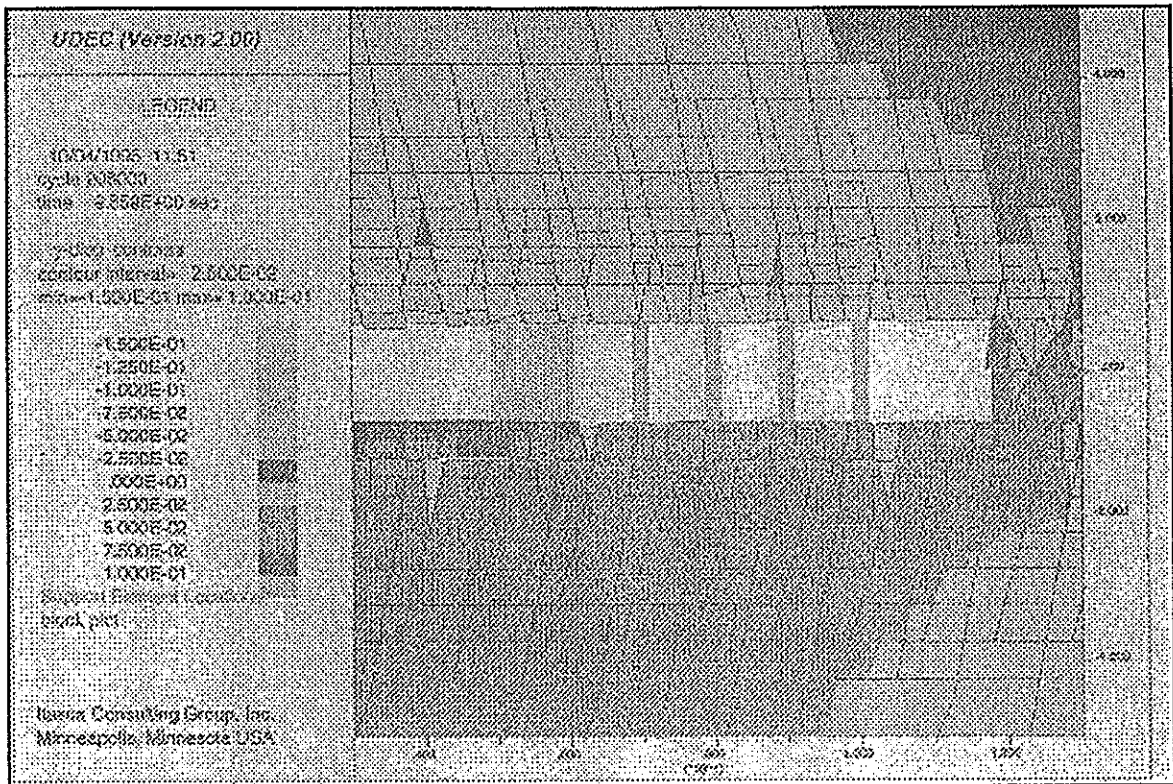


Figure 14(a) 0.5m bedding, packs, 20t units at 1m spacing contours of y-displacement

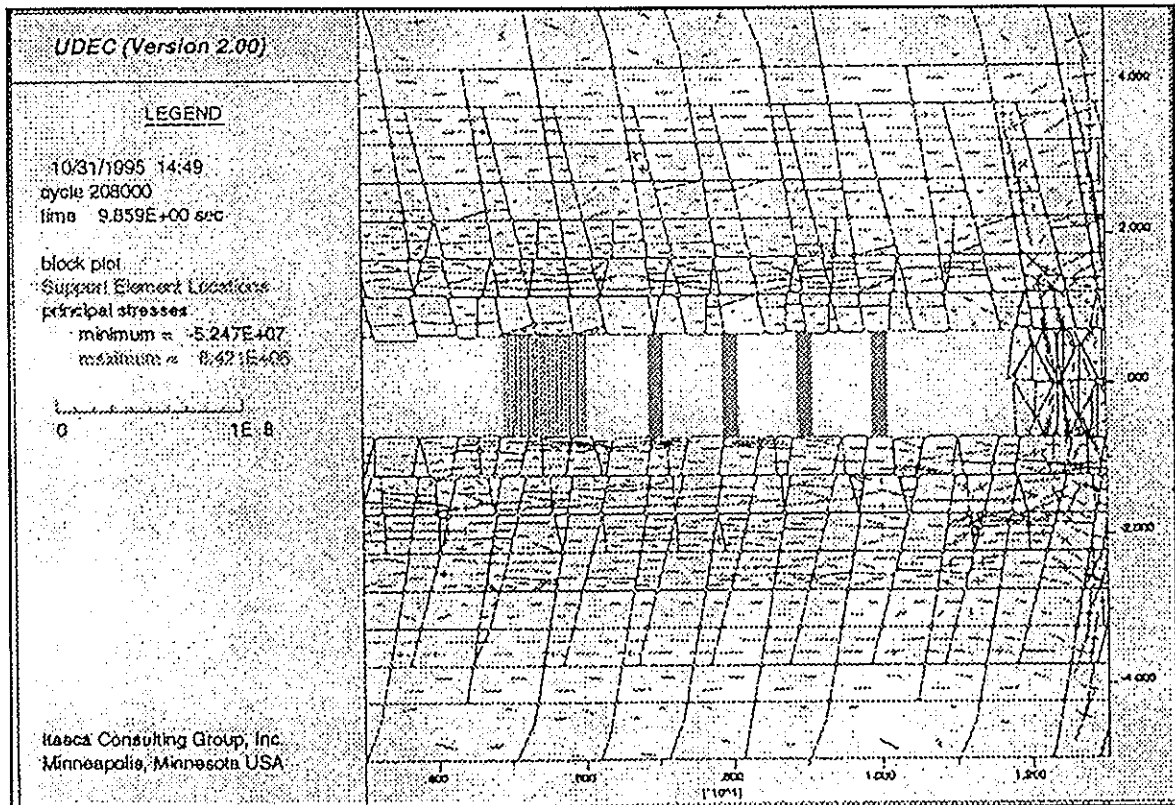


Figure 14(b) 0.5m bedding, packs, 20t units at 1m spacing principal stress tensors

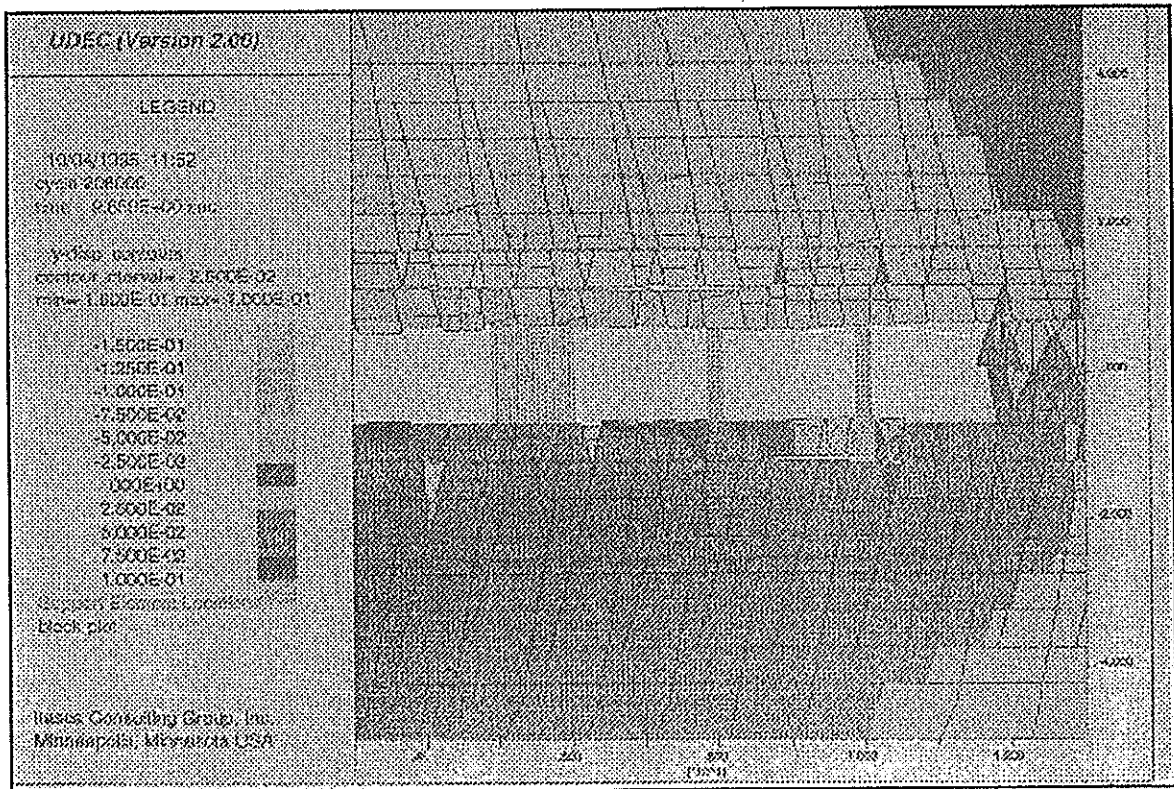


Figure 15(a) 0.5m bedding, packs, 20t units at 2m spacing contours of y-displacement

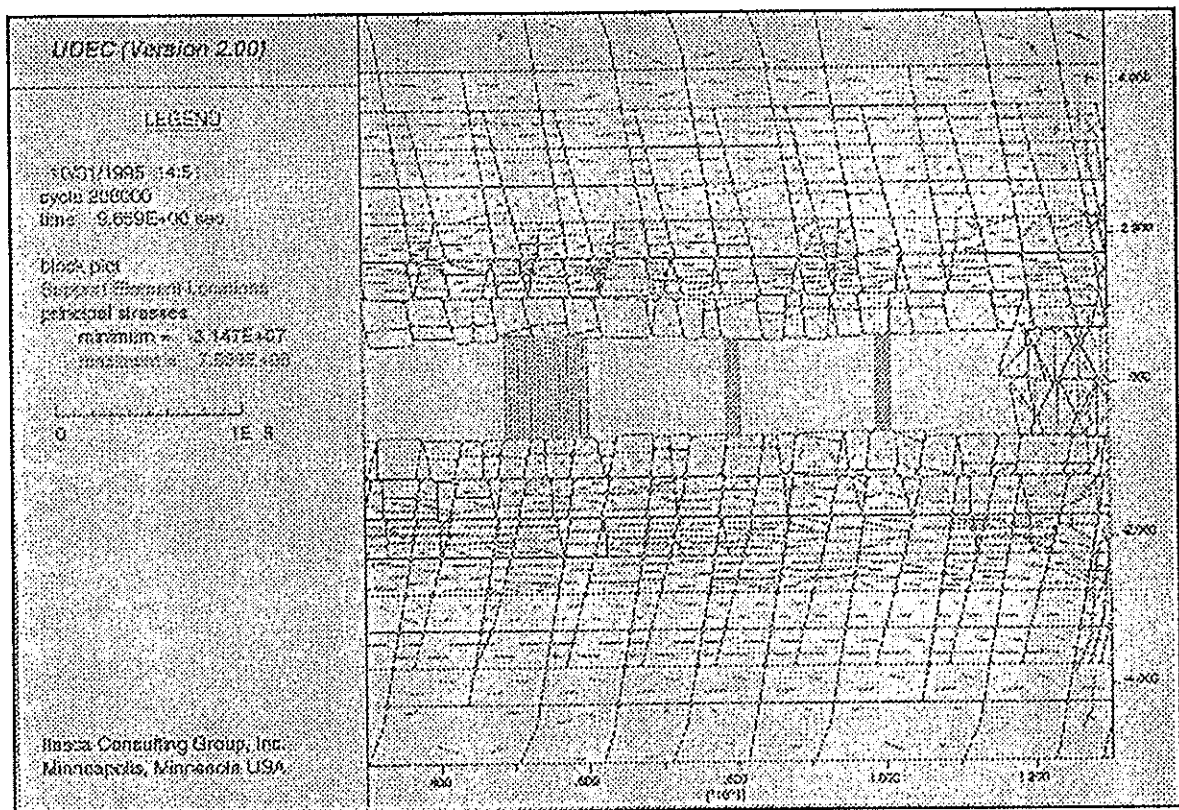


Figure 15(b) 0.5m bedding, packs, 20t units at 2m spacing principal stress tensors

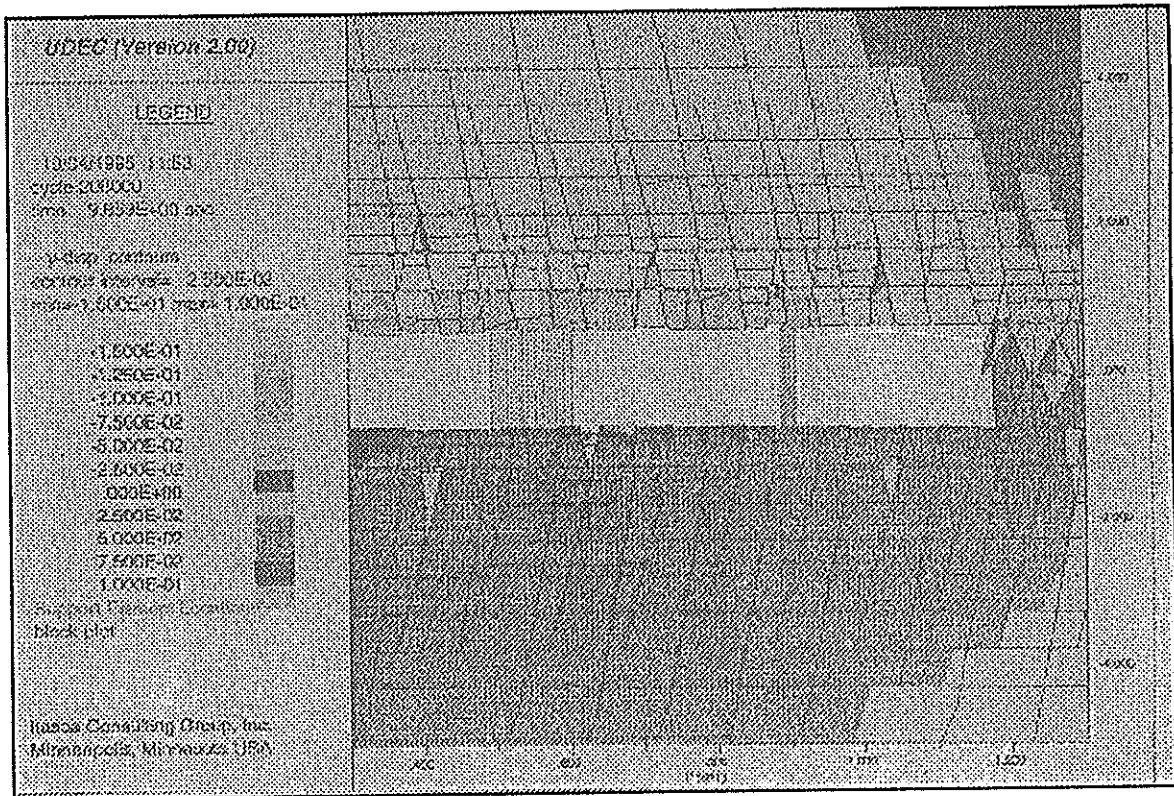


Figure 16(a) 0.5m bedding, packs, 20t units at 3m spacing contours of y-displacement

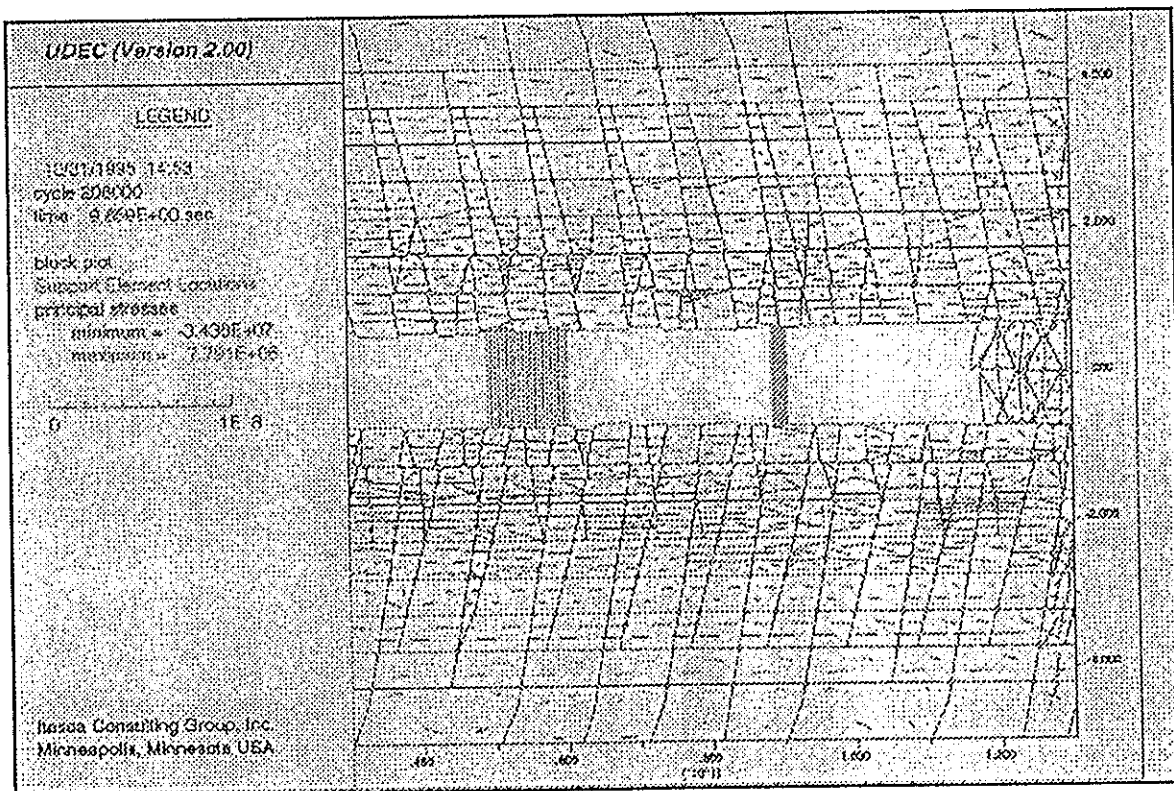


Figure 16(b) 0.5m bedding, packs, 20t units at 3m spacing principal stress tensors

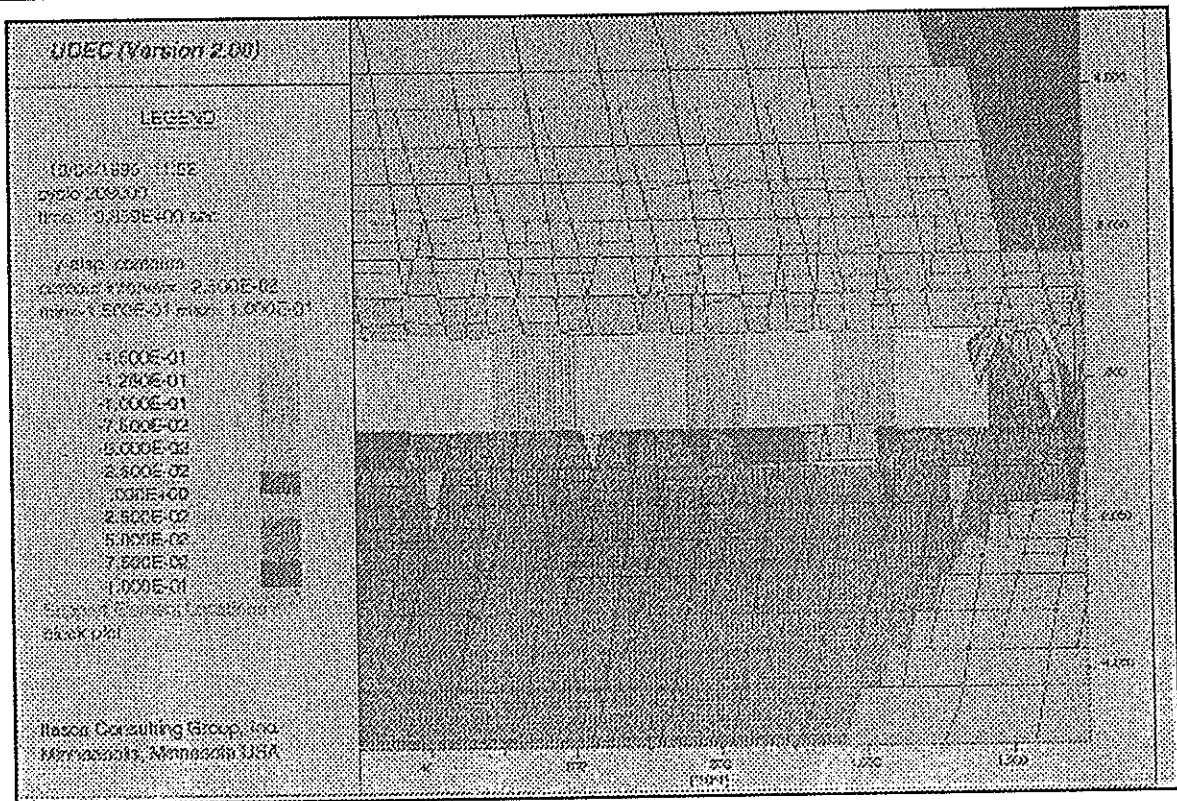


Figure 17(a) 0.5m bedding, packs, 20t units at 2m spacing, 800mm load spreaders contours of y-displacement

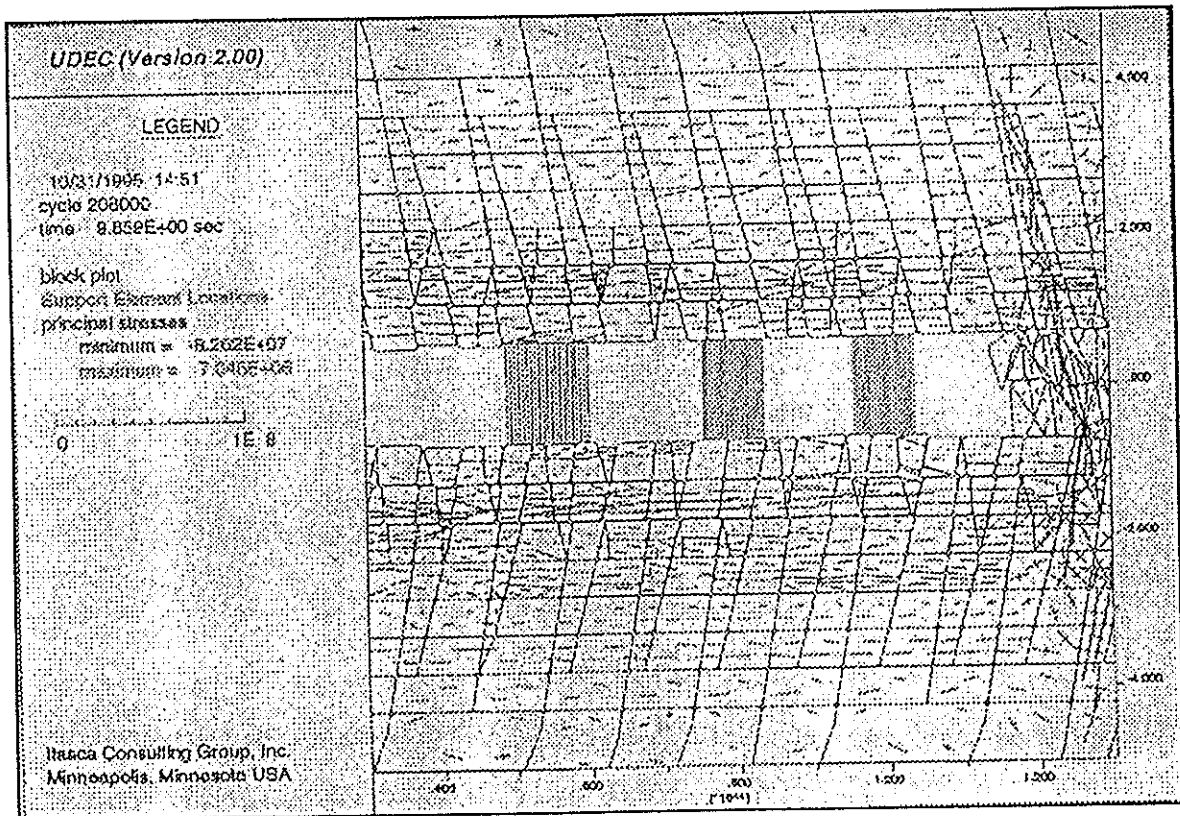


Figure 17(b) 0.5m bedding, packs, 20t units at 2m spacing, 800mm load spreaders principal stress tensors

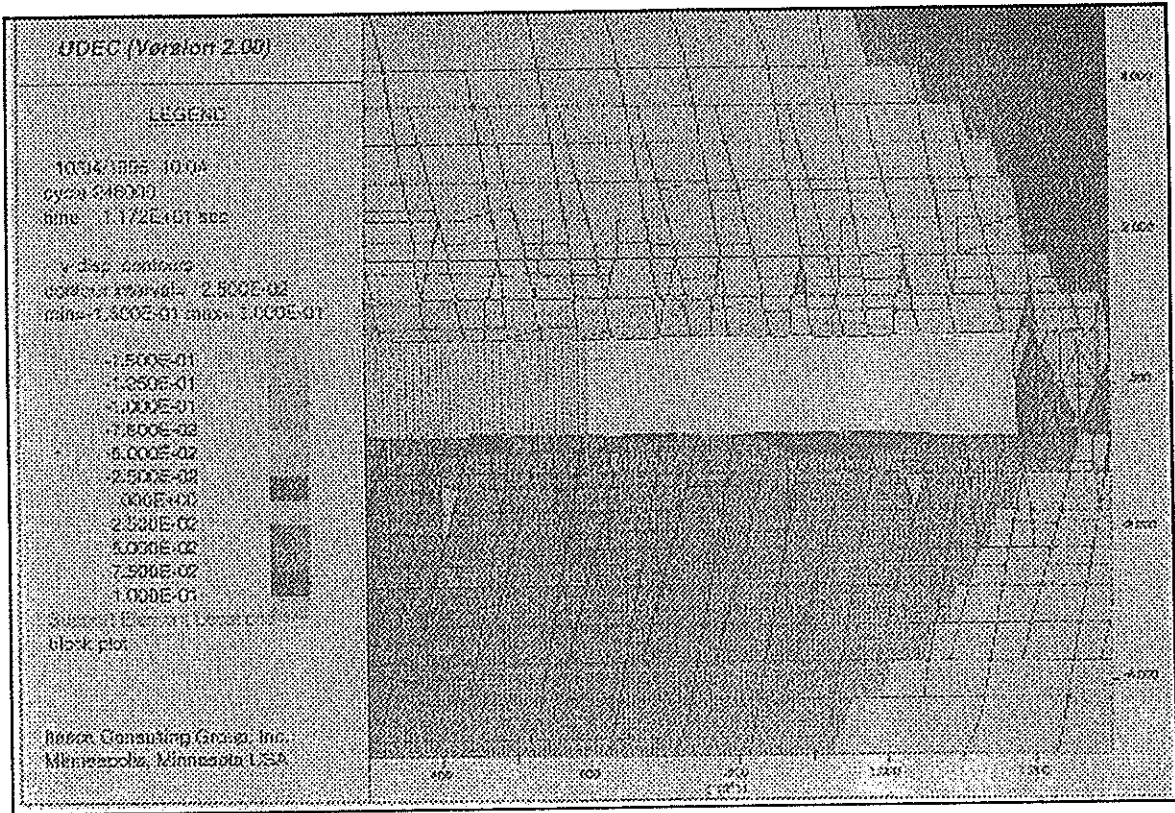


Figure 18(a) 0.5m bedding, backfill, no face area support contours of y-displacement

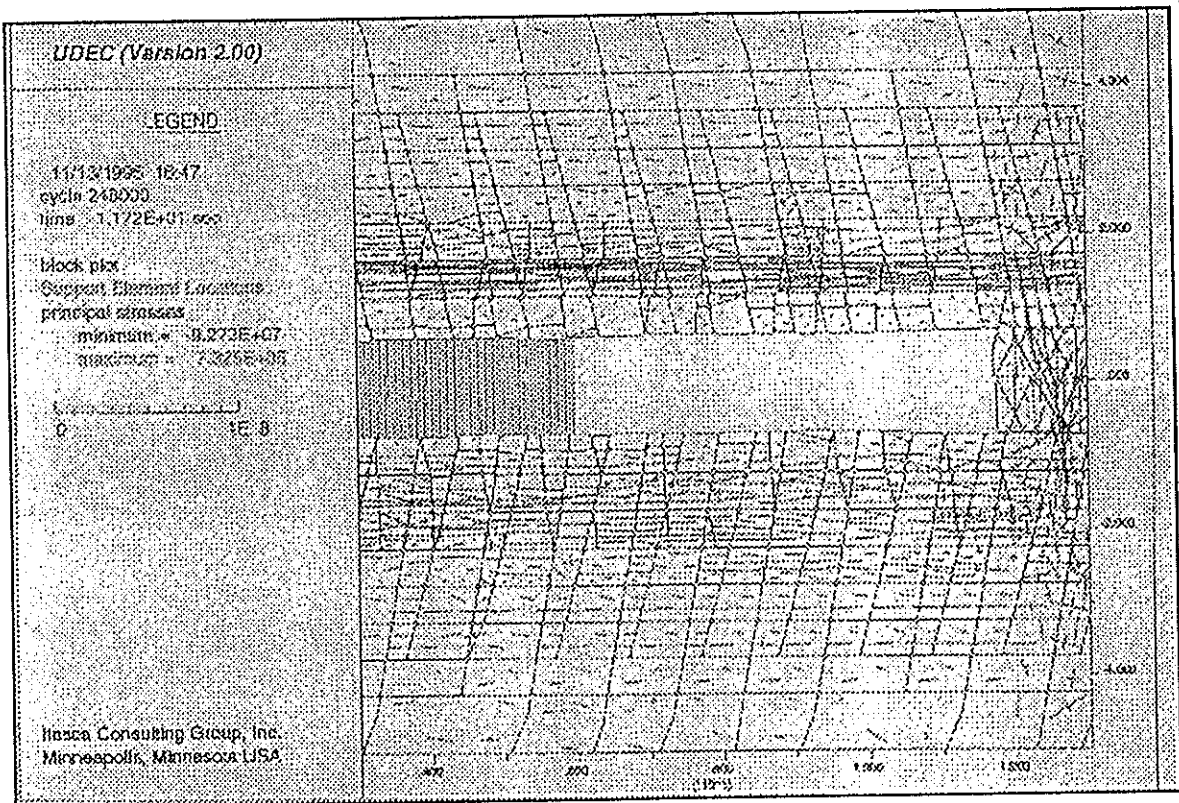


Figure 18(b) 0.5m bedding, backfill, no face area support principal stress tensors

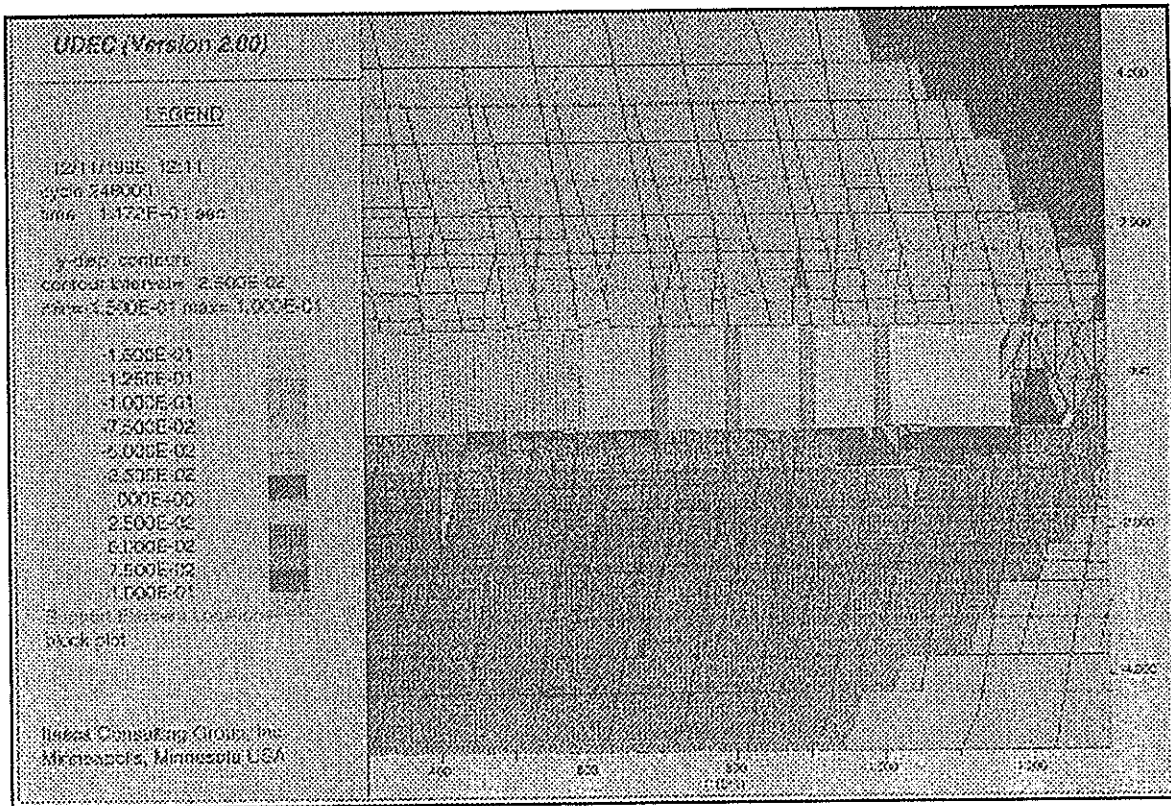


Figure 19(a) 0.5m bedding, backfill, 5t units at 1m spacing contours of y-displacement

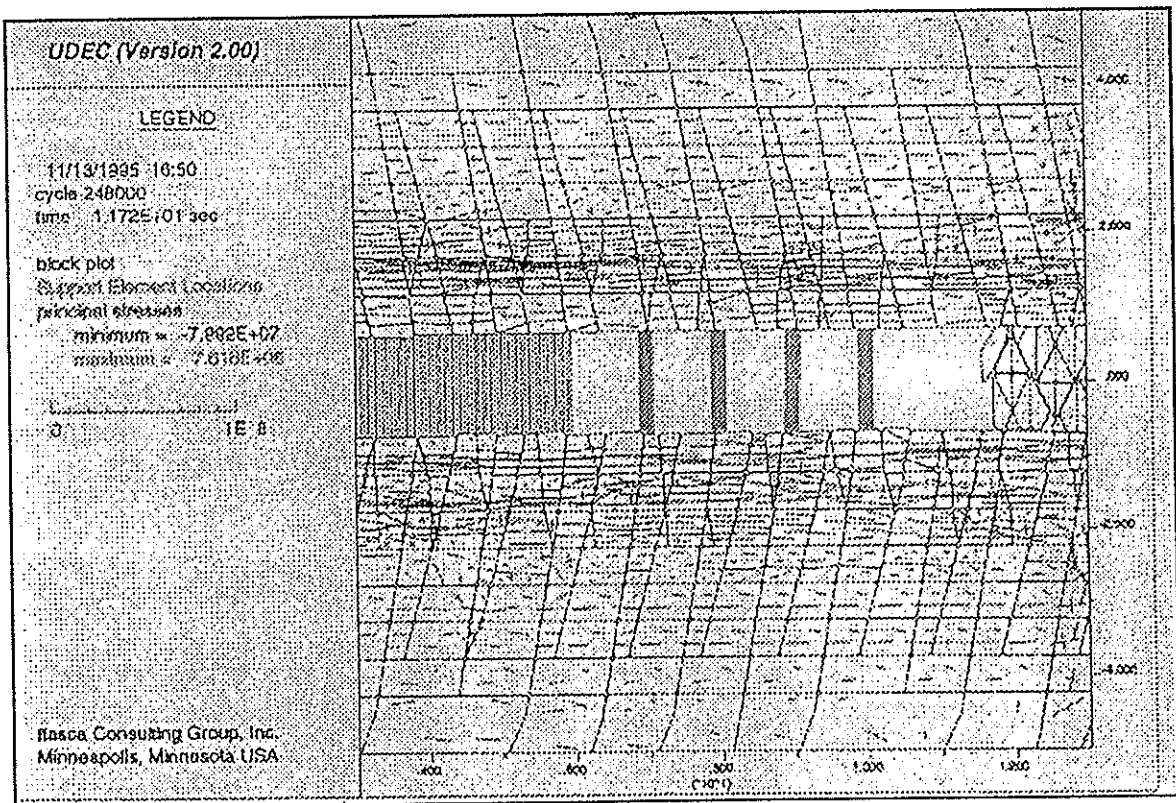


Figure 19(b) 0.5m bedding, backfill, 5t units at 1m spacing principal stress tensors



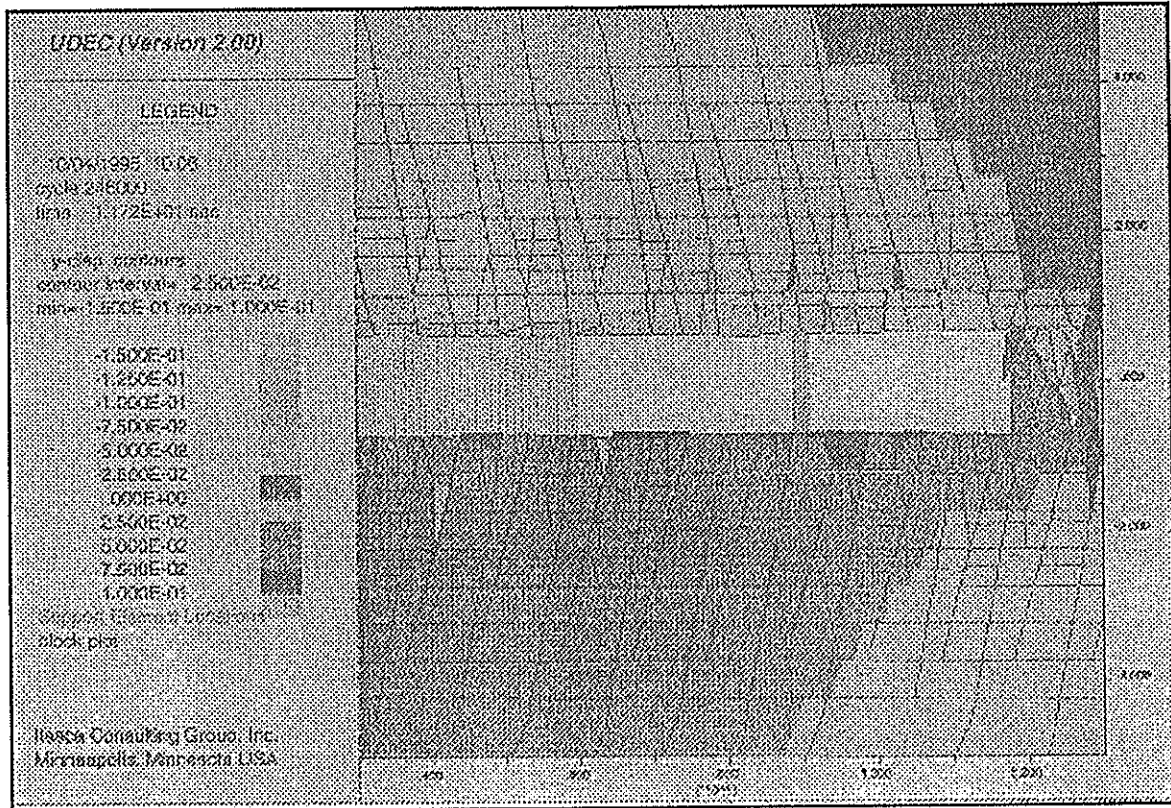


Figure 20(a) 0.5m bedding, backfill, 5t units at 1m spacing contours of y-displacement

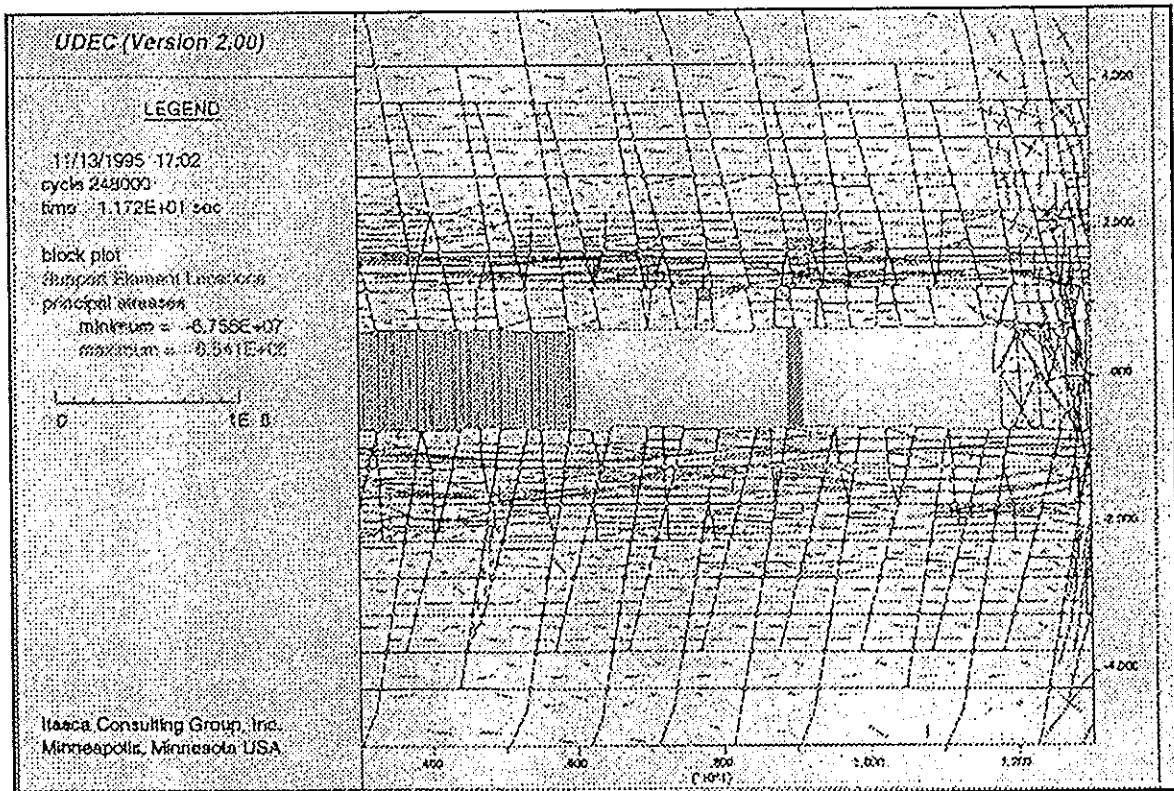


Figure 20(b) 0.5m bedding, backfill, 5t units at 3m spacing principal stress tensors

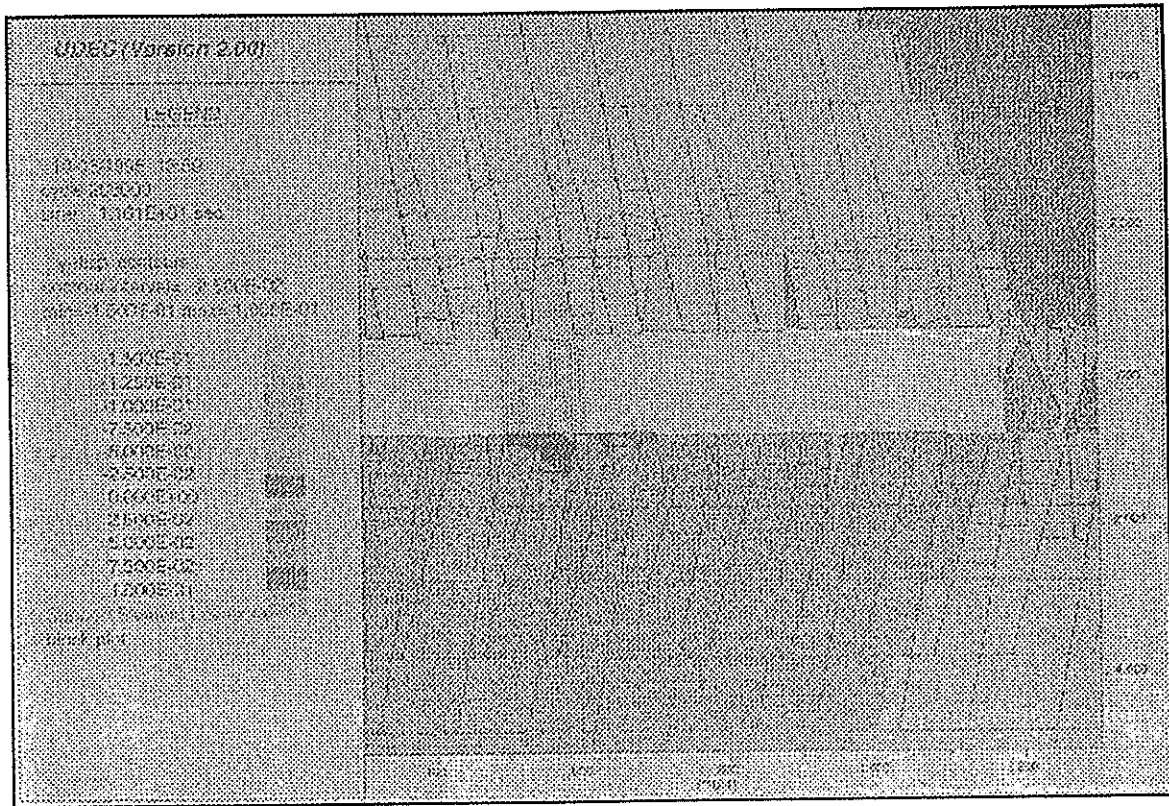


Figure 21(a) 1.0m bedding, packs, no face area support contours of y-displacement

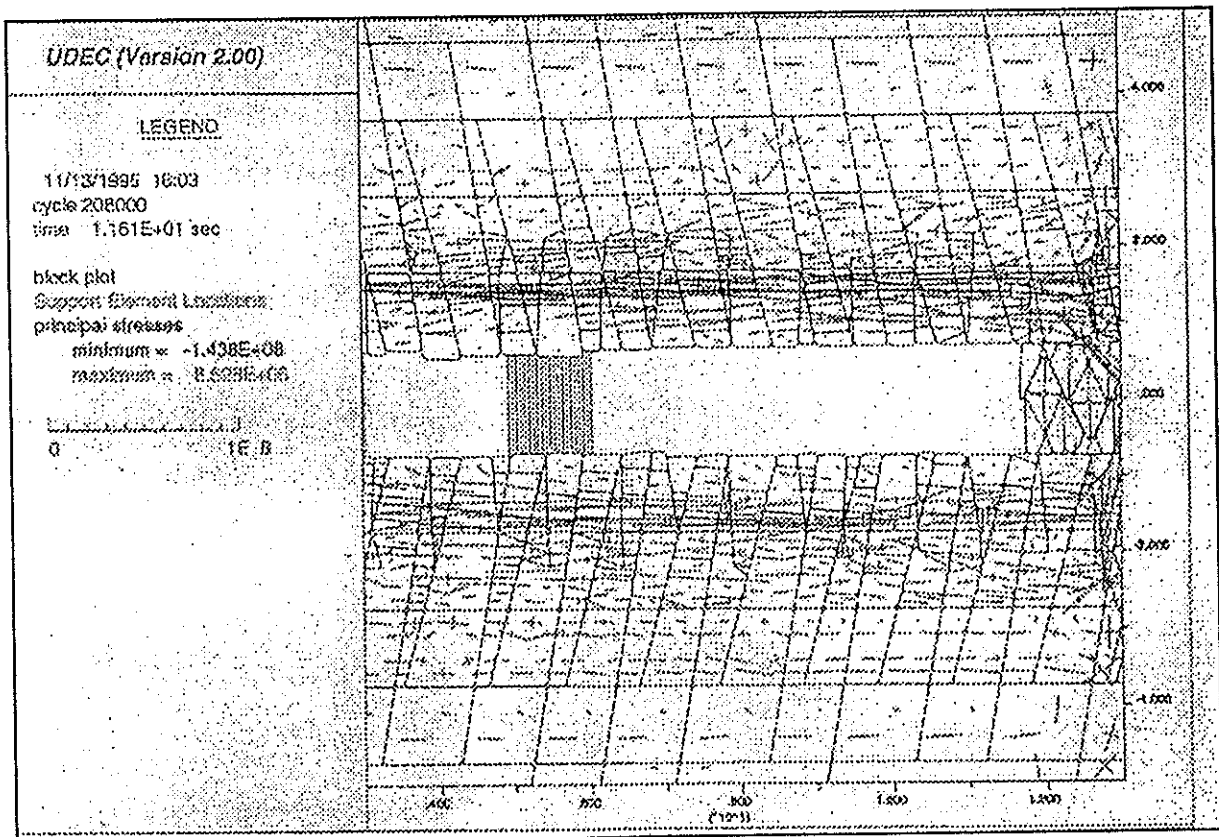


Figure 21(b) 1.0m bedding, packs, no face area support principal stress tensors

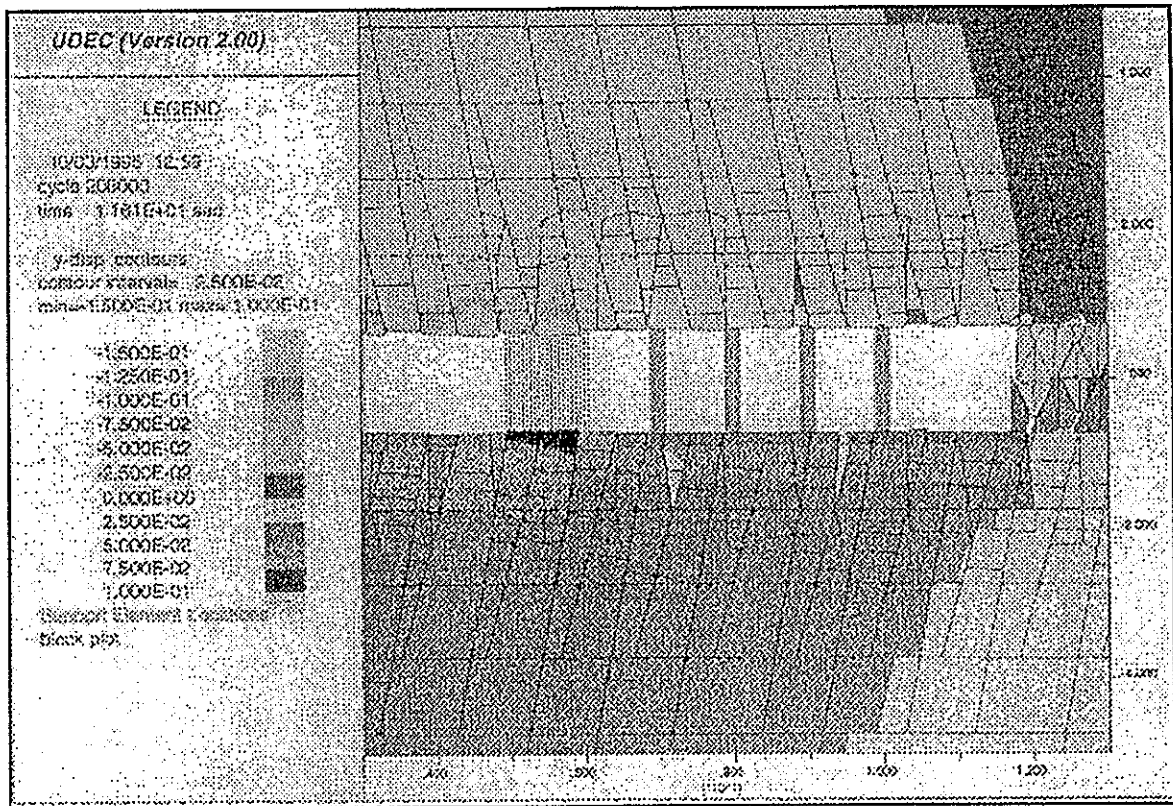


Figure 22(a) 1.0m bedding, packs, 5t units at 1m spacing contours of y-displacement

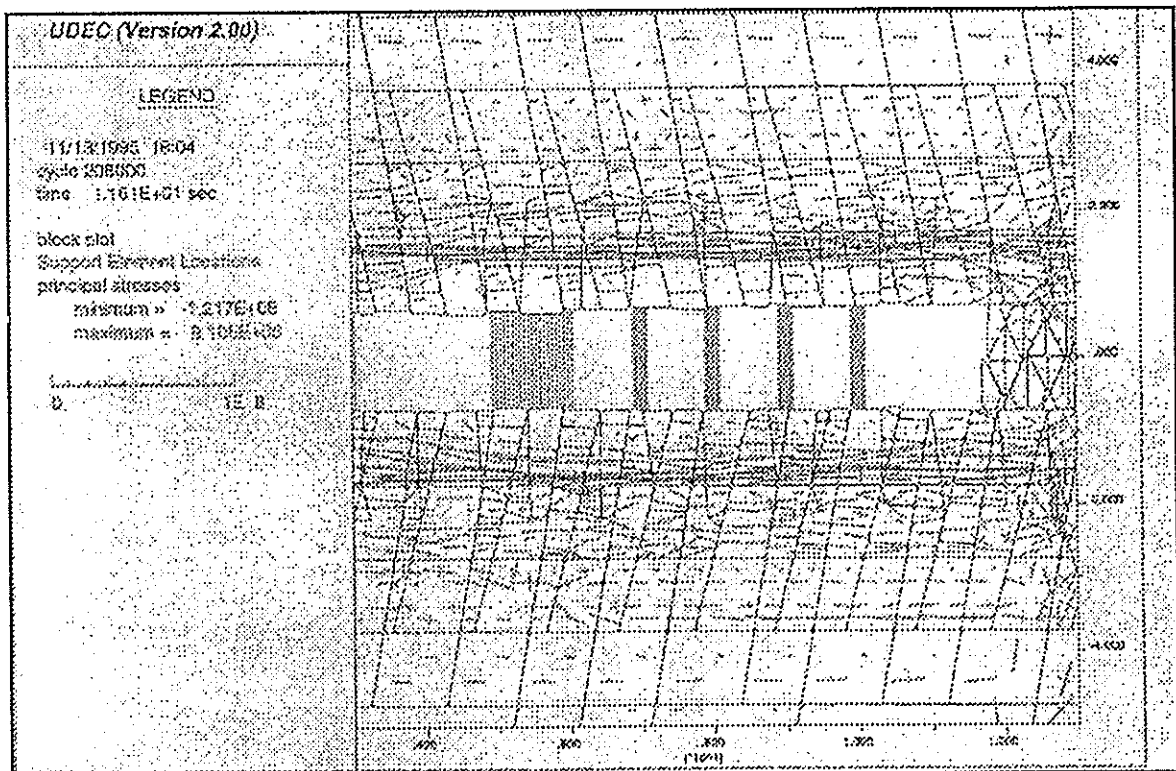


Figure 22(b) 1.0m bedding, packs, 20t units at 1m spacing principal stress tensors

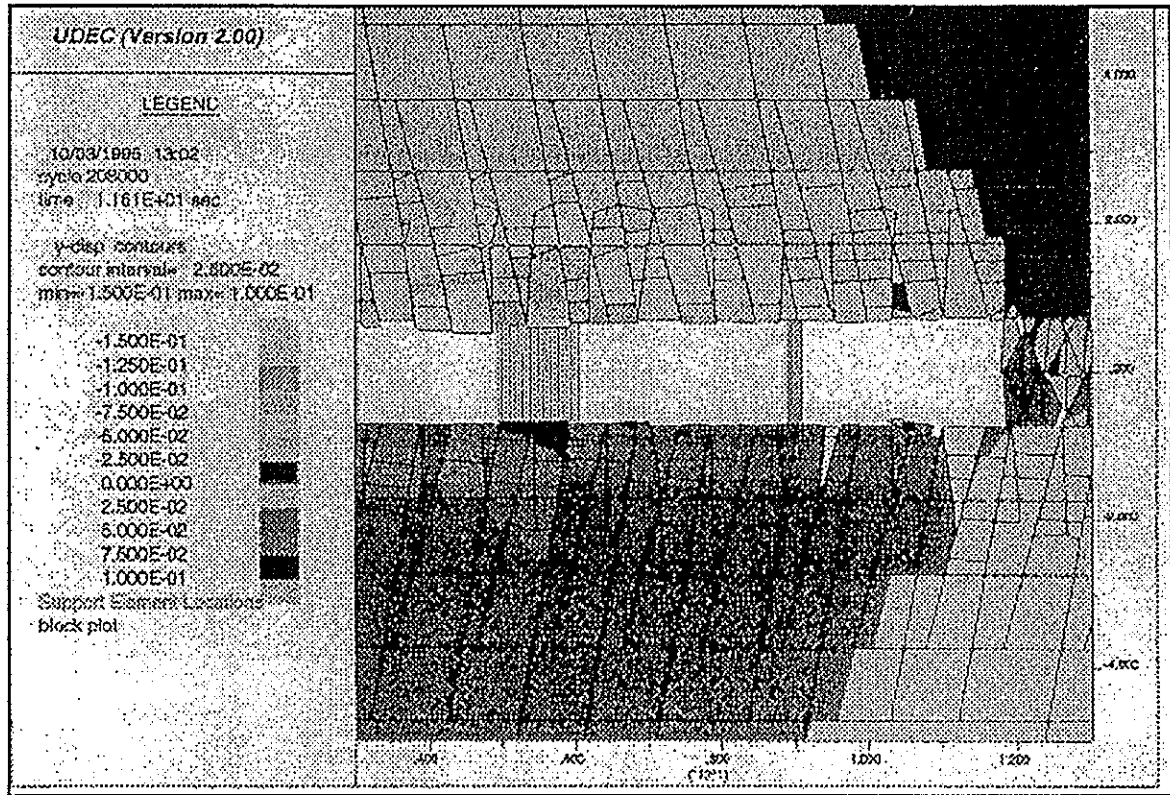


Figure 23(a) 1.0m bedding, packs, 20t units at 2m spacing contours of y-displacement

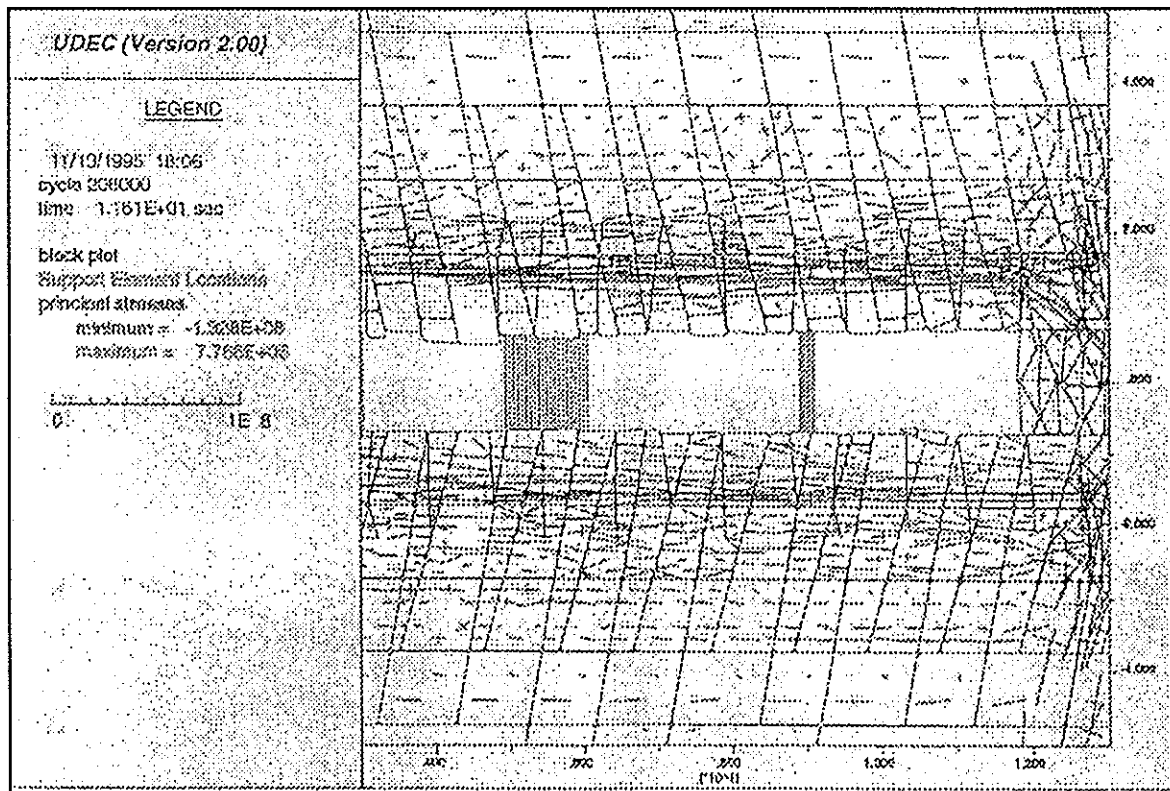


Figure 23(b) 1.0m bedding, packs, 20t units at 2m spacing principal stress tensors

## 5.2 Dynamic loading

In this section a single example of the modelling of the influence of a dynamic loading is presented. The data for this run is discussed in section 4.5. The initial state used is that presented in Figure 15. The loading used to simulate the seismic event is applied to a horizontal slot 20m above the slope. Figure 24 shows the resulting P intensive wave approaching the slope approximately 2 milli-seconds (msecs) after application of the loading, the plot shows contours of vertical velocities. At this time the wave has travelled approximately 11m, this corresponds to a wave speed of close to 5600m/sec which is characteristic of real seismic data. Note that ahead of the wave the rockmass is in equilibrium, numerical noise accounts for slight variations about the zero velocity contour level. A plot of the y-velocity at the point X indicated in Figure 24 is given in Figure 25.

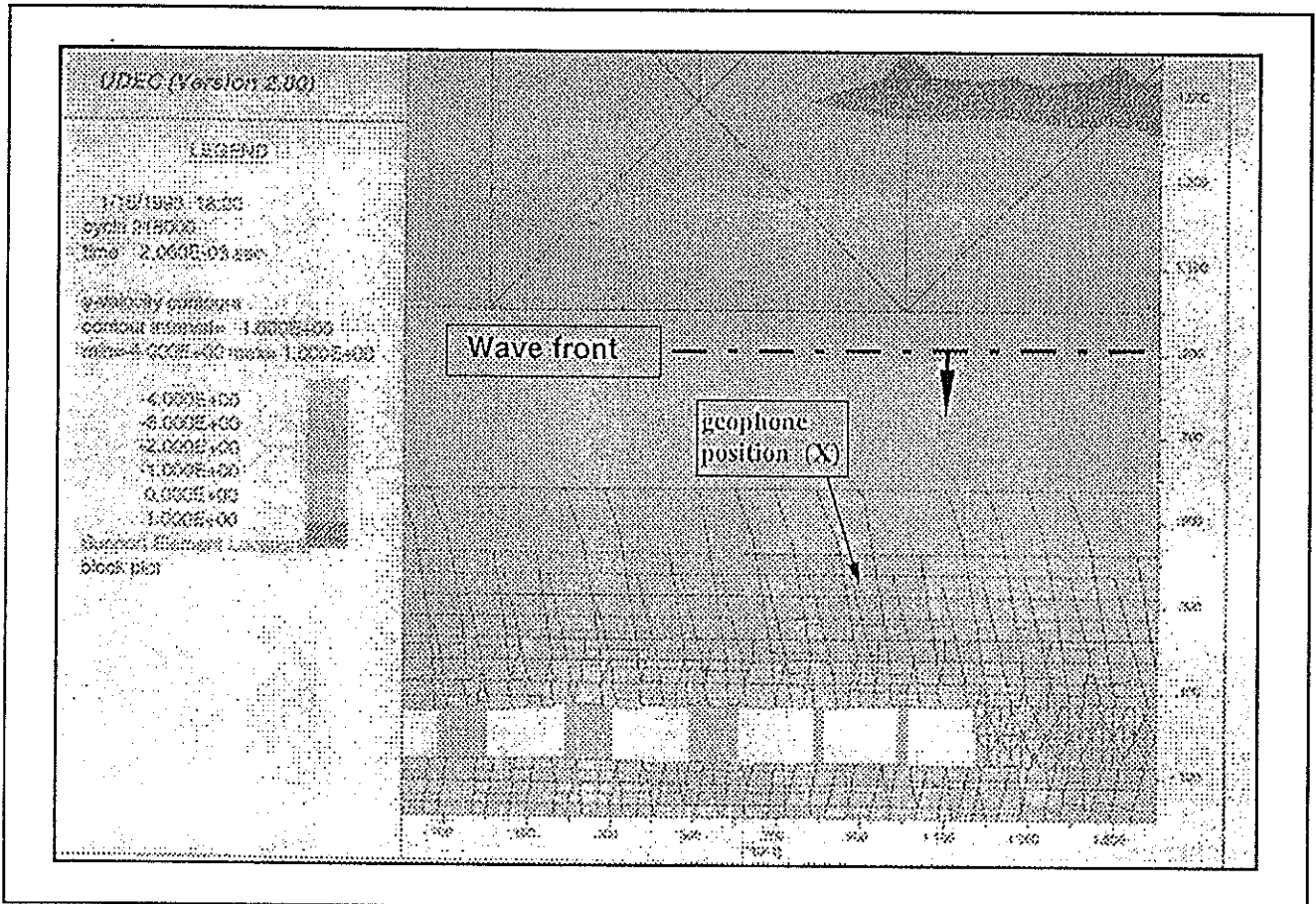


Figure 24 View of seismic P-wave impinging on the slope face area, 2msec after the event

The best way in which to illustrate the models ability to represent a seismic event and its influence on a supported slope is by creating an animation, or *movie*; in this document a series of snap shots are presented in Figure 26. These snap shots show contours of y-velocities in the hangingwall near the face of the slope. The contour intervals are held constant in all these plots and the time at which they were taken are indicated, these times being relative to the initiation of the event. An interpretation of these results is given below but considerable further work is required to understand them fully. Investigation of the performance of support under dynamic loading has been limited mainly because the large run times required. A simulation of the type shown takes in excess of one hundred hours (more than four days) to reach the state shown in the last plot presented. To monitor the full return to a steady state of equilibrium and extent of damage to the hangingwall would require considerably more time, estimated to be in the order of a further five hundred hours.

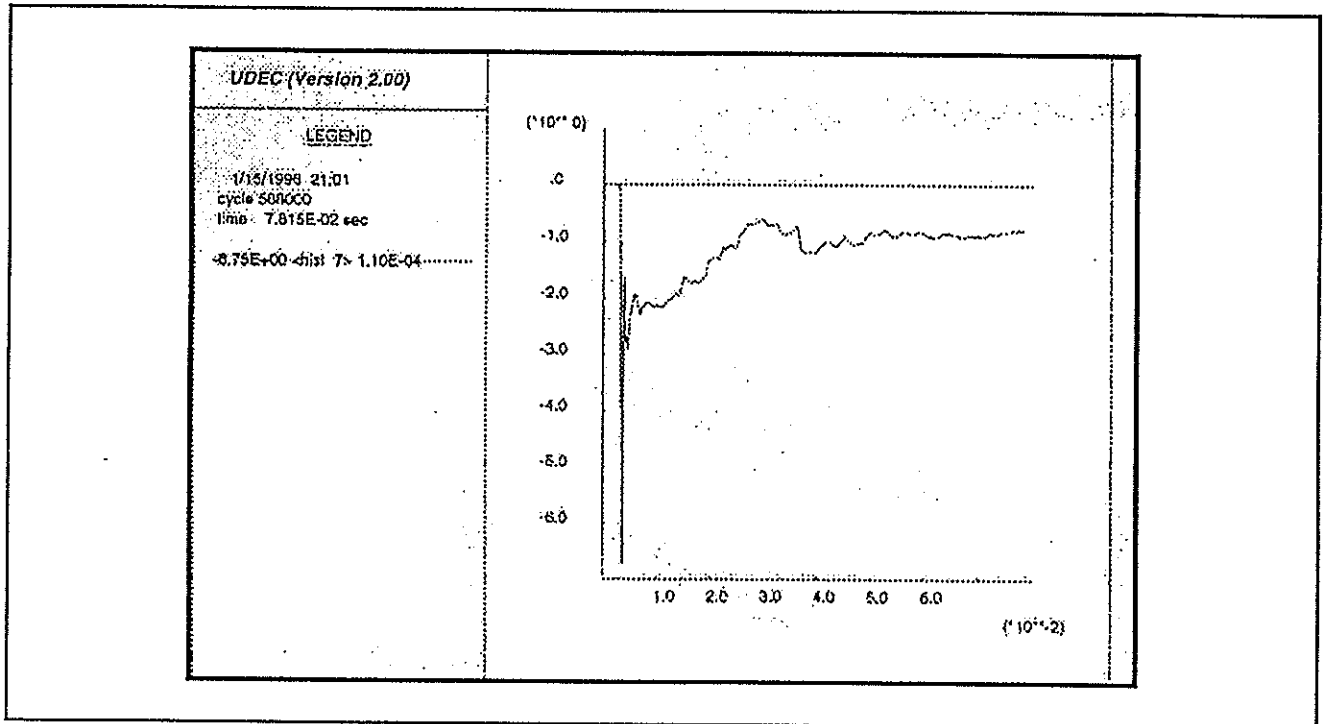


Figure 25 Y-velocity at geophone position (X), see Figure 24

Figure 26(a) shows the initial state of the slope prior to the arrival of the seismic wave, note that some opening of the bedding has taken place. Figure 26(b) is approximately 2msec later, the wave has now entered the blocky region in the skin of the slope, on the left, that is towards the back area the wave has been retarded, while on the right, above the face it has advanced to within a metre of the opening. The hangingwall further back in the slope appears to have been protected by the slight opening on discontinuities and reduced state of stress. The wave seems to have continued to travel at close to 5600m/s in the stressed area above the face although some reflection and refraction of the wave has taken place. In Figures 26(c), (d) and (e), a further 2msec, 4msec and 6msec later respectively, velocities of greater than 4m/sec have been induced in the blocks in the hangingwall at the face; 3m from the face the slope is still protected by the open bedding 1m into the hangingwall. Most of the blocky section of hangingwall rock has picked up a velocity of between 1m/s and 3m/s, it seems that this material lacked the rigidity to fully reflect the wave energy. In the last of these three plots the bedding has started closing between 3m and 4m from the slope face resulting in transfer of some energy to blocks in the slope hangingwall in this area. A further 10msec later, Figure 26(f), the initial opening on the bedding has closed completely and the entire hangingwall to a height of up to 5m has been accelerated to velocities of greater than 1m/s. The volume of rock near the face where velocities are highest, close to 4m/s, is reduced. The final two plots, Figures 26(g) and (h), made at approximately 30msec and 60msec later show further reduction in the maximum block velocity. The region of larger velocities is also influenced by the support, and the kinetic energy in the system appears to be focused into the unsupported surface blocks. Opening on a plane 3m above the slope also takes place with closure due to movement of material below this plane taking place at between 1m/s and 2m/s. Some crushing of the face is also indicated.

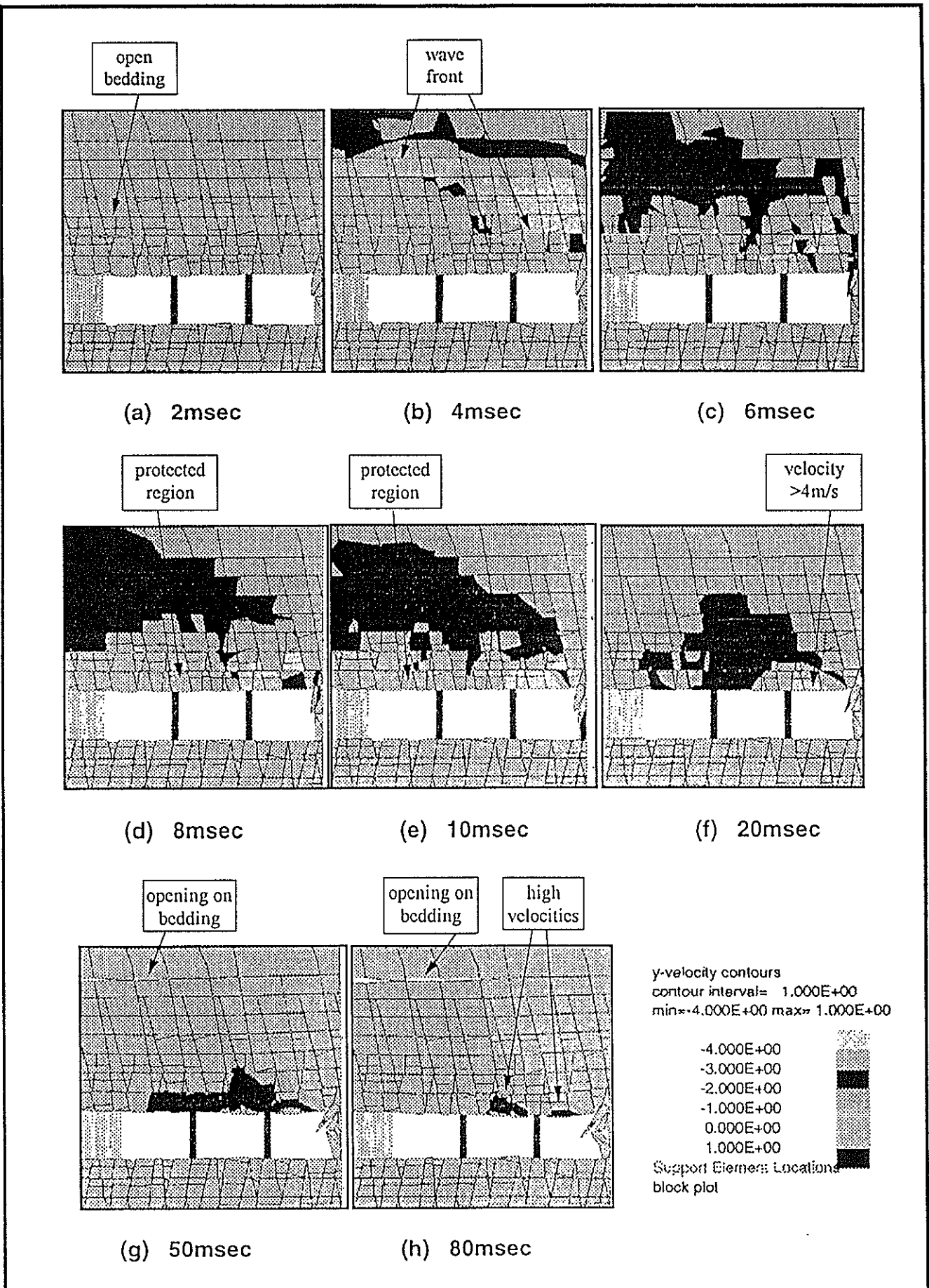


Figure 25 Snap shots of y-displacement contours

## 6. PARAMETER STUDIES

Attention has been focused on temporary supports in the face area. Two different back area support systems have been considered. The main results presented have been obtained with a model that includes reef parallel bedding planes at a spacing of half a meter; some results have also been obtained with a one metre spacing, but no further testing of the sensitivity of the results to details of the fracture pattern has been attempted.

### 6.1 Evaluation of hangingwall stability

The interpretation of results requires an assessment of the instability of blocks in the hangingwall for each support configuration used. Such an assessment is achieved by considering block displacements and stresses, an instability index, between 0 and 1 (0=stable, 1=unstable), is obtained for each block in the face area hangingwall for each these parameters. An overall rating of the stability, expressed as a percentage, is then obtained by weighting the contribution of each blocks index with its mass and normalising with respect to the assessment of the case were no face area support is used. A weighting related to distance to the surface of the hangingwall is also used.

The normalised stability rating,  $R$  is expressed as

$$R = (D - C) / D$$

where

$D$  is the value of the instability rating  $I$  evaluated for the case of no support

and

$C$  is the value of the instability rating  $I$  evaluated for the support configuration being evaluated

The instability rating  $I$  is expressed as

$$I = \sum_j \sum_i [(s_{i,j} \times f_s) + (y_{i,j} \times f_y)] \times m_{i,j} \times w_j$$

where

$s_{i,j}$  is the stress rating for block  $i$  in bedding layer  $j$

$f_s$  is the stress index reliability factor = 0.2

$y_{i,j}$  is the y-displacement rating for block  $i$  in bedding layer  $j$

$f_y$  is the displacement index reliability factor = 1.0

$m_{i,j}$  is the mass of block  $i$  in bedding layer  $j$

and

$w_j$  is the bedding plane weighting factor for the  $j$ th bedding layer. Values of 5,4,3,2 and 1 are used for the 1st, 2nd, 3rd, 4th and 5th bedding layers above the stope respectively

*NOTE the following results are also presented in the main body of this project report*

### 6.2 Trends with varying spacing and support force

A support systems average resistance per square metre is the parameter used in current design practice. Variation of support spacing, while holding a support system's average resistance constant obviously requires variation in support unit resistance (*support force*). Conversely, variation of spacing while holding support unit resistances constant, results in changes to the support system's average resistance. Trends in support performance can be interpreted in different ways by taking into account this coupling. Figures 27(a) and (b) show the trends in hangingwall stability obtained by varying strike spacing and support unit resistances. Recall that a constant dip spacing of 1m is assumed.



Figure 27(a) shows three lines; these lines indicate trends in hangingwall stability with increasing average support system resistance. The support spacing is constant for each trend line, the three lines correspond to spacings of 1m, 2m and 3m.

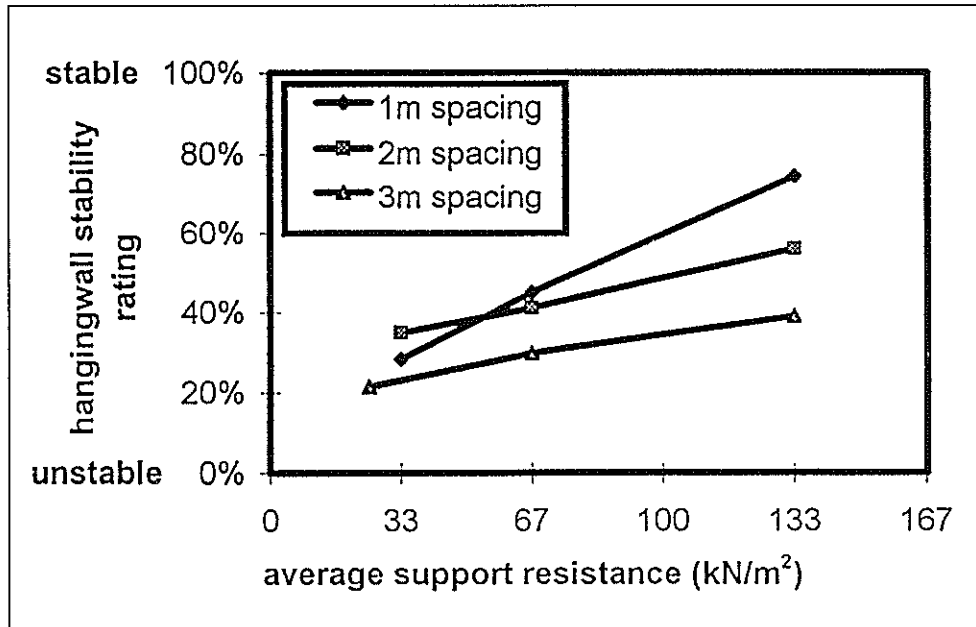


Figure 27(a) Hangingwall stability vs average support resistance at different support spacings (0.5m bedding, back area packs)

Clearly the support unit resistances change along each line; for example, for the case of 1m spacing, the unit resistances at average resistances of 33 kN/m², 66 kN/m² and 133 kN/m² are 5t, 10t and 20t respectively. Note however that the support unit resistances also differ for points corresponding a given average resistance; for example, at a support system average resistance of 33 kN/m², 5t units are used with a spacing of 1m, while 10t and 20t units are used with spacings of 2m and 3m respectively, and at a support system average resistance of 133 kN/m², 20t, 40t and 80t units are used with spacings of 1, 2 and 3m respectively.

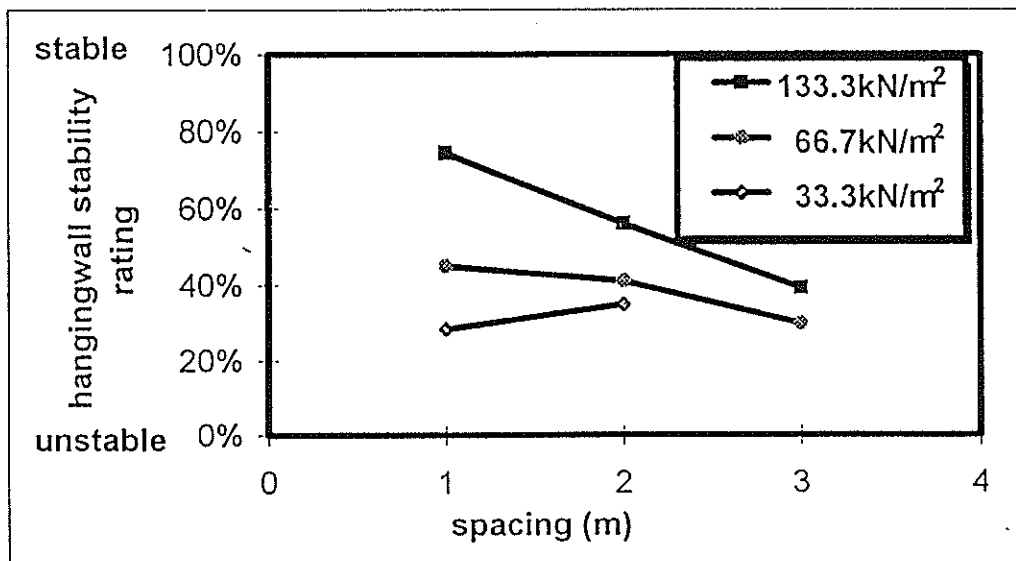


Figure 27(b) Hangingwall stability vs support spacing at different average support resistances (0.5m bedding, back area packs)

Figure 27(b) is an alternative representation of the data used to obtain Figure 27(a). The lines indicate trends in hangingwall stability with varying spacing, the system average resistance is held constant on each line by varying unit resistances.

The improvement in hangingwall conditions with increasing average support resistance that is observed for the case of supports at a 1m spacing in Figure 27(a) was expected. Of interest is the indication that the rate of improvement rapidly decreases with increasing support spacing. This result is obtained by comparing the slopes of the three lines in Figure 27(a). In the case of a 3m spacing there is little improvement with increasing average resistance, in this case the benefit of additional average resistance is countered by the negative influence of high unit force that tends to destabilise the hangingwall by causing a punching mechanism to take place. The influence of this mechanism is also illustrated by the worsening of hangingwall conditions with increasing spacing in Figure 27(b).

The trends show that, if an increase in spacings is desired without changing the hangingwall stability, an increase in average support resistance may be needed.

These results include only support system performance under static conditions, and may be different to trends valid under dynamic conditions. It is reiterated that, the results of the study are purely qualitative and values used and derived in the examples given below should not be used in practice without first collecting sufficient data from an underground support monitoring programme and using it to calibrate the results.

### 6.2.1 Taking changes in dip spacing into account

The influence of dip spacing has been discussed in section 2.3 this theoretical interpretation of the modelling results is used here to obtain trend lines for dip spacings other than 1m. Figure 28 shows the trend lines generated for dip spacings of 1.5m and 2m for a strike spacing of 1m.

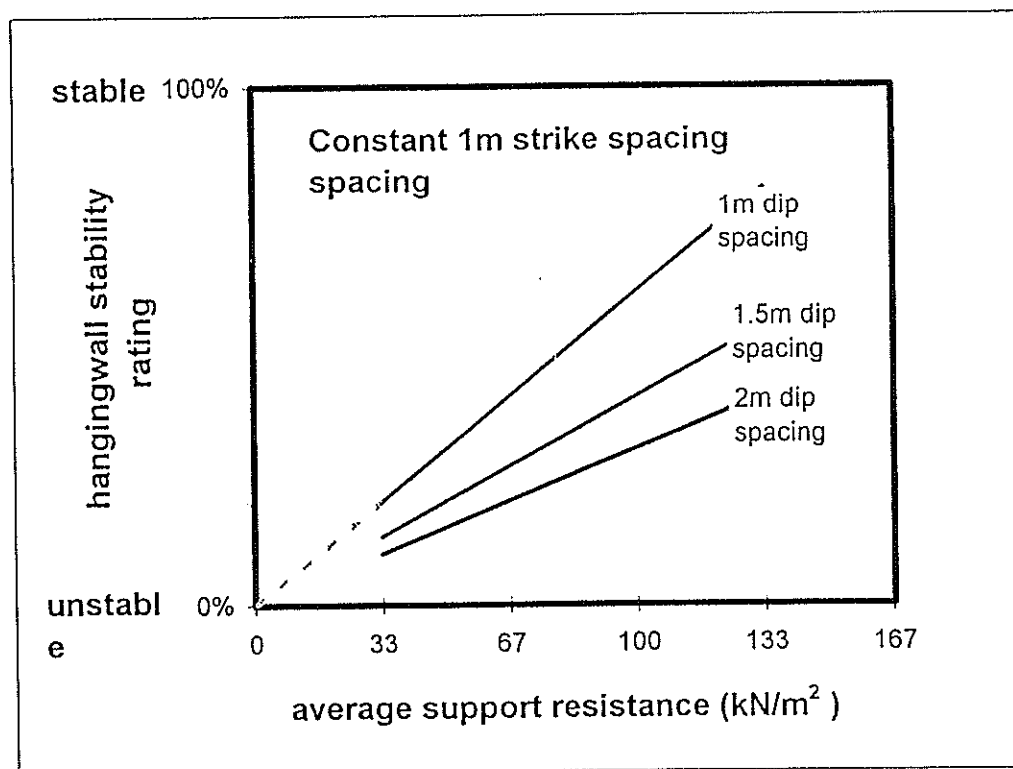


Figure 28 Extending 2D results to consider dip spacing of supports

### 6.3 The influence of load spreaders

Figure 29 shows that the use of load spreaders improves hangingwall stability. This result was obtained with the average support resistance held constant at 66 kN/m<sup>2</sup> and spacing held constant at 2m. In this case the detrimental effects of the punching mechanism are present, though not as pronounced as they are for a 3m spacing. A result obtained with a load spreader for a 3m spacing indicate that the relative improvement may be greater in this case but that it is unlikely that hangingwall conditions will improve beyond those achieved with the lesser support spacing.

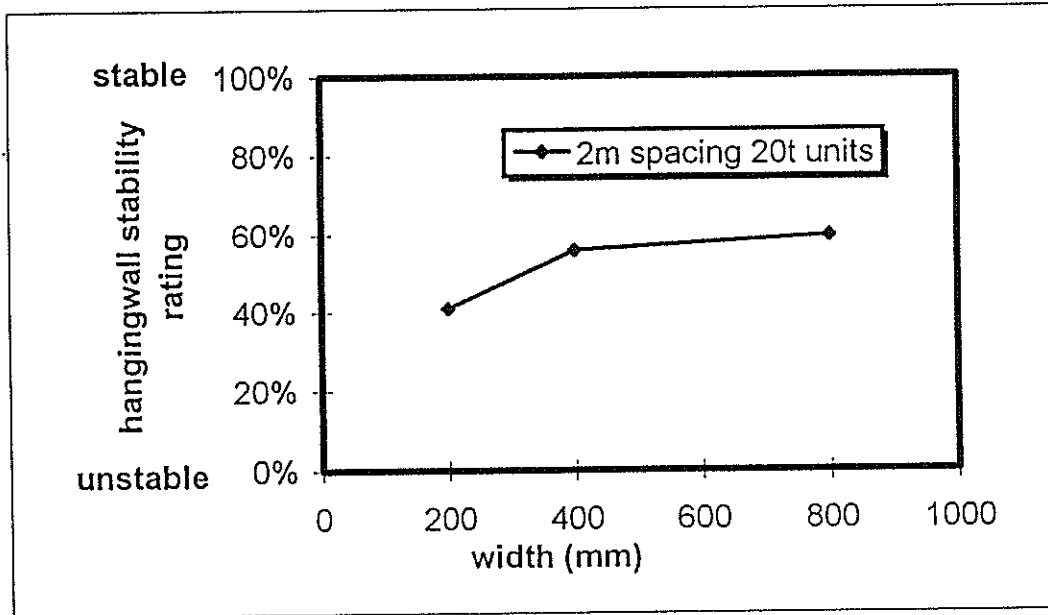


Figure 29 Hangingwall stability vs length of load spreaders (0.5m bedding, back area packs)

### 6.4 Sensitivity to bedding plane spacing

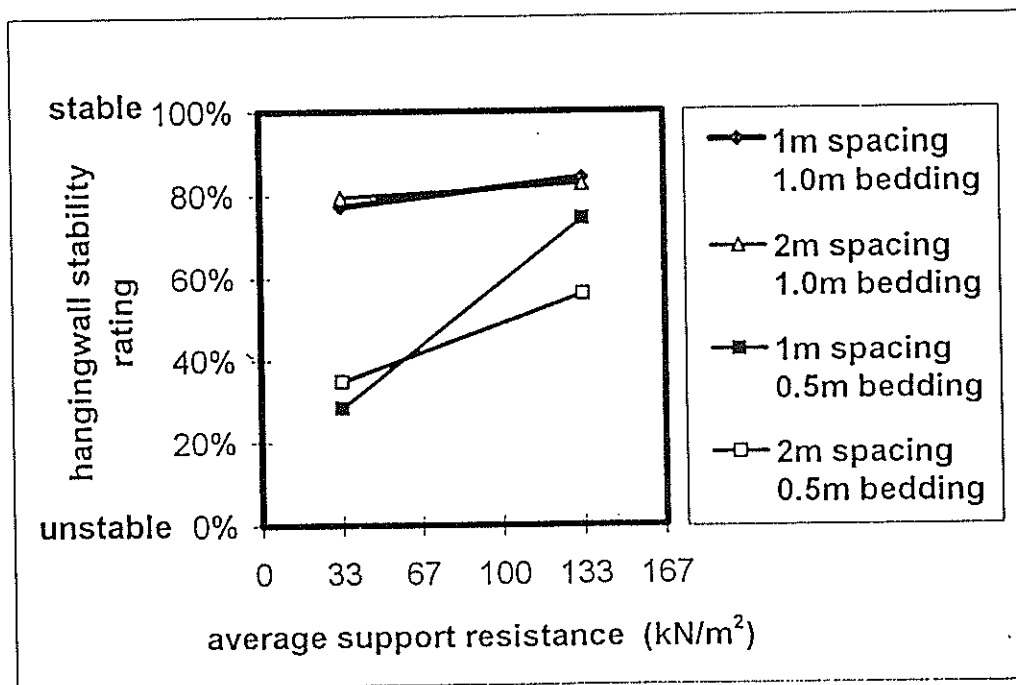


Figure 30 Hangingwall stability vs average support resistance for support spacings of 1m and 2m with different bedding thicknesses

A similar set of results to those obtained for the case of a half metre bedding plane was produced for the case of a one meter bedding. Comparison of results was possible by applying a suitable normalising procedure. On the whole the hangingwall stability improves significantly with this doubling of the bedding plane spacing. The influence of changes in support parameters also seem to be less marked. This is illustrated in Figure 30. This would seem to indicate that lower support resistances may be used, however, this trend is not supported by fallout data which appears to show some correlation between the thickness of bedding and fallouts. Further work is required to obtain a full picture of the trends in hangingwall stability.

### 6.5 The influence of back area support

In the above examples 1.1m square Mat packs at 3m centres were used as back area support. A second set of results was generated using the model with a half metre bedding spacing, in this analysis the back area support system used represented a 46% porosity backfill. A significant improvement in hangingwall conditions was obtained, however, the modelling method used to represent the backfill will tend to exaggerate the influence of the backfill on the face area as the lack of confinement along the face of the backfill is not taken into account. This result is illustrated in Figure 31.

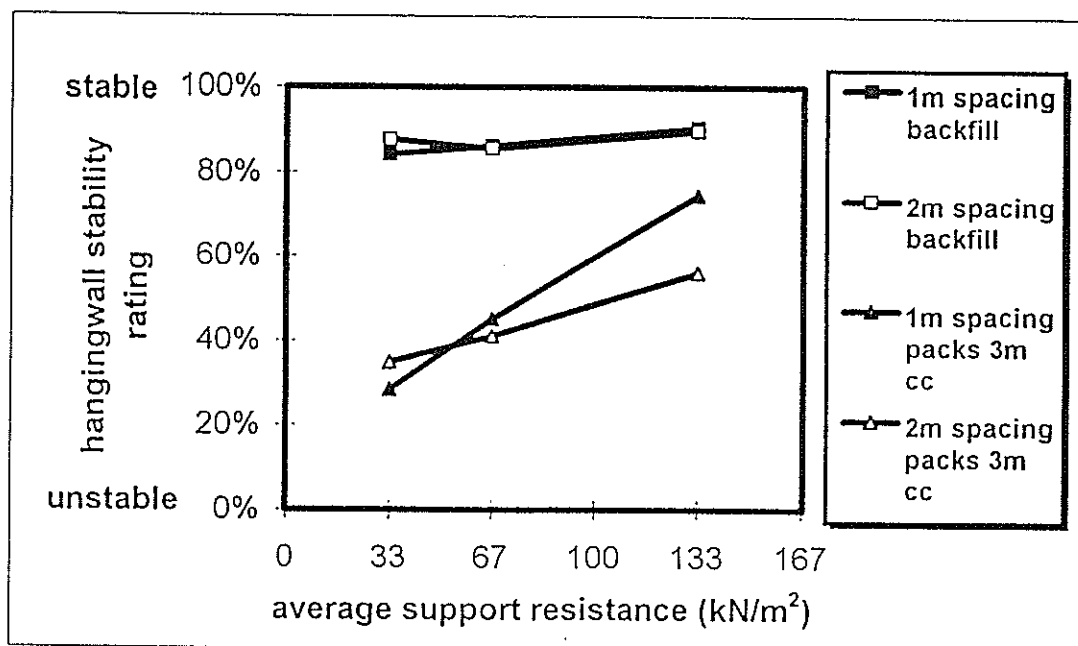


Figure 31 Hangingwall stability vs average support resistance for spacings of 1 and 2m and different types of back area support (0.5m bedding)

## 7. CONCLUSION AND RECOMMENDATIONS

Significant experience has been gained in the application of discontinuum modelling to the study of the complex nature of the interaction between supports and the blocky rockmass in the skin of excavations. Through this modelling work it has been possible to obtain some insights into trends in support system performance that would have been extremely difficult and costly to obtain from a programme of underground monitoring. Not all the initial objectives have been fully achieved; in particular, insufficient progress was made with the modelling of dynamic loading to establish trends in support performance; the basis for modelling of dynamic loading has, however, been established.

The main conclusions of the parameter studies are summarised in point form below.

- Use of head boards gives improved hangingwall stability.
- Increases in total support resistance in the face area improves hangingwall stability, except where large spacings are used as this requires; widely spaced stiff supports tend to activate punching mechanisms.
- Reduced support spacing in general improves hangingwall stability, but this improvement also depends on the total support resistance.

The trends established provide some rationale for selecting a support system, this rationale is described and discussed further in the main body of the report. Unfortunately the results obtained are not as yet detailed enough to establish a complete design procedure for determining support spacing. There is considerable scope for further use of the modelling techniques developed in this project to add clarity to the trends obtained. In particular, the sensitivity to changes in the fracture pattern used in modelling needs to be investigated carefully. True quantitative results are also required before the results can be used in such a procedure. The work has established a starting point from which to design and initiate a programme of underground monitoring aimed at collecting the data needed to calibrate models and hence provide the necessary quantitative dimension to the results. An acceptable practical method of assessing hangingwall stability needs to be developed and included in such a programme of underground monitoring. It is recognised that development of a such a method is extremely difficult.

#### *Other applications*

There is great potential for further application of the modelling technique developed in this project. The techniques developed are well suited to study of the influences of many different aspects of stope support on hangingwall stability in the face area. Only a very few of these support parameters were investigated in this project. The several other parameters which could be studied with little or no change in the model geometry are discussed briefly below.

1. The use of *different back area support systems* has also been briefly looked at; some preliminary results of such a study are discussed above. A more detailed study could show that reductions in back area support may be possible in some circumstances; this would result in major cost savings for the industry, savings, that could be used to improve other aspects of mine safety.
2. The use of *different types of support units* in the face area was briefly investigated during the current study but more attention could be given to such variations. Data for most of the different types of support units used in the industry has been collected, and is presented in the support catalogue compiled as part of this project. In the model the definition of support behaviour is very easily changed as it is specified in a data input file that is separate from those in which the main problem is defined.
3. The influence of different *mining sequences* of face advance and support installation, including variations in the distance of both temporary and permanent supports to the face, would require only simple changes to excavation data provided that face advances of multiples of 0.5m were used.
4. Study of the influences of problems associated with *different stope widths* would require extensive, but simple, changes to geometry data.
5. The model has been constructed in such a way that changes to *stope span* are simply implemented, however, an increase in stope span would lead to an increase in run time. Of particular interest may be changes in behaviour that may take place when complete closure occurs in the stope back areas.
6. Study of the effects of the *depth of mining* requires simply a change to the applied initial and boundary conditions.
7. Adjustment of the model to study the influence of *different combinations of hangingwall and footwall rock types* is easily done by the changing appropriate material properties. Such variations in properties are, however, often associated with other differences in geology, such as differences in bedding. The

fracture patterns around stopes with different hangingwall and footwall rocks are usually quite different to those used in this project, some attention to the definition of the blocky region in the area of interest is therefore needed. The methods developed are being used to model mining of the Ventersdorp Contact Reef where the hangingwall is lava and the footwall maybe one of several types of shale or bedded quartzite. Another suggested application is a study of the influence of the Kharki Shale horizon, above the Basal Reef, on hangingwall stability.

### *Model refinement*

The work reported on here forms a good basis for consideration of support systems that make use of bolting but further investigation of the application of existing modelling tools may be necessary to do this:

Study of the final results and experience gained in producing the many results needed to establish trends has highlighted some areas in which the model used to obtain final results could be further improved. These improvements could not be introduced part way into parametric studies. Recommendations for further refinement of the model are summarised in point form below.

- Adjustments to the representation of the effects of face crushing are needed. While the artificially blocky system used usually provides a fair representation of the influence of face crushing it is a little inclined to lockup and behaves poorly in some circumstances. It also requires too many small blocks and hence contributes unduly to the size of the model. Some alternative representations of face crushing have already been investigated as part of the effort to use the modelling method to investigate the rockmass behaviour around VCR stopes (SIMRAC project GAP102)
- Consideration of the use of quarter symmetry, or a simpler representation of the footwall. This is needed to improve the efficiency of modelling work, particularly with a view to further study dynamic loading.
- Further investigation into the use and calibration of the continuously yielding joint model available in UDEC, or alternatively, development of an improved joint model that can be used to simulate the generation of fractures.
- Improvements in methods available for modelling headboards are necessary, but are possibly not required immediately.
- The method of quantifying hangingwall stability predicted by modelling needs to be refined and calibrated against underground observations.

Some of these recommendations are to be implemented as part of the modelling work in SIMRAC project GAP102 that continues to the end of 1996, others were included in the project proposal GAP300 which has been accepted and will start in 1996.

## APPENDIX 2

# GULLY PACK BEHAVIOUR AND GULLY SUPPORT REQUIREMENTS

### TABLE OF CONTENTS

	page
1 INTRODUCTION	1
2 <i>IN SITU</i> MONITORING OF GULLY PACKS	1
2.1 Hartebeestfontein Gold Mine	4
2.1.1 Site 1 - 80N22 stope, S5 panel	4
2.1.2 Site 2 - 80N22 stope, N4 panel	7
2.2 Western Deep Levels South Mine	9
2.2.1 Site 1 - 84-53 stope, E3 panel	9
2.2.2 Site 2 - 79-49 stope, E1 panel	12
3 PROPOSED YIELDING GULLY PACK	12
3.1 Pack force and stope closure	15
3.2 Gully sidewall closure	17
3.3 Comments	18
4 NUMERICAL MODELLING OF GULLY PACK BEHAVIOUR	18
4.1 Modelling of <i>in situ</i> pack behaviour	18
4.1.1 UDEC modelling	18
4.1.2 FLAC modelling	19
4.2 Modelling of proposed yielding pack	24
5 GULLY SUPPORT REQUIREMENTS	25
5.1 Accident analysis	26
5.2 Fallout thickness distributions	26
5.3 Support requirements	28
6 FURTHER WORK	28

## APPENDIX 2

### GULLY PACK BEHAVIOUR AND GULLY SUPPORT REQUIREMENTS

#### 1 INTRODUCTION

This report documents the work carried out for the gully support section of the SIMRAC GAP032 Stope and Gully Research Project. The purpose of this project was to determine the support requirements of stope gullies under static and dynamic conditions and to provide a gully support design rationale. The project ran from January 1993 to December 1995. During this time extensive underground observations and measurements have been undertaken in stope gullies on a variety of mines and numerical modelling has been carried out. The main areas of research have been the *in situ* behaviour of gully packs and gully sidewalls; the design and *in situ* evaluation of a proposed improved gully pack; and an assessment of the fallout thicknesses and support requirements for the exposed hangingwall along the line of gullies.

The need for this area of research is based on the incidence of accidents which occur in stope gullies and the observation that a large number of gully packs are undermined by the collapse of the underlying gully sidewall and the incidence of pack and gully damage following rockbursts. Accident data from 1991 and 1992 shows that stope gullies account for the second highest incidence of in-stope fatalities after the stope face (Figure 1.1).

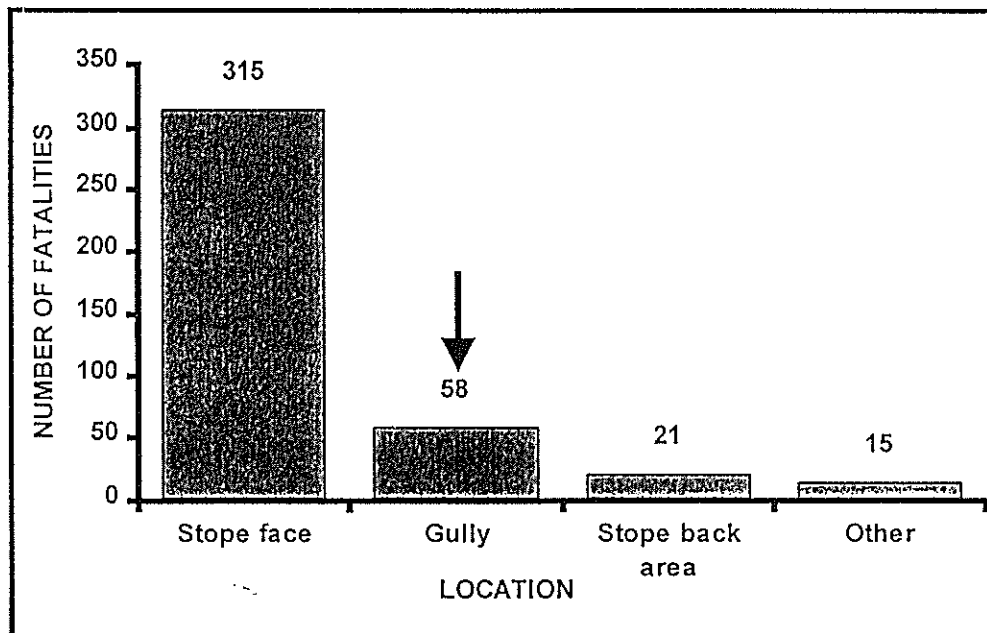


Figure 1.1 Distribution of in-stope rock related fatalities for all mining districts during 1991 and 1992

#### 2 *IN SITU* MONITORING OF GULLY PACKS

Monitoring of gully packs was undertaken at sites on Hartebeestfontein Gold Mine, Western Deep Levels South Mine and Western Holdings Gold Mine. Due to operational problems, successful results were only obtained from Hartebeestfontein and Western Deep Levels. This did however still provide results for gullies in both scattered mining and longwall mining configurations respectively (cf. Figure 2.1).



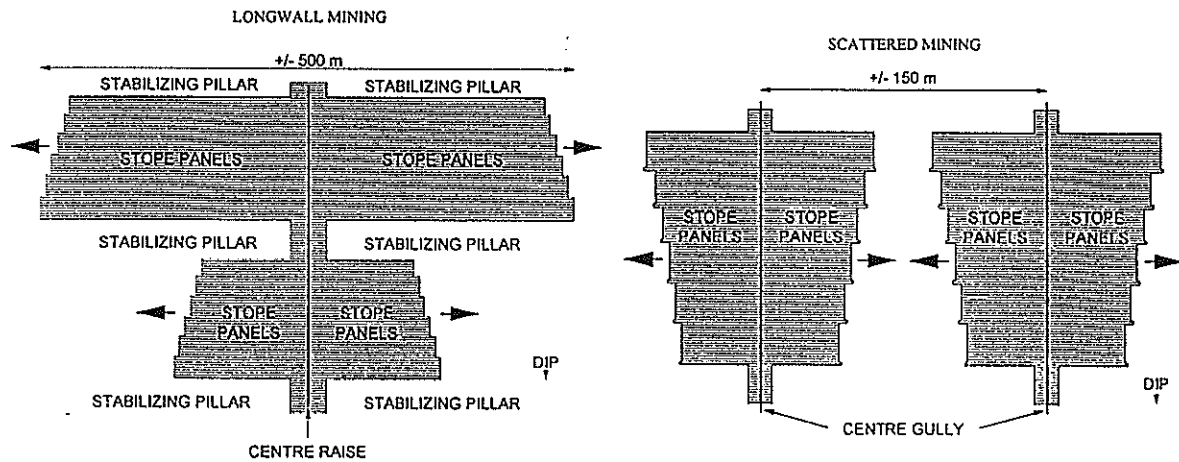


Figure 2.1 Schematics of longwall and scattered mining layouts

At each underground monitoring site a series of three gully packs which were in standard use on the mine were installed and instrumented as part of the normal mining sequence of a gully and panel (Figure 2.2). The instrumentation consisted of four flat pressure load-cells sandwiched between two 10 mm thick steel plates and these were built into each pack during its construction (Figure 2.3). After pack construction was complete pegs were installed into the hangingwall and footwall at each corner of the pack to enable stope closure, and hence pack deformation, to be measured. Similar pegs were also installed in the sidewalls on both sides of the gully, adjacent to the pack, for the associated horizontal movement of the gully sidewalls to be measured. In the case of the follow behind gullies in the longwall situation at Western Deep Levels, these pegs could often only be installed one or more weeks after the pack installation when the gully had been mined past the pack's position.

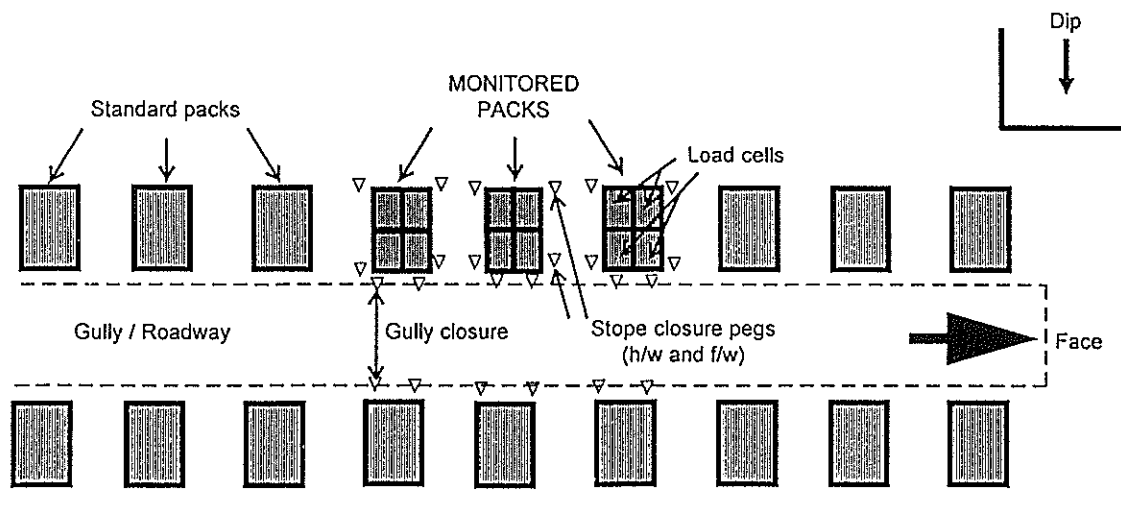


Figure 2.2 Schematic layout of instrumented gully packs and 'standard' gully packs (example of follow-behind gully configuration)

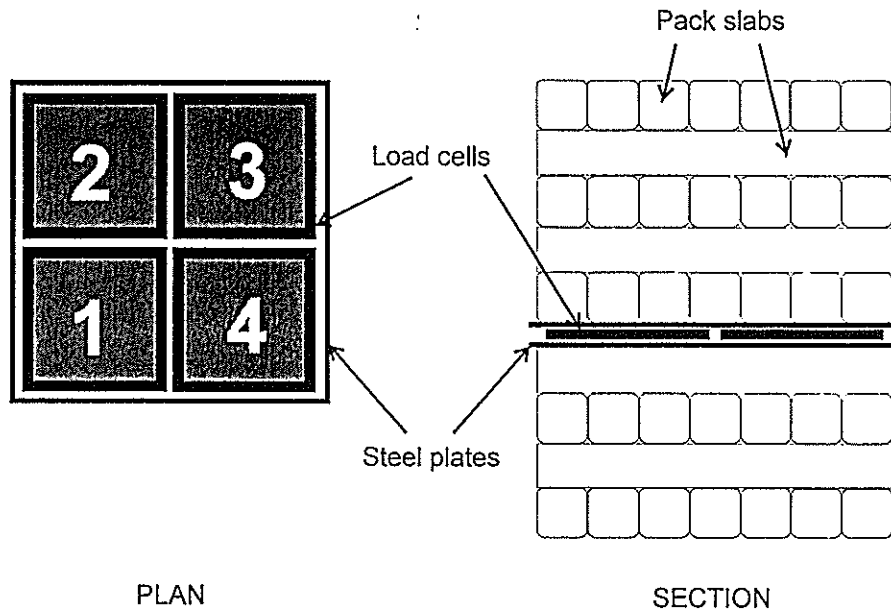


Figure 2.3 Schematic of four load cells installed in a 'standard' gully pack

Mapping of the fractures present in the gully sidewall under the instrumented packs was also conducted to enable possible sidewall failure mechanisms to be determined. In the advance strike gully (ASG) configuration, the pre-existing discontinuities in the footwall rock making up the gully sidewall were expected to be predominantly gully parallel stress induced fracturing (Figure 2.4a). In the follow-behind gully (FBG) configuration, pre-existing discontinuities were expected to be predominantly face parallel stress fractures orientated at right angles to the line of the gully (Figure 2.4b).

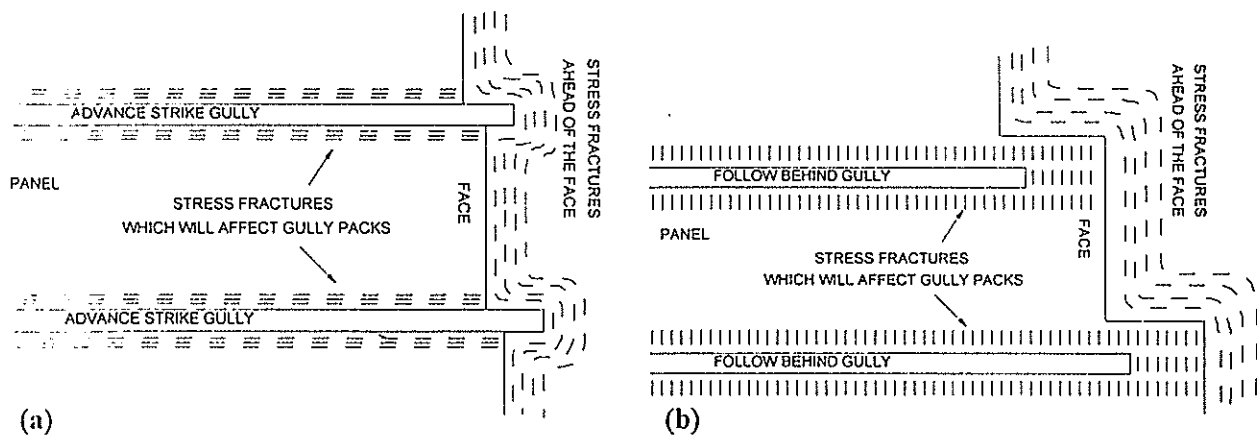


Figure 2.4 Schematic of expected fracture patterns for: (a) advanced strike gully (ASG) and (b) follow-behind gully (FBG) configurations

## 2.1 Hartebeestfontein Gold Mine

Gully packs were monitored at two sites at Hartebeestfontein 6 Shaft.

### 2.1.1 Site 1 - 80N22 stope, S5 panel

Three instrumented 0,75 m x 0,75 m Hercules packs were installed in the 78 level 80N22 stope, S5 panel, at an approximate depth below surface of 2300m. Strike gullies at this location are advanced one or two metres ahead of the stope face and the gully packs are installed several metres behind the gully face. At the completion of monitoring the gully face was 25 m from the first pack. **Figure 2.5** is a schematic of the layout at this site.

Based on stope and gully geometry, the pre-existing discontinuities in the footwall rock at this site were expected to be predominantly gully parallel stress fractures, due to the advance strike gully (ASG) configuration (cf **Figure 2.4a**), and reef parallel bedding planes. Fracture mapping of the site found however that the stress fractures were at approximately 80 degrees to the line of the gully and running up-dip and towards the stope face (see **Figure 2.5**). This unexpected fracture orientation was probably due to the small lead that the ASG was carried ahead of the stope face. A prominent bedding plane, dipping at about 10°, was located in the sidewall about 1 m below the packs and this facilitated the movement of the blocks created by the face parallel fractures, especially in the case of pack 3.

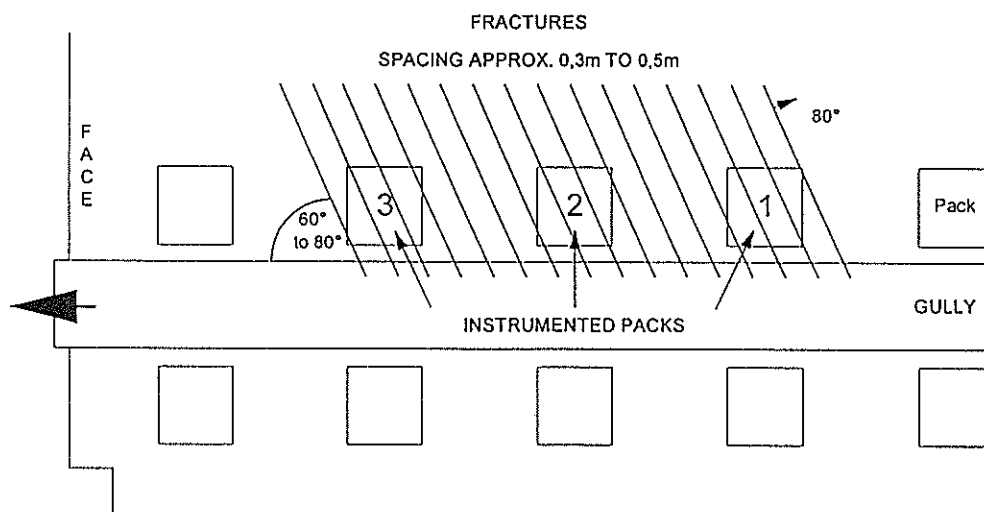


**Figure 2.5** Schematic of fracture pattern observed at Hartebeestfontein 6 Shaft, Site 1

One of the front load cells in the first pack was damaged at an early stage and no readings were obtained from it, this factor needed to be taken into account when interpreting the results (from the remaining three cells) for the whole pack.

The results are presented in graphical form in **Figure 2.6** as pack force vs stope closure and in **Figure 2.7** as pack force vs elapsed time from installation, in days. The average stope closure measured at each pack is equivalent to the average deformation experienced by the pack and can therefore be used in conjunction with the initial height to determine the average strain experienced by the pack. There is quite a variation of peak force from one pack to another, this, however, can be explained from observations made at the site.

Initial average stope widths at each pack were: pack 1, 1115 mm; pack 2, 1237 mm; and pack 3, 1535 mm. A graph of stope closure (i.e. pack deformation) vs time (days) is given in **Figure 2.8**.

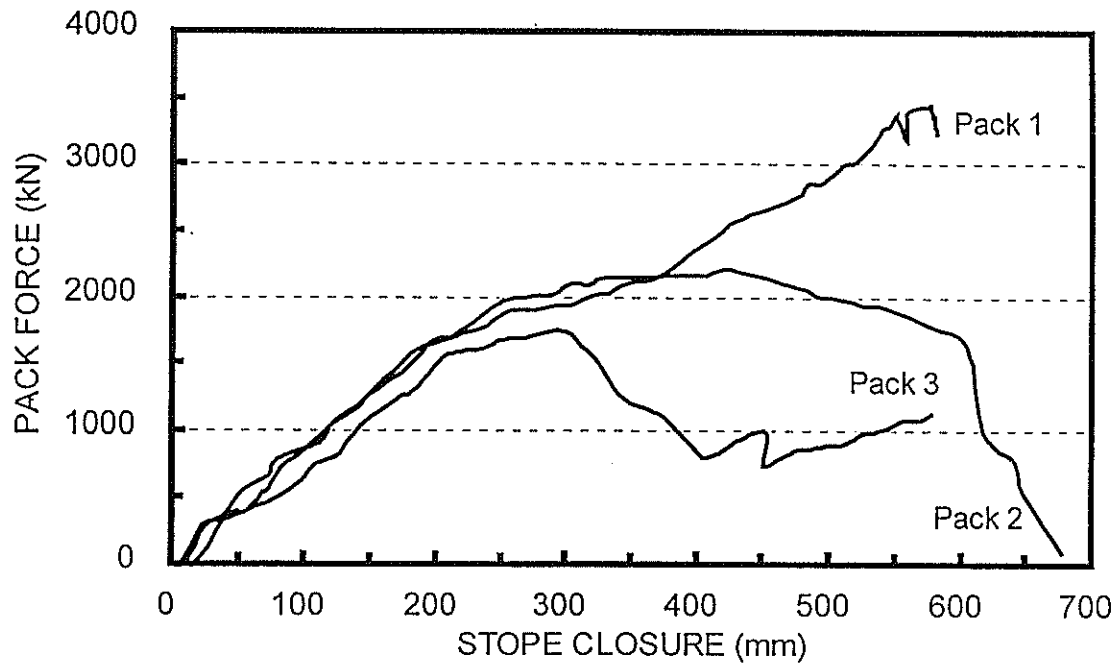


Figure 2.6 Pack force-deformation behaviour at Hartebeestfontein 6 Shaft, Site 1

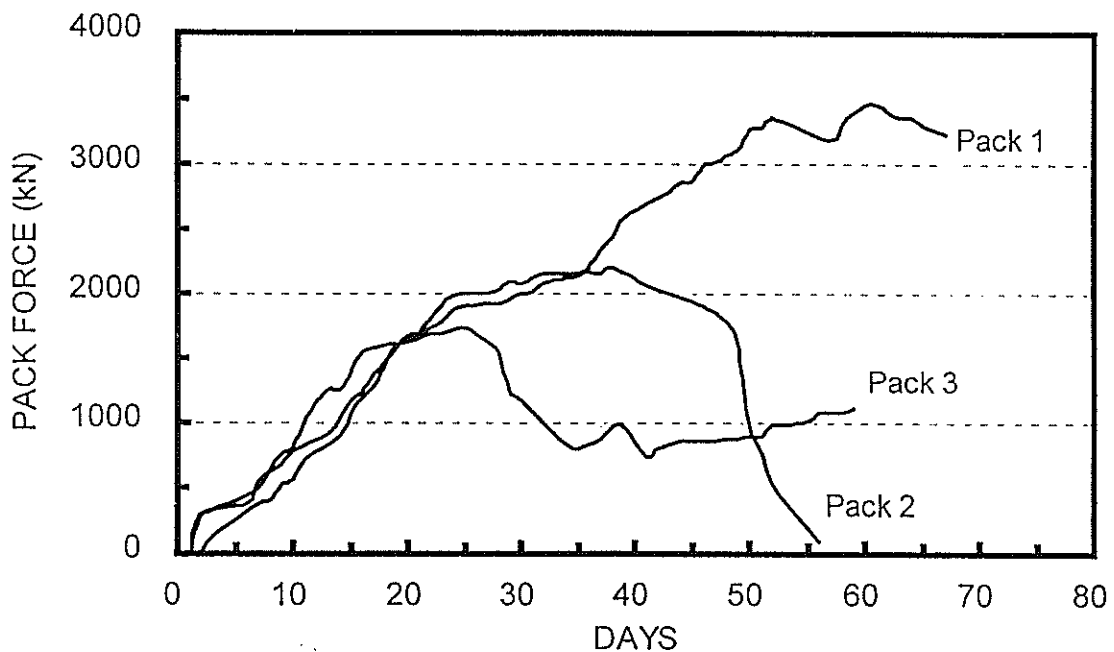


Figure 2.7 Pack force-time behaviour at Hartebeestfontein 6 Shaft, Site 1

In the case of pack 1, there was no appreciable damage (over and above the original stress fracturing) to the gully sidewall underneath the pack and the fractures appear to be locked tightly together. Consequently the total force for the three load cells has continued to rise reaching a peak of about 3450 kN after an average stope closure of 577 mm. This climb was only arrested after about 55 days because of a drop off in load on the cell closest to the gully.

A peak force of about 2000 kN was reached in pack 2, after 282 mm of average stope closure, at which point the force levelled off. After about 40 days some foundation failure (mobilisation of existing fractures) started to occur and after about 50 days virtually all the rock beneath the pack was pushed out into the gully, thus rendering the pack useless.

Pack 3 attained a peak force of about 1700 kN at 300 mm average stope closure after which the force dropped to about 900 kN and stayed around this level until the end of monitoring. Observations showed that the blocks (delineated by the stress fractures and the bedding plane) of footwall rock making up the foundation of this pack had remained *in situ* but had rotated towards the face. The pack had thereby shed load but without becoming totally dislodged and was subsequently able to maintain this lower force and even increase it up to 1000 kN.

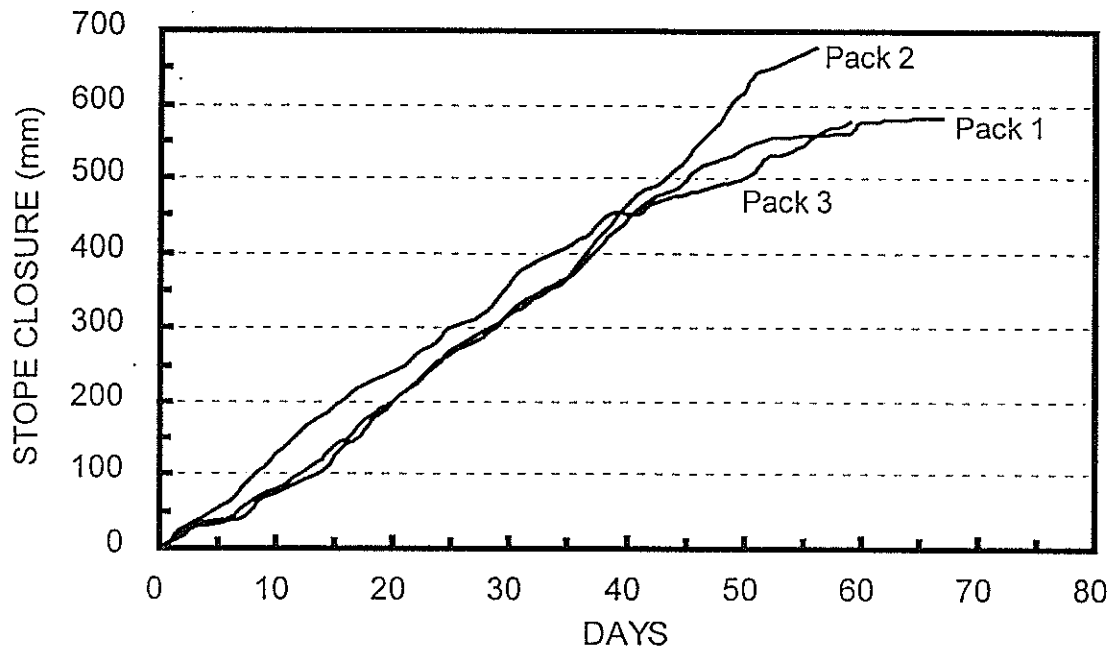


Figure 2.8 Stope closure (pack displacement) at Hartebeestfontein 6 Shaft, Site 1

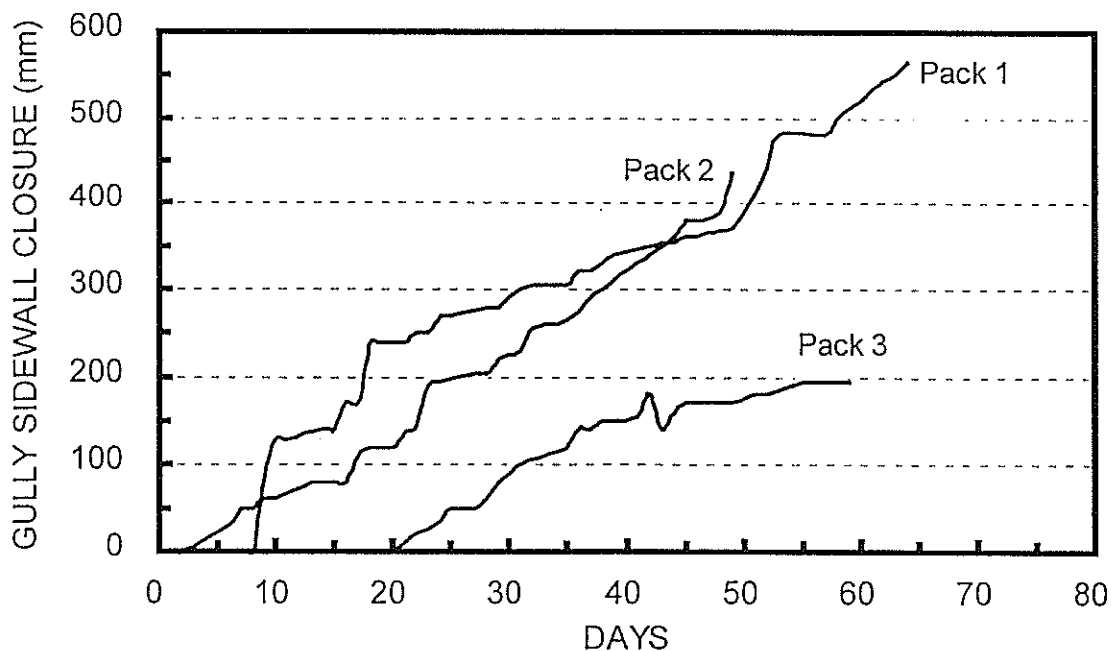


Figure 2.9 Gully sidewall displacement at Hartebeestfontein 6 Shaft, Site 1

The graph of gully sidewall closure (Figure 2.9) shows the displacement that the gully sidewall has undergone due to the load build up in the monitored gully packs and also gives an indication of the amount of damage caused to the sidewall.

### 2.1.2 Site 2 - 80N22 stope, N4 panel

A further three 75x75cm Hercules packs at Hartebeestfontein GM, 6 Shaft 80N22 stope N4 panel strike gully (at an approximate depth below surface of 2300 m) were instrumented (Figure 2.10). The results are included in Figures 2.11 and 2.12 as graphs of force-deformation (stope closure) and force-time (days), respectively. One of the rear load cells in pack 3 was damaged by scraping operations shortly after installation and therefore did not provide any readings. The panel down dip of N4 panel had not yet been mined and therefore, apart from an east siding, it was still solid below the N4 gully.

Initial average stope widths at each pack were: pack 1, 1338 mm; pack 2, 1500 mm; and pack 3, 1293 mm. A graph of stope closure (i.e. pack deformation) vs time (days) is given in Figure 2.13.

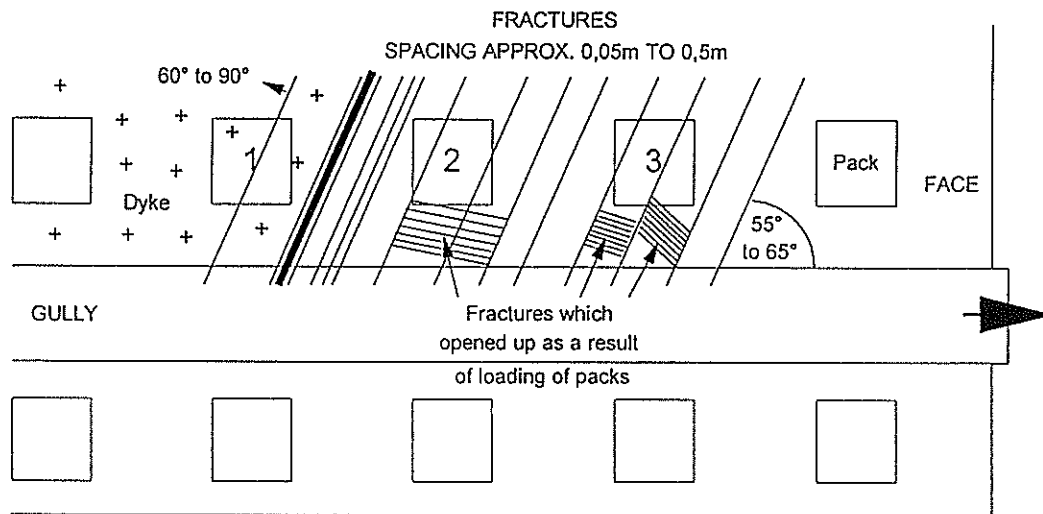


Figure 2.10 Schematic of fracture pattern observed at Hartebeestfontein 6 Shaft, Site 2

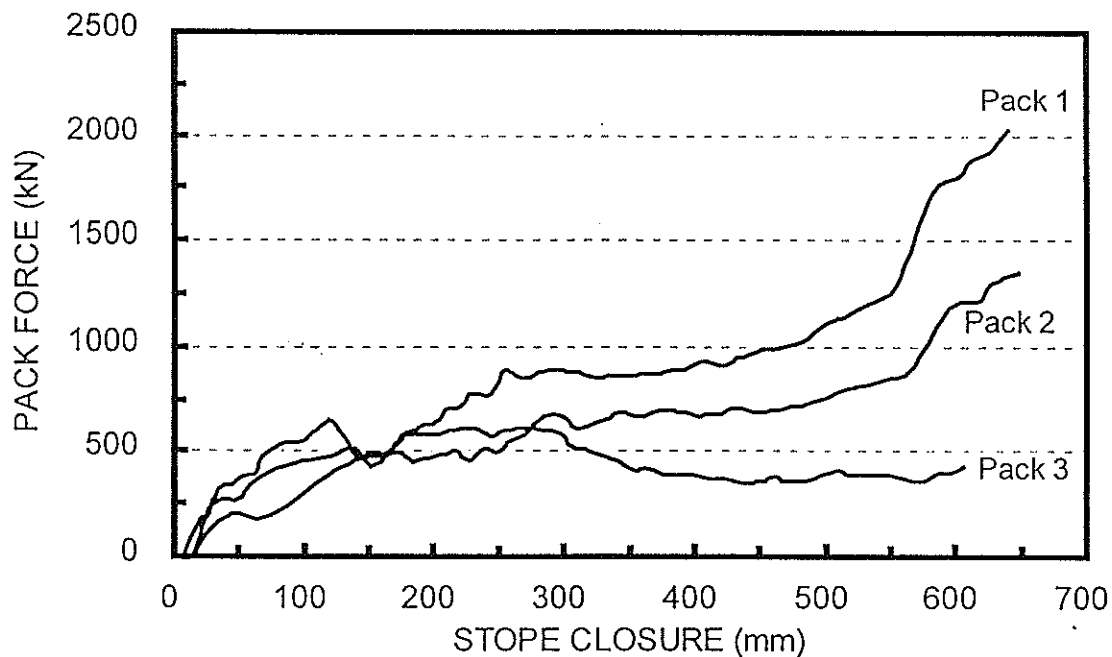


Figure 2.11 Pack force-deformation behaviour Hartebeestfontein 6 Shaft, Site 2

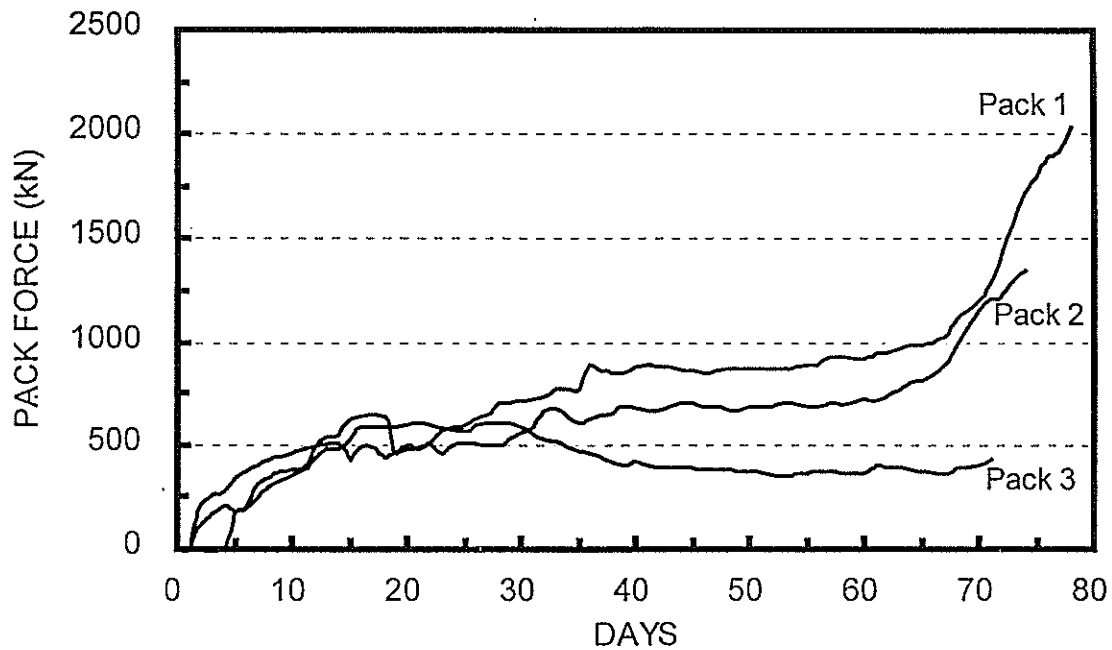


Figure 2.12 Pack force-time behaviour at Hartebeestfontein 6 Shaft, Site 2

There was very noticeable buckling of the three packs towards the gully, with packs 2 and 3 being the worst affected. The movement towards the gully of the middle portion of pack 2 was about 200 mm and for pack 3 it was 300 to 400 mm, whereas in pack 1 this movement was about 100 mm. In all cases the timber at the rear of the packs was much more compressed than that at the front. This was reflected in the build up of load in all the rear load cells and a low or zero load in the front cells. Packs 2 and 3 would almost certainly not have survived a rockburst.

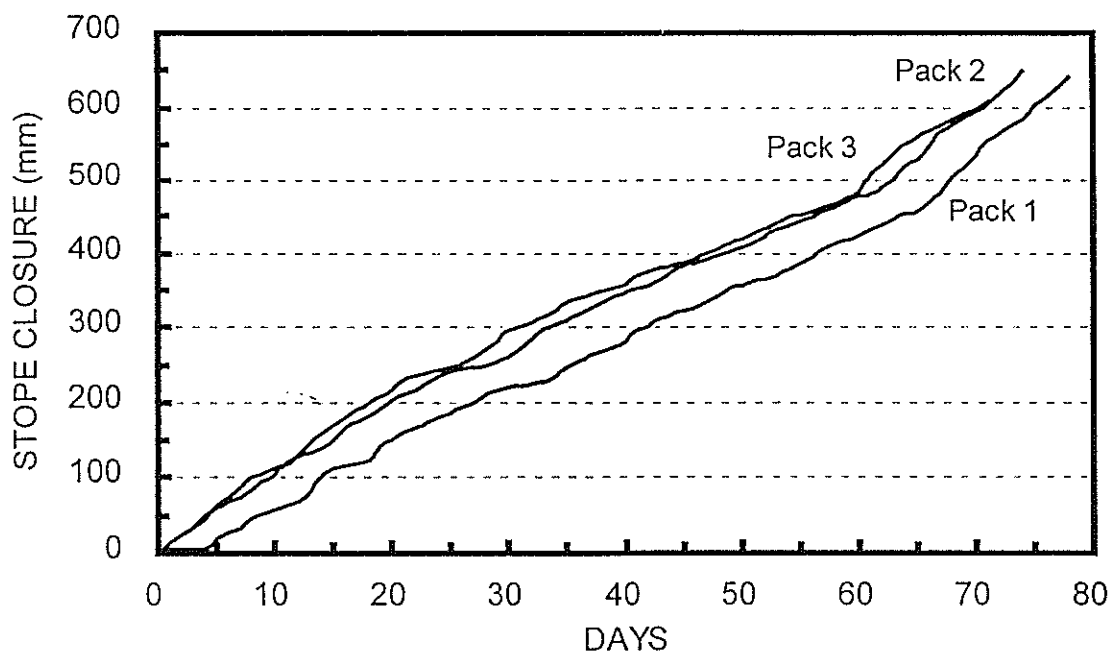


Figure 2.13 Stope closure (pack displacement) at Hartebeestfontein 6 Shaft, Site 2

There was extensive opening up of pre-existing fractures in the footwall beneath pack 3 and to a slightly lesser extent beneath pack 2. The footwall beneath pack 1 remained solid and unaffected. The fractures that opened up were observed to exist at the beginning of the monitoring period and were probably a result of

the development of the ASG. These fractures were approximately perpendicular to and bounded by the face parallel stress induced fractures (see Figure 2.10). The opening of these fractures almost certainly contributed to the lower pack forces recorded in packs 2 and 3 compared to pack 1.

The load in pack 1 reached about 900 kN after 35 days and levelled off until about 60 days at which point it started climbing, reaching about 2000 kN at the end of monitoring. This final pack load was associated with 640 mm of stope closure. The load in pack 2 reached about 700 kN after 33 days and again only started climbing after 60 days, reaching a load of about 1300 kN after 647 mm of average stope closure. The record of load in pack 3 was permanently affected by the damage to one rear load cell reaching 600 kN on the three remaining cells after about 13 days. After 30 days this load dropped to about 400 kN, the level at which it stayed until the end of monitoring. The average stope closure at this stage was 606 mm.

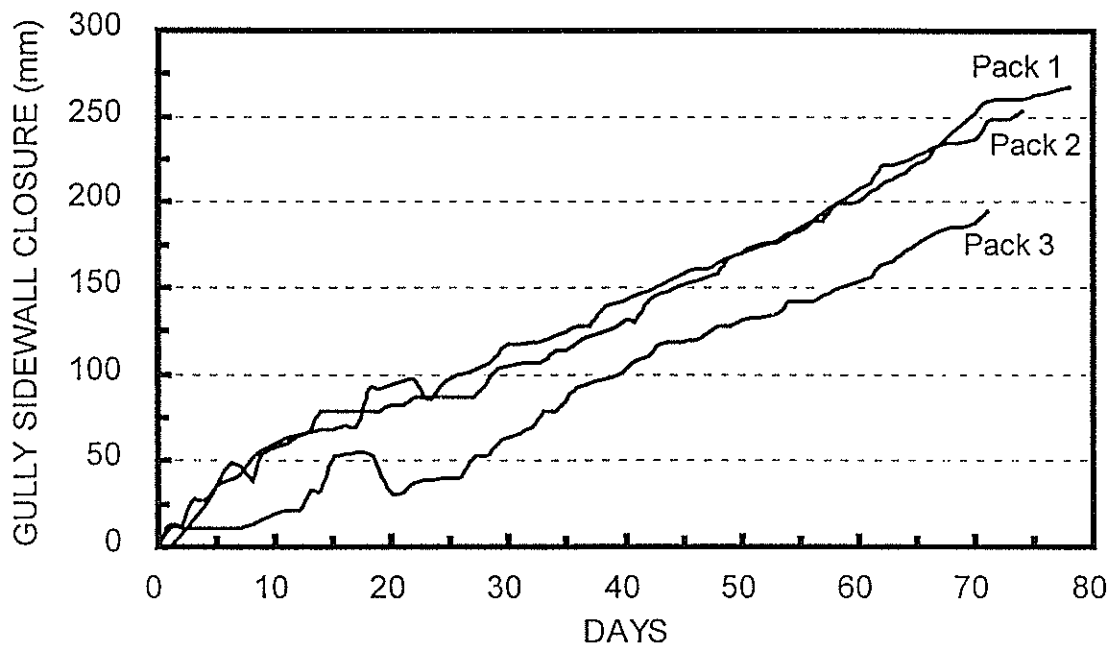


Figure 2.14 Gully sidewall displacement at Hartebeestfontein 6 Shaft, Site 2

The graph of gully sidewall closure (Figure 2.14) shows the displacement that the gully sidewall has undergone due to the load build up in the monitored gully packs and also gives an indication of the amount of damage caused to the sidewall.

## 2.2 Western Deep Levels South Mine

Gully packs were monitored at two sites at Western Deep Levels South Mine.

### 2.2.1 Site 1 - 84-53 stope, E3 panel

Three instrumented 1,1 m x 1,1 m mat packs were installed in the 84-53 stope, E3 panel, at an approximate depth below surface of 2555 m. This mine uses a system of follow behind gullies and therefore the packs were installed in the stope face area before cutting of the gully. The packs were monitored before and after the cutting of the gully. Secondary blasting of the gully sidewall (to facilitate scraping of the panel face) resulted in the first two packs being blasted out. Adequate data was however obtained prior to their being blasted out and the third pack continued to provide data. At the completion of monitoring the gully face was 10 m from the third pack. Figure 2.15 is a schematic of the layout at this site.

Initial average stope widths at each pack were: pack 1, 1134 mm; pack 2, 1330 mm; and pack 3, 1000 mm. A graph of stope closure (i.e. pack deformation) vs time (days) is given in Figure 2.18.



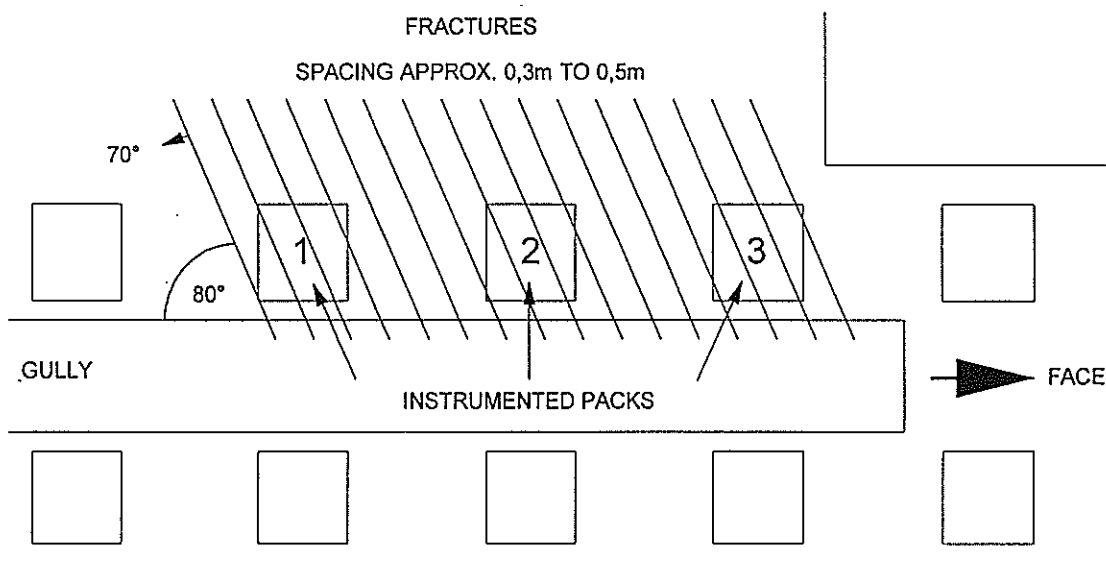


Figure 2.15 Schematic of fracture pattern observed at Western Deep Levels South, Site 1

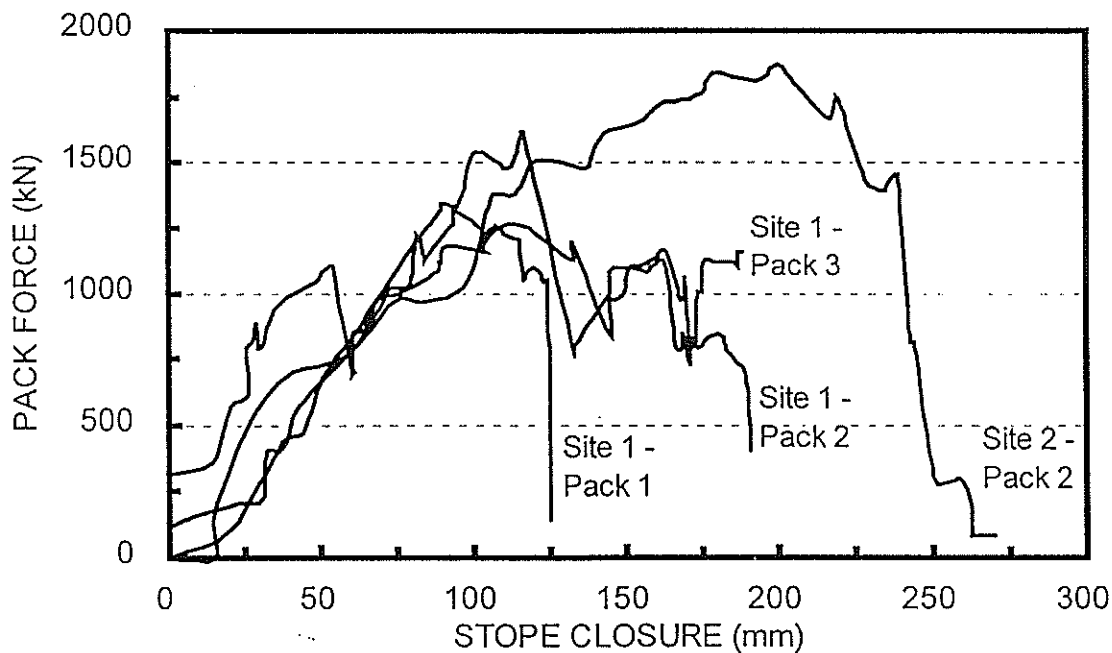


Figure 2.16 Pack force-deformation behaviour at Western Deep Levels South, Sites 1 and 2

Based on stope and gully geometry, the pre-existing discontinuities in the footwall rock at this site were expected to be predominantly face parallel stress fractures orientated at right angles to the line of the gully, and reef parallel bedding planes. Fracture mapping of the site confirmed this, with the stress fractures at approximately 80 degrees to the line of the gully and running up-dip and away from the stope face (see Figure 2.15). Several bedding planes, at approximately 0,3m spacing, daylighted in the gully sidewall under the packs.

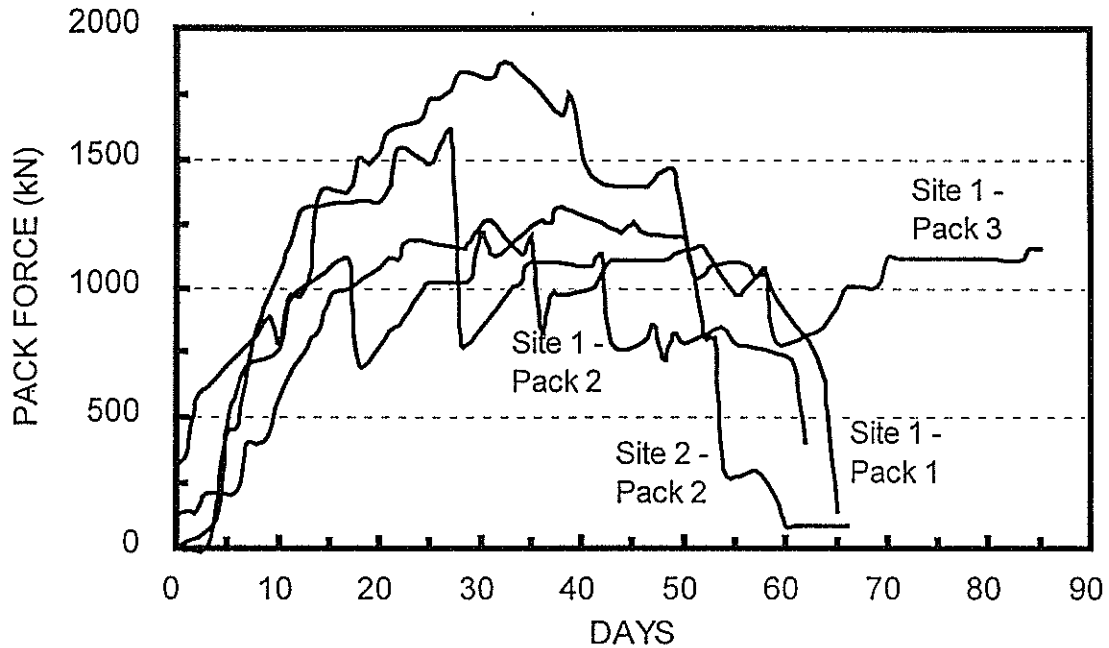


Figure 2.17 Pack force-time behaviour at Western Deep Levels South, Sites 1 and 2

The results are presented in Figures 2.16 and 2.17 as graphs pack force vs stope closure (pack deformation) and pack force vs time (in days), respectively. From these graphs it can be seen that pack forces of between 1250 kN and 1600 kN are reached after average stope closure of about 110 mm. After these forces are reached in the packs there is a levelling off and even a drop off in force with increasing time and closure. This levelling or dropping off of load is accompanied by gully sidewall convergence. The large drops in pack force are associated with the mining of the gully past the packs.

The final drop off in force observed in packs 1 and 2 is considered to be as a result of movement induced on a cross-bedding plane which under lay these packs and was dipping into the gully at 40 degrees.

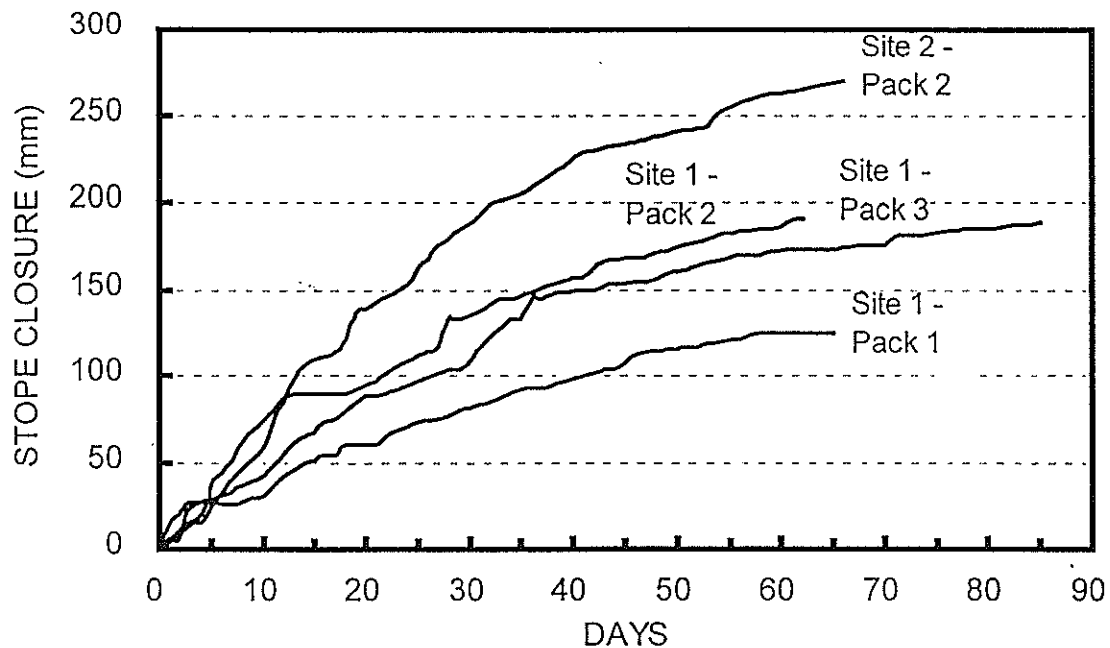


Figure 2.18 Stope closure (pack displacement) at Western Deep Levels South, Sites 1 and 2

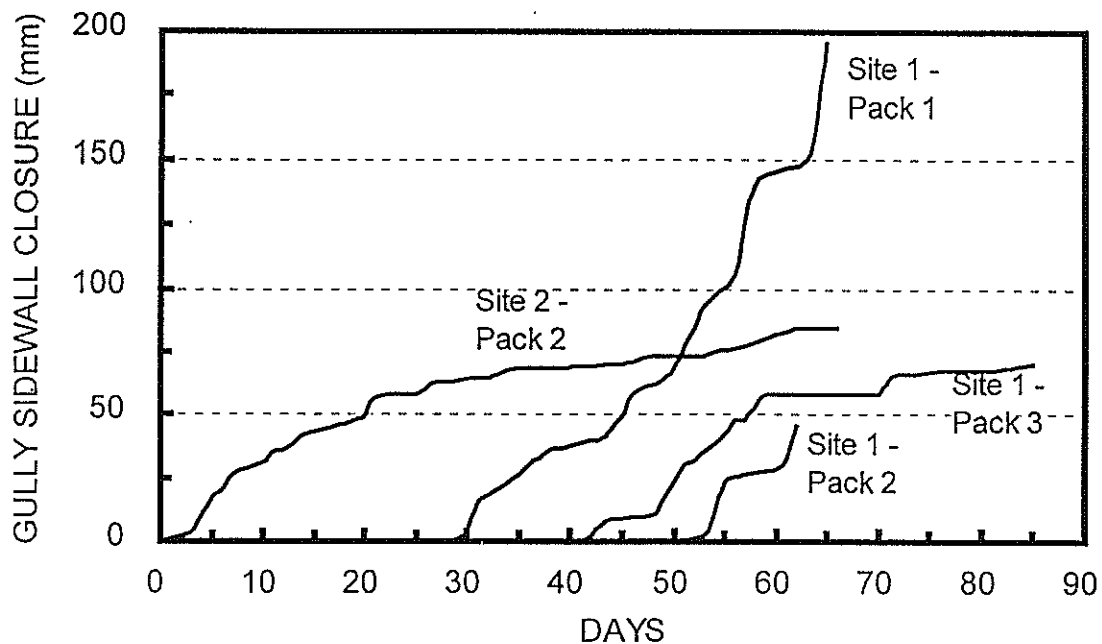


Figure 2.19 Gully sidewall displacements at Western Deep Levels South, Sites 1 and 2

The graph of gully sidewall closure (Figure 2.19) shows the displacement that the gully sidewall has undergone due to the load build up in the monitored gully packs and also gives an indication of the amount of damage caused to the sidewall.

### 2.2.2 Site 2 - 79-49 stope, E1 panel

Three solid timber "8x4" (2 x 1 m) packs in the trackless VCR 79-49, E1 panel were instrumented during November. Unfortunately the first and third instrumented packs at this site were damaged during mining operations and no data could be collected from them. Data from the remaining pack, pack 2, was however obtained and the results are included with those from Site 1 (cf Figures 2.16, 2.17, 2.18 and 2.19). The initial average stope width for pack 2 was 784 mm

This remaining pack 2 was monitored for 66 days and a peak force of about 1800 kN was reached after about 30 days and 180 mm of closure. After 35 days the pack gradually shed load until, after 270 mm of closure, virtually no load was recorded.

## 3 PROPOSED YIELDING GULLY PACK

The results presented above indicate that damage to the gully sidewall under gully packs initiates at pack loads below 2000 kN. Even though the 'standard' packs are capable of sustaining very much higher loads this potential is not achieved due to gully sidewall deformation. The implication being that these packs are over designed for this application and are causing damage to the rock beneath them, i.e. the gully sidewall. With the result that support to the hangingwall is lost and a new pack has to be installed to correct the situation. It is therefore proposed that gully packs be designed to yield below 2000 kN and it is suggested that this yield load be 1000 kN because this forms the lower limit of "failure load" in the majority of cases monitored. Although a yield load of 1000 kN is proposed for the monitored cases, it is not inconceivable that different yield limits could apply to other situations and this can be specifically determined. The proposed force-deformation behaviour for a gully pack with a yield force of 1000 kN is given in Figure 3.1.

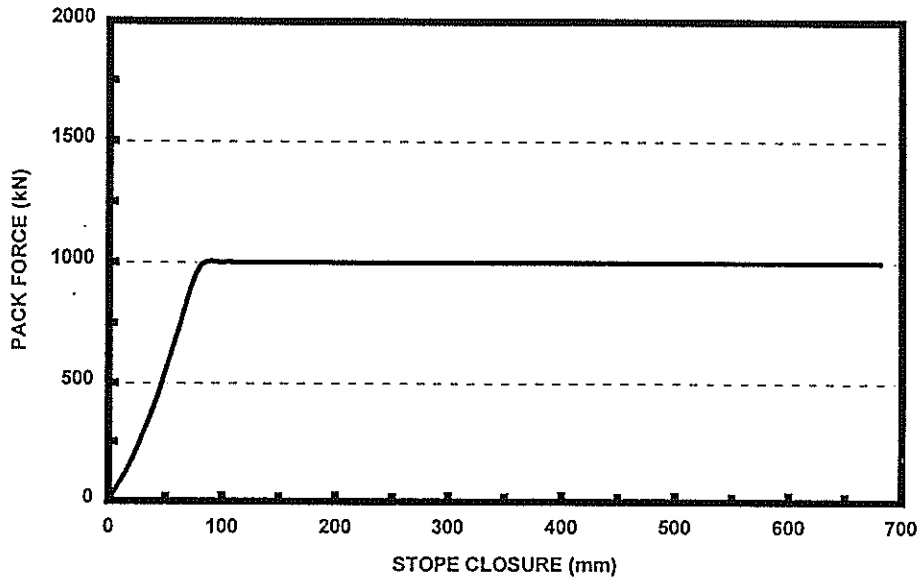


Figure 3.1 Graph showing proposed gully pack 1000 kN yielding behaviour

The effect of different loading rates on the force-deformation behaviour of timber packs (cf Section 2.1.1 in main report), is that the pack behaviour changes markedly. Consequently, the ability of packs to absorb energy is also affected. The difference between normal stope closure rates, typically 5 - 15 mm/day, and closure rates that are believed to occur during some rockbursts, of 1 m/s - 3 m/s, is large, namely a difference in rate of  $10^6$ . This obviously has a significant implication for the performance of timber packs, given their marked loading rate dependant behaviour. It was for this reason that the use of a non-timber material, whose performance is not significantly dependant on loading rate, was considered preferable in the design of a gully pack. The requirement of a yielding pack could also result in packs being constructed of less and possibly cheaper material.

In order to test the validity of the above proposal Grinaker was asked to develop a variation of their 90 x 120 cm "hollow" construction Duraset (reinforced foamed concrete) packs (Figure 3.2) that would yield at 1000 kN. The laboratory determined load-deformation behaviour of one these customised packs is reproduced in Figure 3.3.

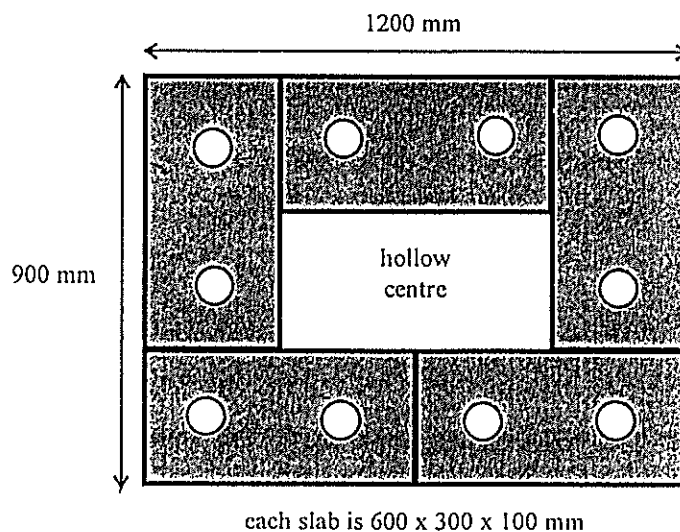


Figure 3.2 Schematic of trial 1000 kN yielding Duraset pack construction

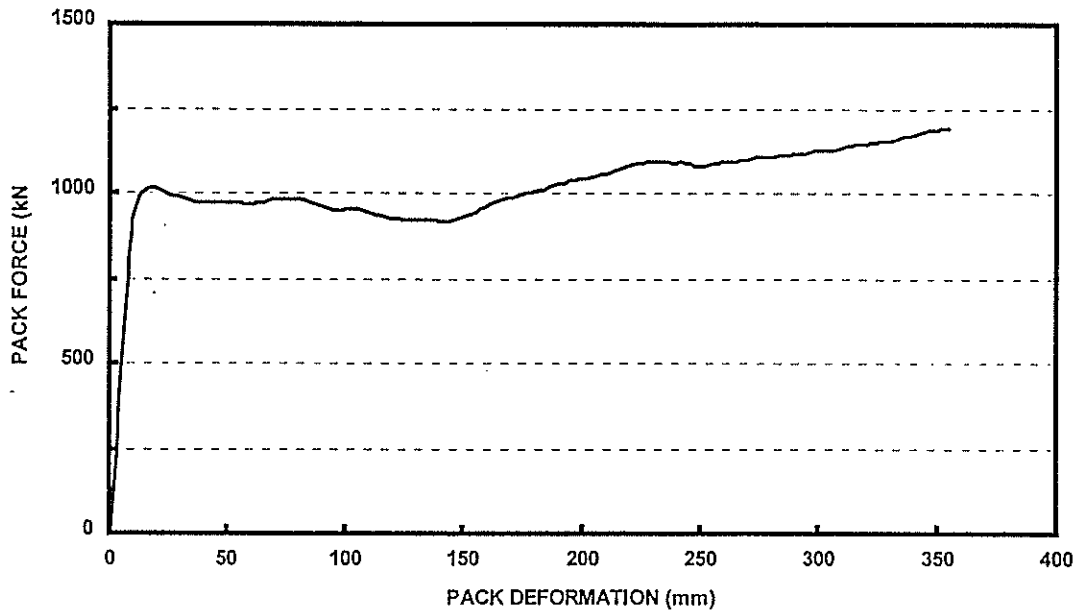


Figure 3.3 Laboratory curve obtained for a 1,3 m high, 1000 kN yielding Duraset pack

Three trial packs with the design yield of 1000 kN were installed at Western Deep Levels South mine in the 87-49 VCR stope, W1 panel at a depth below surface of 2691 m (Figure 3.4). These packs and the associated stope and gully closures were monitored for about 100 days in conjunction with the gully displacement of some adjacent ‘mine standard’ timber packs as a means of assessing the success of the trial packs in reducing gully sidewall damage. This stope was mostly mined as up-dip panels with only periodic and limited on-breast mining being carried out to open up new up-dip face lengths. Consequently the on-strike face advance and follow-behind-gully advance was slow.

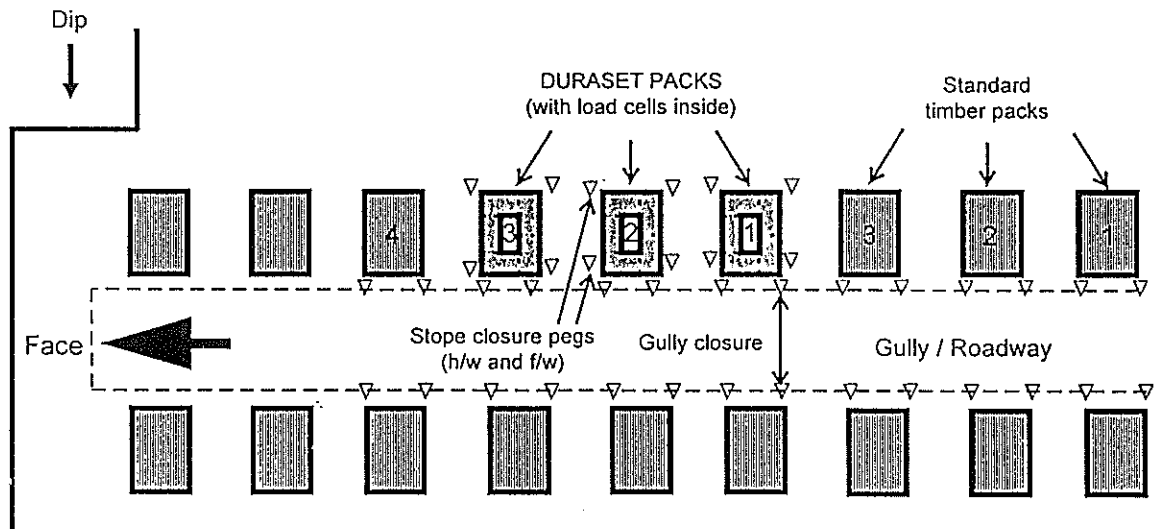


Figure 3.4 Schematic layout of instrumented trial foamed concrete packs

In each of the trial foamed concrete packs, five load cells, corresponding to the five blocks making up a layer, were installed sandwiched between two steel plates. The observed gully sidewall fracturing at this site is indicated in Figure 3.5. Fractures were predominately orientated parallel to the face and near vertical, and were closely spaced. There was also evidence of some blast damage between the packs.

The graphs of pack force vs stope closure (pack deformation) and pack force vs elapsed time (days) are given in Figures 3.6 and 3.7. The gauges and load cells of pack 1 were damaged early on and as a result the pack force curve is affected and not a true reflection of pack 1's behaviour. Pack 2's instrumentation appears to be functioning despite having been slightly dislodged. Two of the gauges for pack 3 were cut off soon after installation but the other three remained functioning.

Initial average stope widths at each pack were: pack 1, 807 mm; pack 2, 916 mm; and pack 3, 1069 mm. A graph of stope closure (i.e. pack deformation) vs time (days) is given in Figure 3.8.

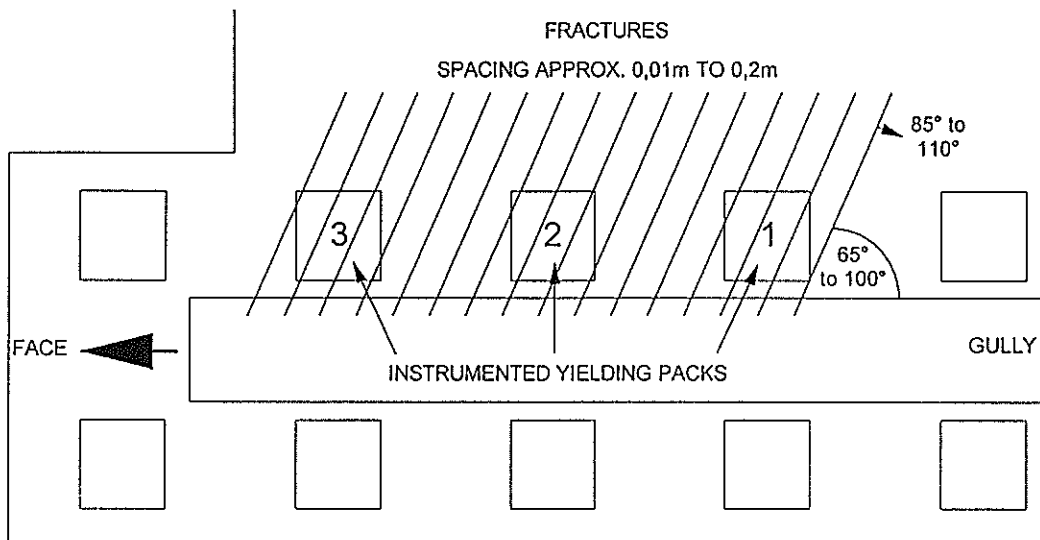


Figure 3.5 Schematic of fracture pattern observed at Western Deep Levels South, Duraset trial site

### 3.1 Pack force and stope closure

The force results for pack 1 are not reliable after the 16 day point due to damage to two of the load cells. The pack does appear to have reached peak load and be yielding at about 600 kN for the period between 3 and 13 days. The drop in force between 13 days and 16 days is associated with the cutting of the gully. The recorded stope closure at this pack reached an average of 293 mm after 97 days, this translates into a strain of 36 per cent and a closure rate of 3 mm/day.

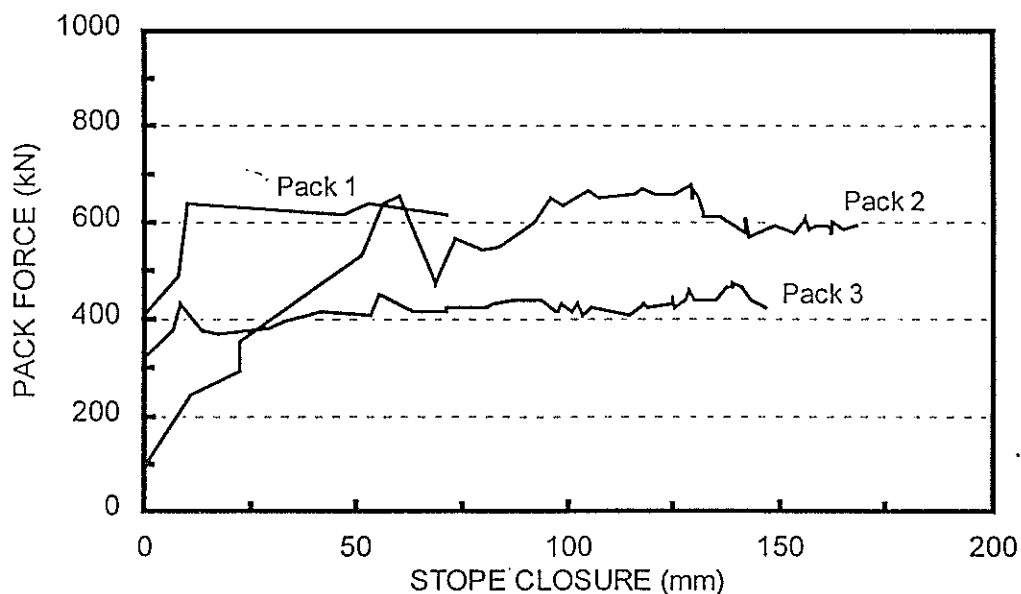


Figure 3.6 Pack force-deformation behaviour at Western Deep Levels South, Duraset trial site

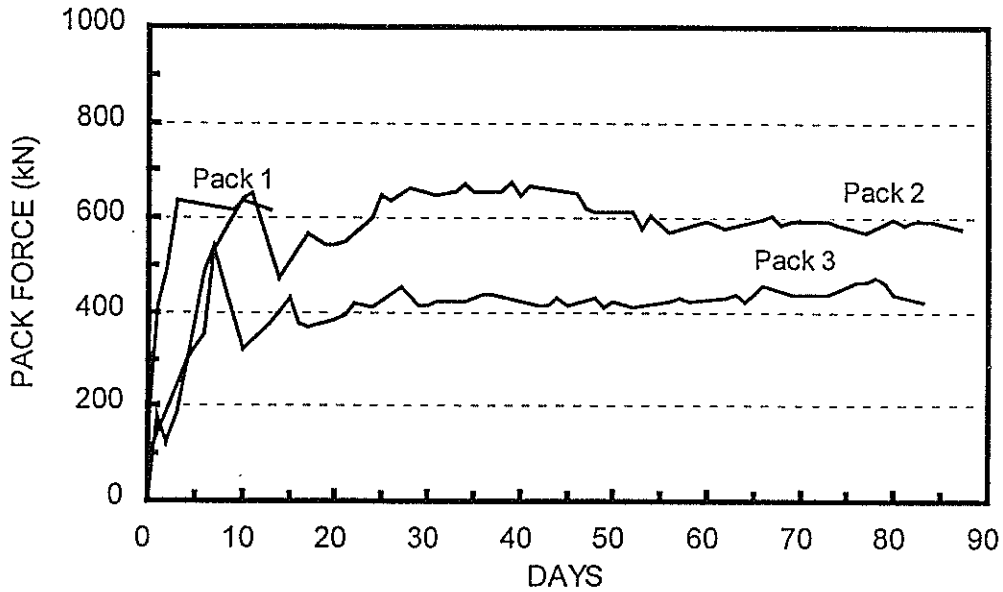


Figure 3.7 Pack force-time behaviour at Western Deep Levels South, Duraset trial site

Pack 2 reached and yielded at about 600 kN from the 10th day onwards, with a dip in load from day 12 to day 24 due to the footwall lifting of the adjacent portion of the gully. The recorded stope closure at this pack reached an average of 168 mm after 87 days, this translates into a strain of 18 per cent and a closure rate of 2 mm/day. However this may not be the full amount of closure because measuring pegs were lost (and were replaced) at various times during the early stages of monitoring.

Pack 3 reached a load of 540 kN on the 7th day before two load cell gauges were damaged. Footwall lifting for the gully also affected the pack force within the first 13 days. Thereafter the remaining three gauges indicate a consistent load of about 420 kN from the 15th day onwards. The recorded stope closure at this pack reached an average of 147 mm after 83 days, this translates into a strain of 14 per cent and a closure rate of under 2 mm/day. This, however, does not reflect the full amount of closure because pegs could not be installed immediately at the time of pack installation and measuring pegs were lost (and were replaced) at various times during monitoring.

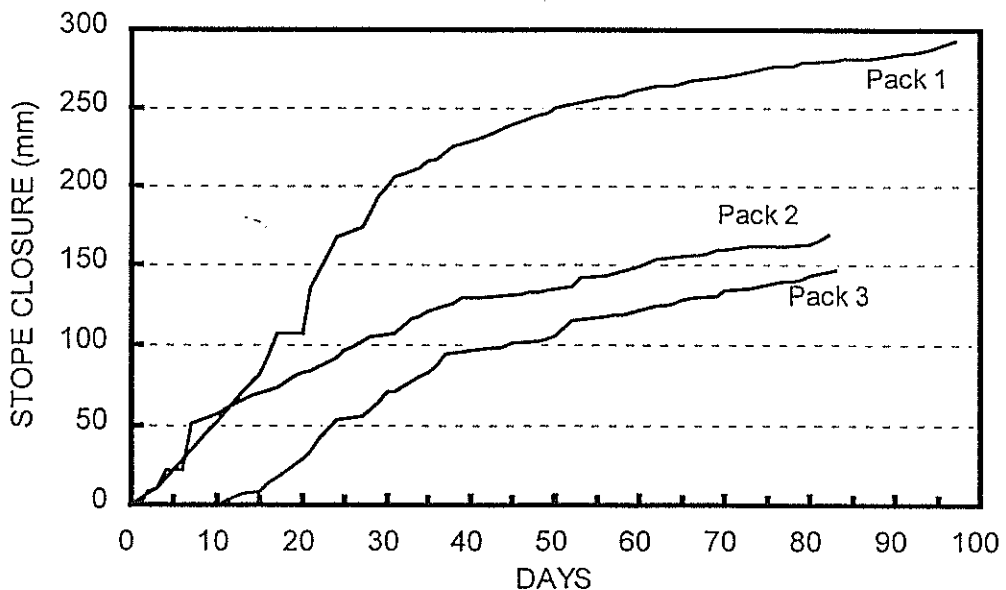


Figure 3.8 Stope closure at Western Deep Levels South, Duraset trial site

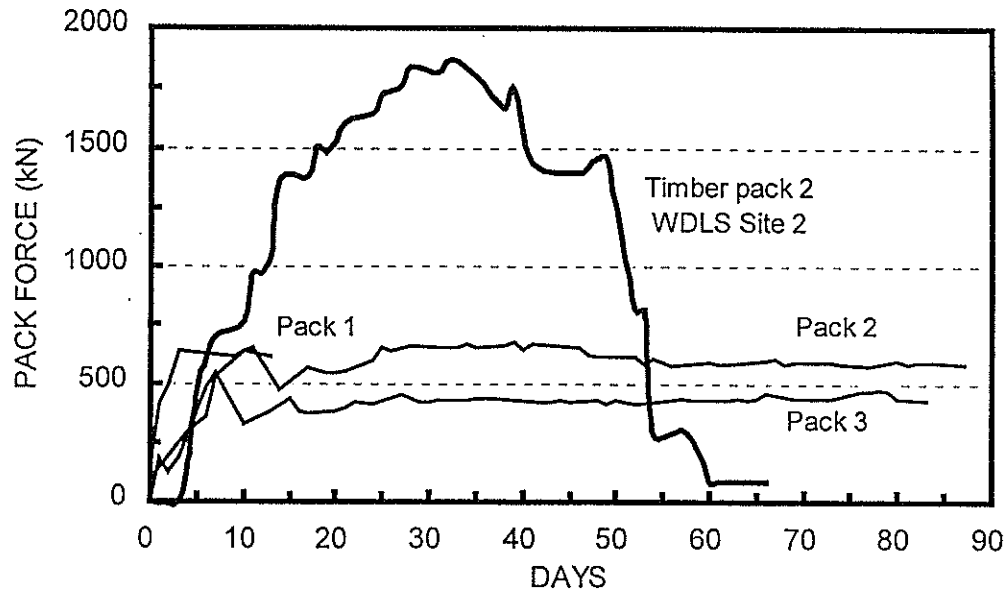


Figure 3.9 Comparison of yielding pack behaviour and 'standard' timber pack behaviour

A comparison of the Duraset packs' force-deformation behaviour with that of a previously monitored timber gully pack at WDL South (Site 2 pack 2) is given in Figure 3.9. The markedly different pack force behaviour for a similar time span can be seen.

### 3.2 Gully sidewall closure

A combination of graphs of gully sidewall closure for the three trial Duraset packs (labelled DP1, DP2 and DP3) and four adjacent 'mine standard' timber packs (labelled TP1, TP2, TP3 and TP4) has been produced (Figure 3.10). Also included as a dashed line is the curve for one of the timber gully packs previously monitored at WDL South (Site 2 pack 2). There appears to be no significant difference in sidewall deformation for the Duraset packs and the timber packs. However the timber packs TP1, TP2 and TP3 were all installed prior to the first Duraset pack but were monitored from the same day as the Duraset pack. Some additional sidewall movement can be expected to have taken place under these timber packs before measurements began.

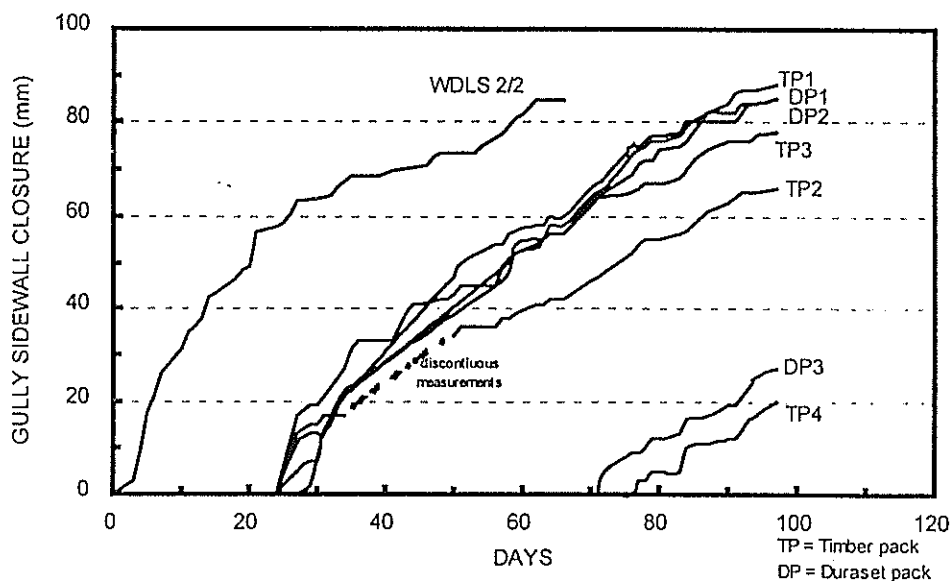


Figure 3.10 Gully sidewall displacements at Western Deep Levels South, Duraset trial site



### 3.3 Comments

Although definite conclusions can not really be made at this stage some aspects are worth noting. The packs do appear to be yielding well but at 60 per cent of their designed yield force. This aspect was discussed with Grinaker to determine possible reasons. The most likely explanation being that because of a very irregular hangingwall profile, a significant amount of blocking was required and this change to the ideal pack construction affected the yield limit. This change in the ideal construction geometry having an effect on the yield limit. Despite the inconclusive gully sidewall measurements, observations made at the site indicate that despite the highly disturbed state of the footwall there was little additional damage being done to the footwall by the trial packs. The same situation was not observed for the timber packs where loss of sidewall rock occurred.

## 4 NUMERICAL MODELLING OF GULLY PACK BEHAVIOUR

Numerical modelling was carried out to investigate possible reasons for the observed and measured *in situ* behaviour of gully packs and gully sidewall and to predict the behaviour of the proposed gully pack support.

### 4.1 Modelling of *in situ* pack behaviour

The assumption that the mobilisation of pre-existing fractures in the gully sidewall is the mechanism by which the gully packs shed load was investigated via numerical modelling. The WDL South case of a single inclined fracture underlying a pack was explored with UDEC and the results confirmed that this was a likely explanation. The case of more numerous fractures was investigated with FLAC 'ubiquitous joint' model. Again, the results confirmed that this provided a mechanism that was consistent with the relevant measured data.

#### 4.1.1 UDEC modelling

As a first step, simulation of some measured behaviour was attempted. UDEC (Universal Distinct Element Code) was selected for this purpose because the fractured nature of the gully sidewall requires a non-linear discrete block modelling approach. The geometry of the model depicted a dip section through a gully with packs on each side and with an unfavourably orientated fracture cutting through the footwall beneath one of the gully packs (Figure 4.1). This geometry was chosen as a starting point because it suits the 2D nature of UDEC and because similar examples were observed in relation to some of the monitored packs. The graphs in Figure 4.2 show a relatively good correlation between the measured and modelled results, although closure is five times greater in the modelling case.

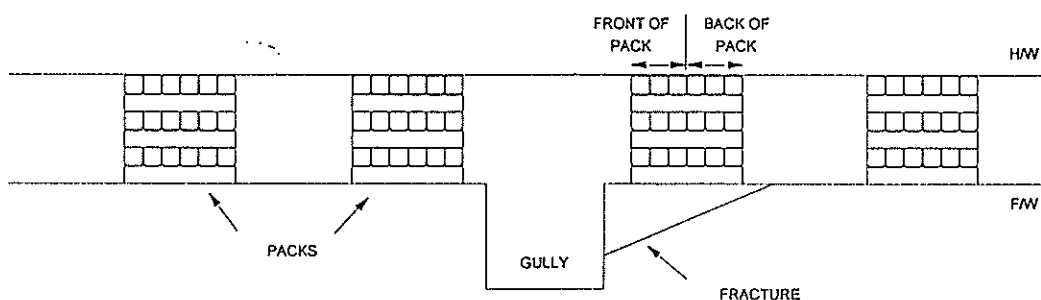


Figure 4.1 Schematic of gully and fracture geometry modelled with UDEC

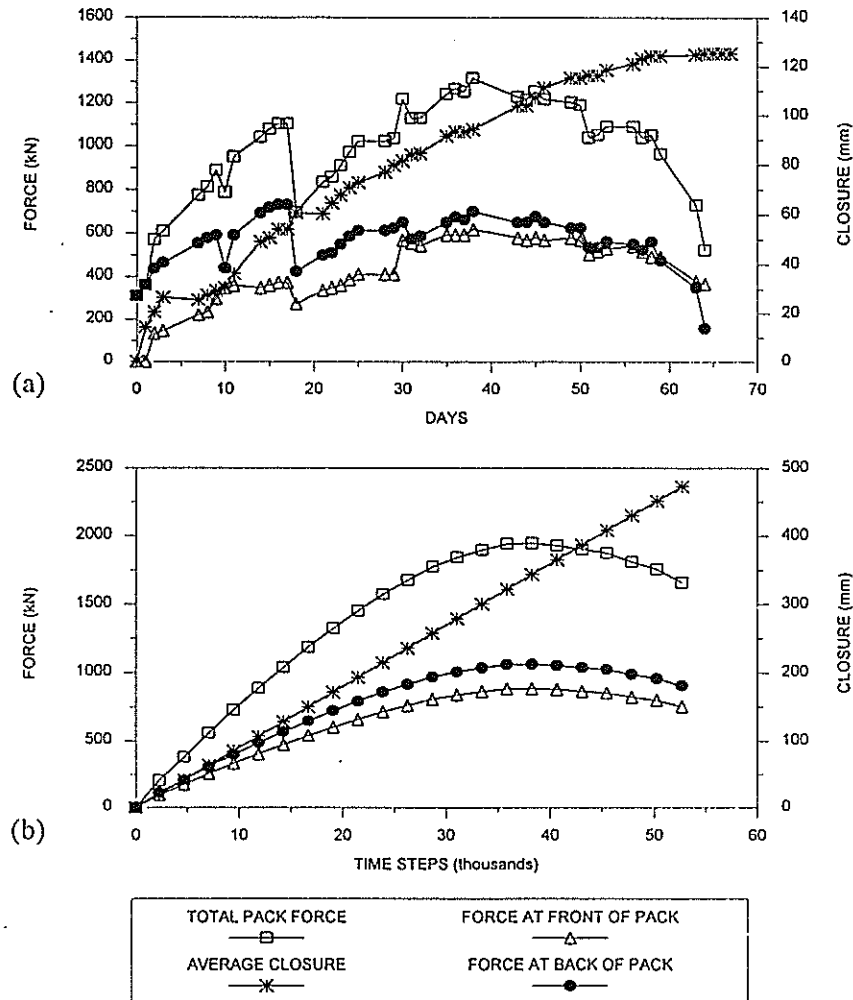


Figure 4.2 Comparison of *in situ* pack behaviour (a) with UDEC modelling results (b)

#### 4.1.2 FLAC modelling

The influence of fracture angle for a pervasive system of fractures (ubiquitous joint model) was investigated with FLAC using a data file developed in conjunction with a Wits University MSc student, Emmanuel Asante. The results of simulations with fracture angles, measured anti-clockwise from the horizontal, of  $0^\circ$ ,  $60^\circ$ ,  $90^\circ$ , and  $120^\circ$  are presented in Figures 4.3 to 4.6, respectively. Part (a) of each figure shows the geometry and an indication of failure (plasticity index) at the end of each run. Part (b) shows the history plot of the load in the gully pack (lower line) and the load in an unaffected in-stope pack (upper line). In each case the top boundary of the model is displaced by a fixed amount and then arrested and brought to equilibrium.

As might be expected the  $60^\circ$  case has a larger region of failure than the  $90^\circ$  and  $120^\circ$  cases because slip can more readily occur into the gully with this orientation. The  $60^\circ$  and  $120^\circ$  cases have, however, the same overall degradation to the load curve (part (b) in each figure) up and till the applied boundary displacement was halted, indicating the same total deformation to the gully sidewall. After the applied displacement is turned off, slip can continue to occur more readily in the  $60^\circ$  case as shown by the more rapid load decay. In the  $0^\circ$  case extensive failure of the ubiquitous joints occurs as the packs punch into the footwall causing it to bulge upwards between the packs and to slip horizontally, however the pack force remains unaffected.

A further study conducted by the Wits student related to the effect of pack distance from gully edge on sidewall damage. The results (Figure 4.7) show very little decrease in sidewall displacement when the pack is more than 50 cm from the gully edge.

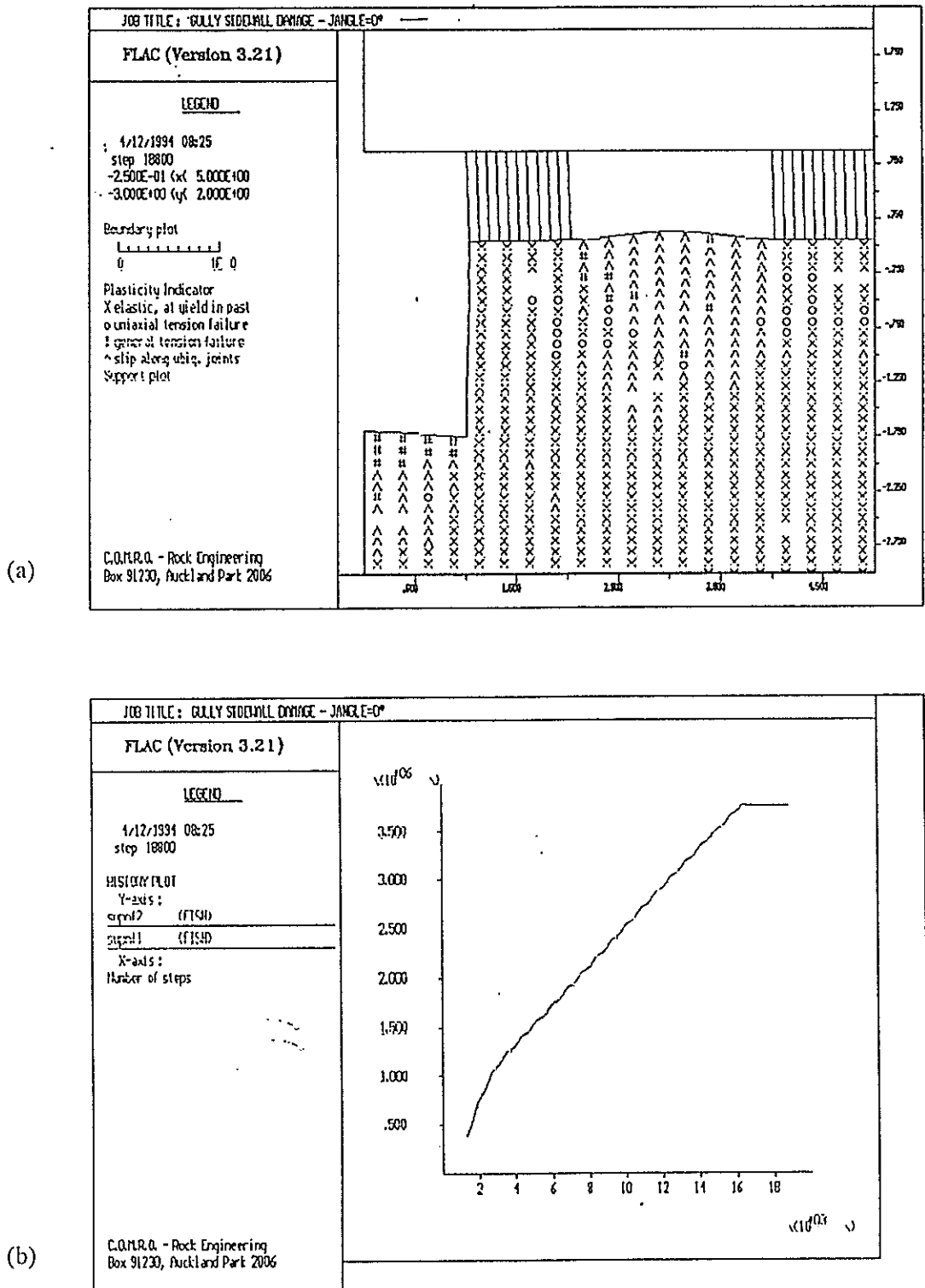


Figure 4.3 Plot of gully sidewall failure (a) and pack force history (b) for 0° fracture angle (FLAC modelling - Wits University student)

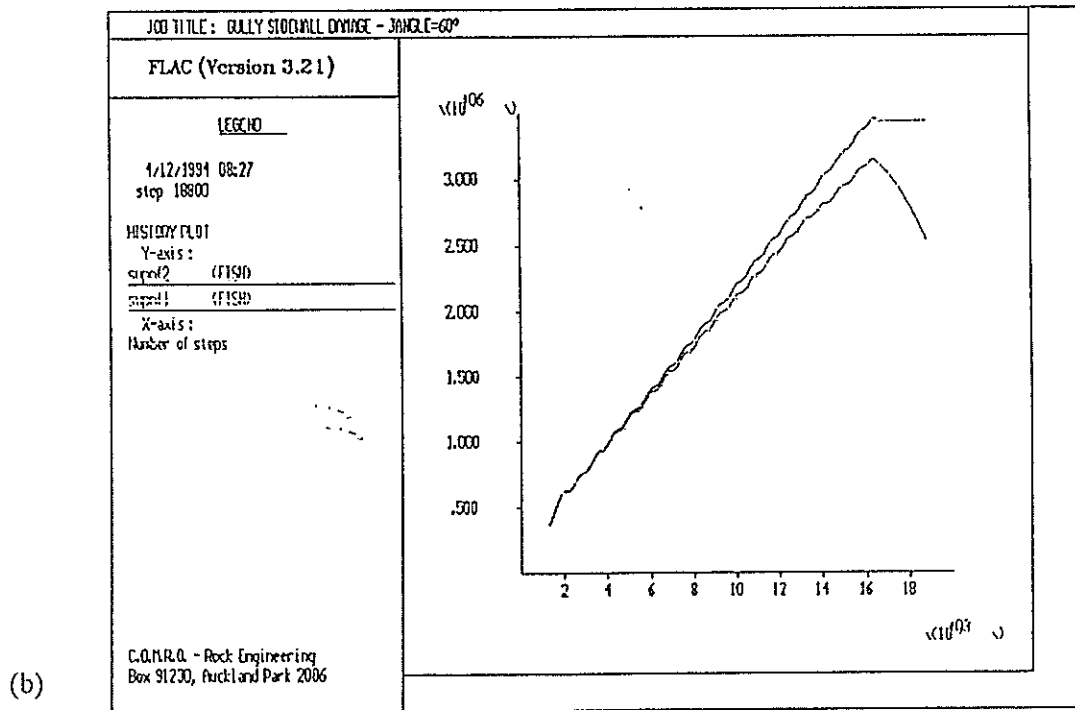
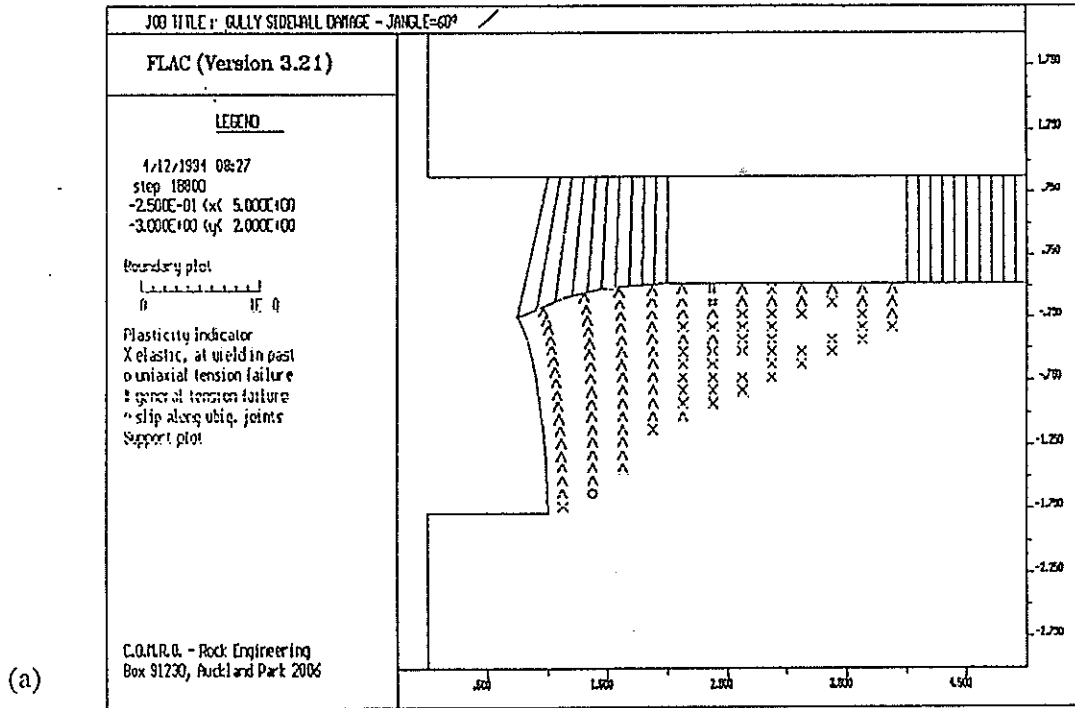


Figure 4.4 Plot of gully sidewall failure (a) and pack force history (b) for 60° fracture angle (FLAC modelling - Wits University student)

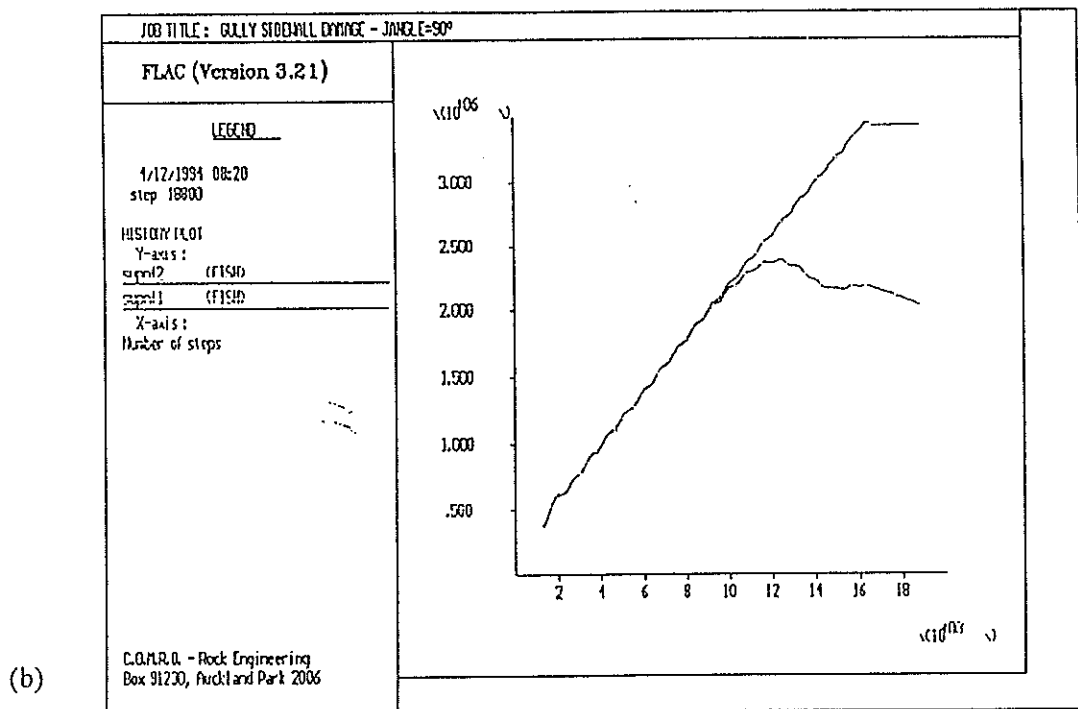
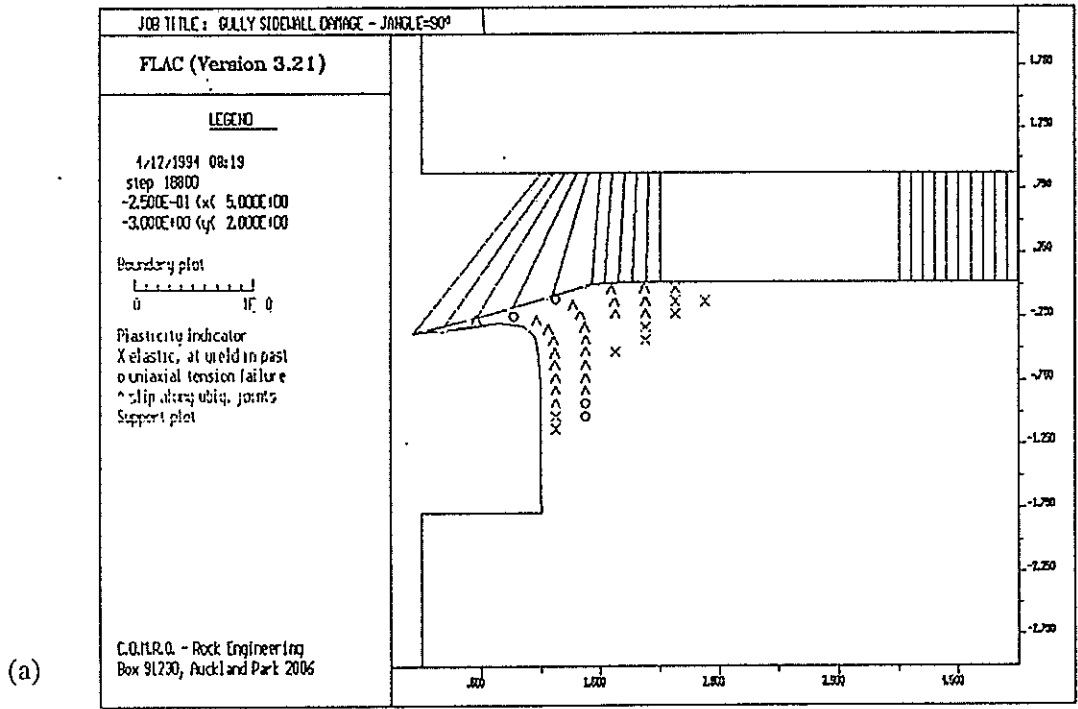


Figure 4.5 Plot of gully sidewall failure (a) and pack force history (b) for 90° fracture angle (FLAC modelling - Wits University student)

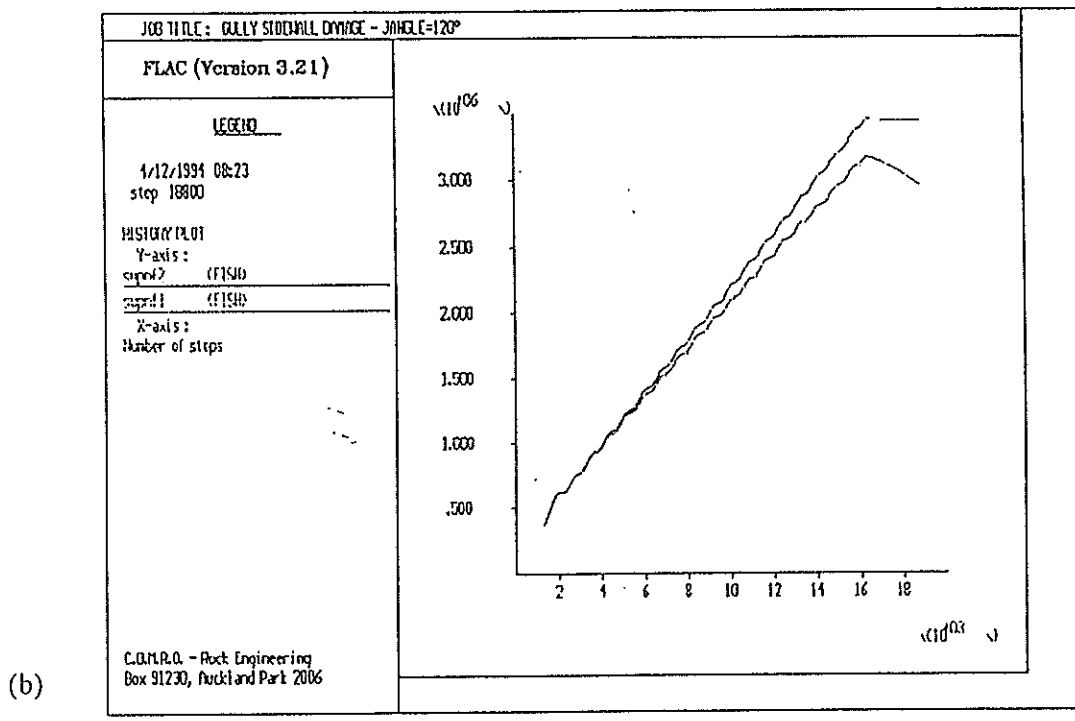
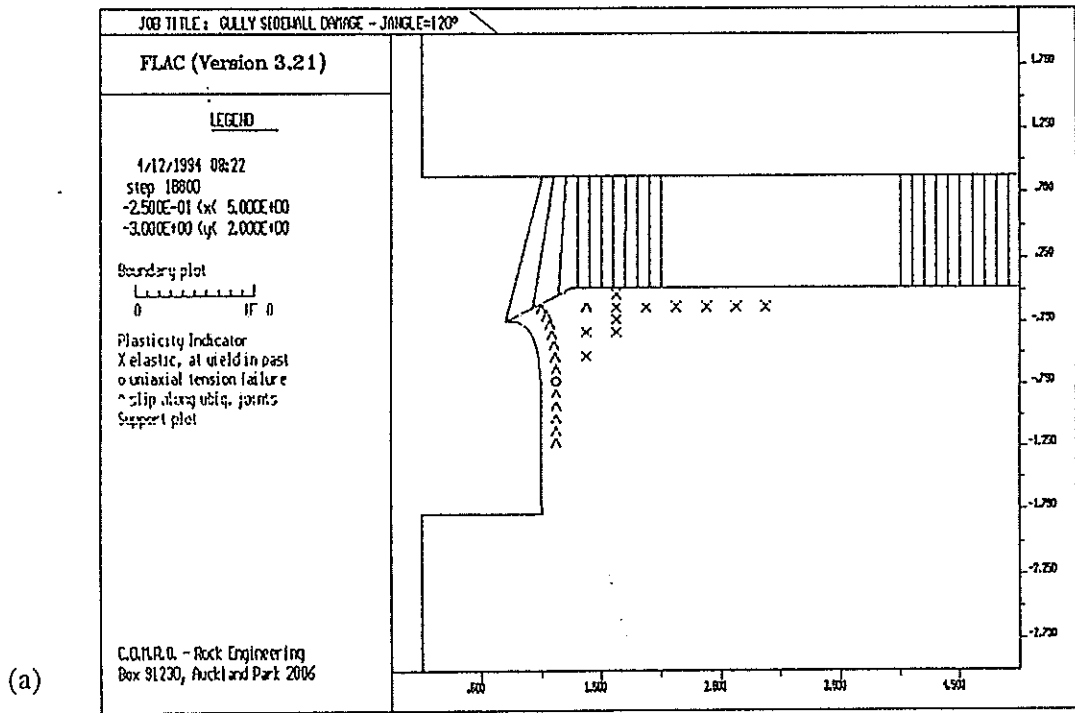


Figure 4.6 Plot of gully sidewall failure (a) and pack force history (b) for 120° fracture angle (FLAC modelling - Wits University student)

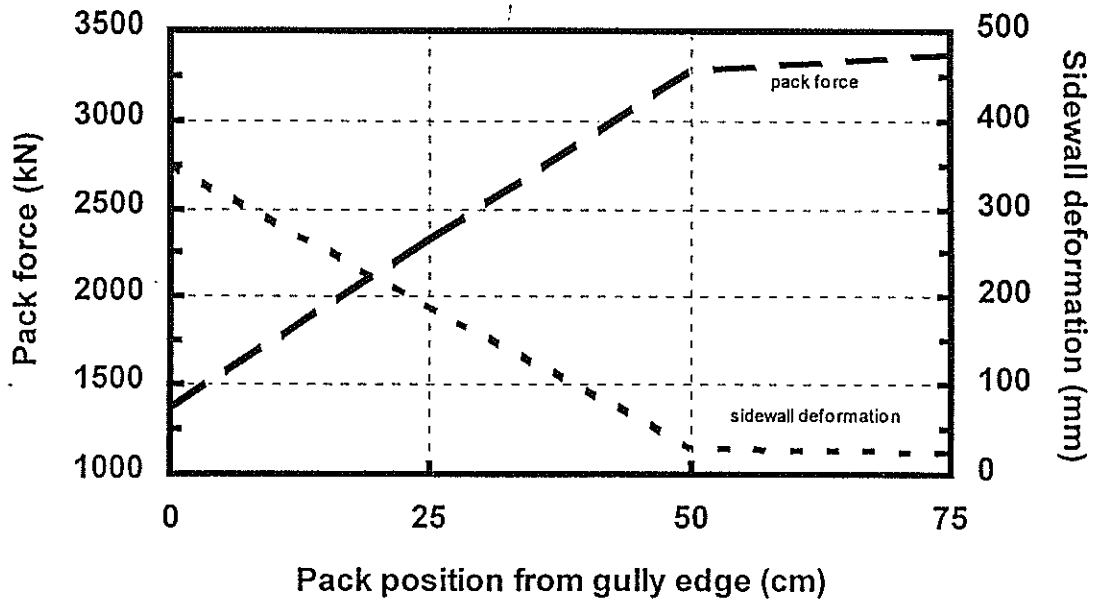


Figure 4.7 Influence of pack position from gully edge (Wits student’s FLAC modelling)

4.2 Modelling of proposed yielding pack

The reduction of sidewall damage that could be expected from the introduction of a 1000 kN yielding gully pack was studied, again with FLAC and UDEC (Figure 4.8). In the FLAC modelling (Figure 4.9 and 4.10), a fourfold reduction in sidewall deformation resulted from the replacement of a ‘standard’ gully pack with a yielding pack. A similar improvement was indicated in the UDEC modelling. These results show a degree of similarity to the *in situ* results obtained for the trial yielding packs presented above and indicate the potential benefit to be gained from using yielding gully packs.

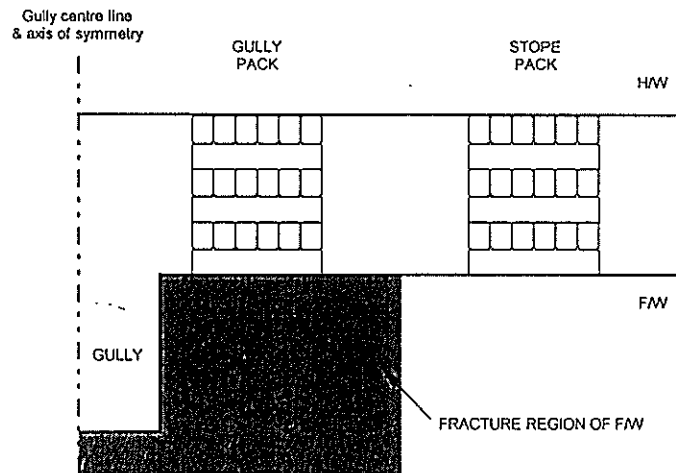


Figure 4.8 Schematic of gully geometry for yielding pack modelling

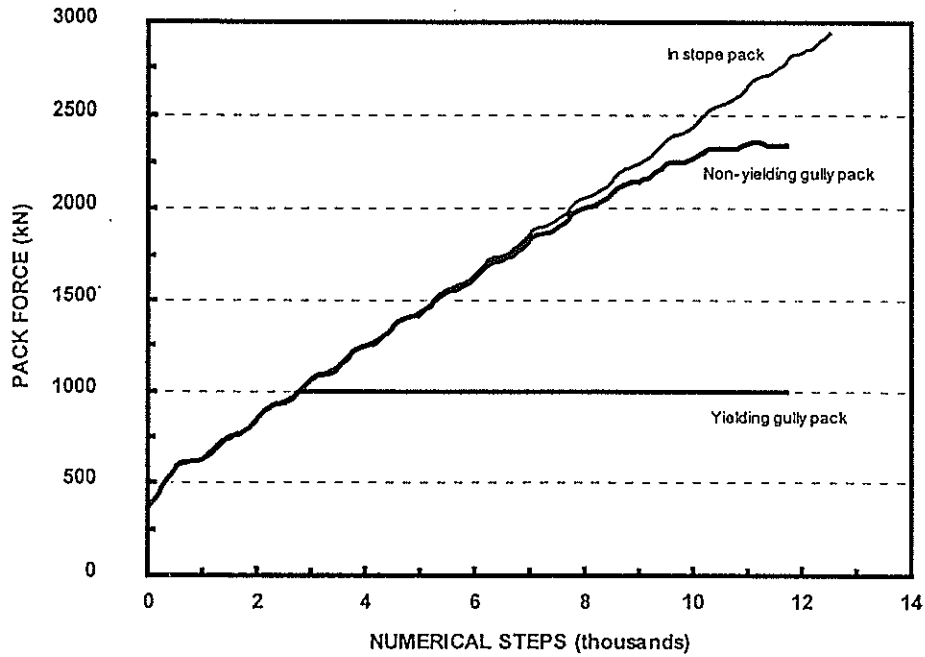


Figure 4.9 Comparison of simulated of '*in situ*' pack behaviour with simulated yielding gully pack response (using FLAC)

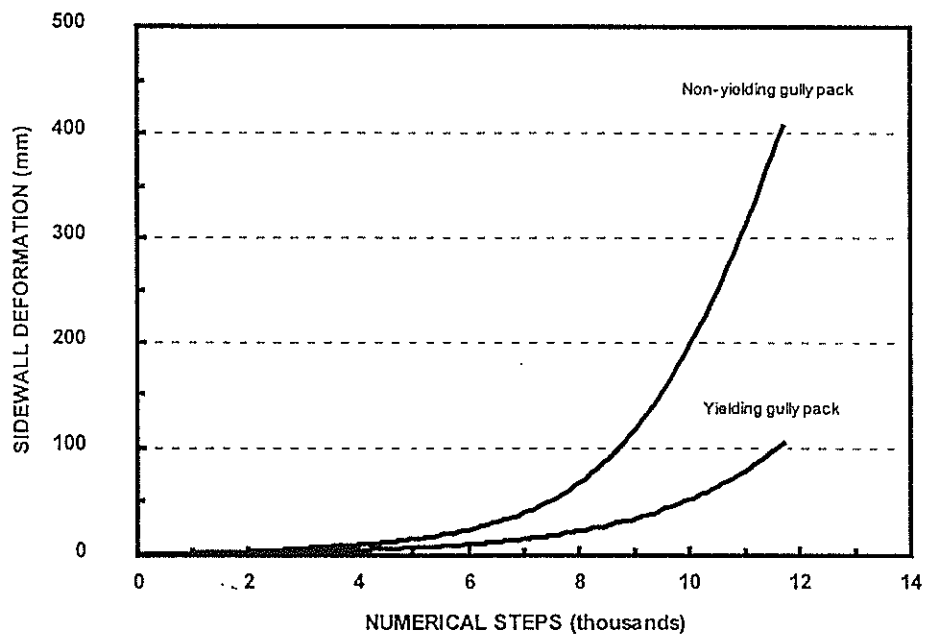


Figure 4.10 Comparison of simulated of '*in situ*' sidewall deformation with deformation induced by simulated yielding gully pack (using FLAC)

## 5 GULLY SUPPORT REQUIREMENTS

In addition to providing support along the sides of the gullies by means of gully packs, support needs to be considered for the exposed section of gully hangingwall which is not directly supported by the two rows of gully packs. It is therefore necessary to be able to design support systems to function in this region of stope gullies.



In order to design a suitable support system it is first necessary to determine the support requirements that must be met and this in turn depends on knowing the thicknesses (heights) of fallouts which have to be prevented. One source of data for fallout dimensions are the GME's fatal accident investigation files. However, due to the relatively small data set for accidents occurring only between the rows of gully packs, the analysis of the GME's fatal accident records has only been able to provide limited information in respect of the thicknesses of fallouts. This problem becomes especially evident when the data is broken down on the basis of reef type or mining district.

In order to address this deficiency a programme of underground measurements was undertaken whereby fallouts were measured in a series of representative gullies located on three major reef horizons. These reefs were: Ventersdorp Contact Reef (VCR), Carbon Leader Reef and Vaal Reef. In each case a cumulative frequency distribution is plotted and fallout thicknesses determined for various percentage limits. This data has then been used to calculate the support resistance requirement for static conditions and an energy absorption requirement for rockburst conditions.

### 5.1 Accident analysis

An initial analysis of the gully accident data for the years 1990, 1991 and 1992 indicated that a support resistance of about 50 kN/m<sup>2</sup> would have been sufficient to prevent 90 % of rockfall accidents occurring in gullies. A graph of cumulative frequency vs height of FOG for all 1991-1992 fatal gully rockfall accidents is given in Figure 5.1. As already described, when this data is broken down on the basis of reef type or mining district it becomes difficult to make reliable assessments. Hence the need for an alternative approach to determining fallout thickness distributions.

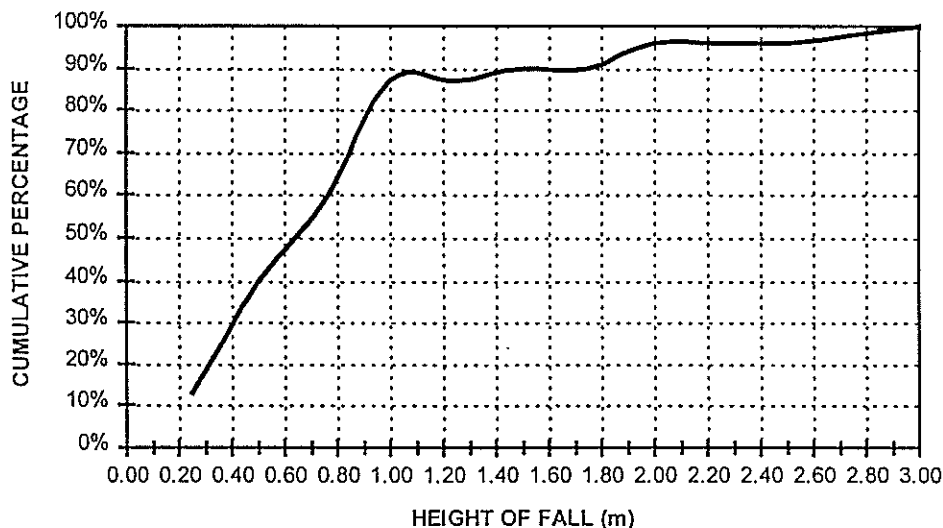


Figure 5.1 Distribution of fatal falls of ground in gullies during 1991 and 1992

### 5.2 Fallout thickness distributions

As already mentioned the alternative approach was to measure fallout heights in a selection of representative gullies on the VCR, Carbon Leader Reef and Vaal Reef. The graphs of cumulative percentage for the fallouts measured on these reefs are given in Figures 5.2, 5.3 and 5.4, respectively. The data presented in these graphs represents 416 measurements on the VCR, 538 measurements on the Carbon Leader and 433 measurements on the Vaal Reef. A total of 27 gullies were surveyed, on a number of mines and at a variety of depths.

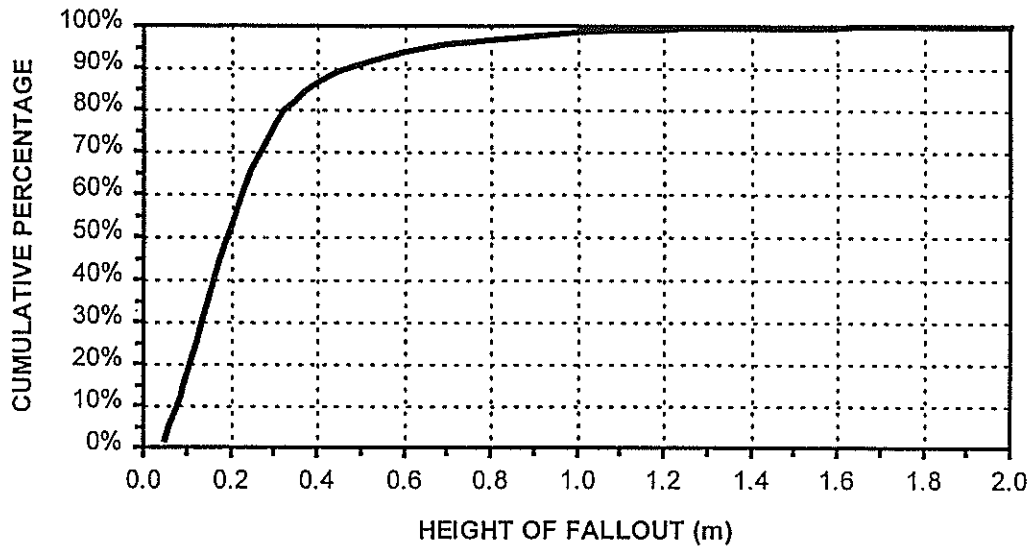


Figure 5.2 Distribution of fallouts in sampled Ventersdorp Contact Reef (VCR) gullies

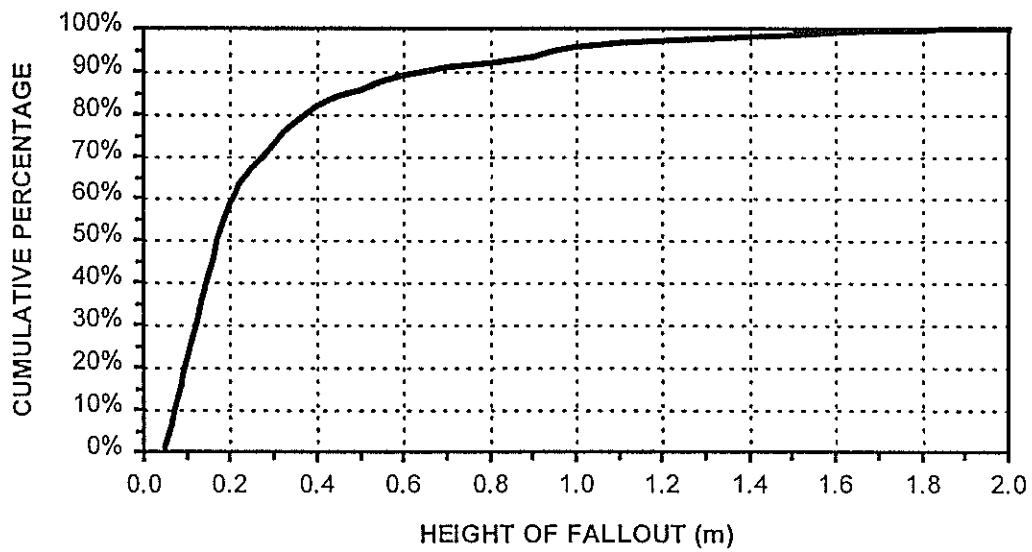


Figure 5.3 Distribution of fallouts in sampled Carbon Leader Reef gullies

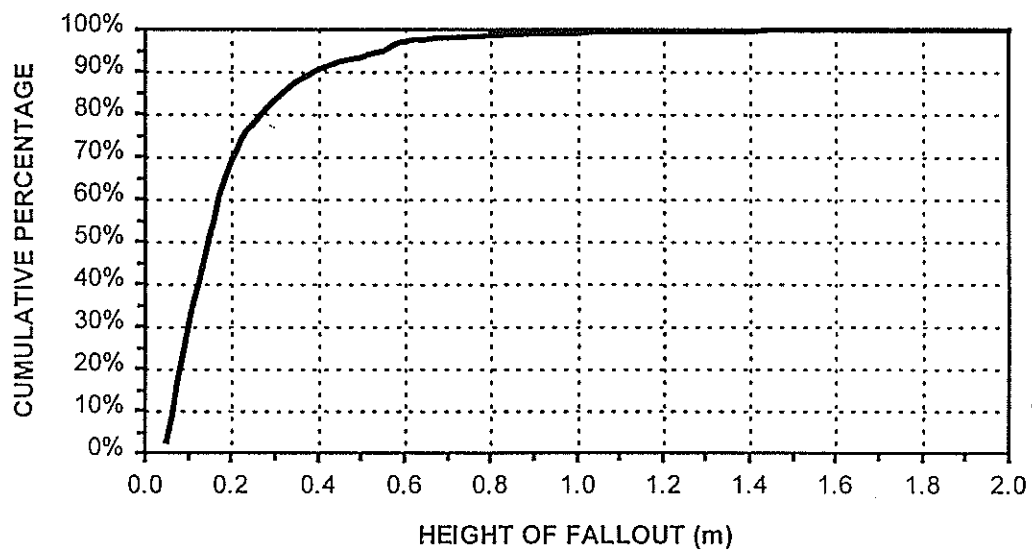


Figure 5.4 Distribution of fallouts in sampled Vaal Reef gullies

### 5.3 Support requirements

Using the fallout distribution graphs and using fallout values for the 90, 95 and 100 per cent frequency levels a table of static (support resistance) and dynamic (energy absorption) support requirements is compiled (Table 5.1). In all cases a density of 2700 kg/m<sup>3</sup>, a gravity value of 9.81 m/s<sup>2</sup>, a velocity of 3 m/s, and an arresting distance of 0,1 m is assumed for a 1 m<sup>2</sup> area of hangingwall.

Table 5.1 Support Requirements for VCR, Carbon Leader Reef and Vaal Reef

Reef Type	Cumulative frequency percentage limit	Fallout thickness m	Support resistance kN/m <sup>2</sup>	Energy absorption kJ/m <sup>2</sup>
VCR				
	90%	0.50	13	7
	95%	0.70	19	10
	100%	1.70	45	25
Carbon Leader				
	90%	0.70	19	10
	95%	1.00	26	15
	100%	2.00	53	30
Vaal Reef				
	90%	0.40	11	6
	95%	0.55	15	8
	100%	2.00	53	30

These support requirements in turn relate to the following support densities (Table 5.2) when using cone bolts to address dynamic conditions. It is assumed that a cone bolt functions with a yielding load of 100 kN under dynamic conditions.

Table 5.2 Cone bolt support densities

Cumulative frequency percentage limit	VCR Cone bolts per m <sup>2</sup>	Carbon Leader Reef Cone bolts per m <sup>2</sup>	Vaal Reef Cone bolts per m <sup>2</sup>
90%	0.7	1.0	0.6
95%	1.0	1.5	0.8
100%	2.5	3.0	3.0

In order for the cone bolts to work effectively and maintain the integrity of the hangingwall during rockburst shakedown it will be necessary to use straps to connect the cone bolts together and create areal coverage. Careful consideration must also be given to the length of bolt used such that the bolt can fulfil its function both during the dynamic phase and the static situation afterwards.

## 6 FURTHER WORK

It should be noted that the above gully support requirements, both for packs and roofbolting, are applicable to the conditions existing in the gullies surveyed. These therefore serve as guidelines, and mines should conduct their own analyses of gully pack behaviour and gully fallouts and determine the support requirements appropriate for their particular conditions.